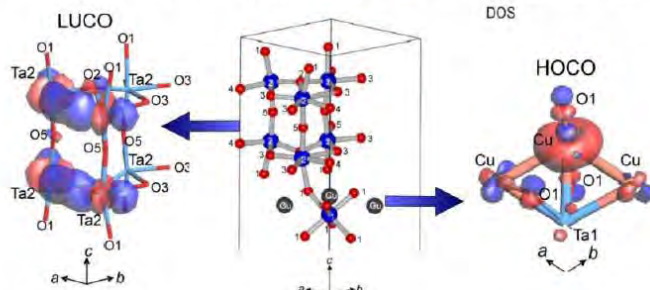
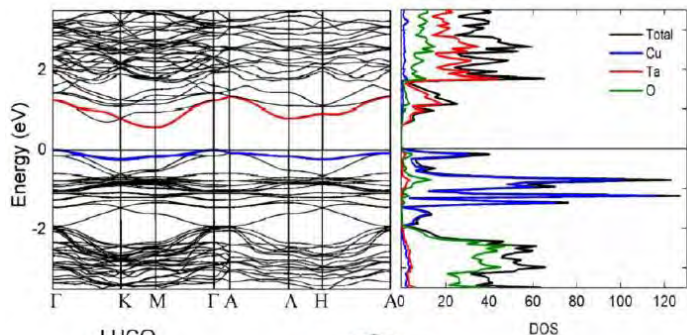


HELIOS SERC

Westin Annapolis Hotel
Annapolis, MD
June 6-9, 2010

Proceedings of the
Thirty-Second
DOE Solar Photochemistry
Research Meeting



Sponsored by:

Chemical Sciences, Geosciences, and Biosciences Division
U.S. Department of Energy

Program and Abstracts

Solar Photochemistry Program Research Meeting

Westin Annapolis Hotel
Annapolis, Maryland
June 6-9, 2010

Chemical Sciences, Geosciences, and Biosciences Division
Office of Basic Energy Sciences
Office of Science
U.S. Department of Energy

Cover Graphics:

The cover figures are drawn from the abstracts of this meeting. One represents a Pt catalyst linked to the stromal end of Photosystem I (Utschig et al., p. 176). Another depicts electronic structure calculations on the semiconductor $\text{Cu}_3\text{Ta}_7\text{O}_{19}$ to obtain densities of states and crystal orbital shapes (Maggard, p. 153).

This document was produced under contract number DE-AC05-06OR23100 between the U.S. Department of Energy and Oak Ridge Associated Universities.

The research grants and contracts described in this document are supported by the U.S. DOE Office of Science, Office of Basic Energy Sciences, Chemical Sciences, Geosciences and Biosciences Division and their invited

FOREWORD

The 32nd Department of Energy Solar Photochemistry Research Meeting, sponsored by the Chemical Sciences, Geosciences, and Biosciences Division of the Office of Basic Energy Sciences, is being held June 6–9, 2010, at the Westin Annapolis Hotel in Annapolis, Maryland. These proceedings include the meeting agenda, abstracts of the formal presentations and posters of the conference, and an address list for the participants.

This conference is composed of the grantees who do research in solar photochemical energy conversion with the support of the Chemical Sciences, Geosciences, and Biosciences Division. The purpose of the meeting is to foster collaboration, cooperation, and the exchange of new concepts and ideas between these researchers. The resultant synergy is a major strength of this program and promulgates the standard of excellence in research required to sustain this program over the years. With this fiscal year comes the arrival of a research Hub for Solar Fuels to the Office of Basic Energy Sciences, which will provide a renewed and expanded center for research in solar photoconversion.

The Solar Photochemistry Research Meeting will have a number of guests this year from related programs in Basic Energy Sciences, including Energy Frontier Research Centers and the Solar Energy Research Center at Lawrence Berkeley National Laboratory. They will make presentations based on their approaches to research in solar photoconversion. Our guest lecturer for this conference will be Professor Laurence Peter from the University of Bath who will draw on his long research experience in semiconductors and semiconductor electrochemistry to present a lecture on new semiconductors for use in solar photoconversion. In the conference sessions that follow there will be presentations on semiconductor photoelectrochemistry, homogeneous and heterogeneous splitting of water, photochemistry of organic molecular systems and photoconversion at nanostructures.

I would like to express my appreciation to Diane Marceau of the Division of Chemical Sciences, Geosciences, and Biosciences, and Loretta Friend and Connie Lansdon of the Oak Ridge Institute for Science and Education for their assistance with the preparation of this volume and the coordination of the logistics of this meeting. I must also thank all of the researchers whose dedication to scientific inquiry and enduring interest in research on solar energy transduction have enabled these advances in solar photoconversion and made this meeting possible.

Mark T. Spitler
Chemical Sciences, Geosciences,
and Biosciences Division
Office of Basic Energy Sciences

Solar Photochemistry Research Conference Overview

Time	Sunday, June 6	Monday, June 7	Tuesday, June 8	Wednesday, June 9	
7:30		Continental Breakfast	Continental Breakfast	Continental Breakfast	7:30
8:00					8:00
8:30		Opening Remarks 8:20	Session V	Session VIII	8:30
8:45		Session I <i>Opening Speaker</i>			8:45
9:00					9:00
9:30					9:30
9:45		Break			9:45
10:00			Break	Break	10:00
10:15					10:15
10:30		Session II	Session VI	Session IX	10:30
11:00					11:00
11:30					11:30
11:50					11:50
12:00		Lunch	Lunch	Lunch	12:00
12:15					12:15
12:45			Lunch		12:45
1:00		Session III	Free Afternoon	Session X	1:15
1:30					1:30
2:00					2:00
2:30					2:30
2:45				Closing Remarks	2:45
3:00	Registration (3:00 - 6:00 P.M.)	Free Time	Free Afternoon		3:00
3:30					3:30
4:00					4:00
4:30					4:30
5:00	No-Host Reception	Session IV	Session VII		5:00
5:30					5:30
6:00					6:00
6:30	Dinner	Dinner	Social Hour Dinner		6:30
7:00					7:00
7:30					7:30
8:00	Reception (cont.)	Posters (odd numbers) Refreshments	Posters (even numbers) Refreshments		8:00
8:30					8:30
9:00					9:00
9:30					9:30

Table of Contents

TABLE OF CONTENTS

Foreword	iii
Overview	iv
Program	xix

Abstracts of Oral Presentations

Session I – Opening Session

Applications of Microwave Reflectance Measurements in Photoelectrochemistry Laurence Peter , University of Bath, United Kingdom	3
---	---

Session II – Photoelectrochemistry I

Sunlight-Driven Hydrogen Formation by Membrane-Supported Photoelectrochemical Water Splitting Nathan S. Lewis , California Institute of Technology	7
---	---

Electrochemical Synthesis of Polycrystalline Photoelectrodes with Controlled Compositions and Architectures Kyoung-Shin Choi , Purdue University	11
---	----

Fundamental Studies of Light-Induced Charge Transfer, Energy Transfer, and Energy Conversion with Supramolecular Systems Joseph T. Hupp , Northwestern University.....	14
---	----

Session III – Photoelectrochemistry II

Mass Transport of Cobalt Mediator in DSSCs and Magnetic Field Effects on Charge-Separated-State Recombination in Copper C-A Dyads Jeremy J. Nelson, Tyson J. Amick, Megan Lazorski, Lance Ashbrook and C. Michael Elliott , Colorado State University.....	21
--	----

Model Dyes for Study of Molecule/Metal Oxide Interfaces and Electron Transfer Processes Elena Galoppini , Rutgers University	24
---	----

Session IV – Computational Approaches to Heterogeneous Solar Photoconversion

- Time-Domain Ab Initio Studies of Nanoscale Structures
for Solar Energy Harvesting and Storage
Oleg Prezhdo, University of Washington..... 31
- Theoretical Studies of Photoactive Molecular Systems: Electron Transfer,
Energy Transport, and Optical Spectroscopy
Richard A. Friesner, Columbia University..... 36

Session V – Charge Transfer in Organic Systems

- Charge Transport in Smart DNA Hairpins and Dumbbells
Frederick D. Lewis, Northwestern University 41
- Structural and Electronic Criteria for Long Distance Charge and Energy Transport
Amy M. Scott, Annie Butler Ricks, Tomoaki Miura, Michael T. Colvin, Raanan
Carmieli, and **Michael R. Wasielewski**, Northwestern University 44
- Tetrapyrrolic Architectures for Fundamental Studies of Light Harvesting and Energy
Transduction
David F. Bocian, University of California Riverside, **Dewey Holten**, Washington
University and **Jonathan S. Lindsey**, North Carolina State University 50

Session VI – Charge Transport in Organic Systems

- "Molecular Wires" for Electrons, Holes and Excitons
John R. Miller, Andrew Cook, Paiboon Sreearunothai, Sadayuki Asaoka,
Norihiro Takeda, Sean McIlroy, Brookhaven National Laboratory,
Julia M. Keller and Kirk Schanze, University of Florida,
Yuki Shibano and H. Imahori, Kyoto University 57
- Measurement of the Distance Scale for Nanoscale Electronic Energy Funneling
by Sub-diffraction Single Molecule Spectroscopy
Joshua C. Bolinger, Matt C. Traub, Takuji Adachi, and **Paul F. Barbara**
University of Texas at Austin 60
- Conjugated Polymers and Polyelectrolytes in Solar Photoconversion
Seoung Ho Lee, Sevnur Kömürlü, Feng Fude, Dan Patel, Jarrett Vella,
Quentin Bricaud, **Valeria D. Kleiman**, **John R. Reynolds**
and **Kirk S. Schanze**, University of Florida..... 63

Session VII – Investigation of Solar Photoconversion with Multidimensional Spectroscopy

- Towards Control of Photochemical Transformations Using Pulse Shaping:
Exploiting Vibrations to Enhance Product Yield in Tetracene Singlet Fission
and in Ligand Dissociation Reactions in Charge-Transfer Excited Metal Complexes
Niels H. Damrauer, Erik M. Grumstrup,
and Paul Vallett, University of Colorado at Boulder 69
- How Hard Is It to Produce 100% Efficient Energy Transfer
in Photosynthetic Light Harvesting?
Graham R. Fleming, Lawrence Berkeley National Laboratory 71

Session VIII – Inorganic Homogeneous Photocatalysis

- Intermediates in Water Oxidation Catalysis through Pulse Radiolysis
Sergei V. Lymar, Brookhaven National Laboratory 79
- Reactions of Hydride Complexes
Carol Creutz, Brookhaven National Laboratory 81
- Photoinitiated Electron Collection in Mixed-Metal Supramolecular
Complexes: Development of Photocatalysts for Hydrogen Production
Shamindri Arachchige, Travis White, Baburam Sedai, Ryan Shaw,
and **Karen J. Brewer**, Virginia Polytechnic Institute 84

Session IX – Novel Chromophores and Environments

- Light Induced Redox Reactions of Photoactive Transition Metal Complexes
Jing Gu, Kristi Lebkowsky, Amelia Neuberger, Jeff Draggich
and **Russell Schmehl**, Tulane University 91
- Solvation and Reaction in Ionic Liquids
Mark Maroncelli, Sergei Arzhantsev, Hui Jin, Xiang Li, Min Liang,
and Durba Roy, Pennsylvania State University 94
- Efficient H₂ Production via Novel Molecular Chromophores and Nanostructures
Arthur J. Nozik, **Arthur J. Frank**, Justin C. Johnson, Nathan R. Neale,
and Soon Hyung Kang, National Renewable Energy Laboratory 98

Session X – Photoconversion with Nanostructures

- Manipulation of Charge Transfer Processes in Semiconductor Quantum Dot Based
Nanoarchitectures
Kevin Tvrdy, Benjamin Meekins, Ian Lightcap, Jin Ho Bang
and **Prashant V. Kamat**, Notre Dame Radiation Laboratory 103

The Role of Surface States in the Exciton Dynamics in CdSe Core and Core/Shell Nanorods Zhong-Jie Jiang, Hoda Mirafzal and David F. Kelley , University of California at Merced.....	108
Graphenes: Basal Plane Photochemistry and Charge Transfer Doping Naeyoung Jung, Haitao Liu, Sunmin Ryu and Louis Brus , Columbia University	111

Poster Abstracts

1. “Electrochemically Wired” Semiconductor Nanoparticles: Toward Vectoral Electron Transport in Hybrid Materials
Neal R. Armstrong, S. Scott Saavedra, Jeffry Pyun 117
2. New Materials and Insights in Molecular Photovoltaic Devices
Mark Thompson, Dolores Perez, Patrick Erwin, Cody Schlenker, EFRC on “Emerging Materials for Solar Energy Conversion and Solid State Lighting” 118
3. Charge Transfer and Core-Valence Excited States for Molecular Systems
Tunna Baruah, Marco Olguin, and R. R. Zope 119
4. Charge Transfer and Energy Transfer in Single-Walled Carbon Nanotube-Semiconducting Polymer Hybrids
Jeff Blackburn, Josh Holt, Andrew Ferguson, Nikos Kopidakis, Kevin Mistry, Matt Beard, Garry Rumbles 120
5. Catalytic Conversion of Carbon Dioxide to Methanol and Higher Order Alcohols at an Illuminated p-Type Semiconductor Interface
A. B. Bocarsly, K. Keets, A. J. Morris, and E. L. Zeitler 121
6. Diode Linkers for the Covalent Attachment of Mn Catalysts to TiO₂ Surfaces
Julio L. Palma, William R. McNamara, Laura J. Allen, Rebecca L. Milot, Karin Brumback, Gary W. Brudvig, Charles A. Schmuttenmaer, Robert H. Crabtree and Victor S. Batista..... 122
7. Modular Nanoscale and Biomimetic Assemblies for Photocatalytic Hydrogen Generation
Kara L. Bren, Richard Eisenberg, Patrick L. Holland, Todd D. Krauss..... 123
8. Development of High Potential Photoanodes for Light Induced Water Oxidation
Gary F. Moore, Hee-eun Song, Rebecca L. Milot, James D. Blakemore, Victor S. Batista, Charles A. Schmuttenmaer, Robert H. Crabtree and Gary W. Brudvig..... 124
9. Electron-Transfer From and In Ionic Liquids
Cherry S. Santos, Madhuri Manpadi, Alex J. Baranowski, Lawrence J. Williams and Edward W. Castner, Jr. 125
10. Hydroxamate Anchors for Water-Stable Attachment to TiO₂
William R. McNamara, Robert C. Snoeberger III, Gonghu Li, Christiaan Richter, Laura J. Allen, Rebecca L. Milot, Charles A. Schmuttenmaer, Robert H. Crabtree, Gary W. Brudvig and Victor S. Batista 126

11.	Dynamic Energy Fluctuations in 3d Molecular Orbitals of Metalloporphyrins and Their Implications in the Ground and Excited State Axial Ligation Revealed by Transient X-ray Absorption Spectroscopy <u>Lin X. Chen</u> , Xiaoyi Zhang, Erik C. Wasinger, Jenny V. Lockard, Andrew B. Stickrath, Michael W. Mara, Klaus Attenkofer, and Guy Jennings, Grigory Smolentsev, Alexander Soldatov	127
12.	Water-Stable, Hydroxamate Anchors for Functionalization of TiO ₂ Surfaces with Ultrafast Interfacial Electron Transfer William R. McNamara, Rebecca L. Milot, Hee-eun Song, Robert C. Snoeberger III, Victor S. Batista, <u>Charles A. Schmuttenmaer</u> , Gary W. Brudvig and Robert H. Crabtree	128
13.	The Crystalline Nanocluster Ti-O Phase: Synthesis of New Clusters and Their Functionalization <u>Philip Coppens</u> and Jason B. Benedict	129
14.	Multi-metallic Complexes for Photoinduced Reactions: Computational Efforts Marco Allard, Brian T. Psciuk, Cláudio N. Verani, John F. Endicott, <u>H. Bernhard Schlegel</u>	130
15.	Photoinduced Reactions of Multi-metallic Complexes: Spectroscopic Probes of Charge-Transfer Excited State Reactivity Marco M. Allard, Onduro S. Odongo, H. Bernhard Schlegel, Cláudio N. Verani and <u>John F. Endicott</u>	131
16.	Nanoscaled Components for Improved Efficiency in a Multipanel Photocatalytic Water-Splitting System <u>Marye Anne Fox</u> and <u>James K Whitesell</u>	132
17.	Multimetallic Complexes for Photoinduced Reactions: Synthetic and Surface-Based Efforts Rajendra Shakya, Frank D. Lesh, Rama Shanmugan, Debashis Basu, Marco M. Allard, H. Bernhard Schlegel, John F. Endicott, <u>Cláudio N. Verani</u>	133
18.	All Inorganic Binuclear Charge Transfer Chromophores: Structure, Electron Transfer Kinetics, and Redox Properties Tanja Cuk, Walter Weare, Marisa MacNaughtan, and <u>Heinz Frei</u>	134
19.	Photochemical Formation of Hydride Donors and Their Reactivities <u>Etsuko Fujita</u> , Diane Cabelli, Brian Cohen, Takashi Fukushima, James T. Muckerman, Dmitry E. Polyansky, Koji Tanaka, Randolph Thummel, and Ruifa Zong.....	135
20.	Charge Injection Behavior of Dye:ZnO Nanocrystal Dyads as a Function of Excited State Potential of the Ruthenium-Based Dye Ryan Hue, Julia Saunders, Adam Huss, Raghu Chitta, Kent Mann, David Blank and <u>Wayne L. Gladfelter</u>	136

21.	Electron Transfer Parameters from Spectroscopy Naoki Ito, Tamal Mukherjee and <u>Ian R. Gould</u>	137
22.	Charged Defects in Excitonic Semiconductors: Their Number, Chemistry and Influence <u>Brian A. Gregg</u> , Ziqi Liang, Michael Woodhouse, Russel A. Cormier.....	138
23.	Biphasic Ionic Liquid-Supercritical CO ₂ Systems for the Photocatalytic Reduction of CO ₂ <u>David C. Grills</u>	139
24.	Porphyrim-Fullerene Polymers for Solar Energy Conversion <u>Devens Gust</u> , Thomas A. Moore, Ana L. Moore, Paul A. Liddell, Gerdenis Kodis, Bradley Brennan and James Bridgewater	140
25.	Anion and Cation Doping of TiO ₂ for Visible Light Photoactivity T. Ohsawa, <u>M. A. Henderson</u> , V. Shutthanandan, A. N. Mangham, and S. A. Chambers	141
26.	Highly Reducing Porphyrim/Metal-Alkylidyne Dyads Benjamin M. Lovaasen, Daniel C. O’Hanlon, Davis Moravec, and <u>Michael D. Hopkins</u>	142
27.	Ultrafast Transient Absorption Microscopy Studies of Carrier Dynamics in Epitaxial Graphene <u>Libai Huang</u> , Gregory V. Hartland, Li-Qiang Chu, Luxmi, Randall M. Feenstra, Chuanxin Lian, Kristof Tahy, Huili Xing	143
28.	Uncommon Approaches to Investigating Water Oxidation Catalysis Jamie Stull, Sergei V. Lyamar, Aurora Clark, <u>James K. Hurst</u>	144
29.	Directed Charge and Energy Transfer in Semiconductor Nanocrystals and Heterostructures E. Ryan Smith, Barbara Hughes, <u>Matt Beard</u> , Arthur Nozik, and Justin Johnson	145
30.	Band Filling Dynamics in Lead Sulfide Quantum Dots Byungmoon Cho, William K. Peters, Trevor L. Courtney, Robert J. Hill, and <u>David M. Jonas</u>	146
31.	The Carotenoid Astaxanthin and its Photooxidative Role under High Light and Salt Stress <u>Lowell D. Kispert</u> , A. Ligia Focsan, Nikolay E. Polyakov, Ans Péter Molnár	147

32.	Photodriven Water Oxidation by New Carbon-Free Molecular Catalysts Qiushi Yin, Yurii V. Geletii, Guibo Zhu, Claire Besson, Yu Hou, Zhuangqun Huang, <u>Tianquan Lian</u> , <u>Djamaladdin G. Musaev</u> and <u>Craig L. Hill</u>	148
33.	Single-Walled Carbon Nanotube Photophysics Xiaoyong Wang, Andrea J. Lee, Lisa J. Carlson, Julie A. Smyder, and <u>Todd D. Krauss</u>	149
34.	Interfacial Charge Separation and Recombination Dynamics in Nanoparticle-Sensitizer-Water Oxidation Catalyst Triads Zhuangqun Huang, Qiushi Yin, Zhen Luo, Jie Song, Yurii V. Geletii, Karl S. Hagen, <u>Djamaladdin G. Musaev</u> , <u>Craig L. Hill</u> , and <u>Tianquan Lian</u>	150
35.	Photochemical Doping of Conjugated Ionomer Interfaces Stephen Robinson, Fuding Lin, Ethan Walker, and <u>Mark Lonergan</u>	151
36.	Computational and Experimental Insights into Photoinduced Oxidation of $[\text{Ru}(\text{mptpy})_2]^{4+}$ and $[\text{Ru}(\text{bpy})_3]^{2+}$ Photosensitizers Alexey Kaledin, Yurii V. Geletii, Zhuangqun Huang, <u>Tianquan Lian</u> , <u>Craig L. Hill</u> , and <u>Djamaladdin G. Musaev</u>	152
37.	Heterometallic Solids for Solar Photoconversion <u>Paul A. Maggard</u>	153
38.	Nanostructured Photocatalytic Water Splitting Systems Seung-Hyun Anna Lee, Landy K. Bladell, John Swierk, Nina I. Kovtyukhova, W. Justin Youngblood, Kazuhiko Maeda, Megan A. Kolarz, Lucas Jellison, and <u>Thomas E. Mallouk</u>	154
39.	New Cyclometallated Iridium Dyes with Nitro Bipyridine Acceptors and Oligothiophene Secondary Electron Donors Kyle R. Schwartz, Raghu Chitta, Jon N. Bohnsack, Darrren J. Cecknowicz, <u>David A. Blank</u> , <u>Wayne L. Gladfelter</u> and <u>Kent R. Mann</u>	155
40.	Excess Electron Spectrum and Heterogeneity in Room Temperature Ionic Liquids Mario del Popolo, Jorge Kohanoff, David Coker, H. V. R. Annapureddy, <u>Claudio J. Margulis</u>	156
41.	Dynamical Arrest and Non-Gaussian Energy Gap Fluctuations in Natural and Artificial Photosynthesis <u>Dmitry V. Matyushov</u>	157
42.	First-Row Transition Metal Complexes as Chromophores for Solar Energy Conversion Allison Brown, Lindsey Jamula, and <u>James K. McCusker</u>	158

43.	Electron Transfer Dynamics in Efficient Molecular Solar Cells Shane Ardo, John Rowley, and <u>Gerald J. Meyer</u>	159
44.	Metal-to-Ligand Charge Transfer Excited States on Surfaces and in Rigid Media: Application to Energy Conversion <u>Thomas J. Meyer</u> , John M. Papanikolas.....	160
45.	Photocatalytic Water Oxidation at the GaN (10 $\bar{1}$ 0) – Water Interface <u>J. T. Muckerman</u> , Y. A. Small, X. Shen, M. S. Hybertsen, <u>J. Wang</u> , P. B. Allen, M. V. Fernandez-Serra, E. Fujita.....	161
46.	Tuning the Photophysical Properties of Group IV Nanocrystals <u>Nathan R. Neale</u> and Daniel A. Ruddy.....	162
47.	First Principles Studies of Optical Absorption and Charge Separation at Donor-Acceptor Interfaces in Organic Nanostructures P. Doak, P. Darancet, S. Sharifzadeh, E. Isaacs, and <u>J. B. Neaton</u>	163
48.	Rapid Synthesis/Screening and Nano-Structuring of Oxide Semiconductor Photocatalysts Allen J. Bard and <u>C. Buddie Mullins</u>	164
49.	D/A Couplings in Binuclear Metal Complexes and the Role of Competing Ligands <u>Marshall D. Newton</u>	165
50.	Multiple Exciton Collection in a Sensitized Photovoltaic System Results in Quantum Yields Greater than One Justin B. Sambur, Thomas Novet and <u>B. A. Parkinson</u>	166
51.	Surface Femtochemistry of Alkali Atom Photodesorption from Noble Metal Surfaces <u>Hrvoje Petek</u>	167
54.	Femtosecond Emission Microscopy of Exciton Dynamics in Semiconductor Nanoparticles Jianhua Bao, Lars Gundlach and <u>Piotr Piotrowiak</u>	168
55.	Imaging Proton-Coupled Electron Transfer Pathways in Natural Photosynthesis <u>Oleg G. Poluektov</u> , Lisa M. Utschig, David M. Tiede and K. V. Lakshmi.....	169
56.	Advances in Re(II) Photo-oxidant Complex Chemistry <u>Dean M. Roddick</u> , Jeramie J. Adams, and Navamoney Arulsamy.....	170
57.	Microwave Absorption Studies of Charge Transfer at Planar Bulk Heterojunction Interfaces <u>Garry Rumbles</u> , Andrew Ferguson, David Coffey, Smita Dayal, and Nikos Kopidakis.....	171

58.	Characterizing Coupled Charge Transport with Multiscale Simulations <u>Jessica M. J. Swanson</u>	172
59.	Single-Chain, Helical Wrapping of Individualized, Single-Walled Carbon Nanotubes by Ionic Poly(Aryleneethynylene)s: New Compositions for Photovoltaic Systems Pravas Deria, Youn K. Kang, One-Sun Lee, Sang Hoon Kim, Tae-Hong Park, Ian Stanton, Dawn A. Bonnell, Jeffery G. Saven, and <u>Michael J. Therien</u>	173
60.	Further Observations on Water Oxidation Catalyzed by Mononuclear Ru(II) Complexes Ruifa Zong, Nattawut Kaveevivitchai, Maya El Ojaimi, and <u>Randolph P. Thummel</u>	174
61.	Mapping Structure with Function in Natural and Biomimetic Photosynthetic Architectures <u>David M. Tiede</u> , Karen L. Mulfort, Nina Ponomarenko, Lin X. Chen, Lisa M. Utschig, Oleg G. Poluektov, and Libai Huang and Gary Wiederrecht.....	175
62.	Photosynthetic Interprotein and Biohybrid Electron Transfer <u>Lisa M. Utschig</u> , Oleg G. Poluektov, Lin X. Chen, Jenny V. Lockard, Sergey D. Chemerisov, Karen Mulfort, David M. Tiede.....	176
63.	Imaging of Energy and Charge Transport in Nanoscale Systems <u>Jao van de Lagemaat</u> and Manuel Romero	177
64.	Transport and Bimolecular Electron Transfer in Ionic Liquids <u>James F. Wishart</u> and Masao Gohdo.....	178
65.	Basic Studies and Novel Approaches for Photoelectrosynthesis <u>J. A. Turner</u> , N. R. Neale, H. Branz, A. J. Frank, M. Beard, S. H. Wei, <u>A. J. Nozik</u> National Renewable Energy Laboratory.....	179
66.	Ultra-stable Molecule-Surface Architectures at Metal Oxides Michelle Cooperrider, Ryan Franking, Kacie Louis, Michael McCoy, and <u>Robert J. Hamers</u> , University of Wisconsin-Madison	180
67.	Metal-Linked Artificial Oligopeptides as Scaffolds toward Photoinitiated Molecular Wires Carl P. Myers, Joy A. Gallagher, Seth Ostheimer and <u>Mary Elizabeth Williams</u>	181
	LIST OF PARTICIPANTS	183
	AUTHOR INDEX	195

Program

**32nd DOE SOLAR PHOTOCHEMISTRY
RESEARCH MEETING**

June 6–9, 2010

**Westin Annapolis Hotel
Annapolis, Maryland**

PROGRAM

Sunday, June 6

3:00 – 6:00 p.m. Registration
5:30 – 9:30 p.m. Reception
6:30 – 8:00 p.m. Dinner

Monday Morning, June 7

SESSION I

Opening Session

Mark T. Spitler, Chair

7:30 a.m. Continental Breakfast

8:20 a.m. Opening Remarks
 Eric Rohlfiing and **Mark Spitler**, Department of Energy

8:45 a.m. **Opening Lecture.**
 Applications of Microwave Reflectance Measurements in Photoelectrochemistry
 Laurence Peter, University of Bath, United Kingdom

9:45 a.m. Coffee Break

SESSION II

Photoelectrochemistry I

John Turner, Chair

10:15 a.m. Sunlight-Driven Hydrogen Formation by Membrane-Supported
 Photoelectrochemical Water Splitting
 Nathan S. Lewis, California Institute of Technology

10:45 a.m. Electrochemical Synthesis of Polycrystalline Photoelectrodes
 with Controlled Compositions and Architectures
 Kyoung-Shin Choi, Purdue University

11:15 a.m. Fundamental Studies of Light-Induced Charge Transfer, Energy Transfer, and Energy Conversion with Supramolecular Systems
Joseph T. Hupp, Northwestern University

12:00 p.m. Lunch

Monday Afternoon, June 7

SESSION III
Photoelectrochemistry II
Gerald Meyer, Chair

1:00 p.m. Mass Transport of Cobalt Mediator in DSSCs and Magnetic Field Effects on Charge-Separated-State Recombination in Copper C-A Dyads
C. Michael Elliott, Colorado State University

1:30 p.m. Model Dyes for Study of Molecule/Metal Oxide Interfaces and Electron Transfer Processes
Elena Galoppini, Rutgers University

SESSION IV
Computational Approaches to Heterogeneous Solar Photoconversion
Marshall Newton, Chair

5:00 p.m. Time-Domain Ab Initio Studies of Nanoscale Structures for Solar Energy Harvesting and Storage
Oleg Prezhdo, University of Washington

5:30 p.m. Theoretical Studies of Photoactive Molecular Systems: Electron Transfer, Energy Transport, and Optical Spectroscopy
Richard A. Friesner, Columbia University

6:30 p.m. Dinner

7:30 p.m. Posters (Odd numbers)
Refreshments

Tuesday Morning, June 8

7:30 a.m. Continental Breakfast

SESSION V
Charge Transfer in Organic Systems
Ian Gould, Chair

- 8:30 a.m. Charge Transport in Smart DNA Hairpins and Dumbbells
Frederick D. Lewis, Northwestern University
- 9:00 a.m. Structural and Electronic Criteria for Long Distance Charge and Energy Transport
Michael R. Wasielewski, Northwestern University
- 9:30 a.m. Tetrapyrrolic Architectures for Fundamental Studies of Light Harvesting and Energy Transduction
David F. Bocian, University of California Riverside, **Dewey Holten**, Washington University and **Jonathan S. Lindsey**, North Carolina State University
- 10:15 a.m. Coffee Break

SESSION VI
Charge Transport in Organic Systems
Ana Moore, Chair

- 10:30 a.m. "Molecular Wires" for Electrons, Holes and Excitons
John R. Miller, Brookhaven National Laboratory
- 11:00 a.m. Measurement of the Distance Scale for Nanoscale Electronic Energy Funneling by Sub-diffraction Single Molecule Spectroscopy
Paul F. Barbara, University of Texas at Austin
- 11:30 a.m. Conjugated Polymers and Polyelectrolytes in Solar Photoconversion
Valeria D. Kleiman, **John R. Reynolds** and **Kirk S. Schanze**, University of Florida

Tuesday Afternoon, June 8

- 12:20 p.m. Lunch

Tuesday Evening, June 8

SESSION VII
Investigation of Solar Photoconversion with Multidimensional Spectroscopy
David Jonas, Chair

- 5:30 p.m. Towards Control of Photochemical Transformations Using Pulse Shaping: Exploiting Vibrations to Enhance Product Yield in Tetracene Singlet Fission and in Ligand Dissociation Reactions in Charge-Transfer Excited Metal Complexes
Niels H. Damrauer, University of Colorado at Boulder

- 6:00 p.m. How Hard Is It to Produce 100% Efficient Energy Transfer
in Photosynthetic Light Harvesting?
Graham R. Fleming, Lawrence Berkeley National Laboratory
- 6:30 p.m. Social Hour
- 7:30 p.m. Dinner
- 8:30 p.m. Posters (Even numbers)
Refreshments

Wednesday Morning, June 9

- 7:30 a.m. Continental Breakfast

Session VIII
Inorganic Homogeneous Photocatalysis
Etsuko Fujita, Chair

- 8:30 a.m. Intermediates in Water Oxidation Catalysis through Pulse Radiolysis
Sergei V. Lymar, Brookhaven National Laboratory
- 9:00 a.m. Reactions of Hydride Complexes
Carol Creutz, Brookhaven National Laboratory
- 9:30 a.m. Photoinitiated Electron Collection in Mixed-Metal Supramolecular
Complexes: Development of Photocatalysts for Hydrogen Production
Karen J. Brewer, Virginia Polytechnic Institute
- 10:00 a.m. Coffee Break

Session IX
Novel Chromophores and Environments
Thomas Mallouk, Chair

- 10:30 a.m. Light Induced Redox Reactions of Photoactive Transition Metal Complexes
Russell Schmehl, Tulane University
- 11:00 a.m. Solvation and Reaction in Ionic Liquids
Mark Maroncelli, Pennsylvania State University
- 11:30 a.m. Efficient H₂ Production via Novel Molecular Chromophores and Nanostructures
Arthur J. Nozik, Arthur J. Frank,
National Renewable Energy Laboratory

Wednesday Afternoon, June 9

12:15 p.m. Lunch

Session X
Photoconversion with Nanostructures
Garry Rumbles, Chair

1:15 p.m. Manipulation of Charge Transfer Processes in Semiconductor Quantum Dot Based Nanoarchitectures
Prashant V. Kamat, Notre Dame Radiation Laboratory

1:45 p.m. The Role of Surface States in the Exciton Dynamics in CdSe Core and Core/Shell Nanorods
David F. Kelley, University of California at Merced

2:15 p.m. Graphenes: Basal Plane Photochemistry and Charge Transfer Doping
Louis Brus, Columbia University

2:45 p.m. Closing Remarks
Mark Spitler and **Richard Greene**, U.S. Department of Energy

Session I

Opening Session

Applications of Microwave Reflectance Measurements in Photoelectrochemistry

Laurie Peter

Department of Chemistry, University of Bath, Bath BA2 7AY, United Kingdom

The kinetics and mechanisms of electrode processes at metal electrodes have been studied extensively. More recently, outer sphere electron-transfer reactions at semiconductor electrodes in the dark have been investigated and interpreted within the context of Marcus theory, but remarkably few studies have focussed on electron transfer kinetics at illuminated semiconductor electrodes. As applied to metal electrodes, conventional electrochemical methods such as cyclic voltammetry, potential step and impedance spectroscopy rely on using changes in electrode potential to perturb the activation energy of electrochemical reactions. These methods are usually not suitable for photoelectrochemical reactions at semiconductor electrodes, where the current is determined by the flux of minority carriers across the interface. In the absence of recombination, the current is determined by the light intensity and does not depend on the heterogeneous rate constant for electron transfer, which is expected to be independent of electrode potential since most of the potential drop appears across the semiconductor space charge region and not the Helmholtz layer (i.e. the activation energy is effectively constant).

However, this does not mean that the rate constants for electron transfer are inaccessible to measurement. In the photocurrent onset region, electron transfer to the redox system competes with electron-hole recombination via surface states. The existence of this potential dependent competition allows deconvolution of the rate constants for electron transfer and surface recombination by using time or frequency resolved photocurrent techniques. Examples of this experimental approach include intensity modulated photocurrent spectroscopy (IMPS) and photoelectrochemical impedance spectroscopy (PEIS). However, neither of these methods provides kinetic information in the photocurrent saturation region, where recombination is absent. The basic problem is that current measurements are not able to distinguish between the current due to transport of electrons or holes to the surface (instantaneous displacement current) from interfacial electron transfer. What is required here is a method that can detect minority carriers "queuing up" at the interface waiting to cross to the redox species in solution. Microwave reflectivity measurements are ideal for this purpose since they detect the local change in conductivity arising from light-induced changes in carrier concentration.

The light induced microwave reflectivity change is related to the perturbation of electron and hole concentrations

$$\Delta R_M = \frac{\Delta P_r}{P_{in}} = S \langle \Delta \sigma \rangle = \frac{S}{d} \int_0^d \Delta \sigma(x) dx = \frac{Sq}{d} \int_0^d [\mu_n \Delta n(x) + \mu_p \Delta p(x)] dx \quad (1)$$

where S is a sensitivity factor, $\Delta \sigma(x)$ is the position dependent conductivity change and μ_n and μ_p are the electron and hole mobilities. It follows from equation 1 that the microwave conductivity change can be calculated by solving the continuity equation for electrons and holes with suitable boundary conditions (diffusion-controlled recombination at the rear contact and a given rate constant for electron/hole transfer at the electrolyte interface). The magnitude of the light-

induced microwave reflectivity change is sensitive to the kinetics of electron transfer because slow electron transfer leads to a build up of minority carriers at the interface, whereas conversely rapid electron transfer prevents substantial build up. This should mean that microwave methods are particularly useful for systems in which electron transfer is slow. This is likely to be the case for multi-electron transfer involving steps with high activation energy. Obvious examples are hydrogen evolution (formation of H⁻ intermediate) and oxygen evolution (4 electron process). Figure 1 illustrates the light induced conductivity change and corresponding microwave reflectivity response calculated as a function of the rate constant for interfacial electron transfer. Figure 2 illustrates the time-dependence of the microwave response, showing the build up and decay that can also be used to obtain the rate constants for charge transfer

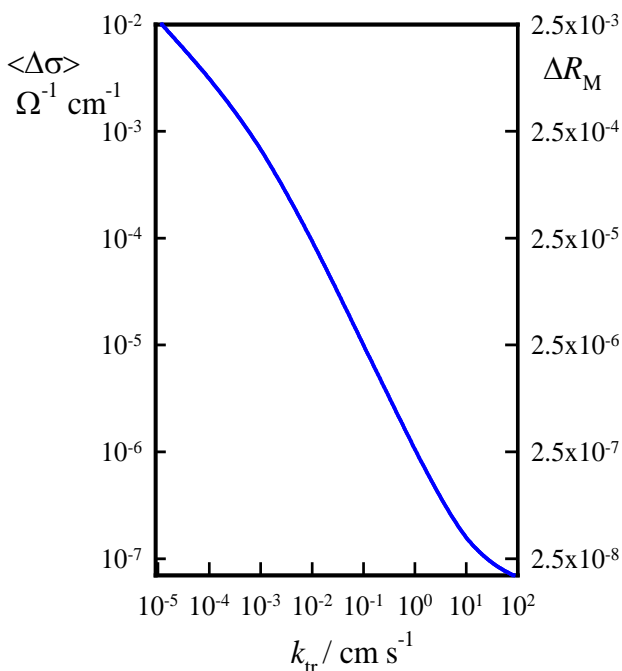


Figure 1. Dependence of the mean light-induced conductivity change on the rate constant. Calculated for low-doped silicon in the photocurrent saturation regime.

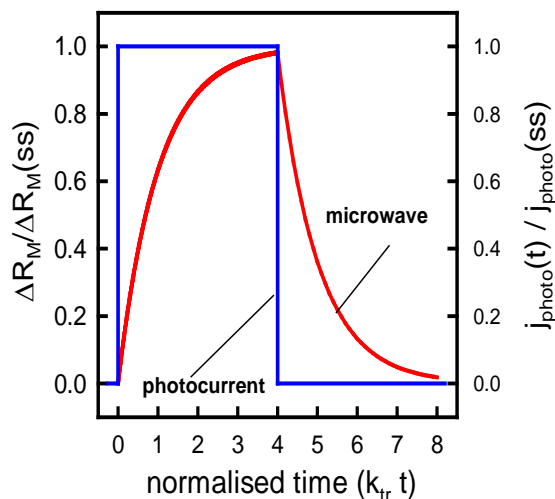


Figure 2. Normalised microwave response showing expected exponential behaviour. Note that the corresponding photocurrent transient contains no useful information.

The application of this technique to study reaction at silicon photoelectrodes will be described and possibilities for application in other systems explored.

References

1. M.J. Cass *et al.* J. Phys Chem. B. **107**, 5857 (2003).
2. M.J. Cass *et al.* J. Phys Chem. **107**, 5864 (2003).
3. L.M. Peter and S. Ushiroda, J. Phys. Chem. B **108**, 2660 (2004).

Session II

Photoelectrochemistry I

Sunlight-driven Hydrogen Formation by Membrane-Supported Photoelectrochemical Water Splitting

Nathan S. Lewis

Division of Chemistry and Chemical Engineering
California Institute of Technology
210 Noyes Laboratory, 127-72, Pasadena, CA 91125

In the past year we made significant progress on each aspect of our solar-driven water splitting scheme proposed under DOE grant number **DE-FG02-05ER15754**. We have demonstrated a high level of control over the material and light absorption properties of our p-Si microwire array photocathodes. We have developed techniques to deposit metal nanoparticles on the wire arrays, and investigated their stability and performance as catalysts for the hydrogen evolution reaction (HER). Toward developing a photoanode, we have modified the bandgap of tungsten oxide (WO_3) with N_2 doping and developed a porous film morphology that improves photoresponse.

Material and light absorption properties of Si microwire arrays

Our p-silicon wire arrays have been shown to have good electronic properties, but their efficiency is limited by their ability to absorb all of the incident light.²⁵ Experimentally and computationally, we demonstrated enhanced absorption with anti-reflective coatings and scattering nanoparticles intercalated within the Si wire array (Figure 1a).

The inexpensive nature of this water splitting membrane relies on controllably removing the microwire arrays from their original substrate. We embedded p-type Si wire arrays in a thin layer of polydimethylsiloxane (PDMS) and removed them from the growth substrate. Following formation of electrical contacts by evaporating a thin layer of Au, we characterized the photoelectrochemical performance of “peeled” wire arrays was characterized using methyl viologen ($\text{MV}^{2+/+}$) as a redox couple. Peeled wire arrays (Figure 1b) demonstrate open circuit voltages of 400mV (under 60 mW cm^{-2} 808nm illumination) and efficiencies comparable to substrate-attached wires (Figure 1c). This verifies the PDMS peeling technique for array transfer and reuse of the growth substrate.²⁷

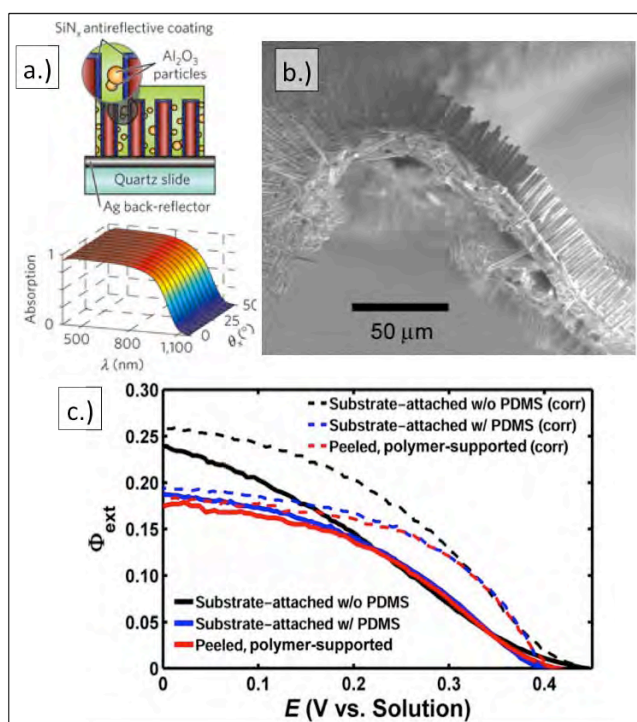


Figure 1. Material properties of p-Si wire arrays a.) absorption of wires with a back reflector, antireflective coating, and scatterers. b.) SEM image of a peeled wire array. C.) Photoelectrochemical performance of a peeled array in $\text{MV}^{2+/+}$ compared to a substrate attached array.

We recently extended the peeling technique to polymers that serve as both structural supports and selectively permeable

membranes. Ongoing research investigates the proton conductivity of wires embedded in perfluorosulphonic acid PTFE copolymer (Nafion).

H₂ productions from wires and radial junctions

We continue to investigate the performance of p-Si wire arrays decorated with nanoparticle metal catalysts as photocathodes for H₂ evolution. Our as-grown wire arrays demonstrate relatively low voltages and current densities when used as HER photocathodes, so we have taken several approaches to improve their efficiency. We have developed techniques to control the diameter and density of wires within the array that serve to increase the filling fraction of absorbing silicon material. We have further developed a process to create n⁺ / p radial junctions within the wires. These radial junctions decouple the catalytic interface from the voltage-generating junction and have the potential to greatly increase performance and efficiency. In initial studies of this radial geometry, Si wire array cells using a Pt catalyst and the light trapping techniques discussed above demonstrate open circuit voltages over 500 mV and H₂ conversion efficiencies of 6% under 100 mW cm⁻² ELH illumination (Figure 2a).²⁸ This represents a significant gain in performance over previous wire devices. As platinum is an expensive and scarce catalyst material, we are now investigating earth-abundant HER catalysts such as Ni and NiMo. We have shown that NiMo has comparable performance to Pt as a dark catalyst, and are currently investigating its performance on p-Si photocathodes (Figure 2b).

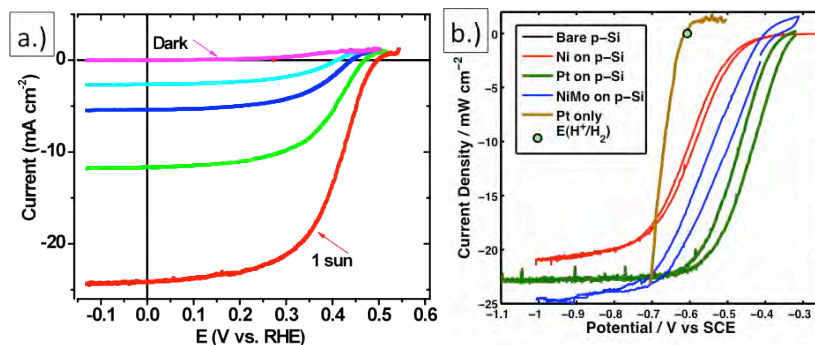


Figure 2: a.) H₂ production from n⁺ / p radial junction wires coated with Pt catalyst in a pH = 1 electrolyte; b.) comparison between Ni, Pt, and NiMo catalysts as HER catalysts on planar p-Si in pH 6.5 buffered solution under 100 mW cm⁻² illumination

Tungsten Oxide photoanodes for water oxidation

Wide bandgap metal oxides are good candidates to drive the water oxidation reaction due to their stability, non-toxicity, low cost, and catalytic activity. However, many metal oxides have excessively high bandgaps that do not capture light efficiently and their material morphology is often impractical for solar applications. We are investigating WO₃ photoanodes for the water oxidation reaction by doping the material to reduce the bandgap as well as structuring the material to enable photocarriers to efficiently reach the water oxidation interface.

Nanoporous WO₃ layers have been fabricated by potentiostatic anodization of tungsten foil in fluoride electrolytes. We have investigated the influence of voltage,

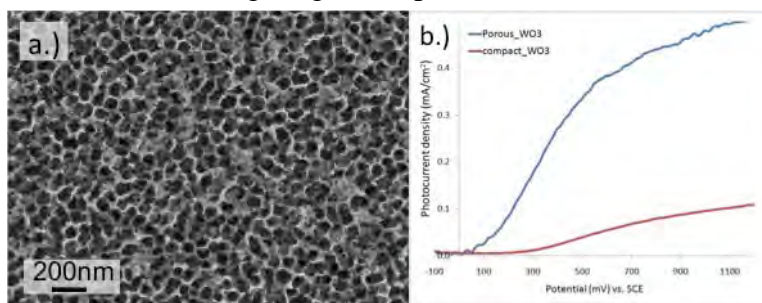


Figure 3: Porous WO₃. a.) SEM image of porous WO₃. b.) Comparison of compact and porous WO₃ photoanodes in pH 4 buffered solution under 100 mW cm⁻² illumination

reaction time, and electrolyte on the morphology of the porous layers. Preliminary results indicate that porous WO_3 electrodes are stable under aqueous conditions, and produce open circuit voltages over 800mV and significantly higher photocurrent densities and external quantum yields than compact WO_3 electrodes (Figure 3b).

We have also developed a method to reduce the bandgap of WO_3 from 2.6eV to 1.8eV by calcining ammonium para- or meta-tungstate in O_2 at 420°C. The resulting material is an orange-red clathrate compound $\text{N}_2 \cdot 24 \text{WO}_3$ is isostructural to the monoclinic crystal system and stable at ambient conditions. This material is responsive to excitation wavelengths as long as 600 nm, compared with a cutoff wavelength of 450 nm for pure WO_3 . Currently, we are working towards higher-absorbing materials and better deposition techniques to yield more efficient photon harvesting and charge-carrier collection in these photoanodes. It is encouraging that we can controllably extend absorption to longer wavelengths and increase the charge carrier collection efficiency in WO_3 , making it a promising photoanode material for water oxidation.

DOE Sponsored Publications 2007-2010

George W. Crabtree and **Nathan S. Lewis**, “Solar Energy Conversion”, *Phys. Today*, **2007**, 60(3), 37.

Nathan S. Lewis, “Toward Cost-Effective Solar Energy Use”, *Science*, **2007**, 315(5813), 798.

James R. Maiolo III, Brendan M. Kayes, Michael A. Filler, Morgan C. Putnam, Michael D. Kelzenberg, Harry A. Atwater, **Nathan S. Lewis**, “High Aspect Ratio Silicon Wire Array Photoelectrochemical Cells”, *J. Am. Chem. Soc.*, **2007**, 129(41), 12346.

Nathan S. Lewis “The World Energy Book (contributed chapter)”, **2007**.

Stephen Maldonado, Anthony G. Fitch, and **Nathan S. Lewis**, “Semiconductor/Liquid Junction Photoelectric Chemical Solar Cells”, in *Series on Photoconversion of Solar Energy Volume III - Nanostructured and Photoelectric Chemical Systems for Solar Photon Conversion*, Mary D Archer; and Arthur J Nozik; Eds., Imperial College Press: London, **2008**, 537.

Brendan M. Kayes, Michael A. Filler, Morgan C. Putnam, Michael D. Kelzenberg, **Nathan S. Lewis**, and Harry A. Atwater, “Growth of Vertically Aligned Si Wire Arrays Over Large Areas ($>1 \text{ cm}^2$) with Au and Cu Catalysts”, *Appl. Phys. Lett.*, **2007**, 91(10), 103110.

Joshua M. Spurgeon, Harry A. Atwater, and **Nathan S. Lewis**, “A Comparison Between the Behavior of Nanorod and Planar Cd(Se, Te) Photoelectrodes”, *J. Phys. Chem. C*, **2008**, 112, 6186.

Nathan S. Lewis, “Powering the Planet”, *MRS Bulletin*, **2007**, 32, 808.

James R. Maiolo III, Harry A. Atwater, and **Nathan S. Lewis**, “Macroporous Silicon as a Model for Silicon Wire Array Solar Cells”, *J. Phys. Chem., C*, **2008**, 112(15), 6194.

Brendan M. Kayes, M. A. Filler, M. D. Henry, J. R. Maiolo III, M. D. Kelzenberg, M. C. Putnam, J. M. Spurgeon, K. E. Plass, A. Scherer, **N. S. Lewis**, H. A. Atwater, “Radial pn Junction, Wire Array Solar Cells”, *Conference Record of the Thirty-third IEEE Photovoltaic Specialists Conference*, **2008**.

Michael D. Kelzenberg, D. B. Turner-Evans, Brendan M. Kayes, Michael A. Filler, Morgan C. Putnam, **Nathan S. Lewis**, Harry A. Atwater, "Single-Nanowire Si Solar Cells", *Conference Record of the Thirty-third IEEE Photovoltaic Specialists Conference*, **2008**.

Joshua M. Spurgeon, Katherine E. Plass, Brendan M. Kayes, Bruce S. Brunschwig, Harry A. Atwater, and **Nathan S. Lewis**, "Repeated Epitaxial Growth and Transfer of Arrays of Patterned, Vertically Aligned, Crystalline Si Wires from a Single Si(111) Substrate", *Appl. Phys. Lett.*, **2008**, 93, 032112.

Katherine E. Plass, Michael A. Filler, Joshua M. Spurgeon, Brendan M. Kayes, Stephen Maldonado, Bruce S. Brunschwig, Harry A. Atwater, and **Nathan S. Lewis**, "Flexible Polymer-Embedded Si Wire Arrays", *Adv. Mater.*, **2008**, 9999,

George W. Crabtree, **Nathan S. Lewis**, David Hafemeister, B. Levi, M. Levine, and P. Schwartz, "Solar Energy Conversion" *AIP Conf. Proc. (Physics of Sustainable Energy)*, **2008**, 1044, 309-321.

Nathan S. Lewis, "Powering the Planet: Where in the World Will Our Energy Come From?", *Energeia*, **2008**, 19(4), 1.

Nathan S. Lewis, "Powering the Planet", *Eng. Science*, **2007**, LXX(2), 12.

George W. Crabtree and **Nathan S. Lewis**, "Solar Energy Conversion", *Phys. Today*, **2007**, 60(3), 37.

Nathan S. Lewis, "Toward Cost-Effective Solar Energy Use", *Science*, **2007**, 315(5813), 798.

James R. Maiolo III, Brendan M. Kayes, Michael A. Filler, Morgan C. Putnam, Michael D. Kelzenberg, Harry A. Atwater, **Nathan S. Lewis**, "High Aspect Ratio Silicon Wire Array Photoelectrochemical Cells", *J. Am. Chem. Soc.*, **2007**, 129(41), 12346.

Nathan S. Lewis "The World Energy Book (contributed chapter)", **2007**.

Nathan S. Lewis, "A Perspective on Forward Research and Development Paths for Cost-Effective Solar Energy Utilization", *ChemSusChem*, **2009**, 2(5), 383.

Shannon W. Boettcher, Joshua M. Spurgeon, Morgan C. Putnam, Emily L. Warren, Daniel B. Turner-Evans, Michael D. Kelzenberg, James R. Maiolo, Harry A. Atwater, and **Nathan S. Lewis**, "Energy Conversion Properties of Silicon Wire-Array Photocathodes", *Science*, **2009**, 327(5962). 185.

Morgan C. Putnam, Daniel B. Turner-Evans, Michael D. Kelzenberg, Shannon W. Boettcher, **Nathan S. Lewis**, and Harry A. Atwater, "10 μm Minority-Carrier Diffusion Lengths in Si Wires Synthesized by Cu-Catalyzed Vapor-Liquid-Solid Growth", *App. Phys. Lett.*, **2009**, 95, 163116.

Joshua M. Spurgeon, Shannon W. Boettcher, Michael D. Kelzenberg, Bruce S. Brunschwig, Harry A. Atwater, and **Nathan S. Lewis**, "Flexible, polymer-supported, Si wire array photoelectrodes", *Adv. Mater.*, **2010**, *In Press*.

Electrochemical Synthesis of Polycrystalline Photoelectrodes with Controlled Compositions and Architectures

Kyoung-Shin Choi
Department of Chemistry
Purdue University
West Lafayette, IN 47907

The overall goal of our research project is to develop various electrochemical synthesis methods to produce polycrystalline photoelectrode materials with optimum compositions and architectures for use in solar hydrogen production. We use electrodeposition as the main synthesis method as it can produce a broad range of semiconductor materials while allowing for an exceptional level of morphology control. We have investigated various strategies to alter nucleation, growth and mass transport processes during electrodeposition to optimize the morphology and interfacial structure of photoelectrodes. We have also developed synthesis conditions to finely tune the compositions of the photoelectrodes (e.g. solid solutions, doping types, doping levels, surface modifications) to improve photon absorption and charge transport properties while reducing electron-hole recombination. The most significant achievements made in morphology and composition tuning during recent years are described below.

Morphology tuning One of the main goals of the morphology tuning of photoelectrodes is to enhance surface areas as well as charge transport properties. We have demonstrated a new strategy of exploiting and manipulating dendritic growth to achieve this goal using a Cu_2O system. We observed that the dendritic branching growth of Cu_2O allowed for facile substrate coverage and high surface roughness without growing a thick film, which resulted in a significantly improved photocurrent compared to electrodes composed of micron-size faceted crystals. In order to further enhance photocurrent, various methods to decrease the nucleation density and increase dendritic crystal domain size were investigated. Since the high surface area of dendritic Cu_2O electrodes is achieved by intricate branching patterns, nucleation density and crystal domain size in the electrodes do not significantly change the total surface area; however, they greatly affect the electrical continuity in the electrode and, therefore, electron-hole recombination and charge transport properties. The electrode shown in Figure 1a composed of dendritic crystals that laterally expand *ca.*

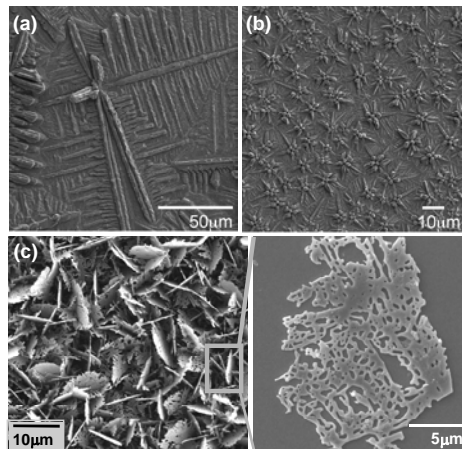


Figure 1. (a-b) SEM images of dendritic Cu_2O electrodes with two different crystal domain sizes; (c) SEM image of Cu_2O electrode composed of 2D dendritic crystals.

$12000 \mu\text{m}^2$ generated more than 20 times higher photocurrent (0.45 mA/cm^2) than the electrode containing dendritic crystals with an average lateral size of $100 \mu\text{m}^2$ (0.02 mA/cm^2 , Figure 1b). The significant increase in photocurrent achieved simply by controlling the crystal sizes in dendritic branching growth, without involving any compositional changes, implies an enormous potential for morphology tailoring in improving properties of polycrystalline electrodes. Continuing this effort, we also identified an electrochemical condition to produce Cu_2O

electrodes composed of two-dimensional (2D) dendritic crystals (Figure 1c). It is quite unusual for Cu_2O with a 3D cubic crystal structure to grow as anisotropic 2D crystals. The Cu_2O electrode composed of 2D dendritic crystals achieved much higher surface areas than Cu_2O electrodes composed of 3D crystals. In addition the thin plate morphology of 2D dendritic crystals served to minimize bulk electron-hole recombination.

Composition tuning

While we investigated various conditions to tune the compositions of photoelectrode materials during electrochemical synthesis, we also developed a simple complementary post-deposition procedure to modify the electrode compositions. One example shown in Figure 2 exploits the unique chemical stability of $\alpha\text{-Fe}_2\text{O}_3$ in a strong alkaline aqueous medium to incorporate of Al^{3+} and Sn^{4+} ions into $\alpha\text{-Fe}_2\text{O}_3$ nanoparticulate electrodes. In this method, a nanostructured Fe_2O_3 electrode was coated with solutions containing Al^{3+} and/or Sn^{4+} ions, and annealed at 500 °C. The heat treatment resulted in the formation of Al_2O_3 and SnO_2 layers on Fe_2O_3 nanoparticles followed by solid state reactions between these layers and the Fe_2O_3 , forming Fe/Al/Sn/O solid solution coatings on each Fe_2O_3 nanoparticle. Due to the high curvature and reactivity of the nanoparticle surface, solid state diffusion reactions can occur at much lower temperatures in nanoparticulate electrodes than in bulk materials. Any residual pure Al_2O_3 and SnO_2 layers that are not incorporated into the solid solution coating layers are easily removed by soaking the electrode in a strong alkaline solution. Our results show that the Fe_2O_3 electrodes treated with Al, Sn, and Al/Sn show significantly enhanced photocurrent responses with negatively shifted V_{oc} values compared to the untreated sample (Figure 2). Various photoelectrochemical characterizations suggest that the presence of the solid solution coating layer efficiently decreases the surface states and therefore electron hole recombination, improving hole transport properties. This simple doping method we developed can be used to optimize or modify compositions of various nanocrystalline electrodes.

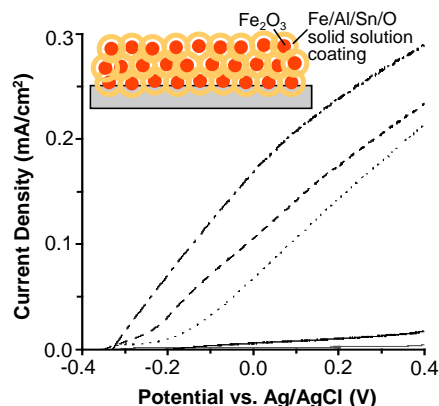


Figure 2. I-V characteristics of Fe_2O_3 electrodes under AM 1.5 illumination after no treatment (—), Al-treatment(---), Sn-treatment(...), and Al/Sn-treatment (-.-). The thin grey solid line shows a dark current of the untreated Fe_2O_3 electrode.

Work in progress/Future directions

Our ability to tailor the morphology and composition of individual inorganic components enables us to build various semiconductor/catalyst and semiconductor/semiconductor multi-component photoelectrodes with systematically varying junction structures and to investigate their effect on the overall photoelectrochemical properties. We have also started investigating electrochemical synthesis conditions to produce ternary compounds as photoelectrodes. Compared to binary compounds, investigations on ternary photoelectrodes for solar hydrogen production have been quite limited mainly due to difficulties in processing them as electrode-type materials although there are many ternary semiconductors that have suitable band gaps and band positions for the photoelectrolysis of water. This study will significantly increase our freedom in selecting appropriate photoanode and photocathode materials to assemble photoelectrochemical cells that can operate without the need of an external bias.

DOE Sponsored Publications (2007-2010)

1. Spray, R. L.; Choi, K.-S. "Electrochemical Synthesis of SnO₂ Films Containing Three-Dimensionally Organized Uniform Mesopores via Interfacial Surfactant Templating" *Chem. Commun.* **2007**, 3655-3657.
2. Santato, C.; López, C. M.; Choi, K.-S. "Synthesis and Characterization of Polycrystalline Sn and SnO₂ Films with Wire Morphologies" *Electrochem. Commun.* **2007**, 9, 1519-1524.
3. Siegfried, M. J.; Choi, K.-S. "Electrochemical Synthesis and Characterization of Cupric Oxide Films" *J. Electrochem. Soc.* **2007**, 154, D674- D677.
4. Steinmiller, E. M. P.; Choi, K.-S. "Electrochemical Construction of Lamellar Structured ZnO Films by Anodic Deposition Using Basic Media" *Langmuir*, **2007**, 23, 12710 -12715.
5. Yarger, M. S.; Choi, K.-S. "Electrochemical Synthesis of Cobalt Hydroxide Films with Tunable Interlayer Spacings" *Chem. Commun.* **2007**, 159-161.
6. Siegfried, M. J.; Choi, K.-S. "Elucidation of New Overpotential-Limited Branching Mechanism for Electrocrystallization of Cuprous Oxide" *Angew. Chem. Int. Ed.* **2008**, 47, 368-372.
7. Choi, K.-S.; Steinmiller, E. M. P. "Electrochemical Synthesis of Lamellar Structured ZnO Films via Electrochemical Interfacial Surfactant Templating" *Electrochim. Acta* **2008**, 53, 6953-6960.
8. Yarger, M. S.; Steinmiller, E. M. P.; Choi, K.-S. "Electrochemical Synthesis of Zn-Al Layered Double Hydroxide (LDH) Films" *Inorg. Chem.* **2008**, 47, 5859-5865.
9. Seabold, J. A.; Karthik, S.; Wilke, R. H. T.; Paulose, M.; Varghese, O. K.; Grimes, C. A. Choi, K.-S. "Photoelectrochemical Properties of Heterojunction CdTe/TiO₂ Electrodes Constructed Using Highly Ordered TiO₂ Nanotube Arrays" *Chem. Mater.* **2008**, 20, 5266-5273.
10. Choi, K.-S. "Shape Control of Inorganic Crystals via Electrodeposition" *Dalton Trans.* **2008**, 5432-5438.
11. McShane, C. M.; Choi, K.-S. "Photocurrent Enhancement of Cu₂O Electrodes Achieved by Controlling Dendritic Branching Growth" *J. Am. Chem. Soc.* **2009**, 131, 2561-2569.
12. Spray, R. L.; Choi, K.-S. "Photoactivity of Transparent Nanocrystalline Fe₂O₃ Electrodes Prepared via Anodic Deposition" *Chem. Mater.* **2009**, 21, 3701-3709.
13. Jung, Y.; Sign, N.; Choi, K.-S. "Cathodic Assembly of Conducting Polymer and Metal-Conducting Polymer Hybrid Films" *Angew. Chem. Int. Ed.* **2009**, 48, 8331-8334.
14. Jung, Y.; Lee, H. I.; Kim, J. H.; Yun, M.-H.; Hwang, J.; Ahn, D.-H.; Park, J.-N.; Choi, K.-S.; Kim, J. M. "Preparation of polypyrrole-incorporated mesoporous carbon-based composites for confinement of Eu(III) within mesopores" *J. Mater. Chem.* **2010**, Available on the web.
15. Choi, K.-S.; Jang, H. S.; McShane, C. M.; Read, C. G.; Seabold, J. A. "Electrochemical Synthesis of Inorganic Polycrystalline Electrodes with Controlled Architectures" *MRS Bull.* **2010** In press.
16. Jung, Y.; Spray, R. L.; Kim, J. H.; Kim, J. M.; Choi, K.-S. "Synthesis of Mesoporous Silica-Polypyrrole Composites via Selective Polymerization in Mesopores Using In-Situ Generated Oxydizing Agents on Silica Surface" **2010**, Submitted.
17. Jang, H. S.; Kim, S. J.; Choi, K.-S. "Electrochemical Synthesis of Cu₂O Electrodes Composed of Two-Dimensional Plate-Like Dendritic Crystals" **2010**, Submitted.

Fundamental Studies of Light-induced Charge Transfer, Energy Transfer, and Energy Conversion with Supramolecular Systems

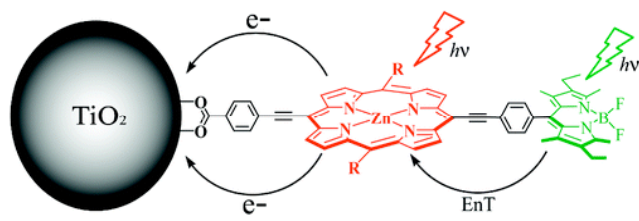
Joseph T. Hupp

Department of Chemistry
Northwestern University
Evanston, IL 60208

Summary of Project. This project seeks to exploit supramolecular chemistry: a) to interrogate and understand fundamental aspects of light-induced charge transfer and energy transfer, and b) to construct solar energy conversion systems that make use of unique assembly motifs to address key conversion efficiency issues. There is a particular focus on the fundamental behavior of new light harvesters and on new redox shuttles useable in dye-sensitized systems. Representative recent results are described below.

1. Supramolecular Chromophoric Assemblies. We have been exploring dye systems that allow us to harvest a large fraction of the visible and near-IR spectrum. Our attention has been on highly conjugated porphyrin systems. The best examples of these systems offer much higher extinction coefficients than the standard ruthenium dyes employed in dye cells and much better spectral coverage than conventional porphyrin molecules.

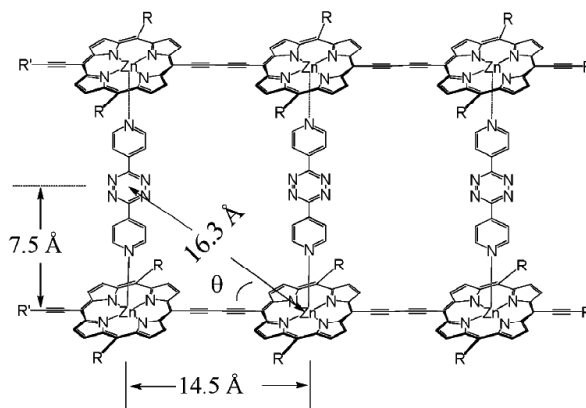
1.1 As described further in paper #24 and illustrated above, a zinc porphyrin derivative (**2**) and zinc porphyrin–bodipy dyad (**3**) have been prepared and applied to dye-sensitized cells.



On the basis of absorption and fluorescence excitation spectra, dyad **3** efficiently transfers energy from the bodipy to zinc porphyrin constituent. **3**-sensitized cells demonstrate higher solar spectral coverage, based on incident photon to current efficiency spectra, and substantially improved power conversion efficiency

compared to that of **2**-sensitized cells. The better performance of **3**-sensitized cells is attributed largely to the gain in spectral absorbance provided by the bodipy constituent of **3**.

1.2 The supramolecular ladder structure shown at right features highly conjugated porphyrin rails (potential excited-state electron donors) and redox active rungs (potential electron acceptors). Ultrafast spectroscopy studies reveal that ET indeed does occur from the photoexcited rails to the rungs. These studies, however, offer no information about the direction or distance of electron transfer. We found (paper #22) that both could be interrogated via transient DC photoconductivity (TDCP) measurements.

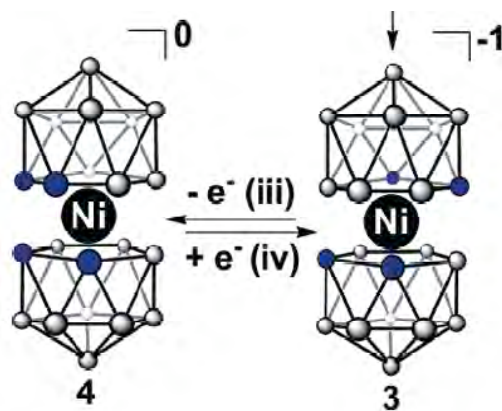


From the measurements we have been able to ascertain that: (a) electrons are preferentially transferred to the outer rungs, (b) the transferred electron is centered on the acceptor rung, (c) the corresponding hole is delocalized over the three porphyrins constituting a rail, and (d) the center of the hole is at the center of the rail, resulting in a charge-transfer distance of ca. 16 angstroms.

2. Shuttles. An optimal photoelectrode will display: a) electron transport that is fast relative to electron recombination with an oxidized dye molecule or electron interception by a redox shuttle (including “fast” shuttles), and b) slow transfer of electrons back to the redox shuttle (including shuttles that are otherwise highly reactive). Condition (a) ensures efficient charge collection and therefore, good photocurrents. Condition (b) is equivalent to mandating low dark currents and is a requirement for achieving good photovoltages.

2.1 Cobalt polypyridyl complexes have previously shown promise. As described further in paper #32, a series of cobalt-containing redox couples, based on $[\text{Co}(1,10\text{-phenanthroline})_3](\text{ClO}_4)_2$ and its derivatives, were prepared for use as regenerators/shuttles in dye-sensitized cells featuring modified TiO_2 photoelectrodes. Electron lifetimes were then extracted from open-circuit voltage decay measurements. Cells employing alumina barrier/passivation layers exhibited higher open-circuit voltages as shuttles with more positive redox potentials were used, with the $\text{Co}(5\text{-nitro-phen})_3^{3+/2+}$ couple exhibited open circuit photovoltages, V_{oc} , as high as 844 mV. Analysis of the open-circuit voltages and electron lifetimes indicated Marcus normal-region behavior for back electron transfer from the TiO_2 photoanode to these compounds.

2.2 As described in papers 28 and 30, a new series of non-corrosive redox shuttles has been developed based on bis(dicarbollide)Ni(IV/III) species. We find that dye regeneration is fast, even at low Ni(III) concentrations, and photovoltages are relatively high, reaching more than 850 mV. Open-circuit voltage decay measurements were used to probe the kinetics of interception of injected electrons by Ni(IV). The interception reaction was found to be three orders of magnitude slower than with ferrocenium, but two orders of magnitude faster than with triiodide. The kinetic differences versus ferrocenium reflect substantial inner-shell reorganization during Ni(IV) reduction. In contrast to cobalt shuttles, no problems due to slow shuttle diffusion were encountered.



3. Miscellaneous Studies. A handful of molecular photophysical studies of other kinds have been completed. Other work concerned photophysical properties of Pt(II)-based chromophores and mechanistic behavior of triads containing these chromophores (for example, paper #19). Here we made use of the unique information provided by TDCP measurements to answer unresolved questions concerning configuration mixing and charge transfer within these systems.

DOE Sponsored Publications 2007-2010

1. "Comparison of Interfacial Electron Transfer Through Carboxylate and Phosphonate Anchoring Groups" C. She, J. Guo, S. Irle, K. Morokuma, H. Zabri, D. L. Mohler, F. Odobel, K.T. Youm, F. Liu, J. T. Hupp, and T. Lian, *J. Phys. Chem. A*, **2007**, *111*, 6832-6842.
2. "Mechanism for Zirconium Oxide Atomic Layer Deposition using Bis(methylcyclopentadienyl)methoxymethyl Zirconium," J. W. Elam, S. D. Elliott, M. C. Faia, A. Zydor, J. T. Hupp, M. J. Pellin, *Appl. Phys. Lett.*, **2007**, *91*, 253123.
3. "ZnO Nanotube Dye-Sensitized Solar Cells," A. B. F. Martinson, J. W. Elam, J. T. Hupp, and M. J. Pellin, *Nano Letters*, **2007**, *7*, 2183-2187.
4. "Novel Photoanode Architectures and Tunneling Barriers," T. W. Hamann, A. B. F. Martinson, J. W. Elam, M. J. Pellin and J. T. Hupp, *ACS Fuel Division Preprints*, **2007**, *52*, 778-779.
5. "Transparent Conducting Oxides at High Aspect Ratios by ALD," M. J. Pellin, J. W. Elam, J. A. Libera, A. B. F. Martinson, and J. T. Hupp, *ECS Transactions* **2007**, *3*, 243-246.
6. "Probing Exciton Localization/Delocalization: Transient DC Photoconductivity Studies of Excited States of Symmetrical Porphyrin Monomers, Oligomers and Supramolecular Assemblies," C. She, J. E. McGarrah, S. J. Lee, J. L. Goodman, S. T. Nguyen, J.A.G. Williams, and J. T. Hupp, *J. Phys. Chem. A*, **2009**, *113*, 8182-8186.
7. "Intramolecular Energy Transfer within Butadiyne-Linked Chlorophyll and Porphyrin Dimer-Faced, Self-assembled Prisms," R. F. Kelley, S. J. Lee, T. M. Wilson, Y. Nakamura, D. M. Tiede, A. Osuka, J. T. Hupp, and M. R. Wasielewski, *J. Am. Chem. Soc.*, **2008**, *130*, 4277-4284.
8. "Atomic Layer Deposition of Tin Oxide Films Using Tetrakis(dimethylamino) Tin," J. W. Elam, D. A. Baker, A. J. Hryn, A. B. F. Martinson, M. J. Pellin, J. T. Hupp, *JVST A*, **2008**, *26*, 244-252.
9. "Atomic Layer Deposition of Indium-Tin Oxide Thin Films Using Non-Halogenated Precursors," J. W. Elam, D. A. Baker, A. B. F. Martinson, M. J. Pellin, J. T. Hupp, *J. Phys. Chem. C*, **2008**, *112*, 1938-1945.
10. "Aerogel Templated ZnO Dye-Sensitized Solar Cells," T. W. Hamann, A. B. F. Martinson, J. W. Elam, M. J. Pellin, J. T. Hupp, *Adv. Mater.*, **2008**, *20*, 1560-1564.
11. "Fast Energy Transfer within a Self-Assembled Cyclic Porphyrin Tetramer," R. A. Jensen, R. F. Kelley, S. J. Lee, M. R. Wasielewski, J. T. Hupp, D. M. Tiede, *Chem. Comm.*, **2008**, 1886-1888.
12. "Hollow Porphyrin Prisms: Modular Formation of Permanent, Torsionally Rigid, Nanostructures via Templated Olefin Metathesis," K.-T. Youm, S. T. Nguyen, J. T. Hupp, *Chem. Comm.*, **2008**, *29*, 3375-3377.

13. "Atomic Layer Deposition of TiO₂ on Aerogel Templates: New Photoanodes for Dye-Sensitized Solar Cells," T. W. Hamann, A. B. F. Martinson, J. W. Elam, M. J. Pellin, J. T. Hupp, *J. Phys. Chem. C*, **2008**, 112, 10303-10307.
14. "Radial Electron Collection in Dye-Sensitized Solar Cells," A. B. F. Martinson, J. W. Elam, J. Liu, J. T. Hupp, M. J. Pellin, T. J. Marks, *Nano Lett.*, **2008**, 8, 2862-2866.
15. "Advancing Beyond Current Generation Dye-Sensitized Solar Cells," T. W. Hamann, R. A. Jensen, A. B. F. Martinson, H. V. Ryswyk, J. T. Hupp, *Energy Environ. Sci.*, **2008**, 1, 66-78.
16. "Outer-sphere Redox Couples as Shuttles in Dye-Sensitized Solar Cells. Performance Enhancement Based on Photoelectrode Modification via Atomic Layer Deposition," T. W. Hamann, O. K. Farha, J. T. Hupp, *J. Phys. Chem. C*, **2008**, 112, 19756-19764.
17. "Anodic Aluminum Oxide Templated Channel Electrodes via Atomic Layer Deposition," J. W. Elam, A. B. F. Martinson, M. J. Pellin, J. T. Hupp, *ECS Transactions*, **2008**, 6.
18. "Toward Plasmonic Solar Cells: Protection of Silver Nanoparticles via Atomic Layer Deposition of TiO₂," S. Standridge, G. C. Schatz, J. T. Hupp, *Langmuir*, **2009**, 25, 2596-2600.
19. "Electron Transfer in Platinum (II) Diimine Centered Triads: Mechanistic Insights from Photoinduced Transient Displacement Current Measurements," J. E. McGarrah, J. T. Hupp, S. Smirnov, *J. Phys. Chem. C*, **2009**, 113, 6430-6436.
20. "Electron Transport in Dye-Sensitized Solar Cells Based on ZnO Nanotubes: Evidence for Highly Efficient Charge Collection and Exceptionally Rapid Dynamics," A. B. F. Martinson, M. S. Góes, F. Fabregat-Santiago, J. Bisquert, M. J. Pellin, J. T. Hupp, *J. Phys. Chem. C.*, **2009**, 113, 4015-4021.
21. "Surface Passivation of Nanoporous TiO₂ via Atomic Layer Deposition of ZrO₂ for Solid-State Dye-Sensitized Solar Cell Applications," T. C. Li, M. S. Góes, Francisco Fabregat-Santiago, Juan Bisquert, Paulo R. Bueno, Chaiya Prasittichaia, Joseph T. Hupp, Tobin J. Marks, *J. Phys. Chem. C*, **2009**, 113, 18385-18390.
22. "Photoinduced Electron Transfer from Rail to Rung within a Self-assembled Porphyrin Oligomeric Ladder," C. She, S.-J. Lee, J. E. McGarrah, J. Vura-Weis, M. R. Wasielewski, H. Chen, G. C. Schatz, M. A. Ratner and J. T. Hupp, *Chem. Commun.*, **2010**, 46, 547-549.
23. "Dye-Sensitized Solar Cells: Sensitizer-Dependent Injection into ZnO Nanotube Electrodes," R. A. Jensen, H. Van Ryswyk, C. She, J. M. Szarko, L. X. Chen, J. T. Hupp, *Langmuir*, **2010**, 26, 1401-1404.
24. "Dye Sensitized Solar Cells: TiO₂ Sensitization with a Bodipy-Porphyrin Antenna System," C. Y. Lee, J. T. Hupp, *Langmuir*, **2010**, 26, 3760-3765.

25. "Solvent-induced configuration mixing and triplet excited state inversion: insights from transient absorption and transient DC photoconductivity measurements," C. She, A. A. Rachford, X. Wang, S. Goeb, A. O. El-Ballouli, F. N. Castellano and J. T. Hupp, *Phys. Chem. Chem. Phys.*, **2009**, *11*, 8586 - 8591.
26. "Distance Dependence of Plasmon Enhancement in Dye-Sensitized Solar Cells," S. Standridge, G. C. Schatz, J. T. Hupp, *J. Am. Chem. Soc.*, **2009**, *131*, 8407-8409.
27. "Excess Polarizability Reveals Exciton Localization/Delocalization Controlled by Linking Positions on Porphyrin Rings in Butadiyne-Bridged Porphyrin Dimers," C. She, S. Easwaramoorthi, P. Kim, S. Hiroto, I. Hisaki, H. Shinokubo, A. Osuka, D. Kim, J. T. Hupp, *J. Phys. Chem.*, **2010**, *114*, 3384–3390.
28. "Ni(III)/(IV) Bis(dicarbollide) as a Fast, Non-Corrosive Redox Shuttle for Dye-Sensitized Solar Cells," T. Li, A. Spokoyny, C. She, O. Farha, C. Mirkin, T. Marks, J.T. Hupp, *J. Am. Chem. Soc.*, **2010**, *132*, 4580–4582.
29. "Porphyrin Sensitized Solar Cells: TiO₂ Sensitization with a π -extended porphyrin possessing two anchoring groups," C. Y. Lee, C. She, N. C. Jeong, and J. T. Hupp, **2010**, submitted.
30. "Electronic Tuning of Ni-based Bis(dicarbollide) Redox Shuttles In Dye-Sensitized Solar Cells," A. M. Spokoyny, T. C. Li, O. K. Farha, C. W. Machan, C. She, C. L. Stern, T. J. Marks, J. T. Hupp, and C. A. Mirkin, **2010**, submitted.
31. "The Role of Electronic Couplings in Linear Porphyrin Arrays Probed by Single-Molecule Fluorescence Spectroscopy," J. Yang, J. Lee, C. Y. Lee, N. Aratani, A. Osuka, J. T. Hupp, D. Kim, **2010**, submitted.
32. "Dye-Sensitized Solar Cells: Driving-Force Effects on Electron Recombination Dynamics with Cobalt Based Shuttles," M. DeVries, M. J. Pellin, J. T. Hupp, *Langmuir*, ASAP.

Session III

Photoelectrochemistry II

Mass Transport of Cobalt Mediator in DSSCs and Magnetic Field Effects on Charge-Separated-State Recombination in Copper C-A Dyads

Jeremy J. Nelson, Tyson J. Amick, Megan Lazorski, Lance Ashbrook and C. Michael Elliott
 Department of Chemistry
 Colorado State University
 Fort Collins, CO 80523

Mass-transport of cobalt-based mediators in DSSCs. The most familiar mediator for dye sensitized solar cells is I/I_3^- . While I/I_3^- remains the “gold-standard”, it has well known limitations. Arguably the biggest are its reactivity and non-ideal redox potential. Certain

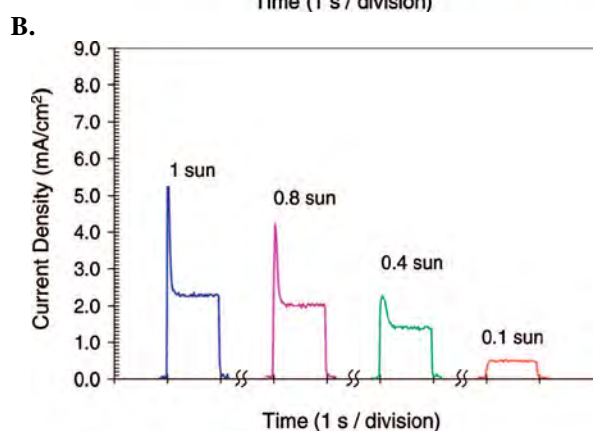
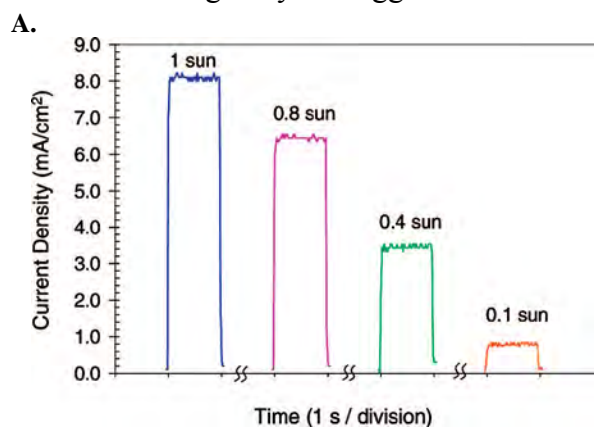
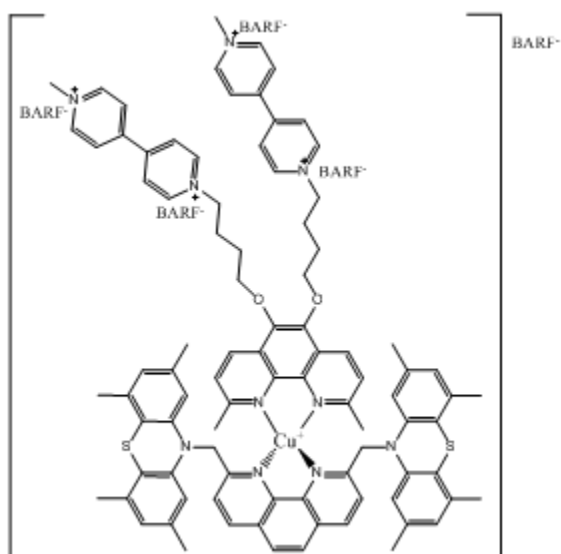


Figure 1. Current Density vs. time for A. I/I_3^- and B. $Co(DTB)_3^{2+/3+}$ mediated DSSCs with 1 s duration light pulses at different illumination intensities.

trisbipyridinecobalt (II/III) complexes have appropriate heterogeneous electron-transfer rates (e.g., fast regeneration of oxidized dye, slow recombination with photoinjected electrons, etc.) to rival I/I_3^- . Based solely on consideration of the rates of these critical electron-transfer processes, $Co(DTB)_3^{2+/3+}$ (DTB = 4,4'-di-*t*-butyl-2,2'-bipyridine) and I/I_3^- should be equally good mediators in DSSCs; yet they are not. Under AM 1.5 illumination, J_{ss} is invariably at least 20% smaller for a $Co(DTB)_3^{2+/3+}$. Short-circuit current density vs. time plots for DSSCs illuminated with ca. 1s pulses of light at different intensities, shown in Figure 1, illustrate why. For the $Co(DTB)_3^{2+/3+}$ mediated cell there is an initial spike in current which decays to a lower steady-state value. The maximum current at the initial spike scales with light intensity, but the steady-state current does not. For the I/I_3^- mediated cell, the steady state current is reached almost instantaneously. These data indicate that, in the $Co(DTB)_3^{2+/3+}$ -mediated cell, the current is limited by solution mass transport. We employed Rotated Disk Electrode (RDE) voltammetry to quantitatively evaluate rates of mediator diffusion within the pore structures of TiO_2 photoanodes.

Accomplishing this task required fabrication of a rotatable electrode with a mesoporous TiO_2 layer on its surface. The key findings from this study are that: (1) Within mesoporous TiO_2 the diffusion coefficient is $\times 7-10$ larger for I_3^- than for $Co(DTB)_3$ whereas, in bulk solution the difference is only $\times 2.5$. (2) A small but significant selective interaction exists between the TiO_2 and $Co(DTB)_3^{2+/3+}$ results in $Co(DTB)_3^{2+/3+}$ partitioning into the photoanode. The same interaction is absent for I_3^- and neutral species.

Magnetic Field Effects in the charge separation kinetics of Cu(I) C-A dyads. The complex



I

Figure 2. A heteroleptic Cu(I) C-A diad.

shown in Figure 2 was prepared in an effort to generate a donor-chromophore-acceptor (D-C-A) triad based on Cu(I) which: (1) cleanly assembles in solution; (2) is the thermodynamically favored product and (3) undergoes multistep, photoinduced charge separation. Complex **I** meets all of these requirements except multistep charge separation. Unfortunately, the putative donor moieties fail to reduce photogenerated Cu(II) in this ligand environment (probably for thermodynamic reasons). Nonetheless, singlestep photoinduced charge separation does occur for **I**, generating a long-lived Cu(II)-MV⁺ charge separated state (CSS). Consequently, **I** can be considered as a simple C-A type diad. What is most interesting about this system is that the decay kinetics for the Cu(II)-MV⁺ CSS exhibit very dramatic magnetic field effects (MFE). Figure 3 shows the effect on the recombination kinetics of very modest (ca. 0.05 T) applied magnetic field. These results strongly suggest that the Cu(II)-MV⁺ “radical pair” is formed with considerable triplet character and that spin-chemical considerations are more important in Cu(I) based photoinduced charge transfer systems than has been previously appreciated.

Absorbance vs. Time for [Cu(diTMPTZ)(Acceptor)]⁺(BARF)₅ at 600 nm in the Presence and Absence of a Magnetic Field

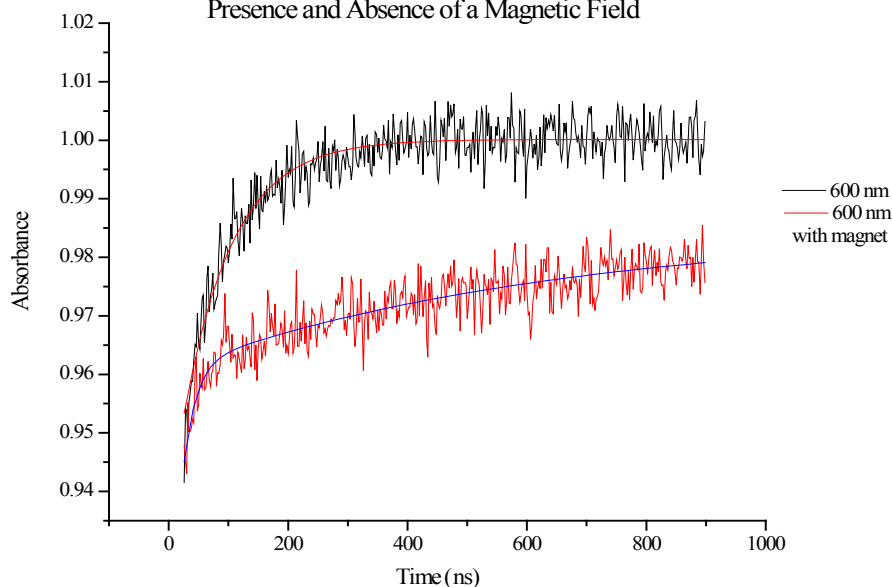


Figure 3. Transient absorption decays measured at 600 nm for MV⁺ formed from **I** after excitation at 450 nm. Black curve was in the absence of a magnetic field and is fit with a single exponential. Red curve is with an applied field of ca. 0.05 T and is fit with a biexponential.

DOE Sponsored Publications 2007-2010

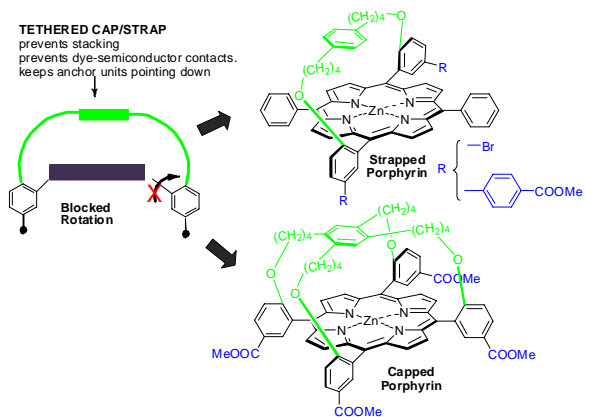
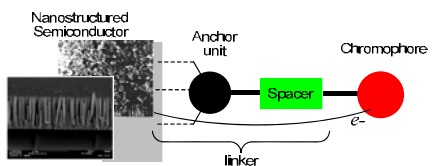
1. J.M. Weber; M.T. Rawls; V.J. MacKenzie; B.R. Limoges; C.M. Elliott. "High Energy and Quantum Efficiency in Photoinduced Charge Separation" J. Amer. Chem Soc. 129, 313-320 (2007).
2. M.T. Rawls; G. Kollmannsberger; C.M. Elliott; U.E. Steiner. Spin Chemical Control of Photoinduced Electron-Transfer Processes in Ruthenium(II)-Trisbipyridine-Based Supramolecular Triads: 2. The Effect of Oxygen, Sulfur, and Selenium as Heteroatom in the Azine Donor," J. Phys. Chem A, 111, 3485-3496 (2007).
3. M.J. Scott; J.J. Nelson; S. Caramori; C.A. Bignozzi; C.M. Elliott. "*cis*-dichloro-bis(4,4'-dicarboxy-2,2-bipyridine)osmium(II)-Modified Optically Transparent Electrodes: Application as Cathodes in Stacked Dye Sensitized Solar Cells," Inorg. Chem. 46(24), 10071-10078 (2007).
4. M.J. Scott; M. Woodhouse; B.A. Parkinson; C.M. Elliott. "Spatially Resolved Current-Voltage Measurements -- Evidence for Non-Uniform Photocurrents in Dye-Sensitized Solar Cells," J. Electrochem. Soc. 155(3) B290-B293 (2008).
5. K. Harada; M. Riede; K. Leo; O.R. Hild; C.M. Elliott. "Pentacene Homojunctions: Studies for Electron and Hole Transport Properties and Related Photovoltaic Responses," Physical Review B 77, 195212 (2008).
6. J.J. Nelson; T.J. Amick; C.M. Elliott. "Mass Transport of Polypyridyl Cobalt Complexes in Dye-Sensitized Solar Cells with Mesoporous TiO₂ Photoanodes," J. Phys. Chem C 112(46), 18255-18263 (2008).
7. M.T. Rawls, I. Kuprov, C.M. Elliott, U.E. Steiner. "Spin Relaxation in Ru-Chromophore-Linked Azine/Diquat Radical Pairs," in Carbon-Centered Radicals and Radical Cations (Malcolm DE Forbes, Ed., Wiley, New York) in press 2009.
8. H.-K. Seo, H.-S. Shin, E.-K. Suh, C.M. Elliott. "A Novel Approach for the Synthesis of Rutile Titania Nanotubes at Very Low Temperature," submitted to Journal of Vacuum Science & Technology B., 2010.
9. H.-K. Seo, C. M. Elliott, and H.-S. Shin, "Synthesis of TiO₂ Films for Dye Sensitized Solar Cells using Atmospheric Pressure Plasma Jet," submitted to Chem. Comm., 2010.
10. S.K. Sarkar, JY Kim, D.N. Goldstein, N.R. Neale, K. Zhu, C.M. Elliott, A.J. Frank, S.M. George. "In₂S₃ Atomic Layer Deposition and Its Application as a Sensitizer on TiO₂ Nanotube Arrays for Solar Energy Conversion," J. Phys. Chem. C. DOI: 10.1021/jp9086943, Publication Date: April 13, 2010.

Model Dyes for Study of Molecule/Metal Oxide Interfaces and Electron Transfer Processes

Elena Galoppini
Department of Chemistry
Rutgers University
Newark, NJ 07102

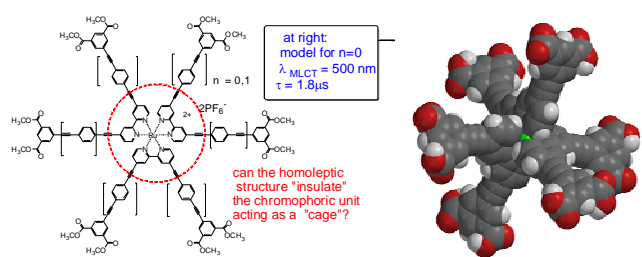
The controlled chemical modification of nanostructured semiconductor surfaces and the study at the molecular level of photochemical and electronic processes at this fundamentally interesting, and complex, boundary are of great importance for solar energy conversion.^{4,10} The scope of this research is to design and synthesize model dyes to control the molecule/semiconductor contact (binding, orientation, aggregation, distance) and to study how such parameters influence binding and interfacial charge transfer processes. We will describe our progress in two areas of research. The presentation will also outline future plans and research directions.

1. Synthetic Work and Binding Studies. In the past three years we have worked on the design and synthesis of three kinds of molecular models: *(a) Large footprint linkers.*^{3,9,13} Tripodal linkers with anchoring groups in *meta* position, and wider footprints were prepared to provide a better match with the TiO₂ surface lattice. On colloidal TiO₂ and ZrO₂ films and planar surfaces, the linker provided spacing control but sensitizer-sensitizer interactions were still observed on colloidal films. Structural considerations suggest that this may largely be due to the significant presence of “necking” regions in the films. We continue to coordinate the experiments with theoretical work from Persson. Adsorption isotherm and binding constant for *m*- and *p*-tripods were compared on crystal anatase and rutile by Parkinson and differences were found only on A001. *(b) Porphyrin models.*^{2,5,7,11,15,iii} Rigid-rod and tetrachelate Zn(II) porphyrins were studied on TiO₂ and ZrO₂ films differing in morphology: nanoparticles, nanorods, nanotubes and planar rutile. We found that the compound binding planar to the surface through a biphenyl unit was the most efficient sensitizer in solar cell. In the past year we have developed capped porphyrins to restrict the conformational freedom of the linker group, and to prevent (or limit) both direct contacts with the semiconductor and porphyrin stacking. *(c) Homoleptic Ru Complexes* The TiO₂ colloidal thin films employed for the injection studies are made of porous films made of spherical nanoparticles in close contact with each other. Bound or unbound molecules may “touch” nearby particles. To avoid (or minimize) injection on nearby nanoparticles and a distribution of binding orientations on the surface, we have prepared the first two examples of rigid-rod homoleptic and symmetric (“star”) complexes. They both exhibited long excited state lifetimes (1.7 us) and single exponential decays in solution. This design should increase the binding probability, avoid any kind of “head down” binding interactions, and eliminate contact of the Ru complex with the surface, while



ensuring an excellent attachment to the surface. We just started to study the “star” compounds bound to TiO₂ films.

Photophysical studies (steady state and time resolved emission, absorption, electrochemical and photoelectrochemical properties, FT-IR-ATR) in solution and bound to TiO₂, ZrO₂, ZnO colloidal films and ZnO nanorods of the recently synthesized model dyes shown are in progress, and the key results will be discussed in the talk.



2. Electron transfer Studies. We will present the progress in electron injection and recombination dynamics and photoelectrochemical studies of the molecules mentioned above.^{14,i,ii} In the talk we will present work is done in collaboration with Piotrowiak, Meyer and Sundström.

(a) Mid-IR measurements of the injected electrons in the conduction band of TiO₂ semiconductor nanoparticles sensitized by Ru(II)bpy chromophores. The Piotrowiak group has assembled a tunable mid-IR OPA producing sub-100 fs pulses in range 2600-4200 nm (idler) with power of approximately 100 μW. With this instrument we have started the absorption of the conduction band electron in a region that is far from the triplet state of the Ru-dyes (700–1500 nm) and from surface trap states (700 - 1200 nm). We are currently comparing data for N3, Ru 455, and the tripodal Ru(II) complexes. The very first Mid-IR transient absorption data collected indicate that sample preparation and experimental setting need to be optimized to correlate the data with the structural properties of the dyes, as the experiment is very sensible to the film preparation (TiO₂ preparation, oxygen annealing, binding presence of salts etc..). *(b) Charge transfer studies of porphyrin models.*ⁱⁱ Charge transfer studies of rigid-rod and tetrachelate porphyrins by Sundström and calculations by Persson^{6,16} suggests that rotational freedom about the anchoring “legs” in the tetrachelates, and molecules binding flat in the rods greatly complicate the ability to correlate injection and recombination kinetics with the expected binding geometry. These results suggest that more sophisticated considerations and model design have to be applied for controlling the dye binding and understanding how it influences the electron dynamics. The recently synthesized capped porphyrins have not yet been studied. *(c) THz study of sensitized ZnO and TiO₂ nanocrystals.*¹ A powerful technique for investigation of transport mechanisms on picosecond to nanosecond time scales after photoexcitation is time-resolved terahertz (THz) spectroscopy which permits non-contact measurement of (effective) conductivity with sub-picosecond time resolution. Nemeč and Sundström have shown that charge transport in sensitized layers can be very different from that in non-sensitized semiconductors, due to strong electrostatic interaction between injected electrons and dye cations at the surface of the semiconductor nano-particle, and that is different for different semiconductors. At this stage we provided simple models dyes. We continue to collaborate with Sundström in this project and will describe recent results and planned work. *(d)* Finally, we will present some of the preliminary studies of the “star” Ru(II) compounds bound to TiO₂ films with the Meyer’s group.

DOE Sponsored Publications 2007-2010

Submitted

- i. Decreased interfacial charge recombination rate constants with N3-type sensitizers. Maria Abrahamsson, Patrik G. Johansson, Andrew Kopecky, Elena Galoppini and Gerald J Meyer
- ii. Solar Energy Conversion - Natural to Artificial Hynek Němec, Elena Galoppini, Hiroshi Imahori, Villy Sundstrom *Elsevier series of books on Nanoscience: Comprehensive Nanoscience and Technology*. Ed. D Andrews. Elsevier 2010
- iii. Synthesis of Capped Tetrachelate Porphyrins. Chi-Hang Lee, Keyur Chitre and Elena Galoppini *Journal of the Chinese Chemical Society* special issue for 2009 International Symposium on Dye-Sensitized Solar Cells 22-23 October 2009, Jhongli City, Taiwan

Published or Accepted

1. Influence of electron-cation interaction on electron mobility in dye-sensitized ZnO and TiO₂ nanocrystals: A study using ultrafast terahertz spectroscopy H. Němec, J. Rochford, O. Taratula, E. Galoppini, P. Kužel, T. Polívka, A. Yartsev, V. Sundström *Phys. Rev. Lett.* **2010**, **accepted**.
2. Synthesis of Strapped Porphyrins: Towards Isolation of the Chromophore on Semiconductor Surfaces. C.-H. Lee E. Galoppini *J. Org. Chem.* **2010**, **in press**. (Article)
3. Modular Synthesis of Ruthenium Tripodal System with Variable Anchoring Groups Positions for Semiconductor Sensitization. C.-H. Lee, Y. Zhang, A. Romayanantakit, E. Galoppini, **2010 Tetrahedron in press**. doi:10.1016/j.tet.2010.04.005 (Article)
4. Organic aromatic hydrocarbons as sensitizing dye models for semiconductor nanoparticles Y. Zhang , E. Galoppini *ChemSusChem* **2010**, *3*, 410-428. DOI: 10.1002/cssc.200900233 **Invited review**
5. Energy levels alignment of a Zinc(II) Tetraphenylporphyrin dye adsorbed onto TiO₂(110) and ZnO(1120) surfaces S. Rangan, R. Thorpe, R.A. Bartynski, J. Rochford, E. Galoppini *J. Phys. Chem. C* **2010**, *114*, 1139-1147.
6. Calculations of interfacial interactions in pyrene-Ipa rod sensitized nanostructured TiO₂ S. Kalyan Pal, V. Sundström, E. Galoppini, P. Persson, *Dalton Trans.* **2009**, 10021-10031 DOI: 10.1039/b910880g
7. Photoelectrochemical Behavior of Polychelate Porphyrin Chromophores and Titanium Dioxide Nanotube Arrays for Dye-Sensitized Solar Cells N. R. de Tacconi, W. Chanmanee, K. Rajeshwar, J. Rochford, E. Galoppini *J. Phys. Chem. C* **2009**, *113*, 2996-3006. DOI: 10.1021/jp808137s
8. Meta-substituted RuII rigid rods for sensitization of TiO₂. M. Abrahamsson, O. Taratula, P. Persson, G.J. Meyer, E. Galoppini, *J. Photochem. And Photobiology A* **2009**, *206*, 155-163.
9. Large Footprint Pyrene Chromophores Anchored to Planar and Colloidal Metal Oxide Thin Films S. Thyagarajan, E. Galoppini, P. Persson, G. Giaimuccio, G.J. Meyer *Langmuir* **2009**, *25*, 9219-9226

10. Multi-component arrays for interfacial electronic processes on the surface of nanostructured semiconductor nanoparticles. A. Kopecky and E. Galoppini in *Specialistic Periodic Reports on Photochemistry*, Albini, A. Ed.; The Royal Society of Chemistry, Vol 37 **2009** 362-392 DOI: 10.1039/b813865f **Invited Book Chapter**
11. Zn(II) Tetraarylporphyrins Anchored to TiO₂, ZnO and ZrO₂ Nanoparticle Films Through Rigid-Rod Linkers, Rochford, J. ; Galoppini, E. *Langmuir*, **2008**, 24, 5366
12. Heavy Atom Effects on Anthracene-Rigid-Rod Excited States Anchored to Metal Oxide Nanoparticles Giaimo, J. M.; Rowley, J. G.; Meyer, G. J.; Wang, D.; Galoppini, E. *Chemical Physics* **2007**, 339, 146-153.
13. Tripodal Pyrene Chromophores for Semiconductor Sensitization: New Footprint Design Thyagarajan, S.; Liu, A.; Famoyin, O. A.; Lamberto M.; Galoppini, E. *Tetrahedron* **2007**, 63, 7550-7559. doi:10.1016/j.tet.2007.05.055
14. Ru(II)-Polypyridyl Complexes Bound to Nanocrystalline TiO₂ Films Through Rigid-Rod Linkers: Effect of the Linkers Length on Electron Injection Rates Piotrowiak, P.; Galoppini, E.; Wang D.; Myahkostupov, M. *J. Phys. Chem. C* **2007**, 111, 2827-2829. DOI: 10.1021/jp0679257
15. Tetrachelate Porphyrin Chromophores for Metal Oxide Semiconductor Sensitization: Effect of the Spacer Length and Anchoring Group Position Rochford, J.; Chu, D.; Hagfeldt, A.; Galoppini, E. *J. Am. Chem. Soc.* **2007** 129, 4655-4665. DOI: 10.1021/ja068218u
16. Calculated Optoelectronic Properties of Ruthenium Tris-Bipyridine Dyes Containing Oligophenyleneethynylene Rigid Rod Linkers in Different Chemical Environments Lundqvist, M. J.; Galoppini, E.; Meyer, G. J.; Persson P. *J. Phys. Chem. A* **2007**, 111, 1487-1497. DOI: 10.1021/jp064219x

Session IV

*Computational Approaches
to Heterogeneous Solar Photoconversion*

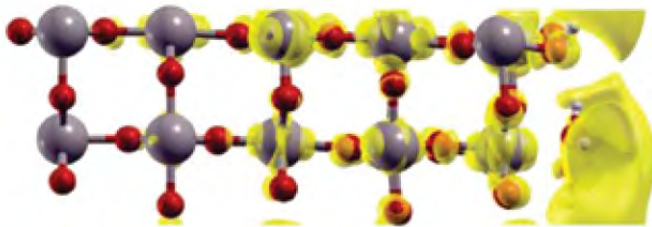
Time-Domain Ab Initio Studies of Nanoscale Structures for Solar Energy Harvesting and Storage

Oleg Prezhdo

Department of Chemistry
University of Washington
Seattle, WA 98195-1700

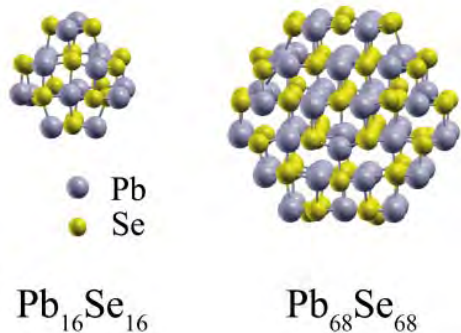
Design of novel materials for solar energy harvesting and storage requires an understanding of the dynamical response on the nanometer scale. A great deal of experimental and theoretical work has been devoted to characterizing the excitation, charge, spin, and vibrational dynamics in molecule-bulk interfaces, semiconductor and metallic quantum dots, carbon nanotubes and graphene ribbons. We have developed state-of-the-art non-adiabatic (NA) molecular dynamics techniques and implemented them within time-dependent density functional theory in order to model the ultrafast processes in these materials at the atomistic level and in real time.

- **Photoinduced electron transfer (ET) across molecular/bulk interfaces [4,6-8,15,23,29]** drives the dye-sensitized semiconductor solar cell. A subject of active research, it creates many challenges due to the stark differences between the quantum states of molecular and periodic systems.



Most recently, we focused on the role of solvent adsorbed at the TiO₂ surface and studied the photoinduced ET dynamics of “wet-electrons”. The simulations indicate that the ET is sub-10fs, in agreement with experiment. Despite large role played by low frequency vibrational modes, the ET is fast due to the strong coupling between the TiO₂ surface and water. The average ET for the system has equal contributions from the adiabatic and NA mechanisms, even though a very broad range of individual ET events is seen in the simulated ensemble. The motions of molecular water have a greater effect on the ET dynamics than the hydroxyl vibrations. The former contribute to both the wet-electron state energy and the water-TiO₂ electronic coupling, while the latter changes only the energy and not the coupling. Delocalized over both water and TiO₂, wet-electrons are supported by a new state created at the interface due to the strong water-TiO₂ interaction. The state cannot exist separately in either material.

- **Quantum dots (QD) [1,3,5,12-14,16,17,20-22,24,30,31]** are quasi-zero dimensional structures with a unique combination of molecular and bulk properties. QDs exhibit new physical phenomena such as the electron-phonon relaxation bottleneck and efficient carrier multiplication, which have the potential to greatly increase the efficiency of solar cells. The efficiency of this process greatly depends on the quality of the QD sample. High-level ab initio calculations on two classes of semiconducting nanocrystals have lead to much



progress on achieving a thorough understanding of the excitation properties of these materials when they are altered with charging, doping or dangling bonds. The calculations show that the

defects introduce new intra-band transitions, blue-shift the optical absorption spectra and push the normal excitonic and multiexcitonic transitions to higher energies. Generally, doping and charging have similar effects on the excited state properties of nanocrystals, while introduction of dangling bonds cause less severe changes, since dangling bonds tend to self-heal.

- **Metal nanoparticles [10,18,27]**

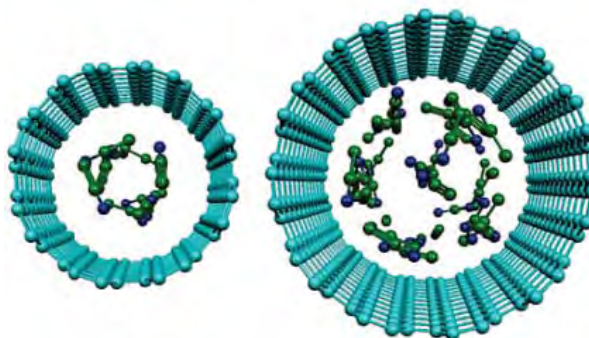
have attracted intense interest in many area of science, including photovoltaics, since plasmon resonances observed in these systems can be used to enhance solar light harvesting. The energy and width of the plasmon resonances play key roles in the applications. We investigated the phonon contribution to the plasmon linewidth, which was largely ignored until recently.



Three types of electronic states in metal nanoparticles were studied corresponding to bulk, surface, and plasmon excitations. The electron-phonon coupling is strongest for bulk states and decreases for surface and plasmon states. The plasmon states dephase within 30–40 fs, which is consistent with the recent experiments. The dephasing time shows weak dependence on the QD size but changes significantly with temperature. The bulk, surface, and plasmon states couple primarily to low-frequency acoustic phonons.

- **Carbon nanotubes (CNT) [9,11,19,24-26,28]** can serve as electron acceptors in solar cell assemblies, possess good chemical stability and large surface area suitable for modification with multifunctional groups. CNTs are exceptional molecular wires, resilient to current-induced failure. Understanding of the electron dynamics mechanisms in CNTs is a key to their use in solar photochemistry. Strong nonradiative decay channels exist in CNT and are responsible for exciton quenching. We simulated the decay of the electronic excitation to its ground state in the (6,4) semiconducting CNT. The decay in the ideal CNT was estimated to occur on a 150 ps time scale and was only weakly dependent on temperature. Defects decreased the excited state lifetime to tens of picoseconds, rationalizing the multiple decay time scales seen in experiments.

Nanoporous activated composite carbon films generate high specific capacitance, laying the foundation for a new generation of supercapacitors. The design requires polar but aprotic solvents such as acetonitrile (AN). We predicted that in contrast to water, which shows inhomogeneous variation of both translational and rotational diffusion with CNT diameter, the diffusion coefficient of AN changes uniformly and can be described by a



simple analytic model. At the same time, the reorientation dynamics of AN vary irregularly in smaller CNTs because of specific packing. The uniform translational diffusion of AN is critical for stable performance of the new generation of supercapacitors for solar energy storage.

Our time-domain atomistic simulations create a detailed picture of these materials. By comparing and contrasting their properties, we provide a unifying description of quantum dynamics on the nanometer scale, resolve several highly debated issues, and generate theoretical guidelines for development of novel systems for solar energy harvesting and storage.

DOE Sponsored Publications 2007-2010

Reviews, Feature Articles and Book Chapters

1. S. A. Fischer, C. M. Isborn, O. V. Prezhdo, "Excited states and optical absorption of small semiconducting clusters: dopants, defects and charging", *Chem. Science*, submitted.
2. S. Garaschuk, V. Rassolov and O. V. Prezhdo "Semiclassical Bohmian dynamics", *Rev. Comp. Chem.*, in press.
3. O. V. Prezhdo "Photoinduced dynamics in semiconductor quantum-dots: insights from time-domain ab initio studies", *Acc. Chem. Res.*, **42**, 2005 (2009).
4. O. V. Prezhdo, W. R. Duncan, V. V. Prezhdo, "Photoinduced electron dynamics at semiconductor interfaces: a time-domain ab initio prospective", *Prog. Surf. Sci.*, **84**, 39 (2009).
5. O. V. Prezhdo, "Multiple excitons and electron-phonon bottleneck in semiconductor quantum dots: Insights from ab initio studies", *Chem. Phys. Lett.–Frontier Article*, **460**, 1 (2008).
6. O. V. Prezhdo, W. R. Duncan, V. V. Prezhdo, "Dynamics of the photoexcited electron at the chromophore-semiconductor interface", *Acc. Chem. Res.*, **41**, 339 (2008).
7. O. V. Prezhdo and W. R. Duncan "Ultrafast heterogeneous electron transfer" in Book *Analysis and Control of Ultrafast Photoinduced Reactions*, Series in Chemical Physics Vol. 87, O. Kühn, L. Wöste (Eds.), Springer, Heidelberg, 2007.
8. W. R. Duncan, O. V. Prezhdo, "Theoretical studies of photoinduced electron transfer in dye-sensitized TiO₂", *Ann. Rev. Phys. Chem.*, **58**, 143 (2007).

Articles in Peer-Reviewed Journals

9. A. Ueta, Y. Tanimura, O. V. Prezhdo, "Distinct infrared spectral signatures of the 1,2- and 1,4-fluorinated single-walled carbon nanotubes: A molecular dynamics study", *J. Phys. Chem. Lett.*, in press.
10. Z. Guo, W.-Z. Liang, O. V. Prezhdo, "Ab initio study of phonon-induced dephasing of plasmon excitations in silver quantum dots", *Phys. Rev. B*, in press.
11. V. V. Chaban, O. N. Kalugin, B. F. Habenicht, O. V. Prezhdo, "The influence of the rigidity of a carbon nanotube on the structure and dynamics of confined methanol", *J. Phys. Soc. Japan*, in press.
12. S. A. Fischer, A. B. Madrid, C. M. Isborn, O. V. Prezhdo, "Multiple exciton generation in small Si clusters: A high-level, ab initio study", *J. Phys. Chem. Lett.*, **1**, 232 (2010).
13. Kim H.-D., A. B. Madrid, O. V. Prezhdo, "Symmetric band structure and asymmetric ultrafast electron-hole relaxation in silicon and germanium quantum dots: time-domain ab initio simulation", *Dalton Transact., Solar Energy Conversion*, **45**, 10069 (2009).
14. A. B. Madrid, H.-D. Kim, O. V. Prezhdo, "Phonon-induced dephasing of excitons in silicon quantum dots: multiple exciton generation, fission and luminescence", *ACS-Nano*, **3**, 2487 (2009).

15. S. A. Fischer, W. R. Duncan, O. V. Prezhdo, "Ab initio nonadiabatic molecular dynamics of wet-electrons on the TiO₂ surface", *J. Am. Chem. Soc.*, **131**, 15483 (2009).
16. C. M. Isborn, O. V. Prezhdo, "Quantum dot charging quenches multiple exciton generation: first-principles calculations on small PbSe clusters", *J. Phys. Chem. C*, **113**, 12617 (2009).
17. H. Bao, B. F. Habenicht, O. V. Prezhdo, X. Ruan, "Temperature dependence of hot-carrier relaxation in a PbSe quantum dot: An ab initio study", *Phys. Rev. B*, **79**, 235306 (2009).
18. D. S. Kilin, K. L. Tsemekhman, S. V. Kilina, A. V. Balatsky, O. V. Prezhdo, "Photoinduced conductivity of a DNA-templated composite nanowire", *J. Phys. Chem.*, **113**, 4549 (2009).
19. D. A. Yarotski, S. V. Kilina, A. A. Talin, S. Tretiak, O. V. Prezhdo, A. V. Balatsky, A. J. Taylor "Scanning tunneling microscopy of DNA-wrapped carbon nanotubes", *Nano Lett.*, **9**, 12 (2009).
20. S. V. Kilina, D. S. Kilin, O. V. Prezhdo, "Breaking the phonon bottleneck in PbSe and CdSe quantum dots: time-domain density functional theory of charge carrier relaxation", *ACS-Nano*, **3**, 93 (2009).
21. H. Kamisaka, S. V. Kilina, K. Yamashita, O. V. Prezhdo "Ab Initio study of temperature and pressure dependence of energy and phonon-induced dephasing of electronic excitations in CdSe and PbSe quantum dots", *J. Phys. Chem. C.*, **112**, 7800 (2008).
22. C. M. Isborn, S. V. Kilina, X. Li, O. V. Prezhdo, "Generation of multiple excitons in PbSe and CdSe quantum dots by direct photoexcitation: first-principles calculations on small PbSe and CdSe clusters", *J. Phys. Chem. C*, **112**, 18291 (2008).
23. W. R. Duncan, O. V. Prezhdo, "Temperature independence of the photoinduced electron injection in dye-sensitized TiO₂ rationalized by ab initio time-domain density functional theory", *J. Am. Chem. Soc.*, **130**, 9756 (2008).
24. B. F. Habenicht, S. V. Kilina, O. V. Prezhdo, "Comparative analysis of electron-phonon relaxation in a semiconducting carbon nanotube and a PbSe quantum dot", *Pure & Appl. Chem.*, **80**, 1433 (2008).
25. B. F. Habenicht, O. N. Kalugin, O. V. Prezhdo, "Ab initio study of phonon-induced dephasing of electronic excitations in narrow graphene nanoribbons", *Nano Lett.*, **8** 2510 (2008).
26. O. N. Kalugin, V. V. Chaban, V. V. Loskutov, O. V. Prezhdo, "Uniform diffusion of acetonitrile inside carbon nanotubes favors supercapacitor performance", *Nano Lett.*, **8**, 2126 (2008).
27. D. S. Kilin, O. V. Prezhdo, Y. Xia, "Shape-controlled synthesis of silver nanoparticles: Ab initio study of preferential surface coordination with citric acid", *Chem. Phys. Lett.*, **458**, 113 (2008).
28. B. F. Habenicht, H. Kamisaka, K. Yamashita, O. V. Prezhdo, "Ab initio study of vibrational dephasing of electronic excitations in semiconducting carbon nanotubes", *Nano Lett.* **7**, 3260 (2007).
29. W. R. Duncan, C. F. Craig, O. V. Prezhdo, "Time-domain ab initio study of charge relaxation

- and recombination in dye-sensitized TiO₂”, *J. Am. Chem. Soc.*, **129** 8528 (2007).
30. D. S. Kilin, K. Tsemekhman, O. V. Prezhdo, E. I. Zenkevich, and C. v. Borczykowski, “Ab initio study of exciton transfer dynamics from a core-shell semiconductor quantum-dot to a porphyrin-sensitizer”, *J. Photochem. Photobiol. A – Chem., Spec. Iss. “Theoretical Aspects of Photoinduced Processes in Complex Systems”*, **190** 342 (2007).
31. S. V. Kilina, C. F. Craig, D. S. Kilin, O. V. Prezhdo, “Ab initio time-domain study of phonon-assisted relaxation of charge carriers in a PbSe quantum dot”, *J. Phys. Chem. C* **111** 4871 (2007).

Theoretical Studies of Photoactive Molecular Systems: Electron Transfer, Energy Transport, and Optical Spectroscopy

Richard A. Friesner
Department of Chemistry
Columbia University
New York, NY 10027

The present project has two principal long term goals. The first is to develop computational methodology that is capable of modeling charge separation, electron transport, energy transport, and optical spectroscopy in complex molecules and materials. The second objective is to apply these methods to systems of interest to the DOE solar photochemistry program. We have made progress in both of these areas in the current granting period. In the methods development area, we have focused on an intensive examination of the accuracy and reliability of density functional theory (DFT) and have developed a highly promising, novel approach to improving the quality of DFT results. We have also implemented TDDFT excited state methods in Jaguar, in collaboration with Todd Martinez at the University of Illinois. In applications, we are focusing at present on TiO₂ nanoparticles and understanding charge transport in the Gratzel cell, and on modeling metal-containing catalysts for water oxidation.

We have made substantial progress in developing our novel localized orbital correction (LOC) DFT method. A number of papers have already been published (some of which are enumerated below [4,8]) but there are also a large number of new improvements that are currently in progress. Below we briefly summarize the current status of the method, and where we expect to be in a 3-6 month period as the new developments are completed.

The current DFT-LOC algorithm is capable of remarkably accurate predictions for thermochemistry (both reaction energies, transition states, ionization potentials, electron affinities) for molecules containing first and second row atoms, with average errors around 1 kcal/mole, comparable to what is achieved by coupled cluster theory at a dramatically lower cost. Very large data sets have been examined and the methodology appears to be robust (for example, 105 chemical reactions are included in our data set for evaluating transition state energetics). Transition metals continue to pose a severe challenge for all DFT methods. In ref. 4, atoms and small gas phase molecules are examined, and the average error is reduced from ~5-10 kcal/mole to ~1-1.5 kcal/mole for ionization potentials and bond energies.

Our current efforts are focused on building a complete initial version of the DFT-LOC method that can be implemented in our Jaguar electronic structure code and distributed to users, including experimental as well as theoretical groups. Such a complete method is expected to possess the following features: (1) applicability to a continuous potential surface rather than just stationary points such as minimum energy and transition state configurations; (2) more accurate treatment of typical transition metal complexes including relative energies of spin configurations and bond energies; (3) realistic treatment of dispersion energy which is not present in many widely used DFT functionals.

To construct this model we add to the standard B3LYP DFT functional a molecular mechanics functions which contains localized orbital corrections as well as corrections for dispersion

energies. We have fit our dispersion model to ~1000 high level calculations taken from the literature via an automated search program which downloads relevant structures and energies; this is a much larger data set than has been used previously. Average errors for our current dispersion model are in the range of ~0.5 kcal/mole for intermolecular interactions for nonpolar, hydrogen bonded, and charged complexes, a huge improvement over the native performance of B3LYP. The combination of this model with the LOC model provides a robust description of compounds containing first and second row atoms. For transition metal containing systems, we are currently studying a data set of octahedral complexes in an attempt to understand the systematic errors made by B3LYP in calculating the different energies of different spin states.

Our research plan for the current DOE funding cycle was to work on the new DFT methods until sufficient progress had been made for new insights to be obtained in the applications efforts. We believe that this point has been reached and consequently we have begun new calculations on TiO₂ nanoparticles and water oxidation catalysts. For the TiO₂ nanoparticle work, conducted in collaboration with Dr. Louis Brus, the first step is to build and converge models that are substantially larger than our previous efforts (ref. [7]) and we have preliminary results for a model that is 3x larger than the largest previous cluster we had investigated, including passivation with the appropriate water derived ligands. This model, and others of a similar size, will enable us to investigate the differences between surface and interior sites in the cluster which is critical to building an atomic level description of the trapping states in the material, a key objective of the project.

The study of water oxidation catalysts is a new effort for this research program. We have started by looking at a number of ruthenium based systems developed by Meyer and coworkers. Our initial goal here is to make sure we can converge wavefunctions and geometries, and generally obtain reasonable results as compared to what is in the literature. However, a fundamental objective is to use the insights we have gained from our localized orbital correction approach, and the transition metal test cases we have examined, to assign better energetics to the various possible reactants, products, and transition states. We have documented the errors made by current DFT methods and noted that they are particularly large, and erratically distributed, for transition metal containing systems. In addition to the intrinsic errors in functionals, there are also serious concerns about converging the wavefunction to the ground state for various complicated systems, and this problem becomes worse when there are multiple metals. We have built machinery to automatically cycle through a large number of initial guesses to make sure that we are examining all possible electronic states so as not to become trapped in an excited state. The combination of this protocol with the LOC based corrections, and a proper treatment of dispersion interactions, should yield energetics that can be appropriately compared with experimental data.

Going forward, our principal goals are to deliver our improved DFT method to the user community (including scientists in the DOE program) and to advance our investigations of the chemistry of the TiO₂ and water oxidation systems. A hypothesis we will be examining for the Gratzel cell and related systems is that small ions such as Li⁺ or H⁺ move with the hopping electrons to the electrode and are needed to stabilize the trapping states at suitable energies. There is substantial experimental evidence that this hypothesis may be correct. For the water oxidation systems, we are not yet at the point where the crucial problems with the calculations can be identified, but we hope to reach that point during the next year.

DOE Sponsored Publications 2007-2010

1. Chen, Yiing-Rei, Lei Zhang, Mark S. Hybertsen, Theoretical study of trends in conductance for molecular junctions formed with armchair carbon nanotube electrodes, *Phys. Rev. B*, 76, 11, 115408 (2007).
2. Ko, Chaehyuk, David K. Malick, Dale A. Braden, Richard A. Friesner and Todd J. Martinez, Pseudospectral time-dependent density functional theory, *J. Chem. Phys.*, 128, 10, 104103, (2008).
3. Bochevarov, Artem D., and Richard A. Friesner, The densities produced by the density functional theory: Comparison to full configuration interaction, *J. Chem. Phys.*, 128, 3, 034102 (2008)
4. Rinaldo, David, Li Tian, Jeremy N. Harvey, and Richard A. Friesner, Density Functional Localized Orbital Corrections for Transition Metals, *J. Chem. Phys.*, 129, 164108-164123 (2008).
5. Goldfeld, Dahlia A., Artem D. Bochevarov, and Richard A. Friesner, Localized orbital corrections applied to thermochemical errors in density functional theory: The role of basis set and application to molecular reactions, *J. Chem. Phys.*, 129, 21, 214105, (2008).
6. Schneebeli, Severin T., Michelle Lynn Hall, Ronald Breslow, and Richard Friesner, Quantitative DFT Modeling of the Enantiomeric Excess for Dioxirane-Catalyzed Epoxidations, *J. Am. Chem. Soc.*, 131, 11, 3965-3973 (2009).
7. Wang, Ting, and Richard A. Friesner, Computational Modeling of the Electronic Structure of Oligothiophenes with Various Side Chains, *J. Phys. Chem. C*, 113, 6, 2553-2561 (2009).
8. Blagojevic, Vladimir, Yiing-Rei Chen, Michael Steigerwald, Louis Brus, and Richard A. Friesner, A. Quantum Chemical Investigation of Cluster Models for TiO₂ Nanoparticles with Water-Derived Ligand Passivation: Studies of Excess Electron States and Implications for Charge Transport in the Gratzel Cell, *J. Phys. Chem. C*, 113, 46, 19806-19811 (2009).

Session V

Charge Transfer in Organic Systems

Charge Transport in Smart DNA Hairpins and Dumbbells

Frederick D. Lewis

Department of Chemistry, Northwestern University, Evanston, IL 60201

The principle objective of this project is to investigate the mechanism and dynamics of photoinduced charge separation processes in systems which possess an electron donor and electron acceptor separated by aromatic spacers having a face-to-face or π -stacked geometric relationship. The hydrogen-bonded base pairs which constitute the core of duplex DNA form an extended one-dimensional π -stacked array with an average stacking distance of 3.4 Å. The possibility that these base pairs might serve as a pathway for charge transport was advanced nearly 50 years ago. Our approach to the study of electron transfer in DNA is based on the use of synthetic conjugates in which a chromophore serves as a linker or capping group in stable hairpin structures (Chart 1). Second generation systems possess chromophores at both ends of a dumbbell structure (Chart 1). Selective excitation of the chromophore can effect the injection of charge (electrons or holes) into the base pair domains. The chromophores also serve as reporters for the dynamics and efficiency of charge separation in these “smart” hairpin and dumbbell structures. The published results of this project during the period 2007-2010 are reported in the references.¹⁻¹¹

Singlet and Triplet State Hole Injection in Hairpin Systems. The mechanism and dynamics of charge separation and charge recombination in synthetic DNA hairpins possessing a stilbenedicarboxamide linker (Chart 2) and a single guanine-cytosine base pair have been reinvestigated.³ Reversible hole injection to neighboring adenines resulting in the formation of the stilbene-adenine contact radical ion pair occurs on the picosecond time scale. The mechanism for charge separation has been revised from single step superexchange to a multi-step process consisting of hole injection followed by hole transport and hole trapping by guanine.

The dynamics of charge separation in hairpins possessing a single G-C base pair and perylenedicarboxamide (Ped)¹ and pyrenedicarboxamide (Pyd)⁴ linkers and a pyrenemonoamide (Pya)⁸ capping group were also investigated. The behavior of Pyd hairpin linker is similar to that of the Sa linker. Reversible hole injection into adenine followed by hole migration and trapping at guanine results in the formation of long-lived radical ion pairs.² The longer lifetime for the Pyd vs. Sa charge-separated state is a consequence of slower charge recombination for the Pyd systems. The Ped linker and Pya capping group are capable of oxidizing neighboring guanine but not adenine and thus do not generate long-lived radical ion pairs. Investigation of the

Chart 1

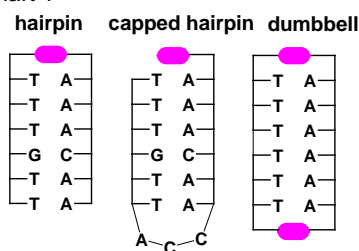
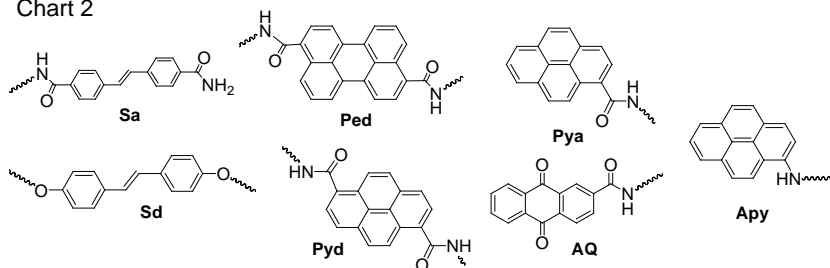


Chart 2



structure of a Pya conjugate by 2D-NMR methods reveals that the pyrene is intercalated between the two terminal base pairs in preference to serving as a capping group for the terminal base pair (Figure 1).



Figure 1

The use of a triplet electron acceptor for hole injection offers the potential advantage of the formation of triplet charge-separated states for which charge recombination is spin forbidden. The dynamics of singlet and triplet charge transfer in DNA-anthraquinone (AQ) conjugates has been investigated by means of femtosecond time-resolved transient absorption spectroscopy.¹⁰ Singlet charge separation and intersystem crossing are found to occur on similar time scales, resulting in the formation of both short-lived singlet radical ion pairs and long-lived triplet radical ion pairs. The dynamics of triplet radical ion pair charge recombination is under continued investigation.

Singlet State Electron Injection in Hairpin Systems. The dynamics of electron injection and quantum yields for photoinduced dehalogenation of halouracils have been investigated in two series of DNA hairpins which possess either an aminopyrene (Apy) or a pyrenecarboxamide (Pya) capping group.^{9,11} The substituted pyrene chromophore serves as an electron donor and is separated from a bromo- or iodouracil electron trap by 1 to 7 A-T base pairs. The Apy chromophore is the stronger electron donor and is capable of reducing both A-T base pairs and halouracils; whereas the Pya is selective for the reduction of the halouracils. Steady-state irradiation in the presence of 0.1 M *i*-PrOH results in loss of halogen and conversion of the halouracil-containing conjugates to the corresponding uracil-containing conjugates in high yield. Dehalogenation occurs via a multi-step mechanisms consisting of electron injection, electron transport to the halouracil, loss of halide, and trapping of the uracilyl radical. Quantum yields for product formation decrease by a factor of two for each additional A-T base pair interposed between the aminopyrene and bromouracil. This distance dependence is similar to that observed in our studies of DNA hole transport in stilbene donor-acceptor capped hairpins; however the quantum yields for product formation are much lower for the Apy conjugates as a consequence of more rapid charge recombination.

Charge Separation in Dumbbell Systems. Nicked dumbbell conjugates possessing donor and acceptor stilbenes (Sa and Sd) separated by a variable number and sequence of base pairs have been employed in our studies of singlet charge separation.^{2,6,7} Hole transport in conjugates possessing either homo-purine (polyA or polyG) or alternating (AT, AG, GC) base-pair sequences is slower than charge recombination, resulting in inefficient charge separation. Higher efficiencies are achieved in diblock polypurine sequences having several adenines followed by a polyG sequences. The adenines in the A-block serve as a rectifier, preventing charge recombination once the hole has entered the G-block. The efficiency of charge separation is independent of the number of bases once the hole has entered the G-block. However, rate constants for hole arrival at the end of the duplex continue to decrease as the number of base pairs increases, in accord with a random walk process having a time constant of ca. 1 ns/base-pair. We have also investigated the dynamics of symmetry-breaking charge separation in dumbbells having two Sa linkers.⁵

DOE Sponsored Publications 2007-2010¹⁻¹¹

- (1) Lewis, F. D.; Zhang, L. G.; Kelley, R. F.; McCamant, D.; Wasielewski, M. R. A perylenedicarboxamide linker for DNA hairpins. *Tetrahedron* **2007**, *63*, 3457-3464.
- (2) Lewis, F. D.; Daublain, P.; Cohen, B.; Vura-Weis, J.; Shafirovich, V.; Wasielewski, M. R. Dynamics and efficiency of DNA hole transport via alternating AT versus poly(A) sequences. *J. Am. Chem. Soc.* **2007**, *129*, 15130-15131.
- (3) Lewis, F. D.; Zhu, H.; Daublain, P.; Sigmund, K.; Fiebig, T.; Raytchev, M.; Wang, Q.; Shafirovich, V. Getting to guanine: mechanism and dynamics of charge separation and charge recombination in DNA revisited. *Photochem. Photobiol. Sci.* **2008**, *7*, 534-539.
- (4) Daublain, P.; Siegmund, K.; Hariharan, M.; Vura-Weis, J.; Wasielewski, M. R.; Lewis, F. D.; Shafirovich, V.; Wang, Q.; Raytchev, M.; Fiebig, T. Photoinduced charge separation in pyrenedicarboxamide-linked DNA hairpins. *Photochem. Photobiol. Sci.* **2008**, *7*, 1501-1508.
- (5) Lewis, F. D.; Daublain, P.; Zhang, L.; Cohen, B.; Vura-Weis, J.; Wasielewski, M. R.; Shafirovich, V.; Wang, Q.; Raytchev, M.; Fiebig, T. Reversible bridge-mediated excited-state symmetry breaking in stilbene-linked DNA dumbbells. *J. Phys. Chem. B* **2008**, *112*, 3838-3843.
- (6) Lewis, F. D.; Daublain, P.; Cohen, B.; Vura-Weis, J.; Wasielewski, M. R. The influence of guanine on DNA hole transport efficiency. *Angew. Chem. Int. Ed.* **2008**, *47*, 3798-3800.
- (7) Vura-Weis, J.; Wasielewski, M. R.; Thazhathveetil, A. K.; Lewis, F. D. Efficient charge transport in DNA diblock oligomers. *J. Am. Chem. Soc.* **2009**, *131*, 9722-9727.
- (8) Siegmund, K.; Daublain, P.; Wang, Q.; Trifonov, A.; Fiebig, T.; Lewis, F. D. Structure and photoinduced electron transfer in DNA hairpin conjugates possessing a tethered 5'-pyrenecarboxamide. *J. Phys. Chem. B* **2009**, *113*, 16276-16284.
- (9) Daublain, P.; Thazhathveetil, A. K.; Wang, Q.; Trifonov, A.; Fiebig, T.; Lewis, F. D. Dynamics of photochemical electron injection and efficiency of electron transport in DNA. *J. Am. Chem. Soc.* **2009**, *131*, 16790-16797.
- (10) Lewis, F. D.; Thazhathveetil, A. K.; Zeidan, T. A.; Vura-Weis, J.; Wasielewski, M. R. Dynamics of ultrafast singlet and triplet charge transfer in anthraquinone-DNA conjugates. *J. Am. Chem. Soc.* **2010**, *132*, 444-445.
- (11) Daublain, P.; Thazhathveetil, A. K.; Shafirovich, V.; Wang, Q.; Trifonov, A.; Fiebig, T.; Lewis, F. D. Dynamics and efficiency electron injection and transport in DNA using pyrenecarboxamide as electron donor and 5-bromouracil as electron acceptor. *J. Phys. Chem. B* **2010**, *asap*.

Structural and Electronic Criteria for Long Distance Charge and Energy Transport

Amy M. Scott, Annie Butler Ricks, Tomoaki Miura, Michael T. Colvin, Raanan Carmieli, and
Michael R. Wasielewski

Department of Chemistry and Argonne-Northwestern Solar Energy Research (ANSER) Center
Northwestern University, Evanston, IL 60208-3113

Scope of the project. We are investigating several related, fundamental problems critical to developing an integrated system for artificial photosynthesis. Studies are in progress to understand how structural dynamics control long distance charge separation and storage in donor-bridge-acceptor (D-B-A) systems by attacking this problem on time scales ranging from femtoseconds to milliseconds using both transient optical and EPR spectroscopy. We are developing the fundamental requirements for energy and charge transport in self-assembling systems having emergent properties as a result of the assembly. We are also exploring how multiple photoinduced charge separation pathways can be used to accumulate redox equivalents at a single redox site to drive catalysts for fuel formation.

Recent Results. Superexchange is the virtual mediation of charge transport from donor to acceptor by bridge orbitals energetically well-separated from those of the donor and acceptor. Charge transfer occurs in a single step with a rate that decays exponentially with distance that is described by the damping factor β . In contrast, sequential charge transport or hopping occurs from the donor to the bridge, as well as between bridge sites, and is weakly distance dependent ($\sim 1/r$) allowing charge to move efficiently at long distances. Which mechanism prevails depends on 1) the magnitude of the donor-to-bridge charge injection barrier as characterized by the energy levels of the system, 2) the energy required for internal and solvent nuclear reorganization, and 3) the overall electronic coupling matrix element, V_{DA} , which depends on the donor-bridge, bridge-bridge, and bridge-acceptor couplings, which, in turn, depend on D-B-A structural dynamics.

For charge recombination (CR), a fourth criterion must be added, that of spin selectivity. The photogenerated singlet radical ion pair (RP) may undergo electron-nuclear hyperfine coupling-induced radical pair intersystem crossing (RP-ISC) to produce the triplet RP, $^1(D^+ \cdot B \cdot A^-) \rightarrow ^3(D^+ \cdot B \cdot A^-)$. The subsequent CR is spin selective; i.e. the singlet RP recombines to the singlet ground state and the triplet RP recombines to yield the neutral local triplet (Figure 1). Controlling spin selectivity can be used to limit energy-wasting CR in artificial photosynthetic systems.

A series of donor-bridge-acceptor (D-B-A) systems have been synthesized in which the same donor, 3,5-dimethyl-4-(9-anthracenyl)-julolidine (DMJ-

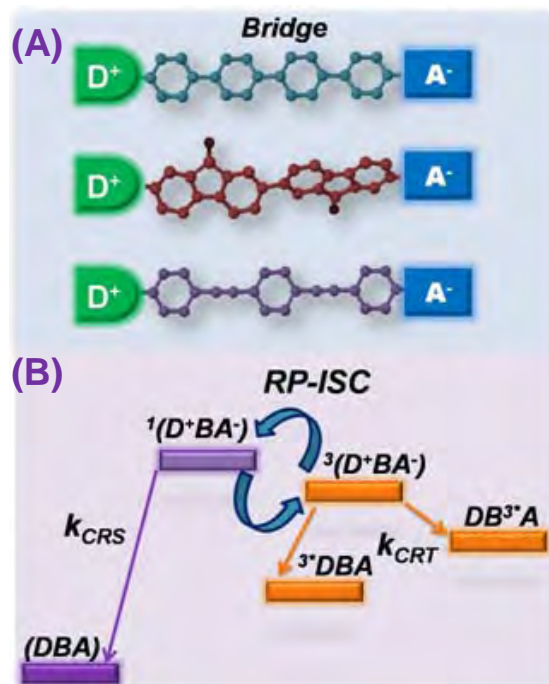


Figure 1. (A) D-B-A systems, where B = FN_{1,3}, PE_{1,3}P, and Ph_{1,5} used in this study. (B) Spin-selective charge transfer scheme.

An), and the same acceptor, naphthalene-1,8:4,5-bis(dicarboximide) (NI), are linked by *p*-oligophenylene (Ph_n) bridging units ($n = 1-5$), fluorenone ($n = 1-3$) (FN_n) and *p*-phenylethynylene ($n = 1-3$) (PE_nP). Photoexcitation of DMJ-An in these systems results in rapid formation of a singlet RP, which undergoes electron-nuclear hyperfine coupling-induced RP-ISC to produce the triplet RP, i.e. $^1(\text{D}^{+\cdot}\text{-B-A}^{\cdot-}) \rightarrow ^3(\text{D}^{+\cdot}\text{-B-A}^{\cdot-})$. Subsequent CR is spin selective; i.e. the singlet RP recombines to the singlet ground state and the triplet RP recombines to yield the neutral local triplet. By monitoring the yield of local triplet production as a function of applied magnetic field, B , the magnitude of the spin-spin exchange interaction, $2J$, can be measured directly, and can be used to estimate V_{DA} because $2J \propto V_{\text{CR}}^2$. Magnetic field effects and time-resolved EPR spectroscopy were used to measure $2J$, and a kinetic analysis of the MFE data was used to separate the rate constants for the spin-selective CR pathways. The data show that the β values for the singlet and triplet CR pathways for the *p*-phenylethynylene and fluorenone bridges are very similar, yet the corresponding β values for the *p*-phenylene bridges are very different, which implies that β for both singlet and triplet CR is *system dependent, not bridge specific*.

Triplet-triplet energy transfer is of increasing importance in molecular systems for both artificial photosynthetic and photovoltaics. Triplet energy transfer (TT) can be analyzed formally as simultaneous hole and electron transfers. TT in molecular systems generally occurs by either strongly distance-dependent single-step tunneling or weakly distance-dependent multi-step hopping. We have studied a series of π -stacked molecules consisting of a benzophenone donor, 1-3 fluorene bridges, and a naphthalene acceptor, and studied the rate of TT from benzophenone to naphthalene across the fluorene bridge using femtosecond transient absorption spectroscopy (Figure 2). We have shown that the dominant TT mechanism switches from tunneling to wire-like hopping between bridge lengths 1 and 2. This represents the first such crossover observed for TT determined by direct observation of the bridge-occupied state.

Future Plans. Our overall plan and main goal is to understand the properties of photodriven redox systems well enough to produce integrated artificial photosynthetic systems that harvest light, separate charge and deliver that charge to catalysts for solar fuels formation.

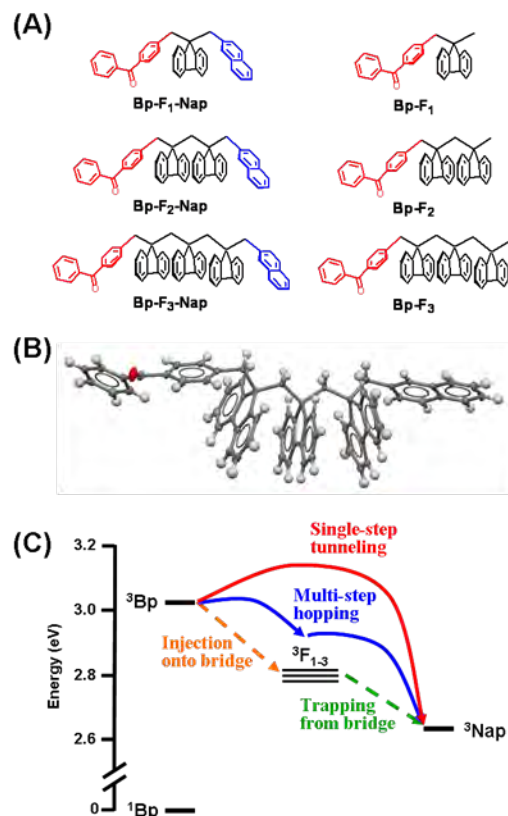


Figure 2. (A) Structures of Bp-F_n and Bp-F_n-Nap molecules. (B) X-ray structure of **Bp-F₃-Nap** showing the cofacial π -stacked arrangement of all chromophores. (C) Energy level diagram of Bp-F_n-Nap showing two mechanisms of TT: single-step tunneling from Bp to Nap, or multi-step tunneling comprised of injection onto the F_n bridge followed by trapping by Nap. The triplet energy of the F_n bridges is independent of n to within 0.02 eV.

Publications Resulting from DOE Grant No. DE-FG02-99ER14999 (2007-2010)

1. Photoinduced Charge Separation in Self-Assembled Cofacial Pentamers of Zinc-5,10,15,20-Tetrakis(perylene-3,4,9,10-tetracarboximide)porphyrin, M. J. Ahrens, R. F. Kelley, Z. E. X. Dance, and M. R. Wasielewski, *Phys. Chem. Chem. Phys.* **9**, 1469-1478 (2007).
2. A Perylenedicarboxamide Linker for DNA Hairpins, F. D. Lewis, L. Zhang, R. F. Kelley, D. McCamant, and M. R. Wasielewski, *Tetrahedron* **63**, 3457-3464 (2007).
3. Solution-Phase Structure of an Artificial Foldamer: X-Ray Scattering Study, R. F. Kelley, B. Rybtchinski, M. T. Stone, J. S. Moore, and M. R. Wasielewski, *J. Am. Chem. Soc.* **129**, 4114-4115 (2007).
4. Ultrafast Energy Transfer within Cyclic Self-Assembled Chlorophyll Tetramers, R. F. Kelley, R. H. Goldsmith, and M. R. Wasielewski, *J. Am. Chem. Soc.* **129**, 6384-6385 (2007).
5. Intramolecular Electron Transfer within a Covalent, Fixed Distance Donor-Acceptor Molecule in an Ionic Liquid, J. V. Lockard and M. R. Wasielewski, *J. Phys. Chem. B*, **111**, 11638-11641 (2007).
6. Scaling Laws for Charge Transfer in Multiply Bridged Donor-Acceptor Molecules in a Dissipative Environment, R. H. Goldsmith, M. R. Wasielewski, and M. A. Ratner, *J. Am. Chem. Soc.* **129**, 13066-13071 (2007).
7. Controlling Energy and Charge Transfer in Linear Chlorophyll Dimers, R. F. Kelley, M. J. Tauber, T. M. Wilson, and M. R. Wasielewski, *Chem. Commun.*, 4407-4409 (2007).
8. Dynamics and Efficiency of DNA Hole Transport via Alternating AT vs. poly(A) Sequences, F. D. Lewis, P. Daublain, B. Cohen, J. A. Vura-Weis, and M. R. Wasielewski *J. Am. Chem. Soc.* **129**, 15130-15131 (2007).
9. Direct Observation of the Preference of Hole Transfer Over Electron Transfer for Radical Ion Pair Recombination in Donor-Bridge-Acceptor Molecules, Z. E. X. Dance, M. J. Ahrens, A. M. Vega, A. Butler-Ricks, D. W. McCamant, M. A. Ratner, and M. R. Wasielewski, *J. Am. Chem. Soc.* **130**, 830-832 (2008).
10. Excited Singlet States of Covalently Bound, Cofacial Dimers and Trimers of Perylene-3,4:9,10-bis(dicarboximide)s, J. M. Giaimo, J. V. Lockard, L. E. Sinks, A. M. Vega, T. M. Wilson, and M. R. Wasielewski, *J. Phys. Chem. A* **112**, 2322-2330 (2008).
11. Reversible Bridge-Mediated Excited State Symmetry Breaking in Stilbene-Linked DNA Dumbbells, F. D. Lewis, P. Daublain, L. Zhang, B. Cohen, J. A. Vura-Weis, M. R. Wasielewski, V. Shafirovich, Q. Wang, and T. Fiebig, *J. Phys. Chem. B* **112**, 3838-3843 (2008).
12. Intramolecular Energy Transfer within Butadiyne-Linked Chlorophyll and Porphyrin Dimer-Faced, Self-assembled Prisms, R. F. Kelley, S. J. Lee, T. M. Wilson, Y. Nakamura, D. M. Tiede, A. Osuka, J. T. Hupp, and M. R. Wasielewski, *J. Am. Chem. Soc.* **130**, 4277-4284 (2008).
13. Intersystem Crossing Mediated by Photoinduced Intramolecular Charge Transfer: Julolidine-Anthracene Donor-Acceptor Molecules, Z. E. X. Dance, S. M. Mickley, M. J. Ahrens, A. Butler-Ricks, M. A. Ratner, and M. R. Wasielewski, *J. Phys. Chem. A* **112**, 4194-4201 (2008).
14. Fast Energy Transfer within a Self-Assembled Cyclic Porphyrin Tetramer, R. A. Jensen, R. F. Kelley, S.-J. Lee, M. R. Wasielewski, J. T. Hupp, and D. M. Tiede, *Chem Commun.* 1886-1888 (2008).

15. Challenges in Distinguishing Superexchange and Hopping Mechanisms of Intramolecular Charge Transfer Through Fluorene Oligomers, R. H. Goldsmith, O. DeLeon, T. M. Wilson, D. Finkelstein-Shapiro, M. A. Ratner, and M. R. Wasielewski, *J. Phys. Chem. A* **112**, 4410-4414 (2008).
16. The Influence of Guanine on DNA Hole Transport Efficiency, F. D. Lewis, P. Daublain, B. Cohen, J. Vura-Weis, and M. R. Wasielewski, *Angew. Chem. Int. Ed.* **47**, 3798-3800 (2008).
17. Unexpectedly Similar Charge Transfer Rates Through Benzo-annulated Bicyclo[2.2.2]octanes, R. H. Goldsmith, J. Vura-Weis, A. M. Vega, S. Borkar, A. Sen, M. A. Ratner, and M. R. Wasielewski, *J. Am. Chem. Soc.* **130**, 7659-7669 (2008).
18. Photoinduced Charge Separation in Pyrenedicarboxamide-Linked DNA Hairpins, P. Daublain, K. Siegmund, M. Hariharan, J. Vura-Weis, M. R. Wasielewski, F. D. Lewis, V. Shafirovich, Q. Wang, M. Raytchev, and T. Fiebig, *Photochem. Photobio. Sci.* **7**, 1501-1508 (2008).
19. Framework Reduction and Alkali-metal Doping of a Triply-interpenetrated Metal-organic Framework Enhances H₂ Uptake, K. L. Mulfort, T. M. Wilson, M. R. Wasielewski, and J. T. Hupp, *Langmuir* **25** 503-508 (2008).
20. Temperature Dependent Conformational Change of meso-Hexakis(pentafluorophenyl) [28]Hexaphyrins(1.1.1.1.1.1) into Möbius Structures, K. S. Kim, Z. S. Yoon, A. B. Ricks, J.-Y. Shin, S. Mori, J. Sankar, S. Saito, Y. M. Jung, M. R. Wasielewski, A. Osuka, and D. Kim, *J. Phys. Chem. A* **113**, 4498-4506 (2009).
21. Towards a n-Type Molecular Wire: Electron Hopping within Linearly-linked Perylenediimide Oligomers, T. M. Wilson, M. J. Tauber, and M. R. Wasielewski, *J. Am. Chem. Soc.* **131**, 8952-8957 (2009).
22. Direct Measurement of Photoinduced Charge Separation Distances in Donor-Acceptor Systems for Artificial Photosynthesis using OOP-ESEEM, R. Carmieli, Q. Mi, A. Butler Ricks, E. M. Giacobbe, S. M. Mickley, and M. R. Wasielewski, *J. Am. Chem. Soc.* **131**, 8372-8373 (2009).
23. Excitation Energy Transfer Pathways within Asymmetric Covalent Chlorophyll *a* Tetramers, V. L. Gunderson, T. M. Wilson, M. R. Wasielewski, *J. Phys. Chem. C* **113**, 11936-11942 (2009).
24. Efficient Charge Transport in DNA Diblock Oligomers, J. Vura-Weis, M. R. Wasielewski, A. K. Thazhathveetil, and F. D. Lewis, *J. Am. Chem. Soc.* **131**, 9722-9727 (2009).
25. Photoinitiated Charge Transport through π -Stacked Electron Conduits in Supramolecular Ordered Assemblies of Donor-Acceptor Triads, J. E. Bullock, R. Carmieli, S. M. Mickley, J. Vura-Weis, and M. R. Wasielewski, *J. Am. Chem. Soc.* **131**, 11919-11929 (2009).
26. Base Pair Sequence and Hole Transfer through DNA: Rational Design of Molecular Wires, J. Vura-Weis, F. D. Lewis, M. A. Ratner, M. R. Wasielewski, in "Charge and Exciton Transport in Molecular Wires", F. Grozema and L. Siebbeles, Eds. Wiley-VCH, Weinheim, 2009.
27. Spin-Selective Charge Transport Pathways through *p*-Oligophenylene-Linked Donor-Bridge-Acceptor Molecules, A. M. Scott, T. Miura, A. Butler Ricks, Z. E. X. Dance, E. M. Giacobbe, M. T. Colvin, and M. R. Wasielewski, *J. Am. Chem. Soc.* **131**, 17655-17666 (2009).

28. Self-Assembly Strategies for Integrating Light Harvesting and Charge Separation in Artificial Photosynthetic Systems, M. R. Wasielewski, *Acc. Chem. Res.* **42**, 1910-1921 (2009).
29. Interrogating the Intramolecular Charge-Transfer State of a Julolidine-Anthracene Donor-Acceptor Molecule with Femtosecond Stimulated Raman Spectroscopy, J. V. Lockard, A. Butler Ricks, D. T. Co, and M. R. Wasielewski, *J. Phys. Chem. Lett.* **1**, 215-218 (2010).
30. Self-Assembly of a Hexagonal Supramolecular Light-Harvesting Array from Chlorophyll Trefoil Building Blocks, V. L. Gunderson, S. M. Mickley, and M. R. Wasielewski, *Chem. Commun.* **46**, 401-403 (2010).
31. Dynamics of Ultrafast Singlet and Triplet Charge Transfer in Anthraquinone-DNA Conjugates, F. D. Lewis, A. K. Thazhathveetil, T. A. Zeidan, J. Vura-Weis, and M. R. Wasielewski, *J. Am. Chem. Soc.* **132**, 444-445 (2010).
32. Photoinduced Electron Transfer from Rail to Rung within a Self-assembled Porphyrin Oligomeric Ladder, C. She, S.-J Lee, K.-T. Youm, K. L. Mulfort, J. E. McGarrah, O. K. Farha, J. Vura-Weis, M. R. Wasielewski, H. Chen, G. C. Schatz, M. A. Ratner and J. T. Hupp, *Chem. Commun.* **46**, 547-549 (2010).
33. Fluorescence Dynamics of Chlorophyll Trefoils in the Solid State Studied by Single Molecule Fluorescence Spectroscopy J.-E. Lee, J. Yang, V. L. Gunderson, M. R. Wasielewski, and D. Kim, *J. Phys. Chem. Lett.* **1**, 284-289 (2010).
34. Rapid Intramolecular Hole Hopping in *meso-meso* and *meta*-Phenylene-Linked Linear and Cyclic Multi-Porphyrin Arrays, T. M. Wilson, T. Hori, M.-C. Yoon, N. Aratani, A. Osuka, D. Kim, and M. R. Wasielewski, *J. Am. Chem. Soc.* **132**, 1383-1388 (2010).
35. Fluorescence Dynamics of Chlorophyll Trefoils in the Solid State Studied by Single Molecule Fluorescence Spectroscopy J.-E. Lee, J. Yang, V. L. Gunderson, M. R. Wasielewski, and D. Kim, *J. Phys. Chem. Lett.* **1**, 284-289 (2010).
36. Rapid Intramolecular Hole Hopping in *meso-meso* and *meta*-Phenylene-Linked Linear and Cyclic Multi-Porphyrin Arrays, T. M. Wilson, T. Hori, M.-C. Yoon, N. Aratani, A. Osuka, D. Kim, and M. R. Wasielewski, *J. Am. Chem. Soc.* **132**, 1383-1388 (2010).
37. Photophysics and Redox Properties of Rylene Imide and Bisimide Dyes Alkylated Ortho to the Imide Groups, J. E. Bullock, M. T. Vagnini, C. Ramanan, T. M. Wilson, T. J. Marks, and M. R. Wasielewski, *J. Phys. Chem. B* **114**, 1794-1802 (2010).
38. Comparing Spin-Selective Charge Transport through Oligomeric Aromatic Bridges in Donor-Bridge-Acceptor Molecules, A. M. Scott, A. Butler Ricks, M. T. Colvin, and M. R. Wasielewski, *Angew. Chem. Int. Ed.* **49**, 2904-2908 (2010).
39. Large Porphyrin Squares from Self-assembling of *meso*-Triazole-Appended L-shaped *meso-meso* Linked Zn(II) Triporphyrins: Synthesis and Efficient Energy Transfer, C. Maeda, P. Kim, S. Cho, J. K. Park, J. Min Lim, D. Kim, J. Vura-Weis, M. R. Wasielewski, H. Shinokubo, and A. Osuka, *Chem. Eur. J.* (in press).
40. Time-resolved EPR Studies of Charge Recombination and Triplet State Formation within Donor-Bridge-Acceptor Molecules having Wire-like Oligofluorene Bridges, T. Miura, R. Carmieli, and M. R. Wasielewski, *J. Phys. Chem. A* (in press).
41. Crossover from Single-Step Tunneling to Wire-like Multi-Step Hopping for Molecular Triplet Energy Transfer, J. Vura-Weis, S. H. Abdelwahed, R. Shukla, R. Rathore, M. A. Ratner, and M. R. Wasielewski, *Science* (submitted).

42. Electron Spin Dynamics as a Controlling Factor for Spin-Selective Charge Recombination in Donor-Bridge-Acceptor Molecules, T. Miura, A. M. Scott, and M. R. Wasielewski, *J. Phys. Chem. C* (submitted).

Tetrapyrrolic Architectures for Fundamental Studies of Light Harvesting and Energy Transduction

David F. Bocian,¹ Dewey Holten² and Jonathan S. Lindsey³

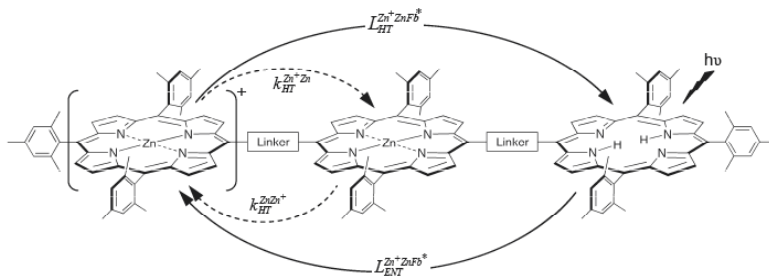
¹Department of Chemistry, University of California Riverside, Riverside, CA 92521

²Department of Chemistry, Washington University, St. Louis, MO 63130

³Department of Chemistry, North Carolina State University, Raleigh, NC 27695

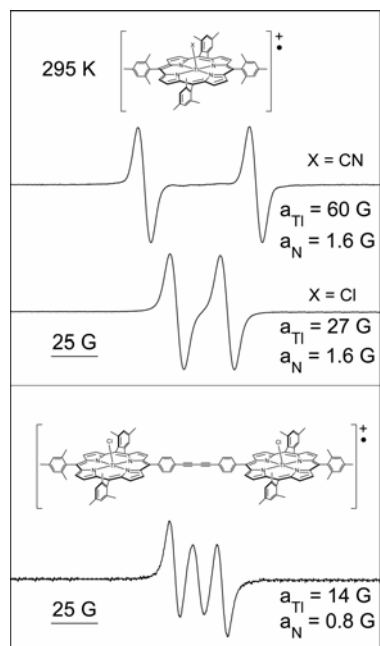
A long-term goal of our program is to design, synthesize, and characterize molecular architectures that provide insights into principles for efficient solar-energy conversion. Efficient solar-energy conversion requires collection of solar light across the visible and near-infrared spectrum, excited-state charge separation, and movement of charge (hole, electron) to prevent charge recombination. Excited-state charge separation in molecular architectures has been widely explored, yet ground-state hole (or electron) transfer, particularly involving equivalent pigments, has been far less studied, and direct quantitation of the rate of transfer often has proved difficult. Prior studies of ground-state hole transfer between equivalent zinc porphyrins using electron paramagnetic resonance (EPR) techniques wherein ¹⁴N hyperfine interactions serve as clock give a lower limit of $\sim(50 \text{ ns})^{-1}$ on the rates. Related prior transient optical studies of hole transfer between inequivalent sites [zinc porphyrin (Zn) and free base porphyrin (Fb)] give an upper limit of $\sim(20 \text{ ps})^{-1}$. These limiting values had established a relatively broad range for the rate of ground-state hole transfer between equivalent sites.

The above considerations prompted us to develop optical methods to probe the ground-state hole-transfer processes in a series of oxidized porphyrin triads (ZnZnFb) to determine the rates between the nominally equivalent sites (Zn/Zn). The strategy builds upon our recent time-resolved optical studies of the photodynamics of dyads wherein a zinc porphyrin is electrochemically oxidized and the attached free base porphyrin is photoexcited. The resulting energy- and hole-transfer processes in the oxidized ZnFb dyads are typically complete within 100 ps of excitation. Such processes are also present in the triads and serve as a starting point for determining the rates of ground-state hole transfer between equivalent sites in the triads. The rate constant of the Zn/Zn hole transfer is found to be $(0.8 \text{ ns})^{-1}$ for diphenylethyne-linked zinc porphyrins and increases only slightly to $(0.6 \text{ ns})^{-1}$ when a shorter *p*-phenylene linker is utilized. The rate decreases slightly to $(1.1 \text{ ns})^{-1}$ when steric constraints are introduced in the diarylethyne linker. In general, the rate constants for ground-state Zn/Zn hole transfer in oxidized arrays are a factor of 40 slower than those for Zn/Fb transfer.



While optical spectroscopic methods provide a direct measurement of the rates of ground-state hole transfer, these methods involve relatively challenging experimental and data analysis protocols. These considerations prompted us to explore other strategies to determine

ground-state hole-transfer rates using EPR spectroscopy. In one approach, ^{13}C labels have been incorporated into specific meso or α -pyrrole carbons of the tetrapyrrole macrocycle. The rationale for incorporating the ^{13}C labels is that the ^{13}C hyperfine coupling is larger (~ 6.4 G for meso ^{13}C atoms) than the ^{14}N hyperfine coupling (~ 1.6 G). The larger ^{13}C hyperfine coupling affords a better opportunity of perform accurate spectral simulations to obtain exact hole-transfer rates. Although a variety of molecules containing site-specific ^{13}C labels have been synthesized, an alternative hyperfine clock is desirable to further enhance the robustness of spectral simulations. Inspection of the characteristics of the nuclei across the periodic table shows that there are relatively few options for alternative hyperfine clocks. By far the best choice of a nucleus is thallium. ^{203}Tl and ^{205}Tl occur naturally in a 30/70 isotope ratio; both are $S=1/2$ nuclei with near equal magnetogyric ratios. Most importantly, the magnetogyric ratio(s) is extremely large, $\sim 60\%$ of that of ^1H . Accordingly, only very small spin density on the Tl metal center yield significant hyperfine splitting. This hypothesis has been explored in a series of prototype monomers and dyads. Simulations of the EPR spectra of both the ^{13}C and $^{203}\text{Tl}/^{205}\text{Tl}$ containing dyads have also been performed to extract exact hole-transfer rates and indicate that these rates fall in the 0.25 – 10 ns range, consistent with the values obtained from the time-resolved optical studies. This approach based on Tl chelates has been extended to a set of dyads containing oligo(*p*-phenylene) and diphenylethyne linkers. For all of these dyads, the activation energies for hole transfer have been obtained from simulations of the spectra as a function of temperature. These studies indicate that hole transfer is governed by a complex interplay of mechanisms.



The vast majority of work over the years in artificial photosynthesis, including our own, has employed porphyrins as surrogates for the naturally occurring (bacterio)chlorophylls. The reliance on porphyrins stems from synthetic expediency despite the lack of red or near-infrared absorption that is characteristic of (bacterio)chlorins and is essential for effective solar-light harvesting. To remedy this deficiency we have developed de novo routes to synthetic chlorins and bacteriochlorins so as to be able to prepare simple analogues of the natural hydrophorphyrins as well as arrange the synthetic hydrophorphyrins in a variety of 3-dimensional architectures. Rational synthetic access is now available to chlorins, 13¹-oxophorbins (which contain the fifth ring characteristic of the natural macrocycles), chlorin-13,15-dicarboximides, bacteriochlorins, and diverse substituted analogues thereof. This set of hydrophorphyrins provides strong absorption in the region 600 – 850 nm. Our present focus concerns the blending of two longstanding threads of our prior work, namely (1) the design, synthesis, and characterization of covalent and self-assembled arrays, and (2) the study of the fundamental (photophysical, redox, MO) properties of monomeric synthetic hydrophorphyrins. The resulting ensembles of synthetic hydrophorphyrins will be the subject of future studies of energy and hole transfer that incorporate newly developed optical and EPR approaches. Collectively, these studies should aid the design of next-generation molecular architectures for studies of solar-energy conversion.

DOE Sponsored Publications 2007-2010

1. “Effects of Substituents on Synthetic Analogs of Chlorophylls. Part 1: Synthesis, Vibrational Properties and Excited-State Decay Characteristics,” Kee, H. L.; Kirmaier, C.; Tang, Q.; Diers, J. R.; Muthiah, C.; Taniguchi, M.; Laha, J. K.; Ptaszek, M.; Lindsey, J. S.; Bocian, D. F.; Holten, D. *Photochem. Photobiol.* **2007**, *83*, 1110–1124.
2. “Effects of Substituents on Synthetic Analogs of Chlorophylls. Part 2: Redox Properties, Optical Spectra and Electronic Structure,” Kee, H. L.; Kirmaier, C.; Tang, Q.; Diers, J. R.; Muthiah, C.; Taniguchi, M.; Laha, J. K.; Ptaszek, M.; Lindsey, J. S.; Bocian, D. F.; Holten, D. *Photochem. Photobiol.* **2007**, *83*, 1125–1143.
3. “Meso-¹³C-Labeled Porphyrins for Studies of Ground-State Hole Transfer in Multiporphyrin Arrays,” Thamyongkit, P.; Muresan, A. Z.; Diers, J. R.; Holten, D.; Bocian, D. F.; Lindsey, J. S. *J. Org. Chem.* **2007**, *72*, 5207–5217.
4. “Tracking Electrons and Atoms in a Photoexcited Metalloporphyrin,” Chen, L. X.; Zhang, X.; Wasinger, E. C.; Attenkofer, K.; Jennings, G.; Muresan, A. Z.; Lindsey, J. S. *J. Am. Chem. Soc.* **2007**, *129*, 9616–9618.
5. “Synthesis and Photophysical Characterization of Porphyrin, Chlorin, and Bacteriochlorin Molecules Bearing Tethers for Surface Attachment,” Muthiah, C.; Taniguchi, M.; Kim, H.-J.; Schmidt, I.; Kee, H. L.; Holten, D.; Bocian, D. F.; Lindsey, J. S. *Photochem. Photobiol.* **2007**, *83*, 1513–1528.
6. “Examination of Tethered Porphyrin, Chlorin, and Bacteriochlorin Molecules in Mesoporous Metal-Oxide Solar Cells,” Stromberg, J. R.; Marton, A.; Kee, H. L.; Kirmaier, C.; Diers, J. R.; Muthiah, C.; Taniguchi, M.; Lindsey, J. S.; Bocian, D. F.; Meyer, G. J.; Holten, D. *J. Phys. Chem. C* **2007**, *111*, 15464–15478.
7. “Ultrafast Stimulated Emission and Structural Dynamics in Nickel Porphyrins,” Zhang, X.; Wasinger, E. C.; Muresan, A. Z.; Attenkofer, K.; Jennings, G.; Lindsey, J. S.; Chen, L. X. *J. Phys. Chem. A* **2007**, *111*, 11736–11742.
8. “Two Complementary Routes to 7-Substituted Chlorins. Partial Mimics of Chlorophyll *b*,” Muthiah, C.; Ptaszek, M.; Nguyen, T. M.; Flack, K. M.; Lindsey, J. S. *J. Org. Chem.* **2007**, *72*, 7736–7749.
9. “Synthesis and Structural Properties of Porphyrin Analogues of Bacteriochlorophyll *c*,” Ptaszek, M.; Yao, Z.; Dhanalekshmi, S.; Boyle, P. D.; Lindsey, J. S. *Tetrahedron* **2007**, *63*, 12629–12638.
10. “Synthesis and Excited-State Photodynamics of a Chlorin–Bacteriochlorin Dyad – Through-Space Versus Through-Bond Energy Transfer In Tetrapyrrole Arrays,” Muthiah, C.; Kee, H. L.; Diers, J. R.; Fan, D.; Ptaszek, M.; Bocian, D. F.; Holten, D.; Lindsey, J. S. *Photochem. Photobiol.* **2008**, *84*, 786–801.
11. “Accessing the Near-Infrared Spectral Region with Stable, Synthetic, Wavelength-Tunable Bacteriochlorins,” Taniguchi, M.; Cramer, D. L.; Bhise, A. D.; Kee, H. L.; Bocian, D. F.; Holten, D.; Lindsey, J. S. *New J. Chem.* **2008**, *32*, 947–958.
12. “Examination of Chlorin–Bacteriochlorin Energy-Transfer Dyads as Prototypes for Near-Infrared Molecular Imaging Probes,” Kee, H. L.; Nothdurft, R.; Muthiah, C.; Diers, J. R.; Fan, D.; Ptaszek, M.; Bocian, D. F.; Lindsey, J. S.; Culver, J. P.; Holten, D. *Photochem. Photobiol.* **2008**, *84*, 1061–1072.

13. “Regiospecifically α - ^{13}C -Labeled Porphyrins for Studies of Ground-State Hole Transfer in Multiporphyrin Arrays,” Muresan, A. Z.; Thamyongkit, P.; Diers, J. R.; Holten, D.; Lindsey, J. S.; Bocian, D. F. *J. Org. Chem.* **2008**, *73*, 6947–6959. *Selected as a featured article.*
14. “Energy- and Hole-Transfer Dynamics in Oxidized Porphyrin Dyads,” Song, H.-E.; Kirmaier, C.; Diers, J. R.; Lindsey, J. S.; Bocian, D. F.; Holten, D. *J. Phys. Chem. B* **2009**, *113*, 54–63.
15. “Determination of Ground-State Hole-Transfer Rates Between Identical Sites in Oxidized Multiporphyrin Arrays Using Time-Resolved Optical Spectroscopy,” Song, H.-E.; Kirmaier, C.; Taniguchi, M.; Diers, J. R.; Bocian, D. F.; Lindsey, J. S.; Holten, D. *J. Am. Chem. Soc.* **2008**, *130*, 15636–15648.
16. “Probing Ground-State Hole Transfer Between Equivalent, Electrochemically Inaccessible States in Multiporphyrin Arrays using Time-Resolved Optical Spectroscopy,” Song, H.-E.; Taniguchi, M.; Kirmaier, C.; Diers, J. R.; Bocian, D. F.; Lindsey, J. S.; Holten, D. *Photochem. Photobiol.* **2009**, *85*, 693–704.
17. “Solution-State Conformational Ensemble of a Hexameric Porphyrin Array Characterized Using Molecular Dynamics and X-ray Scattering,” Mardis, K. L.; Sutton, H. M.; Zuo, X.; Lindsey, J. S.; Tiede, D. M. *J. Phys. Chem. A* **2009**, *113*, 2516–2523.
18. “Chlorin–Bacteriochlorin Energy-transfer Dyads as Prototypes for Near-infrared Molecular Imaging Probes: Controlling Charge-transfer and Fluorescence Properties in Polar Media,” Kee, H. L.; Diers, J. R.; Ptaszek, M.; Muthiah, C.; Fan, D.; Lindsey, J. S.; Bocian, D. F.; Holten, D. *Photochem. Photobiol.* **2009**, *85*, 909–920.
19. “Fast and Robust Route to Hydroporphyrin–Chalcones with Extended Red or Near-Infrared Absorption,” Ruzi , C.; Krayer, M.; Lindsey, J. S. *Org. Lett.* **2009**, *11*, 1761–1764.
20. “Regioselective Bromination Tactics in the De Novo Synthesis of Chlorophyll *b* Analogues,” Muthiah, C.; Lahaye, D.; Taniguchi, M.; Ptaszek, M.; Lindsey, J. S. *J. Org. Chem.* **2009**, *74*, 3237–3247. *Selected as a featured article and as cover art.*
21. “Excited-State Energy Flow in Phenylene-Linked Multiporphyrin Arrays,” Song, H.-E.; Taniguchi, M.; Speckbacher, M.; Yu, L.; Bocian, D. F.; Lindsey, J. S.; Holten, D. *J. Phys. Chem. B* **2009**, *113*, 8011–8019.
22. “Synthesis and Photochemical Properties of 12-Substituted versus 13-Substituted Chlorins,” Mass, O.; Ptaszek, M.; Taniguchi, M.; Diers, J. R.; Kee, H. L.; Bocian, D. F.; Holten, D.; Lindsey, J. S. *J. Org. Chem.* **2009**, *74*, 5276–5289.
23. “Refined Syntheses of Hydrodipyrin Precursors to Chlorin and Bacteriochlorin Building Blocks,” Krayer, M.; Balasubramanian, T.; Ruzi , C.; Ptaszek, M.; Cramer, D. L.; Taniguchi, M.; Lindsey, J. S. *J. Porphyrins Phthalocyanines* **2009**, *13*, 1098–1110.
24. “Linker Dependence of Energy and Hole Transfer in Neutral and Oxidized Multiporphyrin Arrays,” Song, H.-E.; Taniguchi, M.; Diers, J. R.; Kirmaier, C.; Bocian, D. F.; Lindsey, J. S.; Holten, D. *J. Phys. Chem. B* **2009**, *113*, 16483–16493.
25. “Excited-State Photodynamics of Perylene–Porphyrin Dyads 5. Tuning Light-Harvesting Characteristics via Perylene Substituents, Connection Motif, and 3-Dimensional Architecture,” Kirmaier, C.; Song, H.-E.; Yang, E. K.; Schwartz, J. K.; Hindin, E.; Diers, J. R.; Loewe, R. S.; Tomizaki, K.-y.; Chevalier, F.; Ramos, L.; Birge, R. R.; Bocian, D. F.; Lindsey, J. S.; Holten, D. *J. Phys. Chem. B* **2010**, Wasielewski Festschrift, (ASAP).

26. "Expanded Scope of Synthetic Bacteriochlorins via Improved Acid Catalysis Conditions and Diverse Dihydrodipyrin-Acetals," Krayer, M.; Ptaszek, M.; Kim, H.-J.; Meneely, K. R.; Fan, D.; Secor, K.; Lindsey, J. S. *J. Org. Chem.* **2010**, *75*, 1016–1039. *Selected as a featured article.*
27. "Stable Synthetic Bacteriochlorins Overcome the Resistance of Melanoma to Photodynamic Therapy," Mroz, P.; Huang, Y.-Y.; Janjua, S.; Zhiyentayev, T.; Szokalska, A.; Nifli, A.-P.; Sherwood, M. E.; Ruzié, C.; Borbas, K. E.; Fan, D.; Krayer, M.; Balasubramanian, T.; Yang, E. K.; Kee, H. L.; Kirmaier, C.; Diers, J. R.; Bocian, D. F.; Holten, D.; Lindsey, J. S.; Hamblin, M. R. *FASEB J.* **2010**, in press.
28. "De Novo Synthesis of Long-Wavelength Absorbing Chlorin-13,15-Dicarboximides," Ptaszek, M.; Lahaye, D.; Krayer, M.; Muthiah, C.; Lindsey, J. S. *J. Org. Chem.* **2010**, *75*, 1659–1673.
29. "In vitro Photodynamic Therapy and Quantitative Structure-Activity Relationship Studies with Stable Synthetic Near-Infrared-Absorbing Bacteriochlorin Photosensitizers," Huang, Y.-Y.; Mroz, P.; Zhiyentayev, T.; Balasubramanian, T.; Ruzié, C.; Krayer, M.; Fan, D.; Borbas, K. E.; Yang, E. K.; Kee, H. L.; Kirmaier, C.; Diers, J. R.; Bocian, D. F.; Holten, D.; Lindsey, J. S.; Hamblin, M. R. *J. Med. Chem.* **2010**, submitted 12/22/2009.
30. "Structural Studies of Sparsely Substituted Chlorins and Phorbines Establish Benchmarks for Changes in the Ligand Core and Framework of Chlorophyll Macrocycles," Taniguchi, M.; Mass, O.; Boyle, P. D.; Tang, Q.; Diers, J. R.; Bocian, D. F.; Holten, D.; Lindsey, J. S. *J. Mol. Struct.* **2010**, submitted 03/11/2010.
31. "Probing the Rate of Hole Transfer in Oxidized Synthetic Chlorin Dyads via Site-Specific ¹³C-Labeling," Nieves-Bernier, E. J.; Taniguchi, M.; Diers, J. R.; Holten, D.; Bocian, D. F.; Lindsey, J. S. *J. Org. Chem.* **2010**, submitted 03/19/2010.
32. "Synthesis of Oligo(*p*-Phenylene)-linked Dyads Containing Free Base, Zinc(II) or Thallium(III) Porphyrins for Studies in Artificial Photosynthesis," Taniguchi, M.; Lindsey, J. S. *Tetrahedron* **2010**, *68*, submitted 04/13/2010.

Session VI

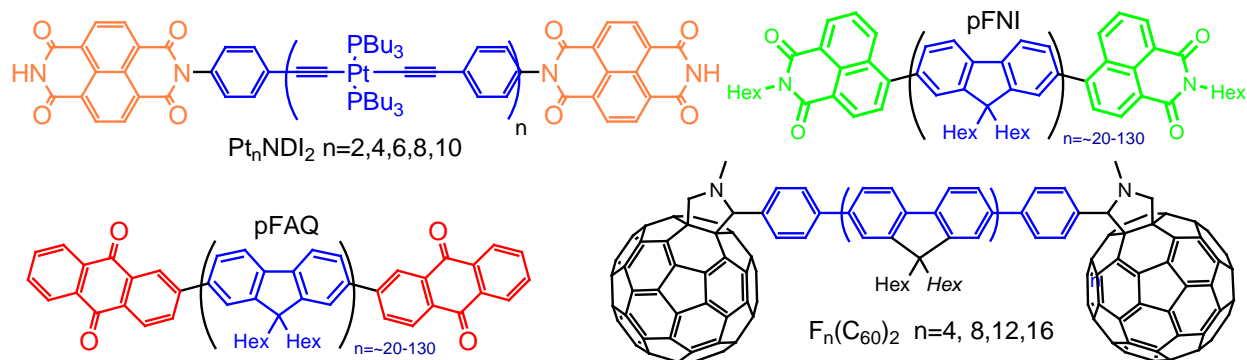
Charge Transport in Organic Systems

"Molecular Wires" for Electrons, Holes and Excitons

John R. Miller, Andrew Cook, Paiboon Sreearunothai, Sadayuki Asaoka, Norihiko Takeda, Sean McIlroy, Julia M. Keller* and Kirk Schanze,* Yuki Shibano[‡] and H. Imahori[‡]
Chemistry Department, Brookhaven National Laboratory, Upton, NY 11973,
*University of Florida, Gainesville, FL 117200 [‡]Kyoto University, Kyoto, Japan.

This research examines the ability of long conjugated molecules to act as “wires” that can facilitate long distance transport. Our interest in transport stems from the potential of organic photovoltaics (OPV) for clean solar energy, but OPV needs to become much more efficient. Reported efficiencies of OPV cells grew rapidly to ~5%, but that growth has stalled during the past few years. We argue that fundamental understanding and disruptive concepts can be the keys to better energy conversion. Transport of excitons, electrons and holes is a central issue. Exciton Transport in OPV cells is characterized by short exciton diffusion lengths, usually 5-8 nm, which limit cell efficiencies. An important series of experiments on isolated chains with end-cap traps reinforced the idea that short diffusion lengths are the result of the fact that exciton transport is an “intrinsically slow process.” The widely-held belief that excitons are necessarily slow limits thinking so that much of the research on cell making examines ways to circumvent the problem of slow excitons, usually through heavily-interdigitated structures including the popular and dominant “bulk heterojunction” concept.

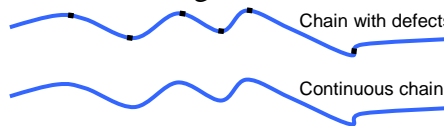
Our research seeks alternatives and asks the question: Can excitons, electrons and holes transport rapidly and efficiently over long distances along conjugated chains? The measurements determine electron and exciton transport in polymers and oligomers having end-cap traps. Structures of molecules under study are shown below and others are in progress.



The measurements photoexcite the molecules to create excitons or inject electrons or holes from the solvent by ionizing the solvent with 5 ps, 9 MeV electron pulses at the Laser Electron Accelerator (LEAF). Detection of transient absorption uses the Optical Fiber Single-Shot detection system which enables experiments with 15 ps time resolution. The experiments find fast electron transport to end caps in oligomers of Platinum acetylides (Pt_nNDI₂ shown top left); transport of triplet excitons created by photoexcitation occurs with similar rates. In fluorene oligomers having C₆₀ trap groups electron transport is also fast. Photoexcitation creates singlet excitons, which might have been expected to transport slowly (~500 ps) based on observations

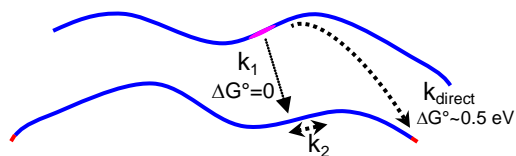
described in the literature. Instead exciton capture is almost twenty times faster, occurring in ~ 10 ps for the $F_{16}(C_{60})_2$ molecule. Electrons injected into the F_n chains are captured in by the C_{60} traps in times < 0.2 ns.

A principal question we ask in these studies concerns the nature of conjugated chains. Many experimental observations support the idea that conjugated polymers are not continuous, but are divided by defects: A common belief is: “..polymer chains can then be regarded as made from a statistical distribution of segments with different conjugation lengths.” The experiments will seek to understand whether transport is continuous or whether it is controlled by defects or other segments. We therefore seek quantitative comparisons with models. The simplest model is that of random 1D diffusion along the chains with reaction upon every encounter with an end trap. Reasons for departures from that simple model can include 1) defects or other segmentation of the chains, 2) imperfect capture at the ends, 3) transport steps of variable lengths, 4) coherent motion, especially for excitons and 5) to relaxation processes occurring on time scales competitive with that of transport.



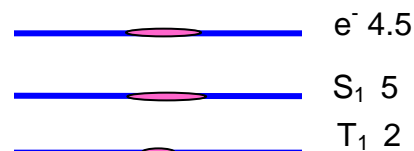
Experiments to examine electron transport in pFNI and pFAQ molecules up to 75 nm in length show evidence of fast transport. The earliest results, available for two years, can be interpreted

only semiquantitatively. Current experiments show that the results are perturbed by ion-pairing in geminate pairs of anions and solvated protons. In the near future new experiments will remedy this perturbation. While they do not play a big role, to obtain high accuracy it is also necessary to take into account bimolecular reactions between polymer chains. Recent experiments have therefore measured rates of bimolecular electron transfer in mixtures of capped and uncapped



chains. These simple experiments require only slow time resolution, but yield important results. Dependence of the rate constants on lengths of the chains show that there is little contribution from the single step mechanism in which an electron on one chain is transferred directly to the trap group on the other chain. Interpretation of the results also supports the conclusion that the rate, k_2 , of transport along the chains, is rapid over long distances.

Transport of triplet excitons is of fundamental importance because dipole (Förster) couplings are not effective, so the electronic coupling matrix elements needed for triplet motion can come only from the exchange (Dexter) mechanism. Direct photoexcitation is usually not viable except in cases of ultrafast intersystem crossing. Triplets can be created by sensitization or by pulse radiolysis, but both involved slow, bimolecular processes leading to slow time resolution. Our results to date shown that triplet transport is fast, but the experiments have established only lower limits for the rates. We are developing methods that may yield higher time resolution. Our earlier results contributed to the notion that electrons and holes in conjugated chains exist as polarons, ~ 4.5 repeat units long in polyfluorenes, although before relaxation they may be more delocalized. Triplet and



singlet excitons are also apparently polarons, ~5 units long for singlets, but much shorter for triplets. Future plans will seek to directly compare transport of electrons, holes, and both singlet and triplet excitons in the same material, with evaluation of the effects of both electronic and nuclear factors including the differences in delocalization lengths. The plans will include extension to films. They will include a collaboration with NREL that will seek to make measurements of both transient absorption with 15 ps time resolution and microwave conductivity measurements on those films.

DOE Sponsored Publications 2007-2010¹⁻⁷

- (1) Shibano, Y.; Imahori, H.; Sreearunothai, P.; Cook, A. R.; Miller, J. R. "A Conjugated "Molecular Wire" for Excitons"; *Journal of Physical Chemistry Letters* **2010**, *ASAP*, 1492-96.
- (2) Schwerin, A. F.; Johnson, J. C.; Smith, M. B.; Sreearunothai, P.; Popovic, D.; Cerny, J.; Havlas, Z.; Paci, I.; Akdag, A.; MacLeod, M. K.; Chen, X. D.; David, D. E.; Ratner, M. A.; Miller, J. R.; Nozik, A. J.; Michl, J. "Toward Designed Singlet Fission: Electronic States and Photophysics of 1,3-Diphenylisobenzofuran"; *Journal of Physical Chemistry A* **2010**, *114*, 1457-1473.
- (3) Sreearunothai, P.; Asaoka, S.; Cook, A. R.; Miller, J. R. "Length and Time-Dependent Rates in Diffusion-Controlled Reactions with Conjugated Polymers"; *Journal of Physical Chemistry A* **2009**, *113*, 2786-2795.
- (4) Holroyd, R. A.; Cook, A. R.; Preses, J. M. "Dynamics of excimer formation and decay in supercritical krypton"; *Journal of Chemical Physics* **2009**, *131*.
- (5) Cook, A. R.; Shen, Y. Z. "Optical fiber-based single-shot picosecond transient absorption spectroscopy"; *Review of Scientific Instruments* **2009**, *80*.
- (6) Asaoka, S.; Takeda, N.; Lyoda, T.; Cook, A. R.; Miller, J. R. "Electron and hole transport to trap groups at the ends of conjugated polyfluorenes"; *Journal of the American Chemical Society* **2008**, *130*, 11912-11920.
- (7) Cardolaccia, T.; Funston, A. M.; Kose, M. E.; Keller, J. M.; Miller, J. R.; Schanze, K. S. "Radical ion states of platinum acetylide oligomers"; *Journal of Physical Chemistry B* **2007**, *111*, 10871-10880.

Measurement of the Distance Scale for Nanoscale Electronic Energy Funneling by Sub-diffraction Single Molecule Spectroscopy

Joshua C. Bolinger, Matt C. Traub, Takuji Adachi, and Paul F. Barbara
Center for Nano and Molecular Science and Technology
University of Texas at Austin
Austin TX, 78712

This research is focused on developing a fundamental understanding of charge separation and charge transfer at organic donor acceptor interfaces in nanostructured binary composites of organic (or organic/inorganic) semiconductors. Despite several years of research using ensemble spectroscopic methods there is no consensus on what factors limit photovoltaic (PV) properties of molecular semiconductors. The tremendous complexity, of such materials, in particular, has severely limited their rational design. New molecular-level experimental and theoretical tools as well as major conceptual breakthroughs are needed to advance our understanding of this type of PV materials. Under support of this grant, we use single molecule spectroscopy (sms) on carefully designed PV interfacial prototypes to obtain new molecular level information on PV mechanisms. We believe that our sms methods will lead to a much better understanding of what molecular-level factors determine the photon to electrical power energy conversion efficiency.

For example we recently developed the first sms methods to make direct, real space measurements of the distant scale for electronic energy funneling in conjugated polymers. We employ a new sub-diffraction optical technique, i.e. Bias modulated Intensity-Centroid spectroscopy (BIC), to accurately measure the distant scales for emission in nano domains of conjugated polymers. The distance scale for electronic energy transfer, R_{ET} , is a critical parameter for organic conjugated polymers for solar energy harvesting. We observe that in highly ordered isolated nanodomains of the prototypical conjugated polymer MEH is shown to be > 60 nm. The observed value far exceeds the energy transfer distances previously reported for bulk organic conjugated materials and furthermore exceeds that predicted by standard theories for single-step energy transfer, e.g. by the Forster resonance energy transfer mechanism. The results suggest that long-range, multistep, electronic energy funneling can occur in conjugated polymer domains with an optimal nanostructure. The extraordinary conformational order of isolated conjugated polymer chain may be the major factor responsible for the observed ultra long-range energy transfer observed in this study.

A semiconductor capacitor-like device (Fig. 1a) structure was used in this study to controllably charge and discharge single polymer molecules with one or more hole (p^+) by modulating the bias across the device in the appropriate range. As the bias is modulated charges are injected from an adjacent hole transport layer that is in contact with the single molecule. The degree of charging of a particular molecule is indirectly measured by recording the synchronously averaged integrated intensity (I_{fl}) of its fluorescence spot (Fig. 1b) as a function of the bias $E(V)$ across the device, which is modulated periodically in a square-wave (Fig. 1c). For the bias conditions in Fig. 1 the quenching is about 60% during the more positive portion of the bias cycle. This level of quenching corresponds to the injection of approximately one p^+ for MEH-PPV with a MW~ 900K, i.e. the range of materials studies in Fig 1. The fluorescence *intensity* centroid of the single isolated conjugated polymer molecule, determined by a 2D Gaussian fitting

procedure of the time-dependent fluorescence images, is observed to be displaced periodically in the sample (x, y) plane as the bias is modulated and, in turn, the degree of quenching is varied due to p^+ injection, see Fig. 1d. The bias dependent centroid displacement can be decomposed into orthogonal (X and Y) directions in the laboratory frame.

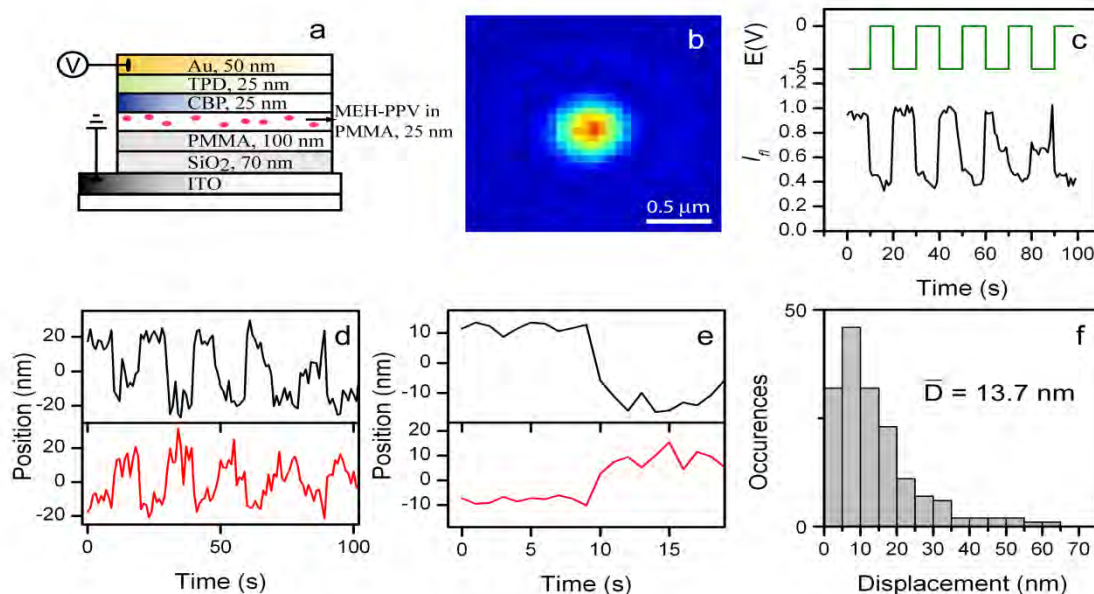


Fig. 1. (a) Device structure of the hole injection device used. (b) False color image of a single molecule of MEH-PPV imbedded in the hole-only device. (c) F-V measurement of the molecule shown in (b) where the fluorescence trajectory is shown in black and the applied bias is shown above, in green. (d) The centroid displacement of the fluorescence point spread function resulting from the applied bias shown in (c) where displacement in the x direction is shown in the top panel (black), and y is shown in the bottom panel (red). (e) Synchronized average of the x (black line) and y (red line) centroid displacement obtained from (c). Histogram of the total centroid displacement for 167 different single molecule MEH-PPV (MW = 900k) transients. Values peak at 12 nm while the mean value is 17 nm.

A striking feature of the results in Fig. 1d is that the centroid displacements as a function of bias are nearly identical from cycle-to-cycle. This allows for synchronous averaging of the displacement data leading to an improved signal-to-noise ratio for X and Y component centroid determination with a STD for X and Y position determination of only 0.5 nm despite a diffraction limit of ~ 300 nm (Fig. 1e). The plateaus in the X and Y component data in Fig. 1e for the vast majority of the molecules investigated exhibit roughly constant values during the uncharged (lower bias) and charged (higher bias) periods reflecting the X,Y centroid positions that correspond to these two cases.

Future research will use BIC to study a series of different conjugated polymer chemical structures to develop molecular-level structure-function relationships for long-range energy transfer in donor-acceptor conjugated polymers blends.

DOE Sponsored Publications 2007-2010

1. **“Effect of electric field on the photoluminescence intensity of single CdSe nanocrystals,”** So-Jung Park, Stephen Link, William M. Miller, Andre Gesquiere, and Paul F. Barbara, *Chem. Phys.*, *341* 169 (2007)
2. **“Single molecule spectroscopy of poly 3-octyl-thiophene (P3OT),”** Rodrigo E. Palacios and Paul F. Barbara, *J. Fl.*, *17* 749 (2007)
3. **“Charging and discharging of single conjugated-polymer nanoparticles,”** Rodrigo E. Palacios, Fu-Ren Fan, John K. Grey, Jungdon Suk, Allen J. Bard, and Paul F. Barbara, *Nature Materials*, *6* 680 (2007)
4. **“Electrogenerated chemiluminescence of single conjugated polymer nanoparticles,”** Ya-Lan Chang, Rodrigo E. Palacios, Fu-Ren Fan, Allen J. Bard, and Paul F. Barbara, *J. Amer. Chem. Soc. (Communication)*, *130* 8906 (2008)
5. **“Detailed investigation of light induced charge injection into a single conjugated polymer chain,”** Joshua C. Bolinger, Kwang-Jik Lee, Rodrigo E. Palacios, and Paul F. Barbara, *J. Phys. Chem. C*, *112* 18608 (2008)
6. **“Single conjugated polymer nanoparticle capacitors,”** Rodrigo E. Palacios, Kwang-Jik Lee, Arnaud Rival, Takuji Adachi, Joshua C. Bolinger, Leonid Fradkin, and Paul F. Barbara, *Chem. Phys.*, *357* 21 (2009)
7. **“Factors controlling hole injection in single conjugated polymer molecules,”** Leonid Fradkin, Rodrigo E. Palacios, Joshua C. Bolinger, Kwang-Jik Lee, William M. Lackowski, and Paul F. Barbara, *J. Phys. Chem. A*, *113* 4739 (2009)
8. **“Light-assisted deep-trapping of holes in conjugated polymers,”** Joshua C. Bolinger, Leonid Fradkin, Kwang-Jik Lee, Rodrigo E. Palacios, and Paul F. Barbara, *Proc. Nat. Acad. Sci.*, *106* 1342 (2009)

Conjugated Polymers and Polyelectrolytes in Solar Photoconversion

Seoung Ho Lee, Sevnur Kömürlü, Feng Fude, Dan Patel, Jarrett Vella, Quentin Bricaud,
Valeria D. Kleiman, John R. Reynolds and Kirk S. Schanze
Department of Chemistry, University of Florida, Gainesville, FL, 32611-7200

Conjugated polymers feature delocalized electronic states that give rise to useful materials properties such as high conductivity for exciton and polaron states. These properties are useful for energy conversion schemes, where visible light harvesting and long distance energy and charge transfer are fundamentally important processes. This DOE program is focused on exploring light harvesting, exciton delocalization and energy transport in a family of conjugated polymers and dendrimers that feature ionic solubilizing groups. These materials, referred to as “conjugated polyelectrolytes” (CPEs) and “conjugated polyelectrolyte dendrimers” (CPE-Ds), are soluble in polar organic solvents and water, and they have a strong propensity to associate with oppositely charged ions and to aggregate under specific conditions. In addition, their surface active nature allows them to be used to construct thin films in which the composition can be controlled on the nanometer length scale. This multi-investigator program seeks to apply photophysical probes to understand fundamental aspects of exciton structure and delocalization in CPEs and CPE-Ds in solution and in thin films at the surface of insulating and semi-conducting surfaces. The presentation will highlight recent work in the area of CPE-Ds in solution and on CPEs in thin film formats.

Conjugated Polyelectrolyte Dendrimers. A series of conjugated polyelectrolyte dendrimers (CPE-Ds) with dendritic side chains has been synthesized and characterized (generations 1 to 3, **G1**, **G2** and **G3**). The core and periphery of the dendrimers consists of diphenylethyne units (a relatively short conjugation length) and branched, ionic peripheral groups provide electrostatic interactions with the solvent to solubilize them in water and methanol. Fundamental photophysics studies show intermolecular and intramolecular aggregation depending on the solvent, pH and dendrimer size. Imaging studies (AFM) and DLS suggest that **G1** dendrimers form 4-5 nm size globular structures comprised of multiple molecules while **G2** and **G3** appear as smaller, single unit, structures (< 2 nm). The relatively small and constant size of **G-2** and **G-3** suggest that their geometric structures disfavor intermolecular aggregation. In solution, these CPE-Ds have long emission lifetimes (8-9 ns) and can undergo energy quenching with cyanine

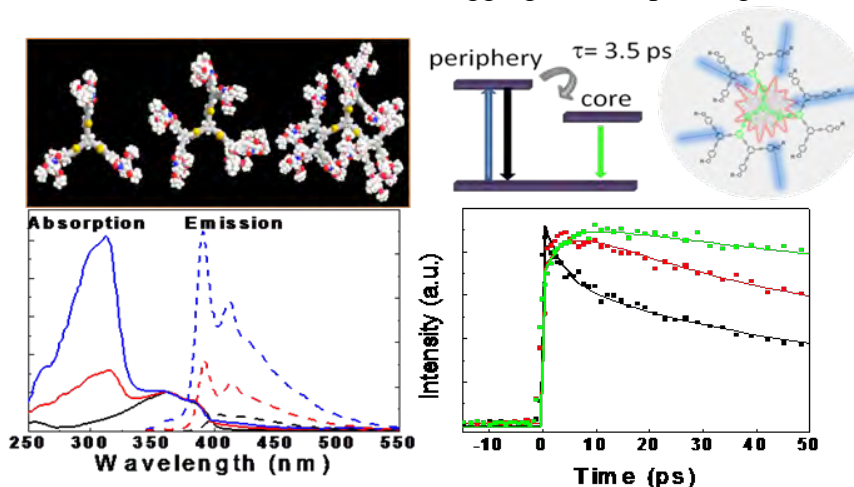


Figure 1. Photophysical studies of conjugated polyelectrolyte dendrimers with energy gradient towards the core of the dendrimer structure. Absorption and fluorescence spectra (lower left) reveal absorption by all units, but fluorescence is dominated by the lower energy chromophores in the core. Time resolved fluorescence (lower right) provides insight concerning the dynamics of intra-dendrimer energy transfer.

dyes. An ionic cyanine dye energy acceptor (DOC) was used to follow the loss of anisotropy and measure the radius of gyration, obtaining larger sizes ($\sim 4\text{-}5$ nm for **G2**, $6\text{-}6.5$ nm for **G3**) associated with solvated dendrimers. Studies of association and quenching with ionic cyanine dyes show large Stern-Volmer quenching constants (K_{SV}), on the order of $10^5\text{-}10^6$ M^{-1} . The solvent-dependent photophysical properties of CPE-Ds reveal that intra-dendrimer interaction becomes stronger in aqueous solution with increasing generation.

In a second line of study, we have explored CPE-Ds with an energy gradient. Two different chemical compositions were considered. In one case the dendrimer core is modified by adding thiophene units which lower the energy of the $S_1\text{-}S_0$ transition. Absorption arises from both the periphery and the core (broader spectrum from unaggregated systems) and it increases linearly with the number of chromophore units. Photophysical studies were performed with the organic precursors to understand intramolecular energy transfer in the absence of aggregation. For the larger dendrimer (**G3**) the absorption and fluorescence excitation spectra match, indicating quantum yield of energy transfer close to unity. Ultrafast timescale time-resolved experiments are applied to follow the dynamics of the energy transfer. For **G1**, there is no energy trap at the core and the natural lifetime of the dendrimer is measured (300 ps). For the second and third generation CPE-Ds, excitation and selective detection of the core emission shows an additional decay component at 44 ps, indicating intramolecular interactions most likely between the dendritic conjugated arms and the periphery. Upon selective excitation of the periphery we observe an even faster component. This component is observed as a decay of the emission from the periphery chromophores and a rise on the emission from the core chromophore, and it is identified with the energy transfer following the gradient. Similar behavior is observed in both dendrimers with a gradient, with the smaller dendrimer presenting a faster time constant, as expected (1.5 and 3.5 ps for **G2** and **G3** respectively).

Conjugated Polyelectrolyte Films. The layer-by-layer polyelectrolyte deposition approach has been optimized and applied to study long distance energy transfer and exciton transport in CPE films. In one line of investigation we have studied singlet-singlet energy transfer between two CPEs with different bandgap across an intervening series of insulating polyelectrolyte layers. The results reveal that the energy transfer distance is modeled well by Förster resonance energy transfer theory. In a second series of studies, singlet exciton transport has been studied through CPE multilayer films to an ITO surface as a quenching interface. These results suggest that the singlet exciton diffusion length is ~ 2.5 nm; however, aggregation in the films serves to trap excitons leading to a decrease in the diffusion length under conditions where aggregation is more pronounced. Finally, in collaboration with Bruce Parkinson at U. Wyoming we have been exploring the structure of CPEs adsorbed at single crystal TiO_2 surfaces.

Future Studies. Work on the CPE-D systems will continue, with emphasis placed on the use of ultrafast fluorescence to determine the timescale for exciton delocalization and transfer within the dendrimers. In addition, studies will explore the dynamics of energy and charge transfer between the dendrimers and ionically associated energy and charge acceptors. Synthetic work will seek to construct mono-disperse, linear conjugated polyelectrolyte oligomers (CPE-O). These systems will be studied to provide quantitative insight concerning exciton structure and dynamics in the structurally more complex CPE (polymer) systems that have been studied previously. Finally, in a new line of investigation we are studying conjugated oligomers and polymers that feature alternating donor and acceptor units in the conjugated system. Preliminary results on these donor-acceptor systems will be presented in the talk.

DOE Sponsored Publications 2007 – 2010

1. Base-free Suzuki polymerization for the synthesis of polyfluorenes functionalized with carboxylic acids, Brookins, R. N.; Schanze, K. S.; Reynolds, J. R. *Macromolecules* **2007**, *40*, 3524-3526.
2. Amplified fluorescence quenching and biosensor application of a poly(para-phenylene) cationic polyelectrolyte, Pinto, M. R.; Tan, C.; Ramey, M. B.; Reynolds, J. R.; Bergstedt, T. S.; Whitten, D. G.; Schanze, K. S. *Res. Chem. Intermed.* **2007**, *33*, 79-90.
3. Base-free Suzuki polymerization for the synthesis of carboxylic-acid functionalized conjugated polymers as dye sensitizers in Graetzel photovoltaic cells Brookins, R. N.; Qiao, Q.; Reynolds, J. R. *Polymer Preprints* **2007**, *48*, 213-214.
4. Effects of polymer aggregation and quencher size on amplified fluorescence quenching of conjugated polyelectrolytes, Jiang, H.; Zhao, X. Y.; Schanze, K. S. *Langmuir* **2007**, *23*, 9481-9486.
5. Hyperbranched conjugated polyelectrolyte bilayers for solar-cell applications, Taranekar, P.; Qiao, Q.; Jiang, H.; Ghiviriga, I.; Schanze, K. S.; Reynolds, J. R. *J. Am. Chem. Soc.* **2007**, *129*, 8958-8959.
6. A conjugated polyelectrolyte-based fluorescence sensor for pyrophosphate, Zhao, X. Y.; Liu, Y.; Schanze, K. S. *Chem. Commun.* **2007**, 2914-2916.
7. Energy transfer dynamics in a series of conjugated polyelectrolytes with varying chain length, Hardison, L. M.; Zhao, X. Y.; Jiang, H.; Schanze, K. S.; Kleiman, V. A. *J. Phys. Chem. C* **2008**, *112*, 16140-16147.
8. Polymer chain length dependence of amplified fluorescence quenching in conjugated polyelectrolytes, Zhao, X. Y.; Jiang, H.; Schanze, K. S. *Macromolecules* **2008**, *41*, 3422-3428.
9. Conjugated polyelectrolytes: Synthesis, photophysics, and applications, Jiang, H.; Taranekar, P.; Reynolds, J. R.; Schanze, K. S. *Angew. Chem. Int. Ed.* **2009**, *48*, 4300-4316.
10. Variable-band-gap poly(arylene ethynylene) conjugated polyelectrolytes adsorbed on nanocrystalline TiO₂: Photocurrent efficiency as a function of the band gap, Jiang, H.; Zhao, X.; Shelton, A. H.; Lee, S. H.; Reynolds, J. R.; Schanze, K. S. *ACS Applied Materials & Interfaces* **2009**, *1*, 381.
11. Convenient synthesis of functional polyfluorenes via a modified one-pot Suzuki-Miyaura condensation reaction, Walczak, R. M.; Brookins, R. N.; Savage, A. M.; van der Aa, E. M.; Reynolds, J. R. *Macromolecules* **2009**, *42*, 1445-1447.
12. Interchain interactions in poly(benzo[1,2-b:4,3-b']dithiophene)s and the effect of substituents on aggregation, Brookins, R. N.; Berda, E.; Reynolds, J. R. *J. Mater. Chem.* **2009**, *19*, 4197-4204.
13. Triplet exciton quenching in a conjugated polyelectrolyte, Jiang, H.; Lee, S.-H.; Zhao, X.; Miller, J. R.; Schanze, K. S., submitted.
14. Water-soluble conjugated polyelectrolytes with dendritic side chains: Synthesis, characterization, and optical properties, Lee, S.-H.; Kömürlü, S.; Zhao, X.; Jiang, H.; Moriena, G.; Kleiman, V. D.; Schanze, K. S., submitted.

Session VII

*Investigation of Solar Photoconversion
with Multidimensional Spectroscopy*

**Towards Control of Photochemical Transformations using Pulse Shaping:
Exploiting Vibrations to Enhance Product Yield in Tetracene Singlet Fission
and in Ligand Dissociation Reactions in Charge-Transfer Excited Metal Complexes**

Niels H. Damrauer, Erik M. Grumstrup, and Paul Vallett
Department of Chemistry and Biochemistry
University of Colorado at Boulder
Boulder, CO 80309

Synthetic and bioenergetic solar energy conversion demands systems with both electronic and reactive complexity. In this program we have been interested in developing new physical tools for their interrogation. Photochemical control of complex systems is becoming a reality using closed-loop adaptive learning procedures in vast parameters spaces made possible by broad-band ultrashort laser pulses. Steps must also be taken to complement control with information about why it occurs and what it says about important degrees of freedom in these systems.

In this project period we first explored how orthogonal control variables discovered using statistical dimension reduction strategies can inform us about control mechanisms. We then developed pulse-shaper based 2D electronic experiments to interrogate systems without changing the experimental setup used for control. These explorations gave us training to develop methodologies to identify when systems are coherently controllable via laser phase manipulations for a given setup (for example a given pump spectrum) and ways to obtain spectral information about systems being controlled by non-resonant multiphoton interactions. We then designed shaping methods to elicit an oscillatory transient absorption (TA) response in systems undergoing multiple exciton generation (MEG), indicating coherent phenomena. Simulations based on the Efros/Nozik coherence model for MEG dynamics showed that pulse-shaping under ideal conditions could uncover coupling constants between non-stationary states such as the thermally hot single- and bi-exciton states. This led us to implement experimental improvements such as the building of a NOPA to obtain shorter (30 fs versus 100 fs) visible excitation pulses. It is noted that subsequent experiments on PbSe QD systems have been inconclusive in part because of stimulated Raman signals involving solvent. We have tools and training in place and are now seeking to identify systems where control involves dynamics as opposed to multi-photon excitation pathways. This talk will explore recent efforts on two fronts.

Polycrystalline tetracene films (generously supplied by Dr. Justin Johnson of NREL) reveal excitonic character in the singlet excited state manifold (near 500 nm excitation). These systems are believed to exhibit prompt and thermally activated singlet fission (related to MEG) where a singlet exciton is converted into two triplets excited states on neighboring tetracene molecules in the lattice. Pump-probe spectra and kinetics following excitation with a bandwidth limited (BWL) pulse at low fluence (~50 nJ/pulse; ~200 μm spot size) reveal a long-lived (> 1.5 ns) absorption feature near 490 nm which we interpret as being due to the triplet and therefore sensitive to its photochemical yield. Coherent oscillations in TA signals are observed for ~ 3 ps with a frequency of 310 cm^{-1} due to a Raman-active vibrational mode. Adaptive control experiments based on the modulation of phase were run with the goal of increasing the 490 nm TA signal. A reduced search space was used that includes pulse trains with variable numbers of pulses, timing (τ) between pulses, and inter-pulse relative phase. Optimizations reveal a 10 -

15% increase in the signal over the BWL pulse. Pulse shapes with $\tau = 450$ fs or $\tau = 225$ fs had comparable fitness and the phase parameter does not appear to matter. **Fig. 1** shows clear evidence of control in a comparison of TA kinetics collected at 490 nm following excitation with a BWL pulse versus a $\tau = 450$ fs optimal pulse. Interestingly, Fourier transformation of an oscillatory signal in 490 nm TA kinetics following excitation with an optimal pulse ($\tau = 225$ fs) shows complete suppression of the 310 cm^{-1} mode but strong enhancement of lower frequency modes (90 cm^{-1} and 130 cm^{-1}) not observed as Raman signals following excitation with a BWL pulse. We hypothesize that these are related to intermolecular motions that alter electronic coupling between the singlet exciton state and the double triplet state and that control leaves remnants of their coherent motion driven by the shaped pulses. Critical next steps include the measurement of fluorescence under conditions where control is taking place and measurement of TA kinetics in magnetic fields. These experiments should help us to determine whether control manipulates singlet exciton population or whether it is manipulating intermolecular nuclear momentum that improves reaction yields. Theoretical efforts are needed both from the perspective of obtaining potential energy surfaces for tetracene dimers (collaboration with Musgrave and Zimmerman; CU Chemical Engineering) as well as explorations of dynamics (collaboration with Eaves CU Chemistry).

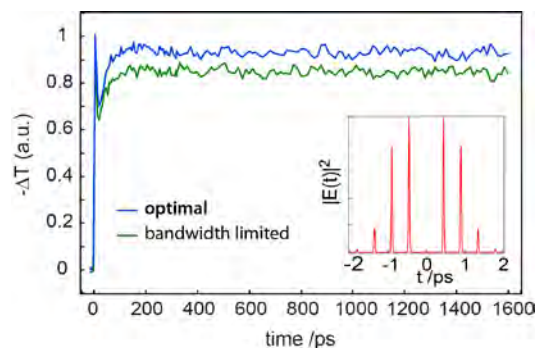
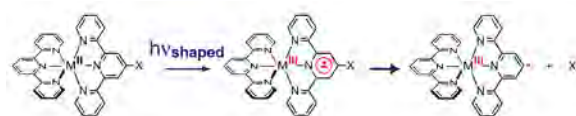


Figure 1. TA kinetics at 490 nm of a tetracene film (~ 90 nm) at 294K following excitation with a 25 fs pulse (50 nJ/pulse) centered at 540 nm (green trace) versus an adaptively-discovered shaped pulse (blue trace). The shaped pulse (intensity is simulated in the inset) is a train with 450 fs interpulse spacing.

A second class of dynamical control problems of interest to us involves metal complexes with an aryl-halide bond in the ligand structure as well as visible MLCT transitions within the complex as a whole. The desire is to achieve electron-transfer-coupled bond breaking reactions (Scheme 1) by controlling halogen bending motion out of the plane of the aryl ligand as a way of circumventing conical intersections between the π^* radical MLCT reactant and the σ -radical product state. In this talk we will describe computational efforts to identify promising molecules. Initial exploration of terpyridine (tpy) systems in Scheme 1 where $M = Ru$ and $X = Br$ and I within an acetonitrile continuum revealed reaction enthalpies endothermic by ~ 0.8 eV for a variety of DFT methods. Using calculations based on thermodynamic cycles we have identified that improvements can be made by tuning the oxidation energy of the complex. We will discuss synthetically tractable bis-heteroleptic bipyridyl species where systematic ancillary ligand modifications lower ΔE_{rxn} to ~ 0.5 eV. Finally we will discuss a tpy system $[Ru(\sigma,6\text{-}Br_2\text{-tpy})(tpy)]^{2+}$ where interligand steric effects lower the C–Br bond dissociation energy and hinders formation of 3dd states. These effects lead to a predicted ΔE_{rxn} of ~ 0.16 eV. This species is also synthetically tractable, is currently being made, and will be a launching point as we go forward with control experiments. The tetracene work, especially the perspective of using more limited search parameters based on pulse sequences, has been critical training and will serve as a template in future control experiments.



Scheme 1

Initial exploration of terpyridine (tpy) systems in Scheme 1 where $M = Ru$ and $X = Br$ and I within an acetonitrile continuum revealed reaction enthalpies endothermic by ~ 0.8 eV for a variety of DFT methods. Using calculations based on thermodynamic cycles we have identified that improvements can be made by tuning the oxidation energy of the complex. We will discuss synthetically tractable bis-heteroleptic bipyridyl species where systematic ancillary ligand modifications lower ΔE_{rxn} to ~ 0.5 eV. Finally we will discuss a tpy system $[Ru(\sigma,6\text{-}Br_2\text{-tpy})(tpy)]^{2+}$ where interligand steric effects lower the C–Br bond dissociation energy and hinders formation of 3dd states. These effects lead to a predicted ΔE_{rxn} of ~ 0.16 eV. This species is also synthetically tractable, is currently being made, and will be a launching point as we go forward with control experiments. The tetracene work, especially the perspective of using more limited search parameters based on pulse sequences, has been critical training and will serve as a template in future control experiments.

DOE Sponsored Publications 2007-2010

1. Grumstrup, E. M.; Shim, S. H.; Montgomery, M. A.; Zanni, M. T.; Damrauer, N. H. Facile Collection of Two-Dimensional Electronic Spectra with Pulse Shaping Technology. *Optics Express* **15**, 16681-16689 (2007)
2. Montgomery, M. A.; Damrauer, N. H. A Convenient Method to Simulate and Visually Represent Two-Photon Power Spectra of Arbitrarily Shaped Broadband Laser Pulses. *New Journal of Physics* (Special Issue on Quantum Control Edited by H. Rabitz) **11**, 105053 (2009).
3. Meylemans, H. A.; Damrauer, N. H. Controlling Electron Transfer through the Manipulation of Structure and Ligand-Based Torsional Motions: A Computational Exploration of Ruthenium Donor-Acceptor Systems using Density Functional. *Inorganic Chemistry* **48**, 11161-11175 (2009). (This study used in-house computational resources made available with this grant)
4. Montgomery, M. A.; Grumstrup, E. M. Damrauer, N. H. Novel One- and Two-Dimensional Fourier Transform Spectroscopies Derived from Amplitude and Phase Switching with Applications to Adaptive Pulse-Shaping Control. (2010) Submitted to *Journal of Chemical Physics*.
5. Grumstrup, E. M.; Damrauer, N. H. Coherent Control of Singlet Fission in Tetracene Thin Films. In preparation
6. Grumstrup, E. M.; Damrauer, N. H. Time Dependant Perturbation Theory Applied to Sinusoidal Spectral Phase Modulation: Insights into Coherent Control Photophysics. In preparation
7. Vallett, P.; Damrauer, N. H. Computational Exploration of Radical Forming Photoreactions Involving Ruthenium Polypyridyl Complexes. In preparation.

How Hard Is It to Produce 100% Efficient Energy Transfer in Photosynthetic Light Harvesting?

Graham R. Fleming

Physical Biosciences Division
Lawrence Berkeley National Laboratory
Department of Chemistry
University of California Berkeley
Berkeley, CA 94720

If the attainment of 100% quantum efficiency in energy transfer from input to target simply involves placing chromophores at a certain density (which in natural systems is $\sim 1M$), then the specific values of the system parameters are not of special interest. However, a recent calculation by Buchleitner and coworkers (ArXiv 0912.3560) finds from a sample of 10^8 configurations of a 10 site model, only 1 in 10^6 give high transfer efficiency. This leads to a number of questions: (1) Can the energy landscape be manipulated to create uni-directional flow to the target site? (2) How important is coherence? (3) How important is constructive/destructive interference along competing pathways to the target? (4) What is the optimal strength of the electron-phonon coupling? (5) Do correlated fluctuations help or hurt? and (6) What is the optimal phonon relaxation timescale?

The control parameters relevant to these questions are: (1) The electronic couplings between components, (2) the strength of the electron-phonon coupling, (3) the site energies of the individual components. Manipulation of all three parameter sets enables: (1) the magnitude and location of delocalized states, (2) the direction and magnitude of transition moments, and (3) the balance of coherent and incoherent energy flow.

Work over the past 2 years to quantify, model, and understand these points will be discussed.

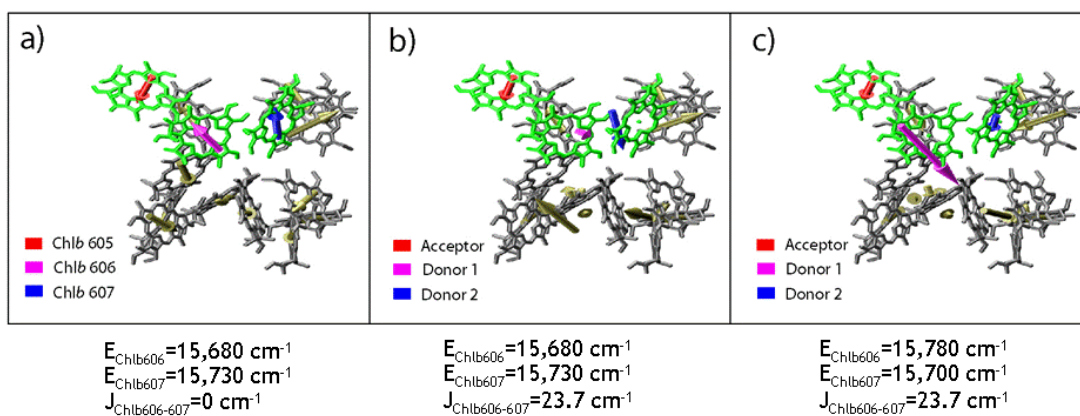


Figure. Interplay of site energies and coupling to determine energy landscape in LHCII.

Publications supported by DOE 2007-2010

- “Two Dimensional Fourier Transform Electronic Spectroscopy: Evolution of Cross Peaks in the Fenna-Matthews-Olson Complex.” G.S. Engel, E. L. Read, T. R. Calhoun, T. K. Ahn, T. Mancal, R. E. Blankenship, and G. R. Fleming. *In Ultrafast Phenomena XV* (Springer, Berlin), 392-394 (2007).
- “Two Dimensional Optical Spectroscopy of Multi-chromophore Protein Complexes.” G.R. Fleming, D. Zigmantas, E. L. Read, T. Mancal and G. S. Engel. *In Ultrafast Phenomena XV* (Springer, Berlin) 326-328 (2007).
- “Evidence for wavelike energy transfer: Quantum coherence in photosynthetic systems.” G. S. Engel, T. Calhoun, E.L. Read, T. K. Ahn, T. Mancal, R. E. Blankenship and G. R Fleming. *Nature* **446**, 782 (2007).
- “Determination of Electronic Mixing in Purple Synthetic Bacteria by Two-Color Three Pulse Photon Echo Peak Shift.” D. Y. Parkinson, H. Lee and G. R. Fleming. *In Ultrafast Phenomena XV* (Springer, Berlin) 537-539 (2007).
- “Measuring Electronic Coupling in the Reaction Center of Purple Photosynthetic Bacteria by Two Color Three Pulse Photon Echo Peak Shift Spectroscopy.” D. Y. Parkinson, H. Lee, and G. R. Fleming. *J. Phys. Chem. B*, **111**, 7449-7456 (2007).
- “Coherence dynamics in photosynthesis: protein protection of excitonic coherence.” H. Lee, Y.C. Cheng and G. R. Fleming, *Science* **316**, 1462 (2007).
- “Multidimensional Ultrafast Spectroscopy Special Feature: Cross-peak-specific two dimensional electronic spectroscopy.” E. L. Read, G. S. Engel, T. Calhoun, T. Mancal, T.K. Ahn, R. E. Blankenship and G. R. Fleming, *PNAS*, **104**, 14203-14208 (2007).
- “Efficient Simulation of Three-Pulse Photon-Each Signals and the Application to Detect Electronic Coupling in a Bacterial Reaction Center.” Y-C. Cheng, H. Lee, and G. R. Fleming *Journal of Physical Chemistry A*, **111**, 9499-9508 (2007).
- “Elucidation of population and coherence dynamics using cross-peaks in two-dimensional electronic spectroscopy” Y-C Cheng, G. S. Engel and G. R. Fleming, *Chemical Physics*, **341**, 285-295 (2007)
- “Coherence Quantum Beats in Two-dimensional Electronic Spectroscopy.” Y-C. Cheng and G. R. Fleming, *J. Phys. Chem. A.*, **112**, 4254-4260 (2008).
- Visualization of Excitonic Structure in the Fenna-Matthews-Olson Photosynthetic Complex by Polarization-Dependent Two-Dimensional Electronic Spectroscopy, E. L. Read, G. S. Schlau-Cohen, G. S. Engel, J. Wen, R. E. Blankenship and G. R. Fleming, *Biophys. J.*, **95**, 847-856 (2008).
- Architecture of a Charge-Transfer State Regulating Light Harvesting in a Plant Antenna Protein, T. K. Ahn, T. J. Avenson, M. Ballottari, Y-C Cheng, K. K. Niyogi, R. Bassi and G. R. Fleming, *Science*, **320**, 794-796 (2008)

Kinetic modeling of charge-transfer quenching in the CP29 minor complex. Y.C. Cheng, T.K. Ahn, T.J. Avenson, D. Zigmantas, K.K. Niyogi, M. Ballottari, R. Bassi, and G.R. Fleming, *J. Phys. Chem. C*, 112(42):13418-23 (2008)

Investigating Energy Partitioning During Photosynthesis Using an Expanded Quantum Yield Convention, T.K. Ahn, T. J. Avenson, G. Peers, Z. Li, L. Dall'Osto, R. Bassi, K. K. Niyogi, and G.R. Fleming, *Chemical Physics*, Villy Sundström Issue, 357, 151-158 (2009).

Grand Challenges in Basic Energy Sciences; G. R. Fleming and M. A. Ratner, *Physics Today*, 60, 28-33, 2008

Dynamics of Light Harvesting in Photosynthesis, Y-C Cheng and G. R. Fleming, *Annual Review of Physical Chemistry*, Vol. 60: 241-262 (2009).

Lutein Can Act as a Switchable Charge Transfer Quencher in the CP26 Light Harvesting Complex. T.J. Avenson, T.K. Ahn, K.K. Niyogi, M. Ballottari, R. Bassi and G.R. Fleming, *J. Biol. Chem.* 284 (5), 2830-2835, 2009.

Pigment Organization and Energy Level Structure in Light-Harvesting Complex 4: Insights from Two-Dimensional Electronic Spectroscopy, E. L. Read, G. S. Schlau-Cohen, G. S. Engel, T. Georgiou, M. Z. Papiz, G. R. Fleming, *J. Phys. Chem B*, 113., 6495-6504 (2009)

Photon Echo Studies of Photosynthetic Light Harvesting, E. L. Read, H. Lee & G.R. Fleming, *Photosynthetic Research*, Govindjee Special Issue, 101, 2, 233, (2009)

On the Adequacy of the Redfield Equation and Related Approaches to the study of Quantum Dynamics in Electronic Energy Transfer. A. Ishizaki and G. Fleming, *J. Chem. Phys.*, 130, 234110 (2009).

Unified Treatment of Quantum Coherent and Incoherent Hopping Dynamics in Electronic Energy Transfer: Reduced Hierarchy Equations Approach, A. Ishizaki and G. Fleming, *J. Chem. Phys*, 130, 234111 (2009)

Nonlinear Optical Methods to Study Condensed Phase Chemical and Biological Dynamics, G. R. Fleming, Lecture for European Virtual University on Lasers; published on-line at: www.mitr.p.lodz.pl/evu/wyklady/ (Jan 2009).

Two-Dimensional Electronic Spectroscopy of the Low-Light Adapted Light Harvesting Complex 4, E. Read, G.S. Schlau-Cohen, G. S. Engel, T. Georgiou, M.Z. Papiz & G.R. Fleming, *In Ultrafast Phenomena XVI: Proceedings of the 16th International Conference Series: Springer Series in Chemical Physics*, Vol. 92, Corkum, P.; De Silvestri, S.; Nelson, K.A.; Riedle, E.; Schoenlein, R.W. (Eds.) (Springer, Berlin) 559-561 (2009).

Mapping Parallel Pathways of Energy Flow in LCHII with Broadband, G.S. Schlau-Cohen, T. R. Calhoun, G.S. Engel, E. Read, N. S. Ginsberg, D. Zigmantas, R. Bassi & G. R. Fleming, *In Ultrafast Phenomena XVI: Proceedings of the 16th International Conference Series: Springer Series in Chemical Physics*, Vol. 92, Corkum, P.; De Silvestri, S.; Nelson, K.A.; Riedle, E.; Schoenlein, R.W. (Eds.) (Springer, Berlin) 598-600 (2009).

Observation of Quantum Coherence in Light Harvesting Complex II by Two-Dimensional Electronic Spectroscopy, T. R. Calhoun, N. S. Ginsberg, Y.-C. Cheng, M. Ballottari, R. Bassi & G. R. Fleming, *In*

Ultrafast Phenomena XVI: Proceedings of the 16th International Conference Series: [Springer Series in Chemical Physics](#), Vol. 92, Corkum, P.; De Silvestri, S.; Nelson, K.A.; Riedle, E.; Schoenlein, R.W. (Eds.) (Springer, Berlin) .406-408, (2009)

Quantum Coherence Accelerating Photosynthetic Energy Transfer, H. Lee, Y.-C. Cheng & G. Fleming, *In Ultrafast Phenomena XVI*: Proceedings of the 16th International Conference Series: [Springer Series in Chemical Physics](#), Vol. 92, Corkum, P.; De Silvestri, S.; Nelson, K.A.; Riedle, E.; Schoenlein, R.W. (Eds.) (Springer, Berlin) 607-609, (2009).

Lutein accumulation in the absence of zeaxanthin restores nonphotochemical quenching in the *Arabidopsis thaliana npq1* mutant, Z. Li, T. K. Ahn, T. J. Avenson, J. A. Cruz, D. M. Kramer, G. R. Fleming, Jay D. Keasling & K. K. Niyogi, *Plant Cell*, 21, 1798-1812, (2009).

Two-Dimensional Electronic Spectroscopy of Molecular Aggregates, N. Ginsberg, Y.-C. Cheng & G. R. Fleming, *Accounts of Chemical Research*, 42, 1352-1363 (2009).

Quantum Coherence Enabled Determination of the Energy Landscape in LHC II, T.R. Calhoun, N.S. Ginsberg, G.S. Schlau-Cohen, Y.-C. Cheng, M. Ballottari, R. Bassi & G.R. Fleming, *J Phys Chem B*, 113, 16295-16295 (2009).

Theoretical Examination of Quantum Coherence in a Photosynthetic System at Physiological Temperature, A. Ishizaki, G. R. Fleming, *PNAS*, 106, 17255-17260 (2009).

The Pathways of Energy Flow in LCHII from Two-Dimensional Electronic Spectroscopy, G. S. Schlau-Cohen, T. R. Calhoun, N. S. Ginsberg, E. L. Read, M. Ballottari, R. Bassi, R. Van Grondelle, G. R. Fleming, *J. Phys Chem B*, 113, 15352-15363 (2009)

Quantum Coherence and its Interplay with Protein Environments in Photosynthetic Electronic Energy Transfer, A. Ishizaki, T. Calhoun, G. Schlau-Cohen, and G. Fleming, *Phys Chem Chem Phys*, (Submitted)

Quantum Superposition in Photosynthetic Light Harvesting: Delocalization and Entanglement, A. Ishizaki and G. Fleming, *New J Phys*, (In Press)

Spectroscopic Elucidation of Uncoupled Transition Energies in the Major Photosynthetic Light Harvesting Complex, LHCII, G.Schlau-Cohen, T.Calhoun, N.Ginsberg, M.Ballottari, R.Bassi, and G. Fleming, *PNAS*, (Submitted)

Session VIII

Inorganic Homogeneous Photocatalysis

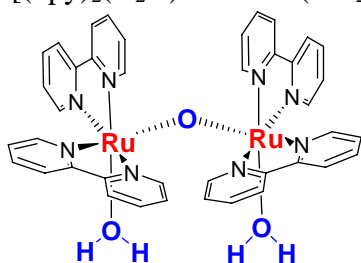
Intermediates in Water Oxidation Catalysis through Pulse Radiolysis

Sergei V. Lymar

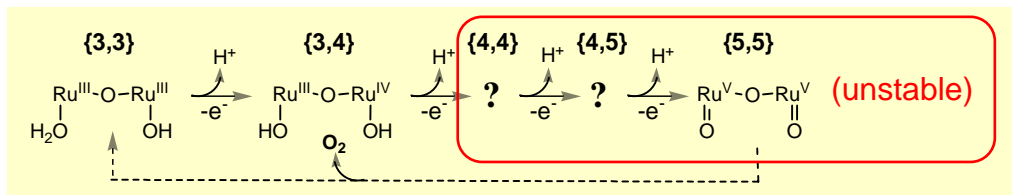
Chemistry Department, Brookhaven National Laboratory, Upton, NY 11973-5000

The goal of this project is to gain mechanistic insight into water oxidation catalysis through the use of pulse radiolysis techniques for generating and characterization of the catalyst transients involved in the catalytic cycle.

Development of catalysts to carry out the four-electron water oxidation at energies and rates consistent with the use of solar light remains the greatest challenge in the photochemical water splitting. Of all homogeneous catalysts that have been examined, the dimeric μ -oxo-bridged ruthenium ion (proposed by Meyer and known as *the blue ruthenium dimer*) *cis,cis*- $[(\text{bpy})_2(\text{H}_2\text{O})\text{Ru}-\text{O}-\text{Ru}(\text{OH}_2)(\text{bpy})_2]^{4+}$ has been the most extensively studied and its capacity for water oxidation has been repeatedly confirmed. Although important features have been discerned, the reaction mechanisms remain to be established. The major impediment in unraveling these and other water oxidation catalysts has been the difficulties in identification and characterization of the reaction intermediates.

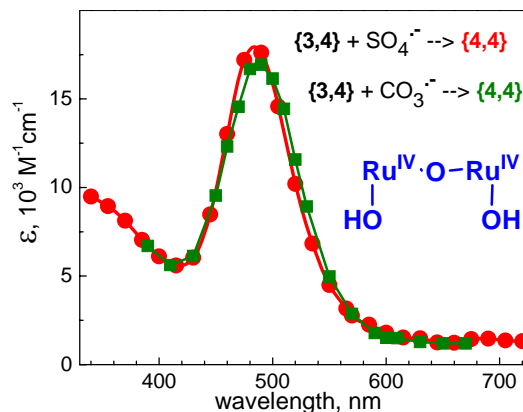


Research from several laboratories, particularly those of Meyer and Hurst, have established that water oxidation catalysis by the *blue dimer* involves its progressive oxidation above the $\text{Ru}^{\text{III}}, \text{Ru}^{\text{III}}$ state (denoted as $\{3,3\}$) with the attendant loss of protons to the ruthenyl $\{5,5\}$ dimer. However, only the $\{3,3\}$ and $\{3,4\}$ states could be characterized over a broad pH range.



We began with the assessments of the reactivity of the $\{3,3\}$ and $\{3,4\}$ states toward the radiolytically-generated radicals focusing on obtaining and characterization of the $\{4,4\}$ state. Of several tested, two convenient systems have been identified. In the $t\text{-BuOH}/\text{S}_2\text{O}_8^{2-}$ system, the hydrated electrons are converted into the $\text{SO}_4^{\cdot-}$ radical ($E^\circ = 2.43 \text{ V}$), which rapidly ($k = 1.5 \times 10^{10} \text{ M}^{-1}\text{s}^{-1}$) oxidizes $\{3,4\}$ to $\{4,4\}$. The kinetic analysis yields the first unambiguous $\{4,4\}$ spectrum shown in the figure. Essentially the same spectrum is obtained by the oxidation of $\{3,4\}$ by the $\text{CO}_3^{\cdot-}$ radical ($E^\circ = 1.57 \text{ V}$) in the $\text{N}_2\text{O}/\text{CO}_3^{2-}$ system; these results make the spectrum assignment definitive. The oxidation by $\text{CO}_3^{\cdot-}$ occurs much slower ($k = 4 \times 10^8 \text{ M}^{-1}\text{s}^{-1}$) possibly indicating the approach to the $\{3,4\}$ reduction potential.

The $\{4,4\}$ complex is found to be unstable in neutral



solution and undergoes further reaction(s) on the time scale of milliseconds to minutes leading to regeneration of {3,4}. Although these processes are not yet fully understood, it appears that a disproportionation of {4,4} is the major contributor.

Other pertinent observations can be summarized as follows: (1) the H atom cleanly reduces {3,4} to {3,3}, (2) the OH[•] radical oxidizes {3,3} to {3,4}, (3) in contrast and unexpectedly, OH[•] attack on {3,4} results in its reduction to {3,3} probably via a bpy-ring adduct, indicating that the catalyst in {4,4} and higher states may be susceptible to nucleophilic

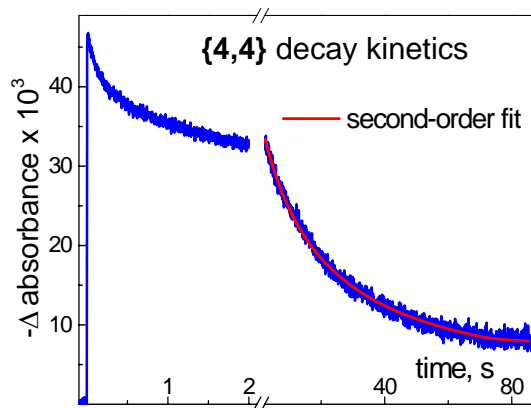
attack by H₂O or OH⁻, (4) the comproportionation reaction {3,3} + {4,4} → {3,4} + {3,4} has been detected, suggesting $E(\{3,4\}) > E(\{3,3\})$ for the reduction potentials, (5) the reaction between {4,4} and the C-centered t-BuOH radical has been observed, suggesting a radical-like nature of the {4,4} state; if confirmed, this finding will have important mechanistic implications.

Future work will further clarify the nature of catalyst transients formed during water oxidation: (1) we will continue characterization of the {4,4} state of “blue dimer” focusing on identification of its protonation state and understanding the decomposition pathways; a set of time-resolved spectra over a range of pH will be obtained and analyzed to unravel the decay mechanism. Analogous study will be attempted for the {4,5} state, (2) it is generally agreed, that {5,5} is the catalytically active form, but it has been difficult to reach this state in a non-rate-determining manner. Radiolysis with large pulses generating sufficient excess of SO₄^{•-} or CO₃^{•-} over {3,4} should allow us to rapidly produce the {5,5} state, thus opening a possibility to observe the details of the O₂-forming step, (3) a set of “blue dimer” congeners with electron-donating and withdrawing ligand substitutions that can modulate reduction potentials and catalytic activities will be included in this study, (4) recently, a novel, all-inorganic, and potentially very robust water oxidation catalyst has been reported. It has a tetranuclear Ru^{IV} core, {Ru₄O₄(OH)₂(H₂O)₄}⁶⁺, sandwiched between supporting polytungstate ligands. In collaboration with Dr. Hill, we have initiated pulse radiolysis in order to detect and describe reactivity of intermediates that may be involved.

This is a collaborative (with Drs. Hurst, Washington State U.) research constituting a minor component of a broader program on the pulse radiolysis application for mechanistic studies; the major part deals with the reactivity of nitrogen oxides and their congeneric acids and anions.

DOE Sponsored Publications 2007-2010

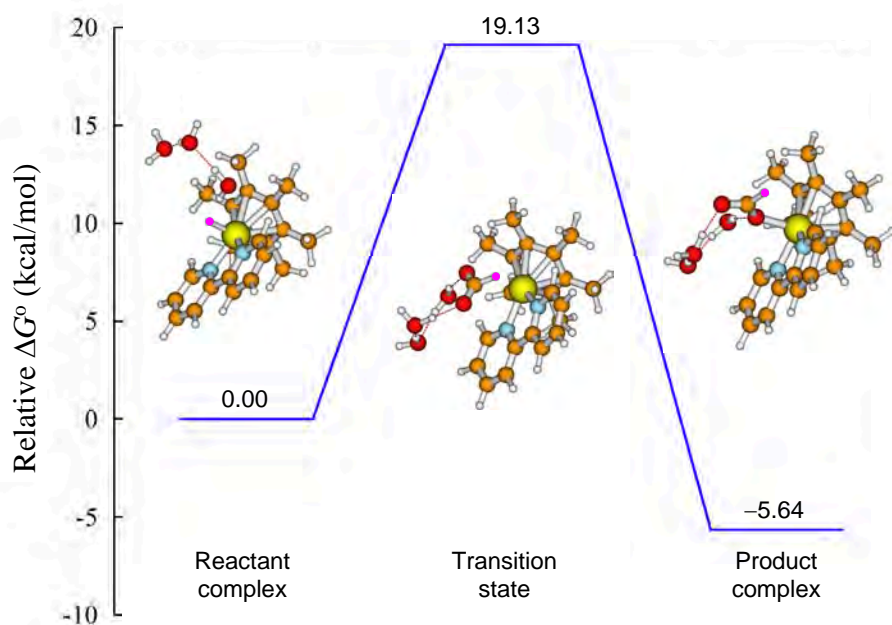
1. Lymar, S. V.; Shafirovich, V. *J. Phys. Chem. B* **2007**, *111*, 6861-6867.
2. Funston, A. M.; Lymar, S. V.; Saunders-Price, B.; Czapski, G.; Miller, J. R. *J. Phys. Chem. B* **2007**, *111*, 6895-6902.
3. Poskrebyshev, G. A.; Shafirovich, V.; Lymar, S. V. *J. Phys. Chem. A* **2008**, *112*, 8295-8302.
4. Cape, J. L.; Lymar, S. V.; Lightbody, T.; Hurst, J. K. *Inorg. Chem.* **2009**, *48*, 4400-4410.



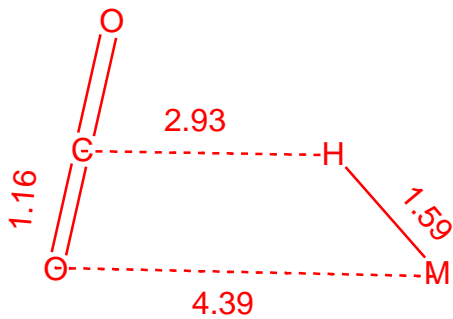
Reactions of Hydride Complexes

Carol Creutz
Chemistry Department
Brookhaven National Laboratory
Upton, NY, 11973-5000

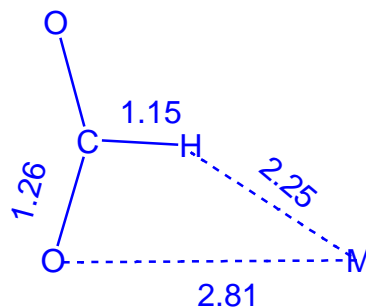
Reactions of hydride complexes of ruthenium(II) with hydride acceptors have been examined for $\text{Ru}(\text{terpy})(\text{bpy})\text{H}^+$, $\text{Ru}(\text{terpy})(\text{dmb})\text{H}^+$ and $\text{Ru}(\eta^6\text{-C}_6\text{Me}_6)(\text{bpy})(\text{H})^+$ in aqueous media at 25 °C (terpy = 2,2',6',2''-terpyridine, bpy = 2,2'-bipyridine, dmb = 4,4'-dimethyl-2,2'-bipyridine). The acceptors include CO_2 , CO, CH_2O , and H_3O^+ . $\text{Ru}(\text{terpy})(\text{dmb})\text{H}^+$ reacts with CO with a rate constant of $1.2(0.2) \times 10^1 \text{ M}^{-1} \text{ s}^{-1}$. Reaction of CO with $\text{Ru}(\eta^6\text{-C}_6\text{Me}_6)(\text{bpy})(\text{H})^+$ was very slow, $k \leq 0.1 \text{ M}^{-1} \text{ s}^{-1}$. $\text{Ru}(\text{terpy})(\text{bpy})\text{H}^+$ and $\text{Ru}(\eta^6\text{-C}_6\text{Me}_6)(\text{bpy})(\text{H})^+$ react with CH_2O with rate constants of $(6 \pm 4) \times 10^6$ and $1.1 \times 10^3 \text{ M}^{-1} \text{ s}^{-1}$, respectively. The reaction of $\text{Ru}(\eta^6\text{-C}_6\text{Me}_6)(\text{bpy})(\text{H})^+$ with acid exhibits straightforward, second-order kinetics, with the rate proportional to $[\text{Ru}(\eta^6\text{-C}_6\text{Me}_6)(\text{bpy})(\text{H})^+]$ and $[\text{H}_3\text{O}^+]$ and $k = 2.2 \times 10^1 \text{ M}^{-1} \text{ s}^{-1}$ ($\mu = 0.1 \text{ M}$, Na_2SO_4 medium). However, for the case of $\text{Ru}(\text{terpy})(\text{bpy})\text{H}^+$, the protonation step is very rapid and only the formation of the product $\text{Ru}(\text{terpy})(\text{bpy})(\text{H}_2\text{O})^{2+}$ (presumably via a dihydrogen or dihydride complex) is observed with k_{obs} ca. 4 s^{-1} . The hydricities of HCO_2^- , HCO^- , and H_3CO^- in water are estimated as +1.48, -0.76, and +1.57 eV/molecule (+34, -17.5, +36 kcal/mol), respectively. Theoretical studies of the reactions with CO_2 have been conducted in an effort to clarify the mechanisms. Results are illustrated below for $\text{Ru}(\eta^6\text{-C}_6\text{Me}_6)(\text{bpy})(\text{H})^+$ with three water molecules.



An abbreviated reaction scheme drawn approximately to scale is shown below. It is the RuH stretching mode and the CO_2 ν_{2a} stretch that take the reactants to the transition state.

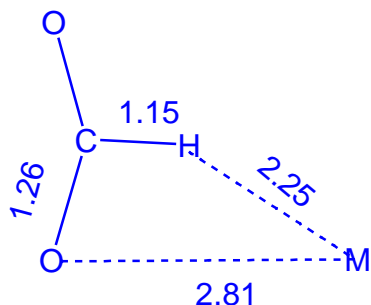


Reactants

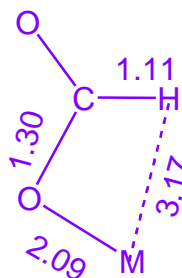


Transition State

This combined motion corresponds to vibrational mode #114 at 1323 cm^{-1} (for terpybpy #68 at 754 cm^{-1}) of the transition state for $\text{Ru}(\eta^6\text{-C}_6\text{Me}_6)(\text{bpy})(\text{H})^+$. In the subsequent step, the transition state is converted to product by relaxation of the formate ion and formation of the Ru-O bond. The similarity of the geometries of the transition state and the relaxed formate complex is noteworthy and relevant to the important (reverse) process of decarboxylation.

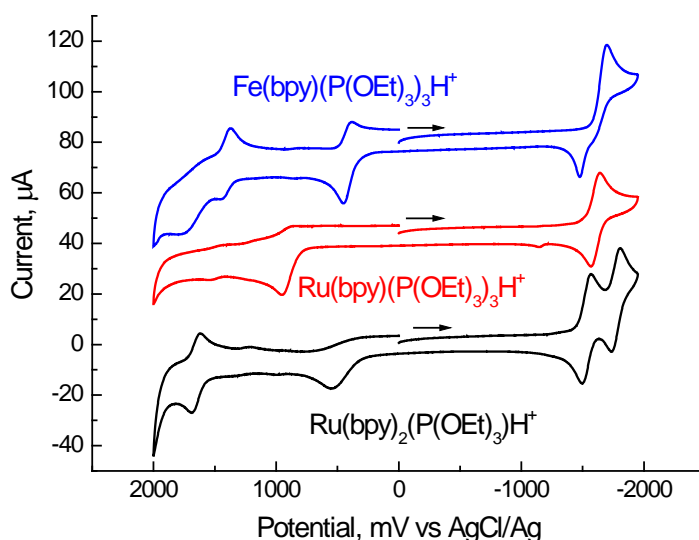


Transition State



Formate Complex

Iron Hydride Complexes. The crystal structures of $(\eta^5\text{-Cp})$ bis and tris TPA complexes (TPA = 1,3,5-triaza-7-phosphatricyclo[3.3.1.1^{3,7}]decane) of iron(II) are reported, as are structures for the hydride complexes, $[\text{Fe}(\text{bpy})(\text{P}(\text{OEt})_3)_3\text{H}](\text{CF}_3\text{SO}_3)$ and $[\text{Ru}(\text{bpy})_2(\text{P}(\text{OEt})_3)_3\text{H}](\text{PF}_6)$. These and a few other compounds have been subjected to electrochemical and spectroscopic characterization. Somewhat surprisingly $\text{Fe}(\text{bpy})(\text{P}(\text{OEt})_3)_3\text{H}^+$ exhibits a quasi reversible oxidation at +0.42 V vs. Ag/AgCl in acetonitrile; $\text{Ru}(\text{bpy})(\text{P}(\text{OEt})_3)_3\text{H}^+$ and $\text{Ru}(\text{bpy})_2(\text{P}(\text{OEt})_3)_3\text{H}^+$ are oxidized irreversibly at +0.90 and +0.55 V, respectively, vs. Ag/AgCl. The reduction site for $\text{Fe}(\text{bpy})(\text{P}(\text{OEt})_3)_3\text{H}^+$ and $\text{Fe}(\text{bpy})(\text{P}(\text{OEt})_3)_3(\text{CH}_3\text{CN})^{2+}$



appears to be the metal and gives rise to a two-electron process. The bpy-centered reductions are negatively shifted in the Ru(II) hydride complexes, compared to the acetonitrile complexes. Fe(bpy)(P(OEt)₃)₃H⁺ and Ru(bpy)(P(OEt)₃)₃H⁺ do not react with CO₂ in acetonitrile, but the one-electron-reduction product of Ru(bpy)₂(P(OEt)₃)H⁺ and two-electron-reduction product of Fe(bpy)(P(OEt)₃)₃H⁺ do. Ru(bpy)₂(P(OEt)₃)H⁺ also reacts slowly with CO₂ to give a formate complex (as reported previously by Albertin et al. *Inorg. Chem.* **2004**, *43*, 1336) with a second-order rate constant of $\sim 4 \times 10^{-3} \text{ M}^{-1} \text{ s}^{-1}$ in methanol.

DOE Sponsored Publications 2007-2010

1. "Low-Spin Iron(II) Complexes Containing P, N, and H Ligands: Structure, Spectroscopy, Electrochemistry and Reactivity", Chen, J. Z., Szalda D., Fujita, E. and Creutz C. (submitted)
2. "Hydride Ion Transfer from and to Ruthenium(II) Complexes in Water: Kinetics and Mechanism", Carol Creutz, Mei H. Chou, Mark D. Doherty, Hua Hou, and James T. Muckerman (submitted)
3. "Hydricities of d⁶ Metal Hydride Complexes in Water", Creutz, C.; Chou, M. H. *J. Am. Chem. Soc.* **2009**, *131*, 2794-2795.
4. "The Coordination Chemistry of Gold Surfaces: Formation and Far-Infrared Spectra of Alkanethiolate-Capped Gold Nanoparticles", Petroski, J.; Chou, M.; Creutz, C. *J. Organomet. Chem* **2009**, *694*, 10.1016/j.jorganchem.2008.11.057.
5. "Binding of Catechols to Mononuclear Titanium(IV) and to 1- and 5-nm TiO₂ Nanoparticles". Creutz, C.; Chou, M. H., *Inorg. Chem.* **2008**, *47*, (9), 3509-3514.
6. "Rapid Transfer of Hydride Ion from a Ruthenium Complex to C₁ Species in Water," Creutz, C.; Chou, M. H. *J. Am Chem. Soc.* **2007**, *129*, 10108 - 10109
7. "Nonadiabatic, Intramolecular Electron Transfer from Ruthenium(II) to Cobalt(III) Complexes," Creutz, C. *J. Phys. Chem B* **2007**, *111*, 6713-6717.

Photoinitiated Electron Collection in Mixed-Metal Supramolecular Complexes: Development of Photocatalysts for Hydrogen Production

Shamindri Arachchige, Travis White, Baburam Sedai, Ryan Shaw, Karen J. Brewer*

Department of Chemistry

Virginia Tech

Blacksburg, VA 24061-0212 (kbrewer@vt.edu)

This project is aimed at developing and studying a class of mixed-metal supramolecular complexes with promising redox and excited state properties. These systems couple charge transfer light absorbing metals to reactive metals such as rhodium(III) that will allow these systems to undergo photoinitiated electron collection (PEC) while possessing reactive metal sites capable of delivering collected electrons to a substrate such as H₂O to facilitate the production of H₂. The factors impacting multi-electron photochemistry and the reduction of water to produce H₂ have been explored aimed at providing a detailed understanding of the mechanism of action of these unique photocatalysts and the factors that impact functioning. The process of collecting electrons at a Rh^{III} center results in the production of a newly reduced Rh^I center that is coordinatively unsaturated and thereby able to interact with substrates, Figure 1.

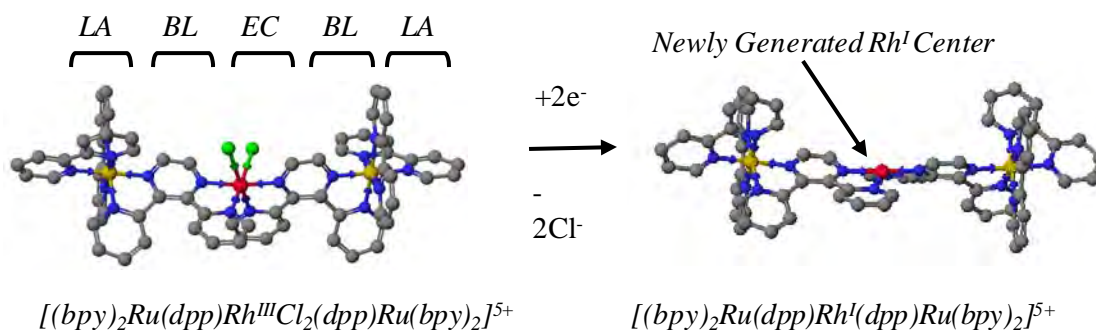


Figure 1. Rearrangement of $[(bpy)_2Ru(dpp)]_2RhCl_2]^{5+}$ following reduction.

Molecular design is at the heart of chemistry providing a means to address complicated issues addressing society. The conversion of the energy from the sun via conversion of water to hydrogen fuel is of significant interest. The processes involved in solar water splitting are complex and involve multielectron chemistry as well as bond breaking and bond making. Reported are structurally diverse supramolecular assemblies with reactive Rh(III) centers that upon excitation are able to multiply reduce and catalyze the reduction of water to produce hydrogen fuel. Polyazine complexes of Ru(II) and Os(II) are widely studied light absorbers (LA) with useful ³MLCT (metal to ligand charge transfer) excited states. Polyazine bridging ligands (BLs) provide coupling to produce large molecular assemblies. This presentation will focus on the design of supramolecular photoinitiated electron collectors for solar hydrogen production and a study of the factors that impact photocatalysis functioning. The ability to synthetic modify these assemblies assists in understanding the complicated redox and spectroscopic properties resulting from many energetically close excited states and complicated excited state dynamics. Illustrative examples of the supramolecular complexes shown to undergo PEC are shown in Figure 2. The systems studied have shown the use of Br bound to the Rh metal center provides for systems with enhanced photocatalytic functioning relative to the previously studied Cl

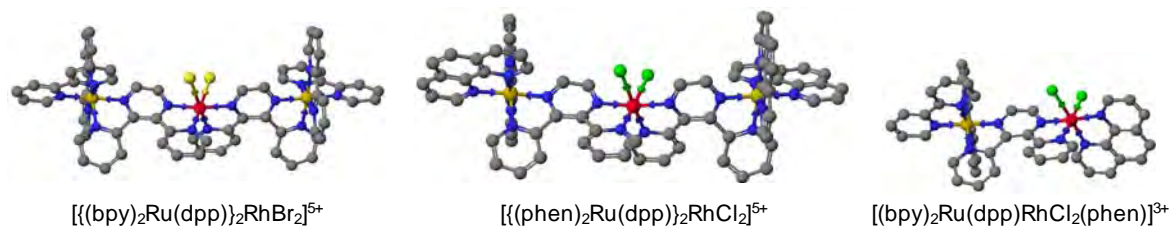


Figure 2. Representative examples of molecular architectures for photoinitiated electron collection and photocatalysis of H_2 formation.

systems. This is indicative of halide loss or electron transfer to the Rh center being kinetically important. Recently we have prepared a new structural motif for PEC, Ru,Rh bimetallic systems that couple one Ru MLCT light absorbing unit to the *cis*- RhX_2 sub-unit important for photocatalysis. The Ru,Rh bimetallics have been shown to undergo PEC producing Rh^I species. Interestingly these Ru,Rh bimetallics are not photocatalysts for the reduction of water to produce H_2 . This illustrates the importance of the Ru,Rh,Ru supramolecular architecture in the production of photocatalytically active systems. This is a key discovery that provides considerable insight into the functioning of the Ru,Rh,Ru supramolecular systems. ESI-MS data show that the Ru,Rh,Ru systems remain intact in the Rh^I form while the Ru,Rh bimetallic systems produce assemblies, presumably through Rh-Rh bond formation. This indicates the steric constraints around the Rh^I center are important to produce active photocatalysts.

The functioning of the photocatalytic system has been studied in detail probing the factors that impact catalyst functioning. The variation of solvent, electron donor, nature of sub-units in the photocatalytic system, headspace volume, light flux and other factors are all utilized to impact photocatalytic function. We have recently shown that our photocatalytic system continues to function after as many as 20 hours of photolysis. We have also shown that turnovers on the order of hundreds are possible within this timeframe under our typical photocatalytic conditions. Details of the study of the functioning of our photocatalytic system will be discussed.

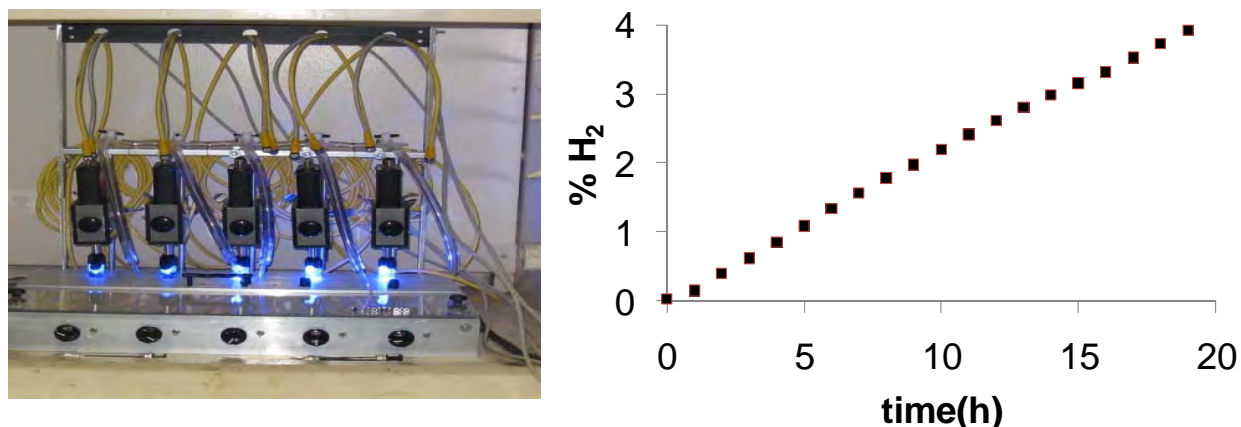


Figure 3. Photocatalysis experiment with real-time hydrogen production.

DOE Sponsored Publications 2007-2010

1. "Rhodium Centered Mixed-Metal Supramolecular Complex as a Photocatalyst for the Visible Light Induced Production of Hydrogen," Mark C. Elvington, Jared Brown, Shamindri Arachchige, Karen J. Brewer *J. Am. Chem. Soc.* **2007**, *129*, 10644-10645.
2. "A Donor-Chromophore Complex Containing the Polyazine Bridging Ligand 2,3-bis(2-pyridyl)pyrazine," Shamindri M. Arachchige, Karen J. Brewer, *Inorg. Chem. Comm.* **2007**, *10*, 1159-1163.
3. "Electrochemistry," Mark Elvington, Karen J. Brewer, *Applications of Physical Methods to Inorganic and Bioinorganic Chemistry*. Edited by Robert A. Scott and Charles M. Lukehart. **2007** John Wiley & Sons, Ltd. ISBN 978-0-470-032176.
4. "A Structurally Diverse Mixed-Metal Complex with Mixed-Bridging Ligands $[[(\text{bpy})_2\text{Os}(\text{dpp})]_2\text{Ru}(\text{dpq})](\text{PF}_6)_{12}$," Ran Miao, Karen J. Brewer, *Inorg. Chem. Commun.* **2007**, *10*, 307-312.
5. "Photochemical Molecular Devices Incorporating Reactive Metals as Supramolecular Solar H₂ Photocatalysts," David F. Zigler, Shamindri Arachchige, Jared Brown, Krishnan Rangan, Eric Chang, Karen J. Brewer, *Prepr. Pap.-Am. Chem. Soc., Div. Pet. Chem.* **2008**, *51(1)*, 1-3. Invited Paper.
6. "Photochemical Hydrogen Production from Water Using the New Photocatalyst $[(\text{bpy})_2\text{Ru}(\text{dpp})]_2\text{RhBr}_2(\text{PF}_6)_5$," Shamindri Arachchige, Jared Brown, Karen J. Brewer *J. Photochem. Photobiol. A: Chem.* **2008**, *197*, 13-17.
7. "Synthesis and Study of the Spectroscopic and Redox Properties of Ru^{II},Pt^{II} Mixed-Metal Complexes Bridged by 2,3,5,6-Tetrakis(2-pyridyl)pyrazine," Shengliang Zhao, Carla Slebodnick, Karen J. Brewer *Inorg. Chem.* **2008**, *47*, 6144-6152.
8. "Ruthenium(II) Polyazine Light Absorbers Bridged to cis-Dichlororhodium(II) Sites in a Bimetallic Molecular Architecture," David F. Zigler, Jing Wang, Karen J. Brewer *Inorg. Chem.* **2008**, *47*, 11342-11350.
9. "Design Considerations for a System for Photocatalytic Hydrogen Production from Water Employing Mixed-Metal Photochemical Molecular Devices for Photoinitiated Electron Collection," Shamindri Arachchige, Jared R. Brown, Eric Chang, Avijita Jain, David F. Zigler, Krishnan Rangan, Karen J. Brewer *Inorg. Chem.* **2009**, *48*, 1989-2000.
10. "Mixed-Metal Supramolecular Complexes Coupling Polyazine Light Absorbers and Reactive Metal Centers," Shamindri M. Arachchige, Karen J. Brewer, in *Macromolecules Containing Metal and Metal Like Elements: Supramolecular and Self-Assembled Metal-containing Materials*, Volume 9, John Wiley and Sons, Martel Zeldin, Editor, **2009**, 295-366.
11. "Solar Energy Conversion Using Photochemical Molecular Devices: Photocatalytic Hydrogen Production From Water Using Mixed-Metal Supramolecular Complexes," Krishnan Rangan, Shamindri M. Arachchige, Jared R. Brown and Karen J. Brewer, *J. Energy and Environ. Sci.* **2009**, *2(4)*, 410-19.
12. "Supramolecular Complexes as Photoinitiated Electron Collectors: Applications in Solar Hydrogen Production," Shamindri M. Arachchige, Karen J. Brewer, *On Solar Hydrogen and Nanotechnology*, Lionel Vayssieres Editor, John Wiley and Sons, **2010**, 589-617.
13. "Synthesis, Characterization, and Study of the Photophysics and Photocatalytic Properties of the Photoinitiated Electron Collector $[(\text{phen})_2\text{Ru}(\text{dpp})]_2\text{RhBr}_2(\text{PF}_6)_5$," Travis A. White, Krishnan Rangan, Karen J. Brewer, *J. Photochem. Photobiol. A: Chem.* **2010**, *209*, 203-209.

14. "Photocatalytic Hydrogen Production from Water," Shamindri M. Arachchige, Karen J. Brewer, *Energy Production and Storage-Inorganic Chemical Strategies for a Warming World, Encyclopedia of Inorganic Chemistry*, Robert Crabtree Editor, John Wiley and Sons, **2010**, in press.

Session IX

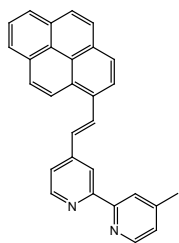
Novel Chromophores and Environments

Light Induced Redox Reactions of Photoactive Transition Metal Complexes

Jing Gu, Kristi Lebkowsky, Amelia Neuberger, Jeff Draggich and Russell Schmehl
Department of Chemistry
Tulane University
New Orleans, LA 70118

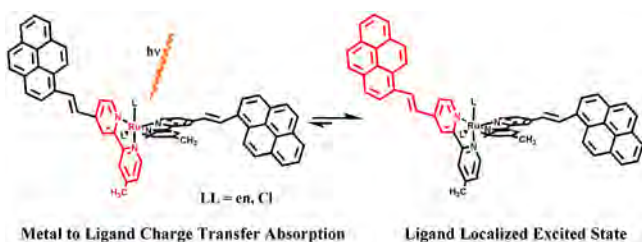
Our work has focused primarily on (A) continued development of spectrophotometrically black chromophores with extended excited state lifetimes, (B) photoinduced electron transfer reactions of square planar Pt(II) complexes and (C) examination of nanoparticulate Ni catalysts in photochemical systems for hydrogen generation.

(A) Development of photoactive black chromophores. An ongoing objective in the past year has been the synthesis and spectroscopic investigation of transition metal complex chromophores that absorb throughout the visible and have lifetimes long enough to be used as sensitizers for photoinduced electron transfer reactions. We have developed a variety of complexes having the Pyvmb ligand (below) that exhibit excited state lifetimes on the order of hundreds of nanoseconds that, as bpy complexes would have very short excited state lifetimes and limited photoactivity. Examples of complexes prepared that exhibit this behavior include $[(\text{Pyvmb})_2\text{Ru}(\text{LL})]$ where $\text{LL} = \text{en}, \text{Cl}_2, \text{SCN}^-$ and CN^- . The unique excited state activity is rationalized in terms of reversible energy transfer between ligand localized and MLCT excited states as shown in the graphic below.



Pyvmb

If the excited state of the complex is ligand localized and the excited state is to be used in reduction of an electron acceptor, a question that arises is whether the oxidation of the chromophore will occur on the ligand or at the more easily oxidized metal center.



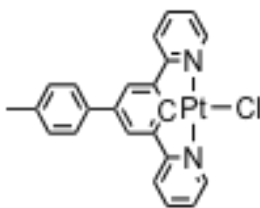
There is a very large difference in the potentials for oxidation of the pyvmb ligand (~ 1.4 V vs. SCE) and the Ru(II) center (0.2 V). If excited state electron transfer results initially in oxidation of the pyvmb ligand, the excited state will be a very weak reducing agent. We have found, through Rehm-Weller analysis of photooxidation of $[(\text{pyvmb})_2\text{RuCl}_2]$ with a series of viologens and diquats that the excited state of the complex is at least a +0.8 V reductant. This work is continuing with other complexes, but the initial result indicates that, while the excited state seems to be ligand localized, photooxidation of the complex occurs at the metal center (and *not* via sequential oxidation of the pyvmb ligand and then the metal center). We are optimistic that this work could lead to a class of chromophores that have absorption throughout the visible, excited state energies in the 1.2 – 1.5 eV range and activity as photochemical reductants.

The other emphasis for this work has been to determine yields for populating the reactive, long-lived triplet excited state. Excitation is into the singlet MLCT state, but relaxation of this state can involve the triplet MLCT state, a triplet metal centered (^3LF) state and the triplet ligand localized state that we believe to be the thermally equilibrated

excited state. Preliminary results using tetracene as a triplet acceptor and $[(\text{pyvmb})_2\text{Ru}(\text{en})]^{2+}$ as the sensitizing chromophore, suggest that the intersystem crossing efficiency for this chromophore is only 0.03 +/- 0.01. The same experiment on the complex $[(\text{pyvmb})_2\text{Ru}(\text{bpy})]^{2+}$ yielded an intersystem crossing yield that is ten times higher.

(B) Square planar Pt(II) complex photoredox reactivity: We have also been examining the excited state photoredox behavior of Pt(II) complexes in solution. Part of the reason for looking at these complexes is that two electron transfer reactions, both oxidative and reductive, could lead to species that could serve as reactants for net two electron processes. For example, oxidation of a Pt(II) complex in the presence of hydroxide could result in a Pt(IV)(OH)₂ complex that could reductively eliminate H₂O₂ and regenerate the Pt(II) complex.

In the past year we have examined light induced redox reactions of ortho-metalated Pt(II) complexes (below) that are derivatives of the terpyridyl complexes above. The complexes, prepared by Garreth Williams lab in the University of Durham, England, are strongly luminescent in solution at room temperature. We have nearly completed a Rhem-Weller free energy dependence for two of the complexes to obtain potentials for the Pt(III/II*) one electron reduction. From this and the excited state energy we can obtain an estimate of the ground state one electron Pt(III/II) potential. This is significant because the one electron potentials for oxidation of square planar Pt(II) complexes are, as far as we know, always completely electrochemically irreversible and also are also kinetically irreversible. Our objective is to follow reaction of the Pt(III) species generated by an irreversible photooxidation.



(C) Photochemical Hydrogen Production Using Nanoparticulate Ni Catalysts: It has become increasingly clear that any realistic photochemical system for production of fuels (whether CO₂ reduction or hydrogen production as a starting point) must have catalysts that are inexpensive and scalable. In an effort to approach first row transition metal catalysts for hydrogen production in photochemical schemes, we began with the examination of nanoparticulate Ni supported in poly-N-vinylpyrrolidone (Ni(PVP)), a system that has been reported to catalytically produce hydrogen when exposed to borohydrides. Our approach was to use a photochemical system employing a Ru(II) complex chromophore (either $[\text{Ru}(\text{bpz})_3]^{2+}$ or $[\text{Ru}(\text{decb})_3]^{2+}$; bpz = 2,2'-bipyrazine and decb = 4,4'-dicarboxyethyl-2,2'-bipyridine) and triethylamine as a sacrificial electron donor in methanol containing a catalytic amount of the Ni(PVP) catalyst. Initial qualitative experiments using a hydrogen specific detector to determine the % H₂ in the head gas over the solution illustrate that hydrogen is produced and continues to be produced over 2-3 days of photolysis. In addition, it appears the number of turnovers of the Ru(II) catalyst is around 50 by the time hydrogen production ceases (in photolysis of a closed system). Control experiments have clearly shown that the chromophore is necessary for hydrogen production. The particle size of the Ni is, on average 3-8 nm (by TEM) and the amount used is small enough that light scattering by the nanoparticulate suspension is minimal. We are beginning work to prepare nanoparticulate Ni catalysts *in situ* via photoreduction, employing capping agents for the growing Ni nanoparticles.

DOE Sponsored Publications 2007-2010

Jing Gu, Jin Chen, Russell H. Schmehl “Using Intramolecular Energy Transfer to Transform non-Photoactive, Visible Light Absorbing Chromophores, into Sensitizers for Photoredox Reactions”, J. Am. Chem. Soc., in press.

Duraisamy Kumaresan, Kristi Lebkowsky, Russell H. Schmehl “Photoinduced charge separation and recombination in solution and in gels of a Pt(II) terpyridyl-naphthalene diimide complex“, J. Photochem. Photobiol., A: Chem., **2009**, 207, 86-93.

Paul Jarosz, K. Lotito, Jacob Schneider, Duraisamy Kumaresan, Russell Schmehl, and Richard Eisenberg “Platinum(II) terpyridyl-acetylidyne dyads and triads with nitrophenyl acceptors via a convenient synthesis of a boronated phenylterpyridine”, Inorg. Chem., **2009**, 48, 2420-28. (with Rich Eisenberg).

Paul Jarosz, Jason Thall, Jacob Schneider, Duraisamy Kumaresan, Russell Schmehl, and Richard Eisenberg ” Synthesis, Characterization, and Photophysical Properties of Platinum(II) Terpyridyl-based Multi-component Systems”, Energy and Environmental Science, **2008**, 1, 573. (collaborative with Rich Eisenberg).

Kosho Akatsuka, Yasuo Ebina, Masaru Muramatsu, Heidi Hester, Russell H Schmehl, Takayoshi Sasaki, Masa-aki Haga “Photoelectrochemical Properties of Alternating Multilayer Films Composed of Titania Nanosheets and Zn Porphyrins”, Langmuir, **2007**, 23, 6730-36. (with Masa-aki Haga)

Duraisamy Kumaresan, Kalpana Shankar, Srivathsa Vaidya and Russell H. Schmehl “Photochemistry and Photophysics of Coordination Compounds: Osmium”, Topics in Current Chemistry, **2007**, 281, 101-42 (invited review.)

Solvation and Reaction in Ionic Liquids

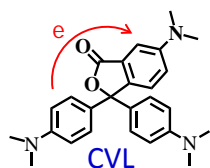
Mark Maroncelli, Sergei Arzhantsev, Hui Jin, Xiang Li, Min Liang, and Durba Roy
Department of Chemistry
The Pennsylvania State University
University Park, PA 16802

Project Scope: Our recent DOE-funded research has centered around two themes: i) understanding the dynamic coupling between photo-induced charge transfer and a solvent environment and ii) characterizing ionic liquids (ILs) as new solvent media relevant to numerous energy applications. During the past three years we have completed extensive surveys of the energetics and dynamics of solvation in ionic liquids,^{1,2,6} characterized the physical properties of a number of these liquids,⁴ developed a coarse-grained model for simulating solute-centered dynamics in ionic liquids,⁸ and examined several prototype intramolecular reactions that probe frictional solute-solvent coupling in conventional^{5,7,9,10} and ionic liquid solvents.^{3,6}

Solvation and Solvation Dynamics in Ionic Liquids: Most of the experimental work we have undertaken using solvatochromic probes to characterize equilibrium and non-equilibrium solvation in ionic liquids was complete early in 2007^{1,2}. This work showed that the solvation free energies and reorganization energies relevant to charge-transfer processes are little different in ionic liquids compared to highly polar conventional solvents like acetonitrile or methanol. But the time-dependence of solvation is vastly different. In keeping with their much higher viscosities, solvation times are roughly 100-fold greater in ionic liquids compared to conventional solvents. Moreover, solvation is broadly distributed in time in these solvents – relaxation over times of hundreds of femtoseconds to tens of nanoseconds are observed.

Our most recent work in this area has involved computer simulations. We have developed an economical coarse-grained model suitable for performing the long (10^{-7} - 10^{-6} s) simulations needed to study solvation dynamics and other solute-based properties in ionic liquids. Published work⁸ discusses the properties of this model as a neat liquid and emphasizes the effect that the ordered lattice-like structure enforced by the strong Coulomb interactions (Fig. 1) leads to high viscosities and slow, heterogeneous ion dynamics. We are currently refining and extending this model and using it to better understand how to describe solvation dynamics in ionic liquids. Future work with these models involve study of intra and intermolecular charge transfer reactions.

Characterization of Charge-Transfer and Frictional Probes: Some of our recent work has entailed



characterizing two types of intramolecular probes of solvent-reaction coupling. The first is the dual fluorescent molecule crystal violet lactone (CVL). Excitation of the S_1 band of CVL initially produces a

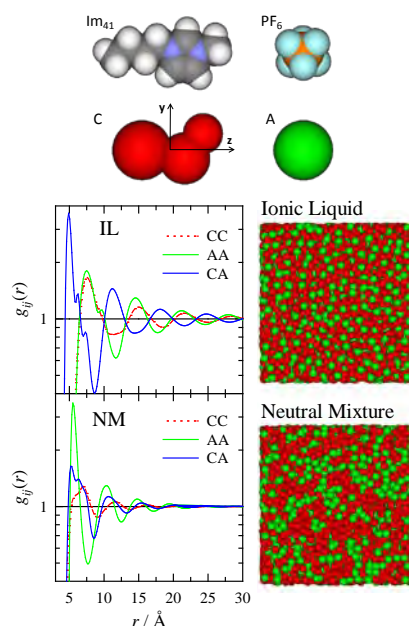


Fig. 1: The coarse-grained IL model and a comparison of the structures simulated for the IL and an equivalent mixture of uncharged C and A species⁸.

locally excited (LE) state on the aminophthalide ring. Subsequent electron transfer from the anilino groups leads to a state with nearly full charge transfer (CT) character. In most conventional solvents, the LE \rightarrow CT reaction occurs with time constants of a few tens of picoseconds and is strongly correlated to solvation times, indicating a small-barrier reaction largely controlled by solvation dynamics¹⁰.

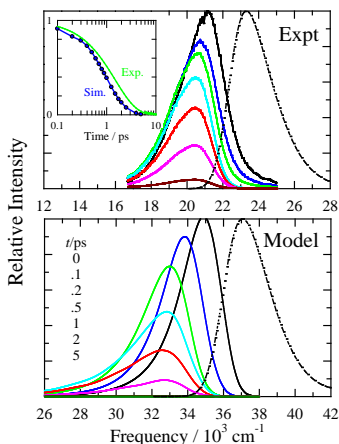


Fig. 2: Experimental (top) and simulated (bottom) absorption and time-resolved emission spectra of DMN in acetonitrile. The inset shows the decay of total emission intensity.

emission spectra of DMN in acetonitrile.

Reactions in ILs: We have examined the charge transfer reactions of CVL and other solutes previously studied in conventional solvents to look for any distinctive features of charge transfer in ionic liquid. In most cases the reaction rates appear to follow the same relationship to solvation times as in conventional solvents, but spectra tend to be more complex as a result of the overlap of solvation and reaction time scales (Fig. 3). More interesting is the fact that the slow and broadly distributed solvation response in ionic liquids leads to heterogeneity in reactions taking place on picosecond and nanosecond timescales. Red-edge excitation enables one to select molecules on the basis solvation energies and thus probe this heterogeneity, as illustrated by the JMDN data shown in Fig. 4³.

We have recently begun investigating bimolecular electron transfer reactions in ionic liquids using fluorescence quenching experiments. Observed rates are often 10-100 times faster than expected based on a viscosity scaling of the rates observed in conventional solvents. Substantial “static” quenching is also typically observed. We are only just starting to understand these effects and how they relate to ionic liquid properties.

We have also undertaken extensive experimental^{6,9} and computational⁷ work on the isomerization reactions of DMN, JDMN, and related molecules. Fluorescence yields of these molecules vary widely with solvation environment due to a fast internal conversion that is effected by a barrierless isomerization in S_1 . Although such molecules have been widely used as sensors of “local fluidity”, little was previously known about how these reactions couple to their surroundings or about the reactive motion involved. We are using semi-empirical potentials derived from electronic structure calculations in classical molecular dynamics simulations to obtain a molecular-level understanding of how these reactions couple to both electrostatic and short-range interactions with a solvent environment. Fig. 2⁷ shows initial attempts to model time-resolved

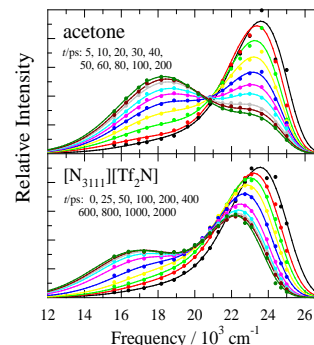
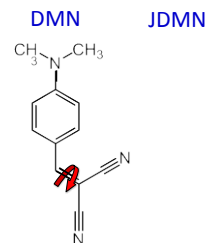


Fig. 3: Area normalized emission spectra of CVL in a conventional solvent and an ionic liquid.

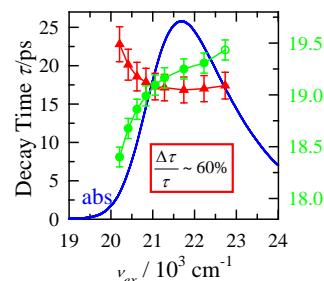


Fig. 4: Excitation wavelength dependence of the emission frequency (green) and lifetime (red) of JMDN in $[N_{ip3111}][Tf_2N]$.

DOE Sponsored Publications 2007-2010

1. Sergei Arzhantsev, Hui Jin, Gary Baker, and Mark Maroncelli, "Measurement of the Complete Solvation Response in Ionic Liquids," *J. Phys. Chem. B* **111**, 4978-4989 (2007).
2. Hui Jin, Gary A. Baker, Sergei Arzhantsev, Jing Dong, and Mark Maroncelli, "Survey of Solvation and Rotational Dynamics of Coumarin 153 in a Broad Range of Ionic Liquids and Comparisons to Conventional Solvents," *J. Phys. Chem. B* **111**, 7291-7302 (2007).
3. Hui Jin, Xiang Li, and Mark Maroncelli, "Heterogeneous Solute Dynamics in Room-Temperature Ionic Liquids," *J. Phys. Chem. J. Phys. Chem. B.* **111**, 13473-13478 (2007).
4. Hui Jin, Bernie O'Hare, Jing Dong, Sergei Arzhantsev, Gary A. Baker, James F. Wishart, Alan J. Benesi, and Mark Maroncelli, "Physical Properties of Ionic Liquids Consisting of the 1-Butyl-3-Methyl Imidazolium Cation with Various Anions and the Bis(trifluoromethylsulfonyl)imide Anion with Various Cations," *J. Phys. Chem. B.* **112**, 81-92 (2008).
5. Min Liang, Hemant Yennawar, and Mark Maroncelli, "2-[(2,3,6,7-Tetrahydro-1H,5H-benzo[*ij*]quinolizin-9-yl)methylene]propanedinitrile" *Acta Cryst. E* **65**, o1687 (2009).
6. H. Jin, "Ultrafast Solution Dynamics: Part I -- Dynamics in Ionic Liquids; Part II - Non-Radiative Deactivation of Malononitriles," Ph. D. Thesis, The Pennsylvania State University, 2009.
7. Chet Swalina and Mark Maroncelli, "Nonradiative Deactivation in Benzylidene Malononitriles," *J. Phys. Chem. C* **114**, 5602-5610 (2010).
8. Durba Roy, Nikhil Patel, Sean Conte, and Mark Maroncelli, "Dynamics in an Idealized Ionic Liquid Model," *J. Phys. Chem. B* (in press).
9. Hui Jin, Min Liang, Sergei Arshantsev, Xiang Li, and Mark Maroncelli, "Photophysical Characterization of Benzylidene Malononitriles as Probes of Solvent Friction," *J. Phys. Chem. B.* (in press).
10. Xiang Li and Mark Maroncelli, "Solvent Controlled Electron Transfer in Crystal Violet Lactone", submitted to *J. Phys. Chem.*

Efficient H₂ Production via Novel Molecular Chromophores and Nanostructures

Arthur J. Nozik, Arthur J. Frank, Justin C. Johnson, Nathan R. Neale, Soon Hyung Kang
Chemical & Materials Sciences Center
National Renewable Energy Laboratory Golden, CO 80401

A. Novel Singlet Fission Chromophores.(J.C. Johnson and A.J. Nozik) (Collaborators: J. Michl, U. Colorado, M. Ratner, Northwestern U.) Single crystal molecular structure and solution photophysical properties are reported for 1,3-diphenylisobenzofuran (**1**), of interest as a model compound in studies of singlet fission (SF). For the first excited singlet and triplet states of **1**, the transient visible absorption spectra, $S_1 \rightarrow S_x$ and sensitized $T_1 \rightarrow T_x$, and single exponential lifetimes, $\tau_F \sim 5.3$ ns and $\tau_T \sim 200$ μ s, are reported. The spectra and lifetimes of $S_1 \rightarrow S_0$ fluorescence and sensitized $T_1 \rightarrow T_x$ absorption of **1** were obtained in a series of solvents, as was the fluorescence quantum yield, $\Phi_F = 0.95$ - 0.99 , with Φ_T always < 0.01 . The first triplet excitation energy of solid **1** ($11\,400$ cm^{-1}) was obtained by electron energy loss spectroscopy. Computations suggest that **1** can exist as two \sim isoenergetic conformers of C_2 or C_s symmetry.

Triplet yields exceeding 100% have been directly measured in thermally evaporated thin films of **1**, compound previously identified to have nearly optimal energy level structure for efficient SF. Figure 1a shows a region of the film with strong intermolecular coupling between two molecules. Triplet formation occurs with time constants of < 250 fs, 2 ps, and 25 ps (Figure 1b). Due to the relatively fast and non-exponential decay of most triplets on a nanosecond time scale in these polycrystalline films, ultrafast transient absorption spectroscopy has been utilized to quantify the true SF yields prior to triplet-triplet annihilation and other forms of nonradiative decay.

The yields have been measured as a function of temperature on films of varying crystal morphology, revealing that inter-chromophore distance and geometry play a large role in determining the SF yield, both in terms of modulating the singlet and triplet energies and by affecting the coupling elements that determine the SF rate. There is evidence that in two distinct types of films, the C_2 and C_s conformers are distributed differently, and this has a large effect on the measured yield.

The effects of chemically connecting two chromophores to create a coupled chromophore pair were considered and how various structural choices alter the thermodynamic and kinetic parameters likely to control SF yield were computed. The electron transfer matrix element and the thermodynamics of SF for several promising chromophore pairs were examined to find the trade-off between the desire to maximize ET and the desire to keep the SF process exothermic.

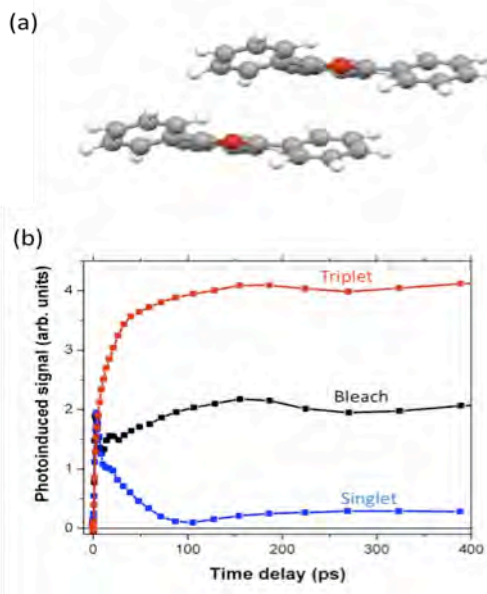


Figure 1. (a) A region of the bulk crystal lattice showing a slip-stacked arrangement. (b) Kinetics of triplet formation and singlet decay in a polycrystalline thin film of **1**.

To identify optimal conditions for SF in small molecular aggregates, we examined the photophysics of a series of covalent dimers of **1** with gradually increasing strength of coupling. In one interesting dimer we believe we observe the lowest quintet state of Q_1 , a state which contains two triplet excitations. We are not aware of other instances of excited quintet state formation upon excitation of a π -electron system, Although the SF yield is only a few percent, it is important because it uncovers the design principles that can lead to higher SF efficiencies.

B. Inverse Opal Photoelectrodes: Strategies for Enhancing Light Harvesting and Charge Transport (N.R. Neale, S.H. Kang, A.J. Frank)

The photophysics underpinning nanostructured solar photochemical systems are strongly tied to two fundamental processes: light harvesting and charge transport. We have been exploring how a nanowire (NW) mesh created by an inverse opal affects the properties of the photoactive material to absorb light and transport photogenerated charges to the collecting photoelectrode.

Cadmium selenide inverse opal films were prepared from electrodeposition within the pores of self-assembled polystyrene colloidal crystal templates. Long-range order within the films is found to be highly dependent on the synthetic conditions. Disorder in CdSe inverse opal films, arising from defects in the template and electrodeposition process, enhances significantly the infrared light (from 800–1300 nm) scattered and trapped within the film.

Light trapping strongly increases the infrared response of the CdSe film. For example, the incident photon-to-current efficiency (IPCE) sub-bandgap photoresponse for nitrogen-annealed, Zn^{2+} -treated CdSe films (Fig. 2) is 0.7% at 855 nm, whereas the IPCE of a nonporous CdSe thin film is essentially negligible. Tauc plots showed the excitation thresholds of all CdSe samples were about 1.7 eV (730 nm).

Compared with CdSe inverse opals, the electrodeposition of *p*-type Cu_xO (Cu_2O & CuO) semiconductor metal oxides and Cu metal in polystyrene bead templates yields more ordered NW mesh inverse opals (Fig. 3b). The Cu metal inverse opals can be partially oxidized electrochemically to provide a core-shell structure in which a Cu metal NW mesh core is covered by a thin Cu_xO shell (Fig. 3a). HR-TEM images and energy dispersive X-ray spectroscopy (EDS) line scan analyses demonstrate that the Cu core is continuous. This Cu core- Cu_xO shell structure has significantly enhanced electrical conductivity (by a factor of ~16) relative to the pure Cu_xO NW mesh photoelectrodes, which is attributable to favorable hole transport afforded by the Cu metal core.

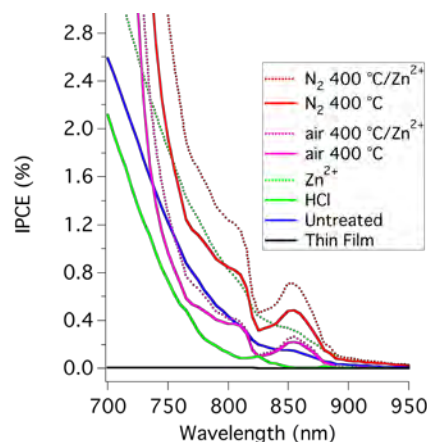


Figure 2. IPCE spectra of subbandgap region for CdSe inverse opal films with various treatments versus a thin film.

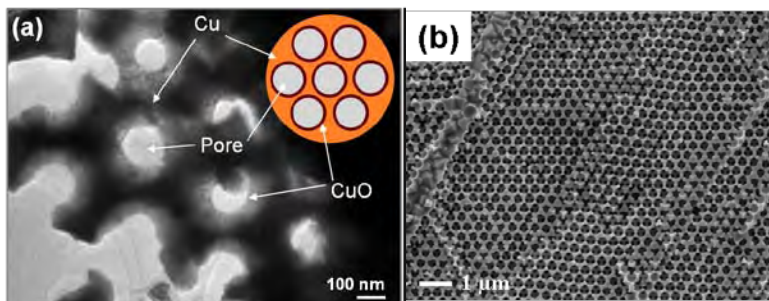


Figure 3. (a) FE-TEM image of metal Cu core- CuO shell inverse opal nanowire mesh electrode showing the film morphology; (b) FE-SEM image of Cu_2O nanowire mesh inverse opal.

DOE Sponsored Publications 2007-2010

1. Schwerin, A. F.; Johnson, J. C.; Smith, M. B.; Sreearunothai, P.; Popovic, D.; Cerny, J.; Havlas, Z.; Paci, I.; Akdag, A.; MacLeod, M. K.; Chen, X. D.; David, D. E.; Ratner, M. A.; Miller, J. R.; Nozik, A. J.; Michl, J. "Toward Designed Singlet Fission: Electronic States and Photophysics of 1,3-Diphenylisobenzofuran", *J. Phys. Chem. A* **2010**, *114*, 1457-1473.
2. Greyson, E. C.; Stepp, B. R.; Chen, X.; Schwerin, A. F.; Paci, I.; Smith, M. B.; Akdag, A.; Johnson, J. C.; Nozik, A. J.; Michl, J.; Ratner, M. "Singlet Fission for Solar Cell Applications: Energy Aspects of Interchromophore Coupling" *J. Phys. Chem. B*, **2010**, published ASAP
3. Johnson, J.C; Michl, J.; Nozik, A.J. Efficient Singlet Fission in Polycrystalline Thin Films of 1,3-Diphenylisobenzofuran, *J. Phys. Chem. B* **2010**, submitted.
4. Johnson, J. C.; Akdag, A.; Chen, X.; Smith, M.; Paci, I.; Ratner, M.; Michl, J.; Nozik, A. J. Toward Designed Singlet Fission: Solution Photophysics of Two Indirectly Coupled Covalent Dimers of 1,3-Diphenylisobenzofuran *J. Phys. Chem.* **2010**, submitted
5. Johnson, J. C.; Akdag, A.; Chen, X.; Smith, M.; Paci, I.; Ratner, M.; Michl, J.; Nozik, A. J. "Toward Designed Singlet Fission: Solution Photophysics of a Directly Coupled Covalent Dimer of 1,3- Diphenylisobenzofuran" *J. Phys. Chem.* **2010**, to be submitted.
6. N.R. Neale, B.G. Lee, S.H. Kang, and A.J. Frank "Infrared Light Trapping in Disordered CdSe Inverse Opals" to be submitted (2010)
7. S.H. Kang, N.R. Neale, K. Zhu, A.F. Halverson, J.Y. Kim, Y. Yan and A.J. Frank "Cu Core-Cu(x)O Shell Nanowire Mesh Inverse Opal Photoelectrodes" to be submitted (2010)

Session X

Photoconversion with Nanostructures

Manipulation of Charge Transfer Processes in Semiconductor Quantum Dot Based Nanoarchitectures

Kevin Tvrdy, Benjamin Meekins, Ian Lightcap, Jin Ho Bang and Prashant V. Kamat
Radiation Laboratory and Department of Chemistry and Biochemistry
University of Notre Dame, Notre Dame, IN 46556

Hybrids of nanostructured architectures and molecular assemblies offer new platforms for the development of next generation solar cells. Of particular interest are the CdSe based

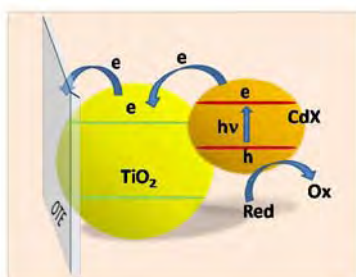


Figure 1 Charge injection from excited semiconductor nanocrystal, CdX (X= S, Se or Te) into TiO₂ nanoparticle

Quantum Dot Solar Cells (QDSC), which have shown great promise towards the development of all-inorganic solar cells with long term stability. For example, CdSe QDs linked to TiO₂ in the QDSCs are capable of injecting electrons into TiO₂ nanoparticles with rate constants as high as 10¹⁰ s⁻¹. By controlling the size of these semiconductor QDs, one can readily tune the band energies as well as the photoresponse of the solar cell. Photoelectrochemical cells derived from CdSe nanocrystals anchored onto TiO₂ nanoparticles (Figure 1) generate stable photocurrents when coupled with sulfide ion based electrolytes. The focus of our current research is to design photocatalyst assemblies by manipulating 1-D semiconductor architectures and to obtain better understanding of interparticle electron transfer and recombination processes in quantum dot based

nanoarchitectures.

TiO₂ nanotube array as scaffolds for improved charge separation. TiO₂ nanotube arrays formed on a Ti substrate by electrochemical anodization provide a convenient method to develop 1-dimensional ordered arrays on a conducting Ti surface. Conversion of TiO₂ nanotube arrays into TiO₂-SrTiO₃ heterostructures by controlled substitution of strontium has been successfully achieved under hydrothermal conditions. The TiO₂-SrTiO₃ composite heterostructures obtained with 1 hour or less hydrothermal treatment (Figure 2) exhibit the best photoelectrochemical performance with a nearly 100% increase in external quantum efficiency at 360 nm. This approach provides a convenient way to design composite semiconductor architectures for dye or quantum dot sensitized solar cells and/or photocatalytic hydrogen production. Li⁺ ion intercalation in TiO₂ nanotubes led to a 3-fold enhancement in photocurrent generation, as this procedure suppresses recombination losses at trap sites.

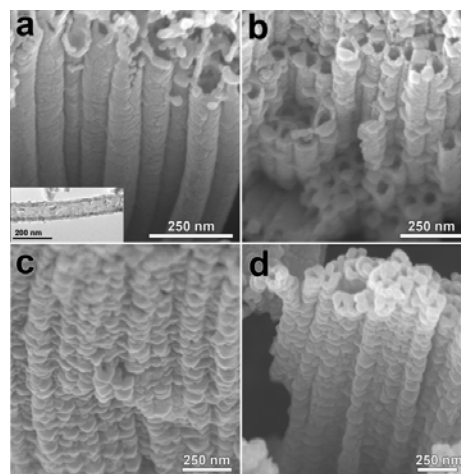


Figure 2 SEM images of TiO₂ nanotubes during exchange of strontium under hydrothermal conditions at times a. 0; b. 1; c. 2 and d. 40 hr.

Dependence of charge injection process on the energy gap. Ability to promote the charge injection from excited CdSe into TiO₂ has important implications in the design of quantum dot sensitized solar cells. We have demonstrated that the charge injection from excited CdSe

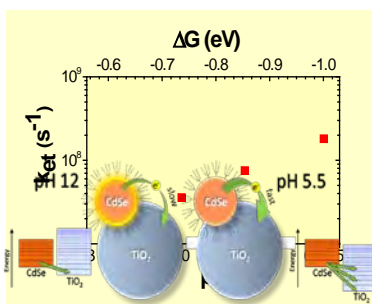


Figure 3. Dependence of electron injection rate constant, k_{et} , on the pH for a TiO₂-CdSe film.

nanocrystals into TiO₂ can be tuned by controlling the particle size. Decreasing the particle diameter increases the driving force for the charge injection as the energy difference between the two conduction bands increases. An alternate way to modulate the energy difference between CdSe and TiO₂ conduction bands is to tune the band edge of TiO₂. Since it is difficult to obtain quantized TiO₂ particles with varying size, one can utilize pH-induced protonation of surface groups which shifts the band edge of TiO₂ (a Nernstian shift of 59 mV/pH unit). For pH 5.5 and 12 this energy difference ($-\Delta G$) decreases from ~ 1.0 eV to ~ 0.61 eV and corresponds a drop in the rate constant of 2×10^8 s⁻¹ to 3×10^7 s⁻¹. The increased rate constants with decreasing pH (Figure 3) further support our earlier argument that the energy difference between the conduction bands of CdSe and TiO₂ is important to attain an efficient charge injection process, and ultimately higher photoconversion efficiency.

Charge transfer interaction between Graphene Oxide (GO) and semiconductor nanoparticles. Recently we have succeeded in attaching semiconductor and metal nanoparticles onto a single graphene sheet. The room temperature construction of a 2-D graphene-based nanomat with semiconductor and metal nanoparticles anchored at separate locations paves the way to use RGO platforms to store and shuttle electrons. The feasibility of this concept has been tested by carrying out stepwise transfer of electrons from photoexcited TiO₂ nanoparticles into GO, followed by a transfer of stored electrons from RGO to Ag⁺ ions. By using separated catalyst particles on the graphene sheet, one can develop a multifunctional photocatalyst system that can selectively carry out reduction and oxidation processes at different sites (Figure 4).

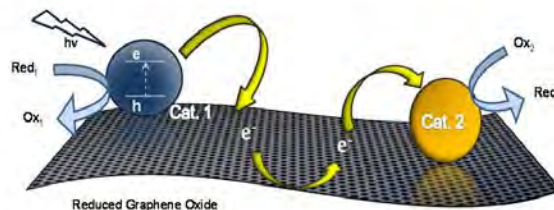


Figure 4. Reduced graphene oxide as a 2D conducting support to carry out selective catalysis at different sites.

Future studies will involve unraveling the mechanistic and kinetic details of charge transfer processes in semiconductor metal composites and electron transport properties of graphene based architectures. In particular, we will focus on the energy gap dependence of charge injection from excited quantum dots (CdSe) and oxide semiconductor (TiO₂, ZnO and SnO₂) particles. A systematic study varying the particle size of CdSe QDs, medium pH and different semiconductor oxides will allow us to attain a wide range of energy gaps ($\Delta E = 0 - 1.2$ eV) and thus probe the electron transfer dependence.

DOE Sponsored Publications 2007-2010

1. Kamat, P. V., *Meeting the Clean Energy Demand: Nanostructure Architectures for Solar Energy Conversion*. *J. Phys. Chem. C* **2007**, *111*, 2834-2860.
2. Robel, I.; Kuno, M.; Kamat, P. V., *Size-dependent Electron Injection from Excited CdSe Quantum Dots into TiO₂ Nanoparticles*. *J. Am. Chem. Soc.* **2007**, *129*, 4136-4137.
3. Kongkanand, A.; Domínguez, R. M.; Kamat, P. V., *Single Wall Carbon Nanotube Scaffolds for Photoelectrochemical Solar Cells. Capture and Transport of Photogenerated Electrons*. *Nano Lett.* **2007**, *7*, 676-680.
4. Kongkanand, A.; Kamat, P. V., *Electron Storage in Single Wall Carbon Nanotubes. Fermi Level Equilibration in Semiconductor-SWCNT Suspensions*. *ACS Nano* **2007**, *1*, 13-21.
5. Sudeep, P. K.; Takechi, K.; Kamat, P. V., *Harvesting Photons in the Infrared. Electron Injection from Excited Tricarbocyanine dye (IR 125) into TiO₂ and Ag@TiO₂ core-shell nanoparticles*. *J. Phys. Chem. C* **2007**, *111*, 488-494.
6. Hasobe, T.; Saito, K.; Kamat, P. V.; Troiani, V.; Qiu, H.; Solladié, N.; Kim, K. S.; Park, J. K.; Kim, D.; D'Souza, F.; Fukuzumi, S., *Organic Solar Cells. Supramolecular Composites of Porphyrins and Fullerenes Organized by Polypeptide Structures as Light Harvesters*. *J. Mater. Chem.* **2007**, *17*, 4160-4170.
7. Arunkumar, E.; Sudeep, P. K.; Kamat, P. V.; Noll, B. C.; Smith, B. D., *Singlet Oxygen Generation Using Iodinated Squaraine and Squaraine-Rotaxane Dyes*. *New J. Chem.* **2007**, *31*, 677 - 683.
8. Hasobe, T.; Fukuzumi, S.; Hattori, S.; Kamat, P. V., *Shape- and Functionality-Controlled Organization of TiO₂-Porphyrin-C₆₀ Assembly for Improved Performance of Photochemical Solar Cells*. *Chemistry, Asian J.* **2007**, *2*, 265-272.
9. Vietmeyer, F.; Seger, B.; Kamat, P. V., *Anchoring ZnO Particles on Functionalized Single Wall Carbon Nanotubes. Excited State Interactions and Charge Collection*, *Adv. Mater.* **2007**, *19*, 2935-2940.
10. Hasobe, T.; Fukuzumi, S.; Kamat, P. V.; Murata, H., *Porphyrin Based Molecular Architectures for Light Energy Conversion*. *Mol. Cryst. Liq. Cryst.* **2007**, *471*, 39-51
11. Jebb, M.; Sudeep, P. K.; Pramod, P.; Thomas, K. G.; Kamat, P. V., *Ru(II)trisbipyridine Functionalized Gold Nanorods. Morphological Changes and Excited-State Interactions*. *J. Phys. Chem. B* **2007**, *111*, 6839 - 6844.
12. Kongkanand, A.; Kamat, P. V., *Interactions of Single Wall Carbon Nanotubes with Methyl Viologen Radicals. Quantitative Estimation of Stored Electrons*. *J. Phys. Chem. C* **2007**, *111*, 9012-9015.
13. Hasobe, T.; Kamat, P. V., *Photoelectrochemistry of Stacked Cup Carbon Nanotube Films. Tube-Length Dependence and Charge Transfer with Excited porphyrin*. *J. Phys. Chem. C* **2007**, *111*, 16626 - 16634.
14. Hasobe, T.; Fukuzumi, S.; Kamat, P. V.; Murata, H., *Fullerene-Based Supramolecular Nanoclusters with poly[2-methoxy-5-(2'-ethylhexyloxy)-p-phenylenevinylene] (MEH-PPV) for Light Energy Conversion*. *Jap. J. Appl. Phys.* **2008**, *47*, 1223-1229.

15. Takechi, K.; Kamat, P. V.; Avira, R. R.; Jyothi, K.; Ramaih, D., *Harvesting Infrared Photons with Croconate Dyes. Chem. Mater.* **2008**, *20*, 265 - 272.
16. Wan, J.; Ferreira, A.; Xia, W.; Chow, C. H.; Takechi, K.; Kamat, P. V.; Guilford Jones, I.; Vullev, V. I., *Solvent Dependence of the Charge-Transfer Properties of a Quaterthiophene-Anthraquinone Dyad. J. Photochem. A* **2008**, *197*, 364-374.
17. Kongkanand, A.; Tvrdy, K.; Takechi, K.; Kuno, M. K.; Kamat, P. V., *Quantum Dot Solar Cells. Tuning Photoresponse through Size and Shape Control of CdSe-TiO₂ Architecture. J. Am. Chem. Soc.* **2008**, *130*, 4007-4015.
18. Brown, P. R.; Takechi, K.; Kamat, P. V., *Single-Walled Carbon Nanotube Scaffolds for Dye-Sensitized Solar Cells. J. Phys. Chem. C* **2008**, *112*, 4776-4782.
19. Muszynski, R.; Seger, B.; Kamat, P., *Decorating Graphene Sheets with Gold Nanoparticles. J. Phys. Chem. C* **2008**, *112*, 5263 - 5266.
20. Brown, P.; Kamat, P. V., *Quantum Dot Solar Cells. Electrophoretic Deposition of CdSe-C₆₀ Composite Films and Capture of Photogenerated Electrons with nC₆₀ Cluster Shell. J. Am. Chem. Soc.* **2008**, *130*, 8890-8891.
21. Williams, G.; Seger, B.; Kamat, P. V., *TiO₂-Graphene Nanocomposites. UV-Assisted Photocatalytic Reduction of Graphene Oxide. ACS Nano* **2008**, *2*, 1487-1491.
22. Matsunaga, Y.; Takechi, K.; Akasaka, T.; Ramesh, A. R.; James, P. V.; Thomas, K. G.; Kamat, P. V., *Excited State and Photoelectrochemical Behavior of Pyrene Linked Phenyleneethynylene Oligomer. J. Phys. Chem. B* **2008**, *112*, 14539-14547.
23. Kamat, P. V., *Quantum Dot Solar Cells. Semiconductor Nanocrystals as Light Harvesters. J. Phys. Chem. C* **2008**, *112*, 18737-18753.
24. Baker, D. R.; Kamat, P. V., *Photosensitization of TiO₂ Nanostructures with CdS Quantum Dots. Particulate versus Tubular Support Architectures. Adv. Funct. Mater.* **2009**, *19*, 805-811.
25. Tvrdy, K.; Kamat, P. V., *Substrate Driven Photochemistry of CdSe Quantum Dot Films: Charge Injection and Irreversible Transformation on Oxide Surfaces. J. Phys. Chem. A.* **2009**, *113*, 3765-3772.
26. Koch, M.; Nicolaescu, R.; Kamat, P. V., *Photodegradation of Polythiophene Based Polymers. Excited State Properties and Radical Intermediates. J. Phys. Chem. C* **2009**, *113*, 11507-11513.
27. Harris, C. T.; Kamat, P. V., *Photocatalysis with CdSe Nanoparticles in Confined Media: Mapping Charge Transfer Events in the Subpicosecond to Second Timescales. ACS Nano* **2009**, *3*, 682-690.
28. Bang, J. H.; Kamat, P. V., *Quantum Dot Sensitized Solar Cells. CdTe versus CdSe Nanocrystals. ACS Nano* **2009**, *3*, 1467-1476.
29. Williams, G.; Kamat, P. V., *Graphene-Semiconductor Nanocomposites. Excited State Interactions between ZnO Nanoparticles and Graphene Oxide. Langmuir* **2009**, *25*, 13869-13873.
30. Farrow, B.; Kamat, P. V., *CdSe Quantum Dot Sensitized Solar Cells. Shuttling Electrons through Stacked Carbon Nanocups J. Am. Chem. Soc* **2009**, *131*, 11124-11131.

31. Baker, D. R.; Kamat, P. V., *Disassembly, Reassembly and Photoelectrochemistry of Etched TiO₂ Nanotubes*. *J. Phys. Chem. C* **2009**, *113*, 17967-17972.
32. Meekins, B. H.; Kamat, P. V., *Got TiO₂ Nanotubes? Lithium Ion Intercalation can Boost Their Photoelectrochemical Performance Three-Fold*. *ACS Nano* **2009**, *3*, 3437–3446.
33. Seger, B.; Kamat, P. V., *Fuel Cell Geared in Reverse. Photocatalytic Hydrogen Production using a TiO₂/Nafion/Pt Membrane Assembly with No Applied Bias*. *J. Phys. Chem. C* **2009**, *113*, 18946 -18952.
34. Kamat, P. V.; Schatz, G., *Nanotechnology for Next Generation Solar Cells* *J. Phys. Chem. C* **2009**, *113*, 15473–15475.
35. Zhang, J.; Bang, J. H.; Tang, C.; Kamat, P. V., *Tailored TiO₂-SrTiO₃ Heterostructure Nanotube Arrays for Improved Photoelectrochemical Performance*. *ACS Nano* **2010**, *4*, 387-395.
36. Gassensmith, J. J.; Matthys, S.; Wojcik, A.; Kamat, P. V.; Smith, B. D., *Squaraine Rotaxane as Optical Chloride Sensor*. *Chemistry, European J.* **2010**, *16*, 2916-2921.
37. Kamat, P. V., *Photosensitization of SnO₂ and Other Dyes*, in *Dye Sensitized Solar Cells*, K. Kalyansundaram, Editor. 2010, EPFL Press, Switzerland: Laussane.
38. Ohtani, M.; Kamat, P. V.; Fukuzumi, S., *Supramolecular Donor-Acceptor Assemblies Composed of Carbon Nanodiamond and Porphyrin for Photoinduced Electron Transfer and Photocurrent Generation*. *J. Mater. Chem.* **2010**, *20*, 582-587.
39. Lightcap, I. V.; Kosel, T. H.; Kamat, P. V., *Anchoring Semiconductor and Metal Nanoparticles on a 2-Dimensional Catalyst Mat. Storing and Shuttling Electrons with Reduced Graphene Oxide*. *Nano Lett.* **2010**, *10*, 577–583.
40. Yu, Y.; Kamat, P. V.; Kuno, M., *CdSe Nanowire Photoelectrochemical Solar Cells Enhanced with Colloidal CdSe Quantum Dots*. *Adv. Funct. Mater.* **2010**, (In Press DOI:10.1002/adfm.200902372).
41. Chakrapani, V.; Tvrdy, K.; Kamat, P. V., *Modulation of Electron Injection in CdSe-TiO₂ System through Medium Alkalinity* *J. Am. Chem. Soc.* **2010**, *132*, 1228-1229.
42. Kamat, P. V., *Graphene based Nanoarchitectures. Anchoring Semiconductor and Metal Nanoparticles on a 2-Dimensional Carbon Support*. *J. Phys. Chem. Lett.* **2010**, *1*, 520-527.
43. Bang, J. H.; Kamat, P. V., *Solar Cell by Design. Photoelectrochemistry of TiO₂ Nanorod Arrays Decorated with CdSe*. *Adv. Funct. Mater.* **2010**, (In Press DOI:10.1002/adfm.200902234).
44. Wojcik, A.; Nicolaescu, R.; Kamat, P. V.; Patil, S., *Photochemistry of Far Red Responsive Tetrahydroquinoxaline-Based Squaraine Dyes*. *J. Phys. Chem. A* **2010**, *114*, 2744-2750.
45. Tvrdy, K.; Kamat, P. V., *Quantum Dot Solar Cells*, in *Comprehensive Nanoscience and Technology* G. Wiederrecht, Editor. 2010, Elsevier: Oxford, U.K.
46. Baker, D. R.; Kamat, P. V., *Tuning the Emission of CdSe Quantum Dots by Controlled Trap Enhancement*. *Langmuir* **2010**, (In Press, DOI:10.1021/la100580g).

The Role of Surface States in the Exciton Dynamics in CdSe Core and Core/Shell Nanorods

Zhong-Jie Jiang, Hoda Mirafzal and David F. Kelley
University of California, Merced
Merced, CA 95343

Static and time-resolved photoluminescence (PL) along with transient absorption (TA) measurements have been used to elucidate the relaxation and recombination dynamics of single excitons and multiexcitons in bare and core/shell CdSe nanorods. The core/shell particles are synthesized from the same cores as used in the optical studies, and both types of particles are studied with and without adsorbed hole acceptors, specifically, hexadecanethiol and phenothiazine (PTZ). Time resolved PL measurements give the exciton population as a function of time. The exciton population is depleted by a combination of radiative and nonradiative decay processes. For these nanorods, the room temperature radiative decay time is about 12 ns. Nonradiative processes which deplete the exciton population include electron or hole trapping at defect (usually surface) states. TA measurements give complementary information: the time dependence of the electrons in the conduction band, that is, conduction band state filling. Thus, the combination of these measurements can elucidate the relative roles of electron and hole trapping in exciton quenching. The dynamics observed in these nanorods are summarized in figure 1, below.

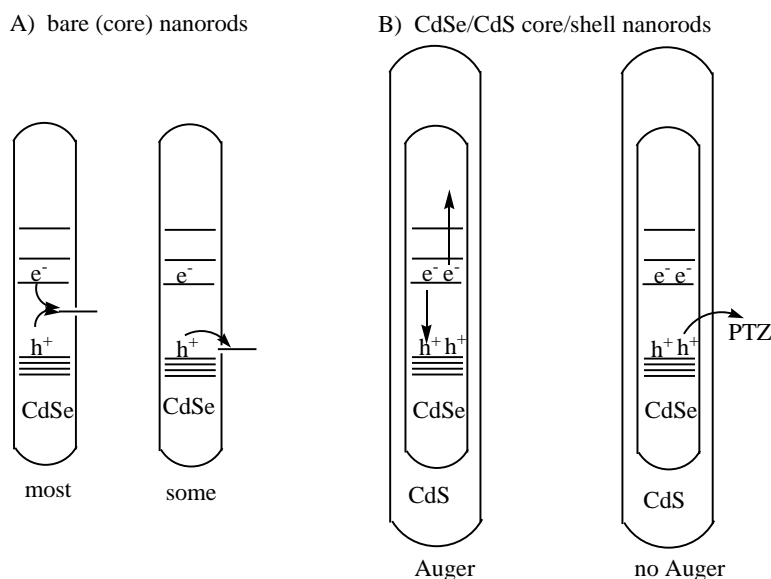


Figure 1. Summary of the dynamical processes in CdSe core and CdSe/CdS core/shell nanorods.

The PL and quantum yield results show that the dynamics of the core particles are dominated by very rapid nonradiative electron-hole recombination. The sample is inhomogeneous and most of these particles are not observed at all – see figure 1A. Of the particles that are observed, most undergo exciton quenching by hole transfer to surface states. This leaves the electron in the conduction band. As a result, the PL decays much more rapidly than the TA bleach, assigned to

conduction band state filling. The high density of mid-gap surface states also rapidly quenches multiexcitons. High fluence excitation produces a significant but small concentration of biexcitons and almost no higher order multiexcitons persisting longer than the electron cooling time of a few picoseconds.

Very different dynamics are observed in the CdSe/CdS core/shell nanorods. These nanorods exhibit high PL quantum yields (>70%), indicating that most of the nonradiative electron-hole recombination sites have been passivated. In this case with low-fluence excitation, the state-filling decay matches the PL decay. This indicates that the CdS shell essentially eliminates surface hole trapping and to the extent that any exciton quenching occurs, it is due to electron trapping. High fluence TA measurements indicate extensive conduction band state filling as shown in figure 2, below. The Auger rate depends on the number of electron-hole pairs and is therefore state dependent, and varies from about 700 ps for the lowest conduction band level (the X0 band) to about 15 ps for the π conduction band level at 3650 cm^{-1} (the X2 band).

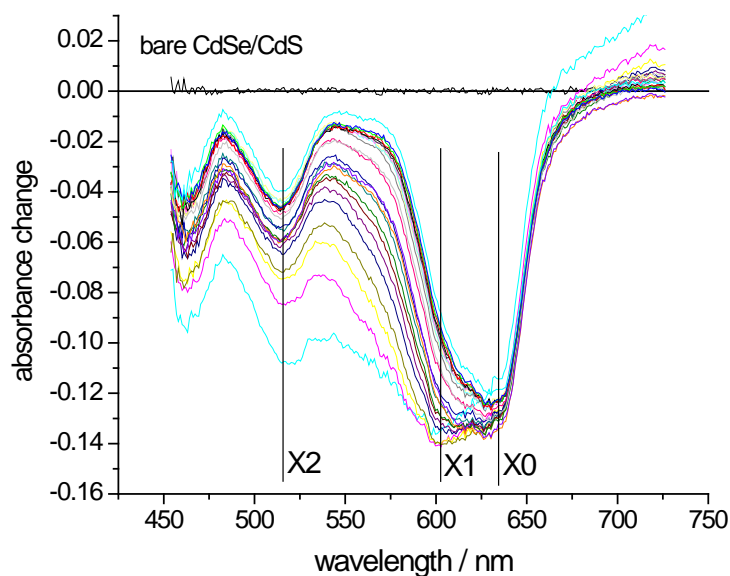


Figure 2. TA spectra of CdSe/CdS core/shell nanorods obtained at 5 ps intervals.

The presence of adsorbed hexadecanethiol or phenothiazine changes these dynamics. The PL decays much faster, due to hole transfer. In addition, the fast TA decay component in the X0 band kinetics assigned to Auger recombination of multiple excitons is almost completely lost. This is assigned to loss of the valence band holes available for Auger recombination. These dynamical changes are accompanied by the appearance of a broad absorption of the $\text{PTZ}^{\cdot+}$ radical cation, which persists for >1ns.

DOE Sponsored Publications 2007-2010

L. C. T. Shoute and D. F. Kelley, "Spatial Organization of GaSe Quantum Dots: Organic/Semiconductor Liquid Crystals" *J. Phys. Chem. C*, **111**,10233, (2007).

Karoly Mogyorosi and David F. Kelley, "Superradiance in GaSe Nanoparticle Aggregates", *J. Phys. Chem. C*. **111**, 579 (2007).

Mirafzal, H.; Kelley, D. F., "Singlet/Triplet Reversal in Strongly-Coupled GaSe Nanoparticle Aggregates" *J. Phys. Chem. C*, **113**, 7139 (2009).

Shao, J.; Mirafzal, H.; Petker, J. R.; Cosio, J. L. S.; Kelley, D. F.; Ye, T., "Nanoscale Organization of GaSe Quantum Dots on a Gold Surface" *J. Phys. Chem. C*, **113**, 19102 (2009).

Jiang, Z.-J.; Leppert, V.; Kelley, D. F., "Static and Dynamic Emission Quenching in Core/Shell Nanorod Quantum Dots With Hole Acceptors" *J. Phys. Chem. C*, **113**, 19161 (2009).

Shea-Rohwera, L. E.; Martin, J. E.; Kelley, D. F., "Increasing the Luminescent Quantum Yield of CdS Nanoparticles Having Broadband Emission" *Journal of The Electrochemical Society*, **157**, J1 (2010).

Jiang, Z.-J.; Kelley, D. F., "The Role of Magic Sized Clusters in the Synthesis of CdSe Nanorods" *ACS Nano*, **4**, 1561, (2010).

Graphenes: Basal Plane Photochemistry and Charge Transfer Doping

Naeyoung Jung, Haitao Liu, Sunmin Ryu and Louis Brus
Chemistry Department, Columbia University, New York, NY 10027

The goal of this DOE solar energy research is to understand how visible light interacts with matter, and how to make neutral excitations evolve into separated electrons and holes, especially in nanoparticles and nanowires. Our specific experiments focus on A) understanding plasmon enhanced spectroscopy and charge-transfer (metal-to-molecule) photochemistry on the surface of metallic particles and B) the spectroscopy and photochemistry of carbon nanotubes and graphene. In my most recent DOE solar talk, I described photochemistry on Ag nanoparticles. In this 2010 talk, I will speak on our graphene efforts. I also work closely with R. Friesner on theoretical DFT studies of photo-excited electrons near surfaces of titanium dioxide nanoparticles.

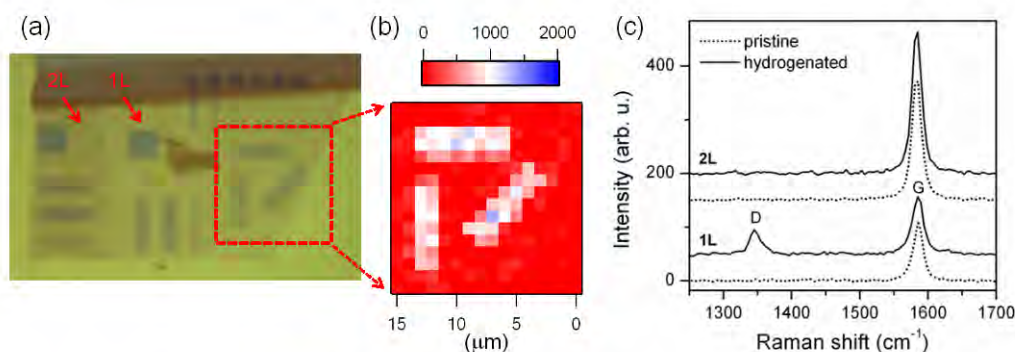
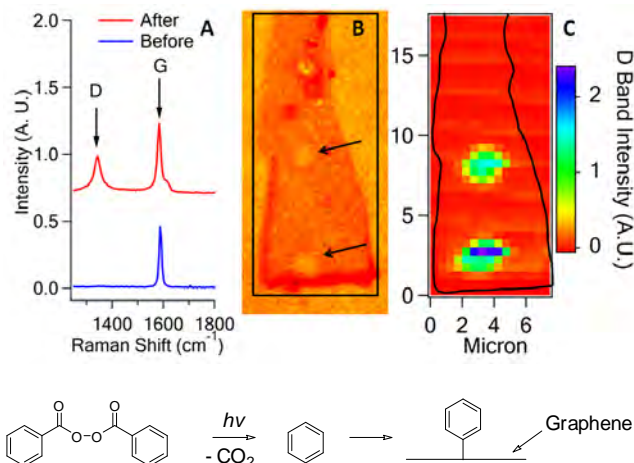


Fig. 1. (a) Optical micrograph of e-beam patterned sample II, which contains 1L, 2L and thick sheets of graphene. The squares and rectangles are crosslinked HSQ etch masks. Non-crosslinked HSQ has been removed by the developer. The 1L area in the dashed square is $15 \times 15 \mu\text{m}^2$. (b) The D band intensity Raman map taken for the dashed square in (a). (c) Raman spectra taken at the center of 1L and 2L graphene squares (area: $4 \times 4 \mu\text{m}^2$) shown in (a), before (dotted) and after (solid) hydrogenation. Data in (b) and (c) were obtained in ambient conditions with $\lambda_{\text{exc}} = 514.5 \text{ nm}$. 3 mW power was focused onto a spot of $\sim 1 \mu\text{m}$ in diameter. Integration time for one pixel is 20 sec.

Graphene has no surface states, and therefore has quite high electrical conductivity, and would be very useful in collecting photogenerated charge. Conductive metallic graphene is 98% transparent at visible wavelengths, and could be used as a transparent window to replace indium tin oxide. More generally, if one could spatially pattern the structure of graphene, one could imagine creation of electrical circuits in single sheets.

Raman spectroscopy is a useful diagnostic tool: the shift of the G band is a measure of graphene doping, and the (defect) D band is a measure of chemical reaction on the basal plane, converting sp^2 carbons into sp^3 carbons. How can one modify graphene to obtain specific shapes and sizes, and to pattern the electrical conductivity? We have explored patterned basal plane graphene photochemistry. The Raman signatures have been used to

study graphene reactions with diatomic oxygen, and with free H atoms as shown above. Patterned e beam irradiation of electron beam resist HSQ creates free H atoms at cross-linking occurs. These H atoms diffuse and react with the graphene surface, creating local C-H bonds. This disrupts the pi conjugation, and creates local insulating regions. Remarkably, the H atom reaction is reversible under mild heating. Single sheet 1L graphene is more reactive than double layer 2L, which is more reactive than triple layer 3L.



We find that patterned graphene photochemistry can be also initiated by direct optical excitation of graphene in the visible. Graphene is a metal with fsec time scale relaxation of optically excited “hot” electrons. Yet there is a small quantum yield of hot electron transfer to species with low lying LUMOs. We find that transfer to adsorbed benzoyl peroxide leads to fast elimination of carbon dioxide, and radical creation. These radicals react with the graphene basal plane, and increase the Raman D band intensity. Prolonged irradiation can cut a hole into the graphene as shown in the figure.

Graphene has a low density of states at the Fermi level, and thus the Fermi level is easily moved by charge transfer doping from the local environment. This can be probed by the shift in the G band. Graphene is strongly perturbed simply by adsorption on SiO_2 . Free-standing, graphene monolayers suspended over an open trench are undoped in air and exhibit very low levels of localized disorder. On SiO_2 spatially inhomogeneous doping is observed. The two-phonon 2D mode of the free-standing graphene monolayers is downshifted in frequency compared to that of the supported region; and the intensity of the 2D band is amazingly sensitive to adsorption.

This sensitivity to local doping is both a problem and an opportunity. Local environmental doping can be used to create graphenes with purposefully shifted Fermi levels. We have carefully studied the doping of few layer graphenes by Br_2 and I_2 . We observe both intercalated dopants, and adsorbed dopants on the top and bottom. Adsorption of bromine on 1L graphene creates a high doped hole density, well beyond that achieved by electrical gating with ionic polymer electrolyte. The 2D Raman band is completely quenched. The 2L bilayer spectra indicate that the doping by adsorbed I_2 and Br_2 is equal on top and bottom layers. Br_2 intercalates into 3L and 4L graphenes, but I_2 does not. The combination of both surface and interior doping with Br_2 in 3L and 4L creates a relatively constant doping level per layer, as shown in the observed G spectra. In contrast, the G spectra of 3L and 4L with surface adsorbed I_2 indicate that the hole doping density is larger on the surface layers than on the interior layers. This adsorption-

induced potential difference between surface and interior layers implies that a band gap opens in the bilayer type bands of 3L and 4L

DOE Publications from this project in the period 2007-2010

- 1) Elena Stolyarova (Polyakova), Kwang Taeg Rim, Sunmin Ryu, Janina Maultzsch, Philip Kim, Louis E. Brus, Tony F. Heinz, Mark S. Hybertsen, and George W. Flynn "High-Resolution Scanning Tunneling Microscopy Imaging of Mesoscopic Graphene Sheets on an Insulating Surface", *Pro. Nat. Acad. Sci. USA* *104*, 9209 (2007).
- 2) F. Wang, G. Dukovic, Y. Wu, M. Hybertsen, L. Brus, T. Heinz, "Auger Recombination of excitons in semiconducting carbon nanotubes" *Springer Series in Chemical Physics* (2007) *88*, 683-685.
- 3) D. Song, F. Wang, G. Dukovic, M. Zheng, E. Semke, L. Brus, T. Heinz, "Observation of the optical Stark Effect in Semiconducting Carbon Nanotubes" *Springer Series in Chemical Physics* (2007), *88*, 674-676
- 4) D. Song, F. Wang, G. Dukovic, M. Zheng, E. Semke, L. Brus, T. Heinz "Direct Measurement of the Lifetime of Optical Phonons in Single-Walled Carbon Nanotubes" *Phys. Rev. Lett.* *100*, 225503-225506 (2008).
- 5) Xiaomu Wu, Peter L. Redmond, Haitao Liu, Yihui Chen, Michael Steigerwald, and Louis Brus "Photovoltage Mechanism for Room Light Conversion of Citrate Stabilized Silver Nanocrystal Seeds to Large Nanoprisms" *J. Am. Chem. Soc.* *130*, 9500-9506 (2008).
- 6) Li Liu, Sunmin Ryu, Michelle R. Tomasik, Elena Stolyarova, Naeyoung Jung, Mark S. Hybertsen, Michael L. Steigerwald, Louis E. Brus, George W. Flynn "Graphene Oxidation: Thickness Dependent Etching and Strong Chemical Doping" *Nano Lett.* *8*, 1965-1970 (2008).
- 7) Louis Brus, "Noble Metal Nanocrystals: Plasmon Electron Transfer Photochemistry and Single Molecule Raman Spectroscopy". *Accts. Chem. Res.* *41*, 1742. (2008)
- 8) Sunmin Ryu, Melinda Y. Han, Janina Maultzsch, Tony F. Heinz, Philip Kim, Michael L. Steigerwald and Louis E. Brus "Reversible Basal Plane Hydrogenation of Graphene" *Nano Lett.* *8*, 4597-4602 (2008).
- 9) Stéphane Berciaud, Sunmin Ryu, Louis E. Brus, and Tony F. Heinz. "Probing the Intrinsic Properties of Exfoliated Graphene: Raman Spectroscopy of Free-Standing Monolayers" *Nano Lett.* *9*, 346-352 (2009).
- 10) Y. Yu, Y. Zhao, S. Ryu, L. Brus, K. Kim and P. Kim "Electric field effect tuning of the graphene work function" *Nano Lett.* *9*, 3430-3434 (2009)
- 11) Vladimir Blagojevic, Yiing-Rei Chen, Michael Steigerwald, Louis Brus, Richard Friesner "Quantum Chemical Investigation of Cluster Models for TiO₂ Nanoparticles with Water-Derived Ligand Passivation: Studies of Excess Electron States and Implications for Charge Transport in the Gratzel Cell" *J. Phys. Chem C* *113*, 19806-19811 (2009).
- 12) Naeyoung Jung, Namdong Kim, Steffen Jockusch, Nickolas J. Turro, Philip Kim, Louis Brus "Charge Transfer Chemical Doping of Few Layer Graphenes: Charge Distribution and Band Gap Formation" *Nano Lett.* *9*, 4133-4137 (2009).

- 13) Haitao Liu, Sunmin Ryu, Zheyuan Chen, Michael L. Steigerwald, Colin Nuckolls, Louis E. Brus “Photochemical Reactivity of Graphene” *J. Am. Chem. Soc.* *131*, 17099-17101 (2009).
- 14) Berciaud, S., Voisin, C., Yan, H., Chandra, B., Caldwell, R., Shan, Y., Brus, L., Hone, J., Heinz, T. “Excitons and High-Order Optical Transitions in Individual Carbon Nanotubes “ *Phys. Rev.* *B81*, 041414R (2010)
- 15) Changgu Lee, Huguen Yan, Louis Brus, Tony Heinz, James Hone, Sunmin Ryu “Anomalous Lattice Vibrations of Single and Few-layer MoS₂” *ACS Nano* Accepted 2010
- 16) Xiaomu Wu, Elizabeth Thrall, Haitao Liu, Michael Steigerwald, Louis Brus “Plasmon Induced Photovoltage and Charge Separation in Citrate Stabilized Gold Nanoparticles” *J. Phys. Chem. C* submitted 2010.
- 17) Stephane Berciaud, Melinda Han, Louis Brus, Philip Kim, and Tony Heinz “Electron and optical phonon temperatures in electrically biased graphene” submitted 2010.

Posters

“Electrochemically Wired” Semiconductor Nanoparticles: Toward Vectoral Electron Transport in Hybrid Materials

Neal R. Armstrong, S. Scott Saavedra, Jeffrey Pyun

Department of Chemistry

University of Arizona

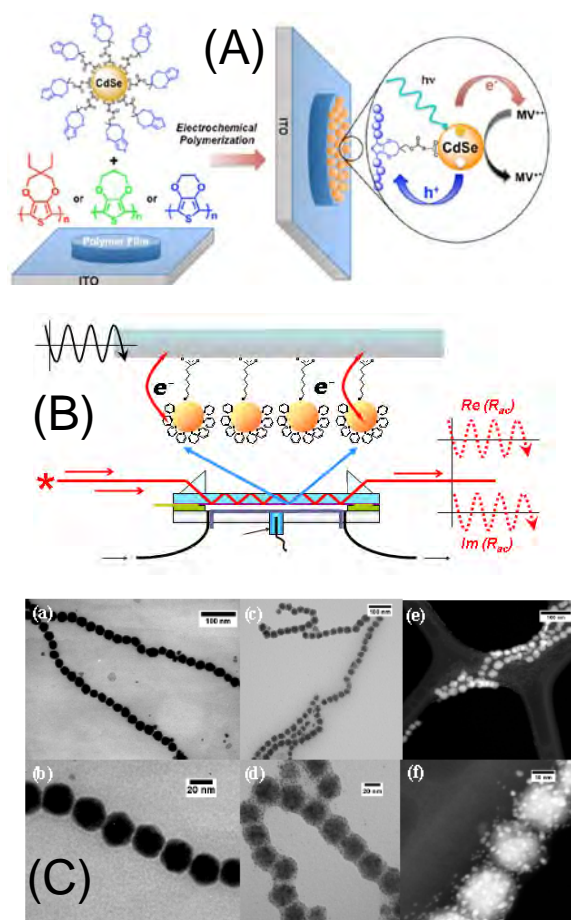
Tucson, Arizona 85721

nra@email.arizona.edu, saavedra@email.arizona.edu, jpyun@email.arizona.edu

Research efforts in this program have focused on three complementary areas: A) photoelectrochemical processes of semiconductor nanocrystals (SC-NCs) capped with electroactive ligands and tethered to thin polymer thin film hosts; B) development of spectroelectrochemical protocols (potential modulated attenuated total reflectance (PM-ATR)) on waveguide substrates to probe the energetics and rates of electron transfer to/from sub-monolayer SC-NC films; C) energetics and electrochemical properties of new oxide nanoparticle materials in which noble metals (Au, Pt) have been incorporated. **A)** Rates of photoelectrochemical processes for polymer-tethered SC-NCs are controlled by energy offsets between E_F of the host polymer (P/P^+) and E_{VB} of the SC-NC, and E_{CB} of the SC-NC and E_{MV^{++}/MV^+} . Quantum size effects control E_{VB} , controlling the rate limiting step in solution photoelectrochemical processes.

B) PM-ATR studies show that E_{CB} for tethered 5 nm CdSe NCs is ca. 0.5 eV closer to vacuum than predicted from our UV-photoemission studies of supported NC monolayers. Switching rates for these CdSe NCs are low and relatively independent of tether length, suggesting that rates are limited by electron injection from an oxide substrate (ITO) which is quite heterogeneous in its electrical activity, with a preponderance of inactive regions.

C) Electrochemical reactivities of magnetically-aligned cobalt oxide nanoparticles can be greatly enhanced through inclusion of Au or Pt nanoparticles inside of/or decorating the surface of, these unique nanomaterials. Further electrochemical and electronic property studies are underway, as is the interrogation of their photoelectrochemical properties (hydrogen production and water splitting).



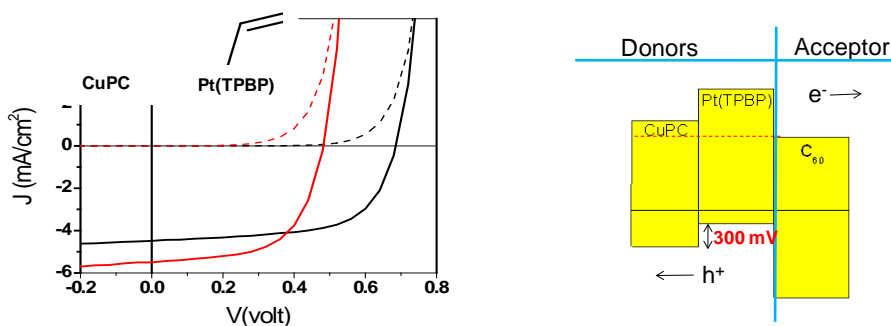
A – Schematic view of photoelectrochemical processes involving thiophene-capped CdSe nanocrystals, electrochemically tethered to host polymer films, providing for sensitized reduction of a solution electron acceptor (e.g. MV^{++}); **B** – Schematic view of CdSe NCs tethered to a waveguide surface, providing for spectroelectrochemical (PM-ATR) estimates of energies for electron injection into the NC (E_{CB}) and rates of bleaching/recovery of the excitonic absorbance; **C** – TEM images of magnetically-aligned cobalt oxide nanoparticles, decorated with metal catalytic sites (e.g. Pt, Au).

New Materials and Insights in Molecular Photovoltaic Devices

Mark Thompson, Dolores Perez, Patrick Erwin, Cody Schlenker
 Department of Chemistry
 University of Southern California
 Los Angeles, CA 90089

There has been a great deal of interest in developing new materials for the fabrication of light emitting diodes (OLEDs). We have prepared a range of intensely materials, which have found application in both monochromatic and white OLEDs. Our approach has involved a systematic study of a range of different materials. We have used a similar approach to develop materials for organic photovoltaic devices (OPVs). I will discuss the development of new materials as donors, acceptors and buffer layers in OPVs. I will discuss the use of metal complexes and organic materials as donor and acceptor materials in organic solar cells. We have investigated a wide range of new and established materials to investigate the connection between the OPV open circuit voltage (V_{oc}) and the energy difference between the donor HOMO and acceptor LUMO energies (ΔE_{DA}). Within closely related families of materials there is a clear correlation between V_{oc} and ΔE_{DA} , however, we have found marked differences between the V_{oc} values for materials systems with very similar ΔE_{DA} values. The devices that we studied here consisted of ITO/donor/ C_{60} /BCP/Al structures (BCP = bathocuproine), with a range of different organic and inorganic donors. We have found a number of examples of materials that give lower ΔE_{DA} values than reference donor/acceptor pairs, but give higher V_{oc} in comparable devices. This is illustrated for Pt porphyrin and Cu-phthalocyanine donors below. I will present a model that we have developed that accurately couples V_{oc} and ΔE_{DA} values with a D/A coupling term. This approach gives us a path to develop high V_{oc} materials

We have explored the use of metal porphyrin complexes as donor materials in OPVs. The complexes we have chosen have high nonplanar structures in the ground state and excited state. I will discuss the use of a range of metallo porphyrin and porphyrin tape compounds, illustrating how these materials can be used to enhance both the efficiency and V_{oc} . This work has recently been extended to a range of parylene-diimide acceptors and related compounds, that fit the model developed with systematic variation of the donor materials.



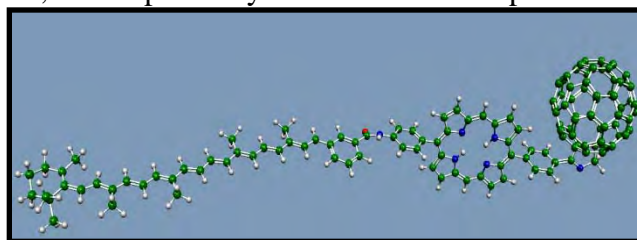
	J_{sc}	V_{oc}	FF	η (%)	ΔE_{DA}
CuPc	5.51	0.482	0.60	1.59	1.7
PtTPBP	4.48	0.685	0.63	1.93	1.4

Charge Transfer and Core-Valence Excited States for Molecular Systems

Tunna Baruah, Marco Olguin, and R. R. Zope

Department of Physics
University of Texas at El Paso
El Paso, TX, 79968

Charge transfer (CT) excitation plays a crucial role in many photo-induced phenomena such as photocatalysis, photovoltaics etc. Most often the systems of interest are quite large such as organic bio-mimetic molecules, polymers, dye molecules adsorbed on nanocrystal surfaces etc. which often prohibits use of highly accurate quantum chemical methods. Time-dependent DFT (TDDFT) within the linear response regime is found to be inadequate in describing the CT excited energies. We have developed a DFT based method to calculate the CT energies of molecular donor-acceptor systems. The CT energies of a donor-acceptor system with zero overlap can be estimated as $IA-EA-1/R$ where IA, EA respectively are the ionization potential of the donor, the electron affinity of the acceptor, and R is the separation between the two molecules. In our method we calculate the energies of CT states as the total energy difference between the ground and the excited states. This method uses the orthogonality between the ground and the excited state *wavefunctions* (constructed from the Kohn-Sham orbitals) as a constraint. We use a perturbative treatment which circumvents diagonalization and thereby avoids convergence issues. The perturbative treatment is carried out variationally to incorporate the polarization and relaxation of the orbitals. The perturbatively updated orbitals are orthogonalized using Lowdin's orthogonalization scheme. The table shows the CT excited state energies of a few gas-phase donor-acceptor systems calculated by our method and compared with the available experimental values or with the estimates according to $(IA-EA-1/R)$. In all the presented cases, the CT excitations are HOMO \rightarrow LUMO excitations.



The perturbative treatment is carried out variationally to incorporate the polarization and relaxation of the orbitals. The perturbatively updated orbitals are orthogonalized using Lowdin's orthogonalization scheme. The table shows the CT excited state energies of a few gas-phase donor-acceptor systems calculated by our method and compared with the available

System	Calc. (eV)	Expt. (eV)	Estimate (eV)
Benzene-TCNE	3.79	3.59	
Toluene-TCNE	3.27	3.36	
Xylene-TCNE	3.04	3.15	
Naphthalene-TCNE	2.74	2.60	
Zn Bchl-Bchl	2.61		2.69
Carotenoid-porphyrin-C ₆₀	2.46		2.50

experimental values or with the estimates according to $(IA-EA-1/R)$. In all the presented cases, the CT excitations are HOMO \rightarrow LUMO excitations.

We have also tested our method for core-valence excitations as measured in X-ray absorption spectroscopy. We have carried out the calculations on a set of small molecules for which experimental values are readily available. The mean absolute error in our calculated values are 0.87eV which is significantly smaller than 24.4eV obtained by TDDFT(B3LYP). This shows that our method can be applied to different types of excitation.

Charge Transfer and Energy Transfer in Single-walled Carbon Nanotube-Semiconducting Polymer Hybrids

Jeff Blackburn, Josh Holt, Andrew Ferguson, Nikos Kopidakis, Kevin Mistry, Matt Beard, Garry Rumbles
National Renewable Energy Laboratory, Golden, CO

Single-walled carbon nanotubes (SWNTs) are two-dimensionally confined quantum wires that have the potential to impact a variety of solar photochemical applications. SWNTs have many properties that are well suited to solar conversion, including strong, size-tunable light absorption and excellent charge carrier mobilities. Additionally, SWNTs interact strongly with many light-absorbing semiconducting polymers, spurring interest in SWNT/polymer hybrid systems tailored for photo-induced charge separation. For such systems to be useful for organic photovoltaics, the fundamental properties of the interface formed between nanotubes and polymers. We strive to understand the interfacial properties that promote or hinder the generation of long-lived charge-separated states in these systems, which include the molecular structure of the interface, SWNT diameter-dependent band offset (charge separation driving force), and SWNT electronic structure.

This poster focuses on our recent studies aimed at rationally designed SWNT/polymer hybrids that promote long-lived photo-induced charge separation. Two semiconducting polymers – poly(3-hexylthiophene) (P3HT) and poly(2-methoxy-5-(2'-ethyl-hexyloxy-1,4-phenylene vinylene) (MEH-PPV) – are shown to disperse high degrees of isolated or lightly bundled SWNTs in a variety of organic solvents. Photoluminescence excitation (PLE) spectroscopy indicates that a significant number of photons absorbed by the polymer in each of these hybrids results in energy transfer to proximal SWNTs. Such energy transfer implies a potential limitation on the yield of charge separation within such hybrids.

Time-resolved microwave conductivity (TRMC) was used to study the dissociation of excitons at the interface between P3HT and SWNTs. It was found that excitation of SWNTs at the second optical transition (S_{22}) did not result in appreciable hole transfer from SWNT to P3HT. In contrast, excitation of the polymer at 2.3 eV results in a 100-fold increase in charge carrier generation relative to a film of P3HT with no SWNTs, an indication of efficient electron transfer from the LUMO of the photo-excited P3HT to the LUMO of semiconducting SWNTs. Furthermore, the lifetime of this charge-separated state was lengthened significantly relative to the lifetime of free charges created on P3HT alone by auto-dissociation of excitons. We also studied blends of P3HT with SWNTs separated by electronic structure into type-pure metallic and semiconducting SWNTs. We found that both the yield and lifetime of the photo-induced charge-separated state is dramatically increased as the percentage of semiconducting SWNTs within the blend is increased. This is the first experimental demonstration of the prevailing theoretical hypothesis that metallic SWNTs should act as efficient recombination centers in such polymer/SWNT systems.

Finally, we present preliminary results aimed at understanding the molecular structure of the interface formed between SWNTs and conducting polymers such as P3HT by nuclear magnetic resonance (NMR) spectroscopy. By doping laser vaporization targets with 20% ^{13}C , and separating the ^{13}C -enriched SWNTs by electronic structure, we have identified for the first time the unique ^{13}C resonances for metallic and semiconducting SWNTs. Ongoing NMR experiments are now focused on probing the effects of SWNT electronic structure on the ground-state interaction between SWNTs and P3HT

Catalytic Conversion Of Carbon Dioxide To Methanol And Higher Order Alcohols at an Illuminated p-Type Semiconductor Interface

A. B. Bocarsly, K. Keets, A. J. Morris, and E. L. Zeitler

Department of Chemistry, Frick Laboratory

Princeton University

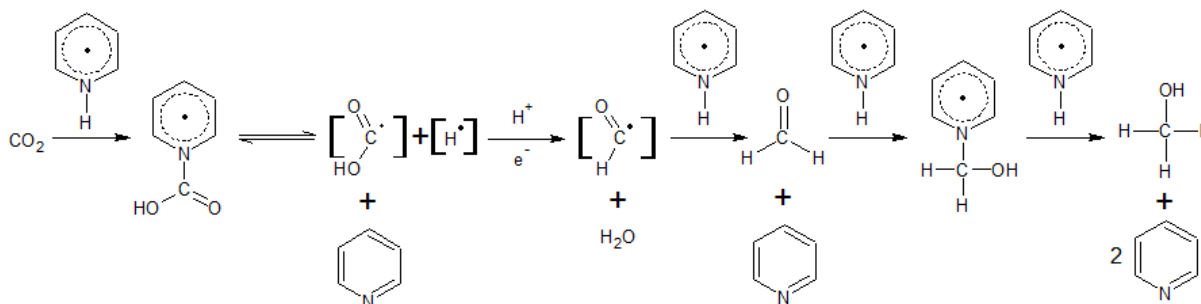
Princeton, New Jersey 08544

It has long been known that certain semiconductor electrodes can be utilized to reduce carbon dioxide in aqueous electrolyte to methanol,¹ and therefore one can consider chemical conversion of CO₂ to fuels as an alternative to the geophysical sequestration approaches that have been put forth recently. However, in most cases, the faradaic yield of methanol at a semiconductor interface is modest. In almost all cases, the overpotentials required to effect the reduction of interest are excessive. Typical overpotentials of ~1V, force the reduction to be driven by an external potential even when semiconductor band edge positions are well matched to the thermodynamics required for carbon dioxide reduction coupled with water oxidation:



The stability of the illuminated semiconductor-electrolyte interface is also problematic.

Previously, we reported that the excessive overpotentials observed for aqueous carbon dioxide reduction at a metal electrode could be reduced substantially by employing a dissolved pyridinium (pyrH⁺) electrocatalyst.² Introduction of a 10mM pyrH⁺ catalyst allows ~1mA/cm² for the conversion of carbon dioxide to methanol with only a 200mV overpotential. Recently, we have ported this chemistry over to an illuminated p-GaP electrode where we have observed for the first time methanol formation at an underpotential with faradaic efficiencies approaching 100%.^{1,3,4} We find that the observed catalysis is associated with a mediated charge transfer process in which pyrH⁺ is reduced by one electron to pyrH•. This species undergoes an inner sphere charge transfer with CO₂ that is best typified as involving a carbamate-like intermediate. A second charge transfer then produces formate, which further reacts with electrode produced pyrH• to eventually produce methanol as outlined in the scheme below.



SCHEME I

We now report that the desired chemistry not only occurs at a p-GaP interface, but also is observed at p-GaAs interfaces and p-GaInP₂ interfaces. In all cases, good faradaic yields are observed when the semiconducting photocathode is operated at an underpotential. Variations in performance and stability are observed as a function of band edge positions and key surface densities of states. In certain cases, the stability of the interface can be enhanced by the addition of a thin metallic interface. For example, while a p-GaAs photocathode is unstable when irradiated in a cell containing aqueous pyrH⁺/CO₂, platinization of the interface introduces a good degree of stability without the formation of a metal on semiconductor shottky barrier.

Variations in product distributions including the formation of higher order alcohols are found to depend on both the catalyst employed (substituted pyrH⁺) and the nature of the electrode interface. Illuminated p-GaP and p-GaInP₂ interfaces are catalytic for the formation of isopropanol with ~30% faradaic yield when appropriately substituted pyridines are employed.

References:

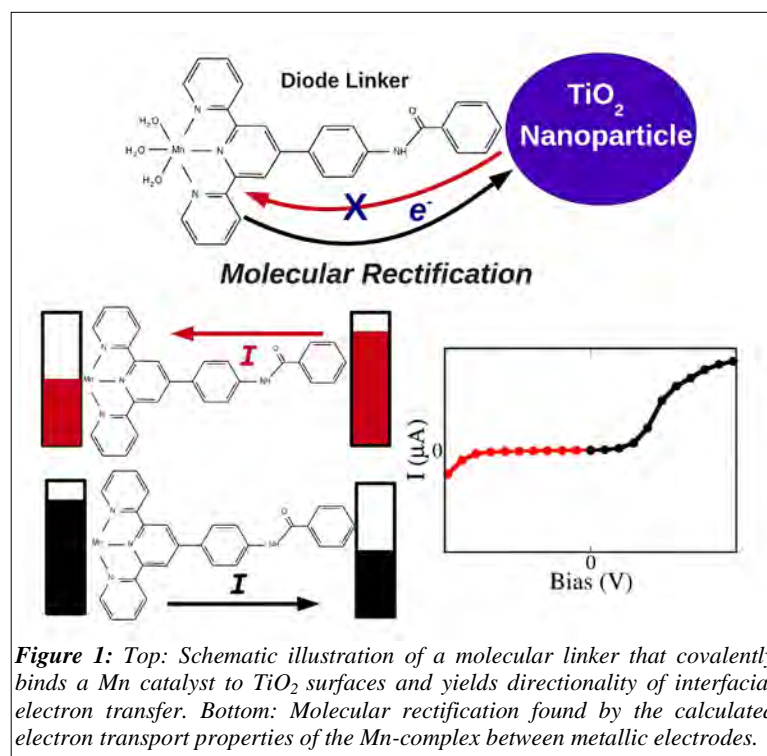
- (1) Barton-Cole, E.; Bocarsly, A. B. In *Carbon Dioxide as Chemical Feedstock*; Aresta, M., Ed.; Wiley-VCH Verlag GmbH & Co.: Weinheim, 2010.
- (2) Seshadri, G.; Lin, C.; Bocarsly, A. B. *J Electroanal Chem* **1994**, 372, 145-150.
- (3) Barton, E. E.; Rampulla, D. M.; Bocarsly, A. B. *J Am Chem Soc* **2008**, 130, 6342-6345.
- (4) Bocarsly, A. B.; Barton-Cole, E. B.; Pending, U. P. O., Ed.; Princeton University: United States, 2009.

Diode Linkers for the Covalent Attachment of Mn Catalysts to TiO₂ Surfaces

Julio L. Palma, William R. McNamara, Laura J. Allen, Rebecca L. Milot, Karin Brumback, Gary W. Brudvig, Charles A. Schmuttenmaer, Robert H. Crabtree and Victor S. Batista

Department of Chemistry
Yale University
New Haven, CT 06520-8107

We characterize the electronic rectification properties of molecular linkers that covalently bind Mn catalysts to TiO₂ surfaces. We focus on Mn-complexes with phenylterpyridine ligands attached to 3-phenyl-acetylacetonate anchors via amide bonds.¹ We find that a suitable choice of the amide linkage yields directionality of interfacial electron transfer, essential to suppress recombination. Our findings are supported by calculations of current-voltage (I-V) characteristics at metallic atomic junctions, based on first-principles methods that combine non-equilibrium Green's function techniques with density functional theory.^{2,3} Our computational results are consistent with EPR measurements, confirming an asymmetry of electron transfer rates for linkers with significant rectification. The reported studies are particularly relevant for the development of photovoltaic, or photocatalytic, devices based on functionalized TiO₂ thin-films where the overall performance is affected by recombination processes competing with interfacial electron injection.



1. McNamara, W. R.; Snoeberger, R. C., III; Li G.; Schleicher, J. M.; Cady, C. W.; Pyatos, M.; Schmuttenmaer, C. A.; Crabtree, R. H.; Brudvig, G. W.; Batista, V. S. *J. Am. Chem. Soc.* **2008**, 130, 14329-14338.
2. Rocha, A. R.; Garcia-Suarez, V.; Bailey, S. W.; Lambert, C. J.; Ferrer, J.; Sanvito, S. *Phys. Rev. B* **2006**, 73, 085414
3. Palma, J. L.; Cao, C.; Zhang, X.-G.; Krstic, P. S.; Krause, J. L.; Cheng, H.-P. *J. Phys. Chem. C* **2010**, 114, 1655-1662.

Modular Nanoscale and Biomimetic Assemblies for Photocatalytic Hydrogen Generation

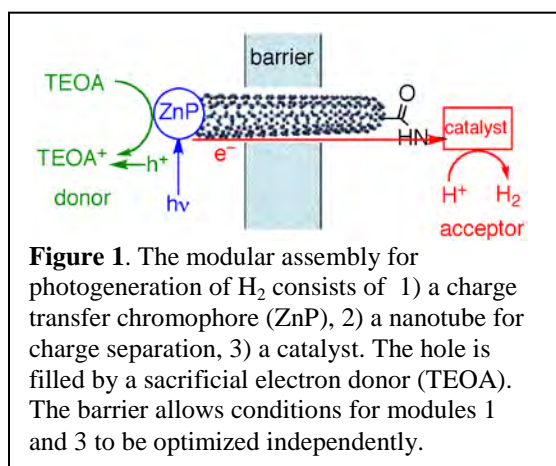
Kara L. Bren, Richard Eisenberg, Patrick L. Holland, Todd D. Krauss

Department of Chemistry

University of Rochester

Rochester, NY 14627

The abundance and availability of solar energy makes it an attractive primary energy source for hydrogen (H_2) generation independent of fossil fuels. The objective of this project is to develop modular nanoscale assemblies for light-driven H_2 generation. The three modules are: 1) peptide-porphyrin-conjugate light-harvesting and charge-transfer chromophores, 2) nanotubes for efficient long-range charge separation through an impermeable barrier, and 3) catalysts for hydrogen production from water based on earth-abundant metals (Fig. 1).

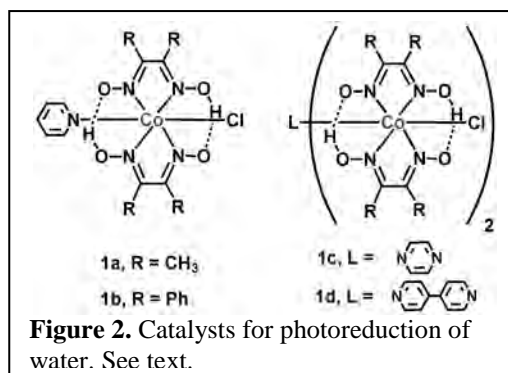


For light-harvesting and photoinduced charge separation (module 1), a series of porphyrin-peptide conjugates have been expressed in *E. coli* from synthetic genes. The peptide designs are based on sequences previously shown to bind to nanotubes. Progress toward characterizing the structure and photophysical properties of these peptides is contributing to our fundamental understanding of how nature uses similar motifs in photosynthesis.

To produce nanotubes for directional electron transfer (module 2), a dense forest of vertically aligned carbon nanotubes (VA-CNTs) was grown by a CVD process using a micro porous silicon

substrate, an e-beam evaporated Fe catalyst, and ethylene gas as the carbon source. After optimization, film thicknesses of over $100 \mu m$ covering a $1 cm^2$ area were achieved. For fabrication of a conductive VA-CNT membrane, a polymer (PMMA) was deposited on the VA-CNTs and heated to facilitate penetration through the entire VA-CNT layer. Toluene was used to expose the carbon nanotube ends. Future work includes conductivity measurements of the VA-CNT membranes and systematic studies of the membrane integrity.

In recent results on module 3, some of us reported a precious-metal-free, homogeneous system for the photo-reduction of water based on the cobaloxime catalyst (Fig. 2), $[Co(dmgh)_2pyCl]$ (1a) (dmgH = dimethylglyoximate, py = pyridine). Other cobalt catalysts under development are $[Co(dpgH)_2pyCl]$ (dpgH = diphenylglyoximate) and $[Co(dmgh)_2Cl]_2L'$ (L' = pyrazine and 4, 4' - dipyridyl) (1b,c,d), which have been found to be active for photogeneration of H_2 . Finally, the nickel and cobalt complexes of "P2N2" (where P2N2 is 1,3,5,7-tetraphenyl-1,5-diaza-3,7-diphosphacyclooctane), previously known to electrocatalyze H_2 formation, have been used for photocatalytic H_2 generation.



Development of High Potential Photoanodes for Light Induced Water Oxidation

Gary F. Moore, Hee-eun Song, Rebecca L. Milot, James D. Blakemore, Victor S. Batista, Charles A. Schmuttenmaer, Robert H. Crabtree and Gary W. Brudvig

Department of Chemistry
Yale University
New Haven, CT 06520-8107

Of the available carbon neutral energy sources, solar is quite promising as it is abundant but unfortunately is diffuse and intermittent in its availability.¹ Thus, devising cost effective methods for efficiently capturing and storing this energy is among the grand challenges of science.^{2, 3} Here, we describe a selection of high potential sensitizers for functionalization of metal oxide surfaces. In these constructs, the function of the sensitizers is to efficiently absorb visible light and use the energy to initiate electron transfer to an attached metal oxide. The injected electrons can ultimately be used to drive hydrogen production at a cathode while the resulting holes (sensitizer radical cations) provide the potential needed to power a water oxidation catalyst supplying the source of electrons.

In preliminary work, we have prepared photoanodes consisting of high potential free-base and zinc bis-pentafluorophenyl porphyrin sensitizers (PF₁₀ and ZnPF₁₀) bearing linkers for functionalization of TiO₂ and SnO₂ nanoparticles. The porphyrin effectively extends the absorption spectrum of the anode into the visible region of the solar spectrum and electrochemical measurements indicate the dyes are thermodynamically capable of water oxidation. Initial THz studies and photoelectrochemical measurements demonstrate that photoexcited PF₁₀ (PF₁₀^{*}) is capable of injecting electrons into the SnO₂ conduction band (CB).

In addition, the zinc derivative forms a photoinduced charge separated state on both TiO₂ and SnO₂. Co-deposition of the photoanode with a molecular based water oxidation catalyst (IrCp^{*}) results in a marked increase in observed photocurrent, consistent with light induced activation of the catalyst (Figure 1).

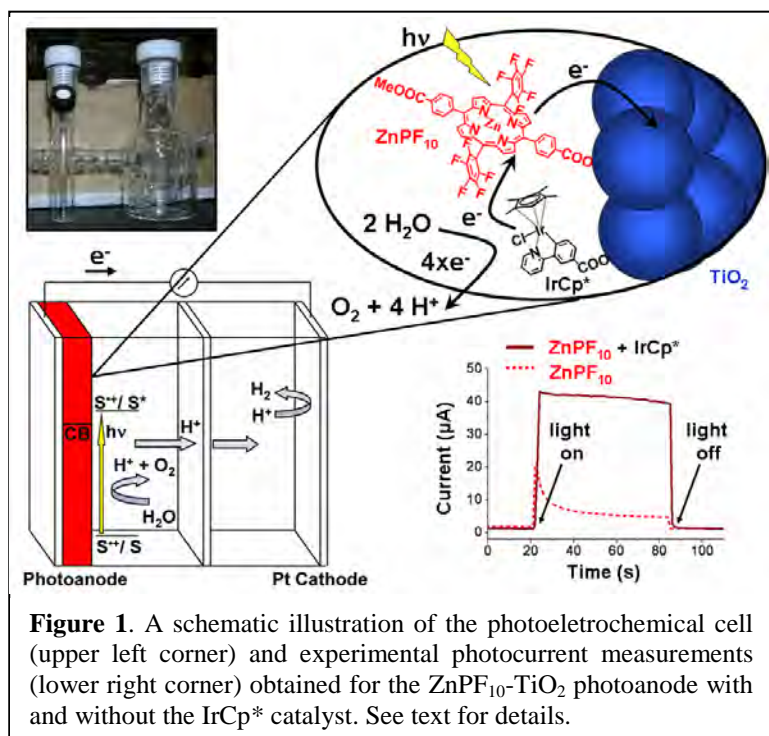


Figure 1. A schematic illustration of the photoelectrochemical cell (upper left corner) and experimental photocurrent measurements (lower right corner) obtained for the ZnPF₁₀-TiO₂ photoanode with and without the IrCp^{*} catalyst. See text for details.

1. *New Sciences for a Secure and Sustainable Energy Future*, U.S. Department of Energy, Washington, DC, December 2008.
2. *Directing Matter and Energy: Five Challenges for Science and the Imagination*, U.S. Department of Energy,

Electron-Transfer from and in Ionic Liquids

Cherry S. Santos, Madhuri Manpadi, Alex J. Baranowski, Lawrence J. Williams and
Edward W. Castner, Jr.

Department of Chemistry and Chemical Biology
Rutgers, The State University of New Jersey
Piscataway, NJ 08854-8066

Ionic liquids (ILs) present an array of complex behaviors when used as solvents for electron-transfer reactions.[1] Nanostructural organization is ubiquitous for these liquids. Solvation dynamics are often heterogeneous, in part because these fragile glass-formers may be supercooled liquids at ambient temperatures. Dynamic heterogeneity of solvation and reactivity has been observed, including for electron-transfer reactions.

To address the complexities of electron-transfer in ionic liquids, we have synthesized a new class of ILs that will serve as strong electron donors by using carboxylate derivatives of the N,N-dimethylaniline (DMA) donor. The first example of the novel electron-donating ionic liquids, $\text{Pyrr}_{14}^+/\text{NTf}_2^-$, is shown below in Fig. 1. The DMAPP⁻ anion shows an oxidation potential 16 mV lower than that of DMA measured in CH_3CN solvent. Photo-induced electron transfer from DMAPP⁻ to the coumarin 152 chromophore is observed to have diffusion-limited reaction rates in THF and CH_3CN solvents. The fluorescence transients for reductive quenching of coumarin 152 by DMAPP⁻ in CH_3CN solution are shown for donor concentrations in the range from 0.02 to 0.5 M. The temperature-dependence of this bimolecular reaction is weak, with an activation enthalpy of 7.6 kJ/mol. This and related new electron-donating ILs will permit electron-transfer studies in both polar solvents and in pure ionic liquids where the IL anion will serve as the electron donor.

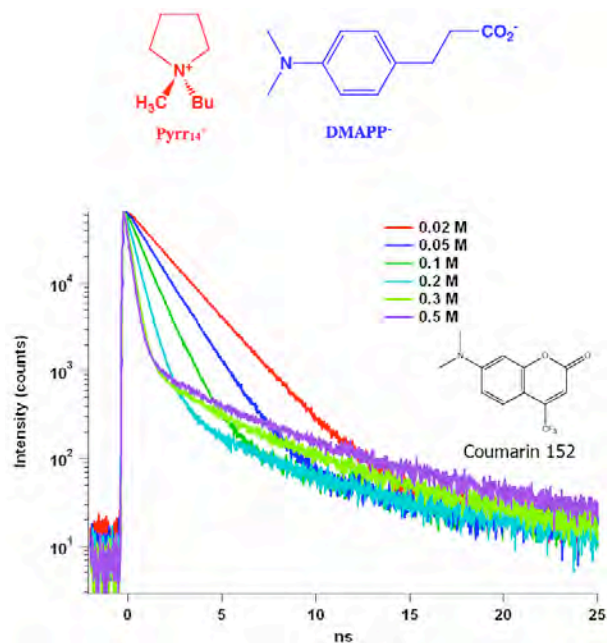


Figure 1. TCSPC fluorescence quenching of coumarin 152 by the ionic liquid anion DMAPP⁻ in CH_3CN . Excitation and emission wavelengths at 400 and 510 nm, respectively.

[1] E. W. Castner, Jr. and J. F. Wishart, 'Spotlight on Ionic Liquids', *J. Chem. Phys.* **132**, 120901 (2010).

Hydroxamate Anchors for Water-Stable Attachment to TiO₂

William R. McNamara, Robert C. Snoeberger III, Gonghu Li, Christiaan Richter, Laura J. Allen, Rebecca L. Milot, Charles A. Schmuttenmaer, Robert H. Crabtree, Gary W. Brudvig and Victor S. Batista

Department of Chemistry
Yale University
New Haven, CT, 06520-8107

Artificial photosynthesis with water splitting normally requires that the components be stably bound to the electrode surface. In the case of oxide semiconductors, such as TiO₂, the typical carboxylate linkers are stable in organic solvent such as MeCN, but not in water. We have, therefore, developed a series of hydroxamate linkers for TiO₂ that prove to be hydrolytically stable in water as well as being able to photoinject electrons into the semiconductor.

Scheme 1 shows the synthetic transformation of ester precursors into hydroxamates. These are doubly deprotonated on binding to TiO₂ from IR data, thus providing tight binding to Ti(IV) analogous to the role of hydroxamates in bacterial siderophores. Fig. 1 shows that irradiating the Mn(II) complex of **2**, bound to TiO₂ leads to photoinjection, accompanied by oxidation of Mn(II) to Mn(III), a step relevant our biomimetic water oxidation strategy. Fig. 2 shows the computational modeling of the binding and injection. Ultrafast THz spectroscopy shows that the hydroxamate is at least as effective as the conventional carboxylate anchor in mediating photoinjection.

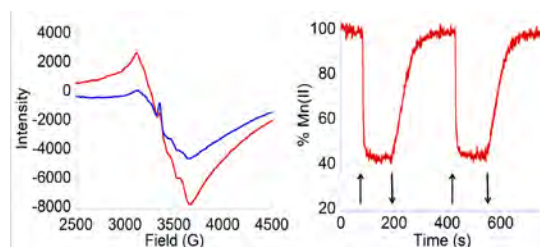
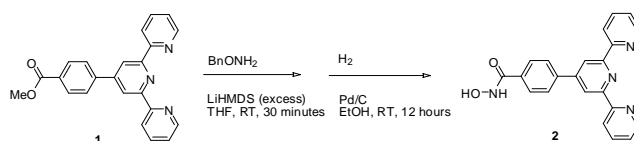


Figure 1. *Left:* EPR spectra at 6 K of **2**-TiO₂ NPs functionalized with Mn^{II}(OAc)₂ in the dark before irradiation (red) and with visible light irradiation (blue); *Right:* Time-dependent Mn(II) %age at 3106 G with light on (↑) and off (↓).

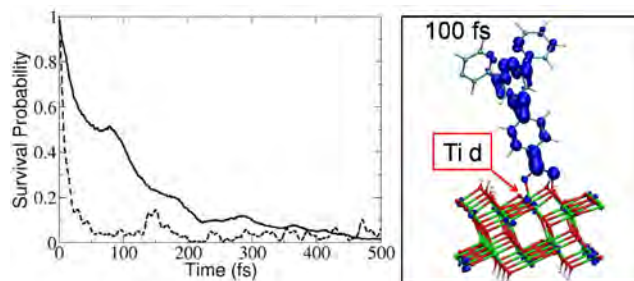


Figure 2. *Left:* Time-dependent probability of the electron to remain in the adsorbate **2** (solid line), compared to the analogous carboxylate-linked adsorbate (dashed line). *Right:* A snapshot of the electronic charge distribution at 100 fs after photoexcitation of **2**.

Dynamic Energy Fluctuations in 3d Molecular Orbitals of Metalloporphyrins and their Implications in the Ground and Excited State Axial Ligation Revealed by Transient X-ray Absorption Spectroscopy

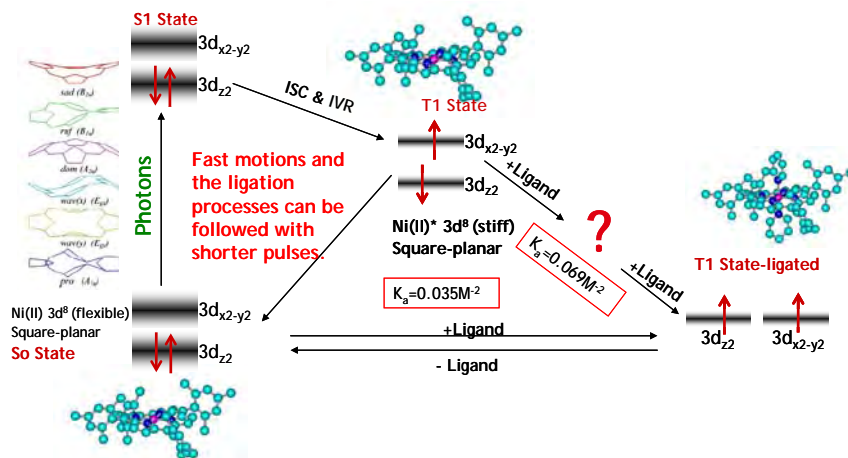
Lin X. Chen^{1,2}, Xiaoyi Zhang³, Erik C. Wasinger^{1,§}, Jenny V. Lockard¹, Andrew B. Stickrath¹, Michael W. Mara², Klaus Attenkofer³, and Guy Jennings³, Grigory Smolentsev⁴, Alexander Soldatov⁴

¹Chemical Sciences and Engineering Division and ³X-ray Sciences Division, Argonne National Laboratory, Argonne, Illinois 60439

²Department of Chemistry, Northwestern University, Evanston, Illinois, 60208

⁴Physics Department, Southern Federal University, Rostov-na-Donu 344090 Russia

The ground state and photoinduced axial ligation mechanisms of a metalloporphyrin, nickel(II) tetramesitylporphyrin (NiTMP), were investigated by static and transient X-ray absorption spectroscopy at Ni K-edge (8.333 keV) and by optical transient absorption. A surprisingly broad (i.e. ~ 1.4 eV) linewidth for the $1s \rightarrow 3d_{x^2-y^2}$ transition in the ground state NiTMP in toluene solution at room temperature has been associated with coordination geometry dependent energy levels of 3d molecular orbitals (MOs) due to the multiple coexistent conformations with severe non-planar distortions. The resulting dynamic energy level fluctuation enables transient degeneracy of the $3d_{z^2}$ and $3d_{x^2-y^2}$ MOs to produce an electronic configuration of two singly occupied ($3d_{z^2}, 3d_{x^2-y^2}$), favoring the axial ligation in the ground state due to the vacancy in $3d_{z^2}$ MO. The photoexcitation at the Q-band also induces the ($3d_{z^2}, 3d_{x^2-y^2}$) configuration and promotes the axial ligation. A unified axial ligation reaction mechanism for the ground state and the photoexcited state therefore is proposed based on the elucidation of the excited state structural dynamics by transient optical and x-ray absorption spectroscopy, as well as by density functional theory calculations. The X-ray transient absorption at $1s \rightarrow 4p_z$ transition energy taken at different time delays after the photoexcitation presents a time sequence of the excited state and ligation processes. The results obtained from this study can be broadly applied to study other metalloporphyrins and metal complexes for their photocatalytic activities involving the transient ligation.



Water-Stable, Hydroxamate Anchors for Functionalization of TiO₂ Surfaces with Ultrafast Interfacial Electron Transfer

William R. McNamara, Rebecca L. Milot, Hee-eun Song, Robert C. Snoeberger III, Victor S. Batista, Charles A. Schmuttenmaer, Gary W. Brudvig and Robert H. Crabtree
Department of Chemistry, Yale University, New Haven, CT 06520-8107

A novel class of derivatized hydroxamic acid linkages for robust sensitization of TiO₂ nanoparticles (NPs) under various aqueous conditions is described. The stability of linkages bound to metal oxides under various conditions is important in developing photocatalytic cells which incorporate transition metal complexes for solar energy conversion.

In order to compare the standard carboxylate anchor to hydroxamates, two organic dyes differing only in anchoring groups were synthesized and attached to TiO₂ NPs. At acidic, basic, and close to neutral pH, hydroxamic acid linkages resist detachment compared to the labile carboxylic acids (Figure 2). Ab initio calculations show that the electron density in the LUMO is in close proximity to the anchor site, thereby allowing charge injection into TiO₂ (Figure 3).

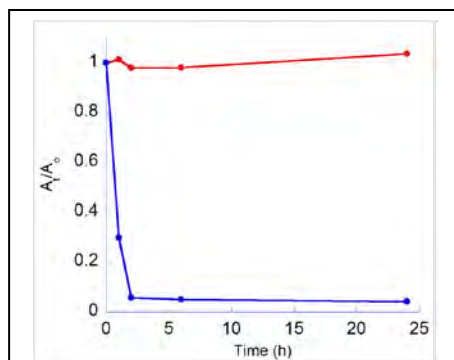


Figure 2. UV/vis spectra of hydroxamate (red) and carboxylate (blue) anchors as a function of time soaking in water.

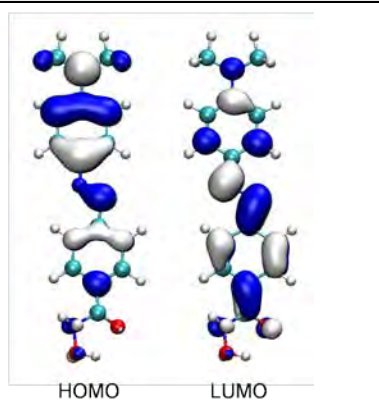


Figure 3. Calculated electron density in HOMO and LUMO of dye with hydroxamate anchor.

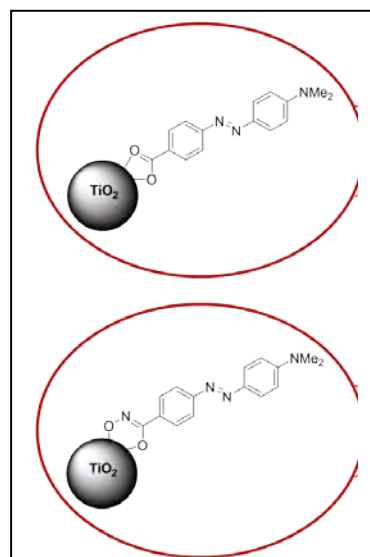


Figure 1. Methyl red-like molecules compared. **2** (top) has a carboxylate linkage to TiO₂, and **4** (bottom) has a hydroxamate linkage.

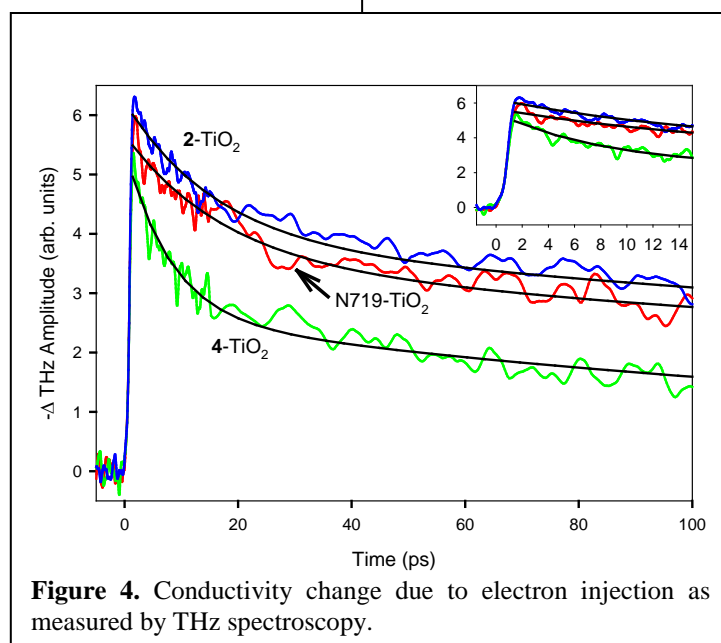


Figure 4. Conductivity change due to electron injection as measured by THz spectroscopy.

The Crystalline Nanocluster Ti-O Phase: Synthesis of New Clusters and Their Functionalization

Philip Coppens and Jason B. Benedict

Department of Chemistry

University at Buffalo, State University of New York,
Buffalo, New York 14260-3000

Despite tremendous progress in the development of dye sensitized solar cells (DSSC) for light harvesting applications, current knowledge of the precise structures of the semi-conductor nanoparticles and the binding modes of adsorbed dye molecules is limited, even though geometric knowledge is crucial for the understanding of their function. To fill this gap, we are synthesizing and characterizing crystalline arrays of well ordered Ti-O clusters.¹ Polyoxotitanates are prepared by the controlled hydrolysis of Ti-alkoxide precursors in suitable solvents using solution and solvothermal techniques; other synthetic routes are being explored. Subsequent crystallization is achieved by slow evaporation, temperature reduction, and vapor diffusion. X-ray analyses show a wide variety of cluster shapes ranging from almost spherical to flattened assemblies. While the structures of these nanoparticles often contain features of the bulk TiO₂ found in DSSCs -anatase and rutile-, the polyoxotitanates also contain titanium undercoordination speculated to be present on and responsible for the reactivity of the surfaces of the pure phase nanoparticles (Figure 1). To date, our structures indicate that monocarboxylic acids (acetic acid, iso-nicotinic acid, *trans*-cinnamic acid, 4-dimethylamino cinnamic acid) deprotonate in the presence of polyoxotitanates and bind to the clusters by bridging two titanium atoms, exclusively. In contrast, crystal structures of products from reactions containing a model diol, catechol, show considerable variation in the observed binding modes and states of protonation. While clusters with up to 18 titanium atoms ($n_{\text{Ti}}=18$) are readily synthesized and have been reported in the literature, the synthesis and crystallization of larger clusters has remained elusive. By varying the synthetic conditions, we have recently extended the range to $n_{\text{Ti}}=28$ (Figure 2) and are expecting further advances. As expected deep colors are obtained when the clusters are functionalized with a range of photosensitizer dyes such as catechol, fluorone black and fluorescein, presumably due to the formation of new ligand-metal charge transfer bands. Once the precise structures are known, photo-induced electron transfer dynamics of the crystalline functionalized nanoclusters can be obtained through time-resolved X-ray diffraction² and ultra-fast femtosecond spectroscopy.

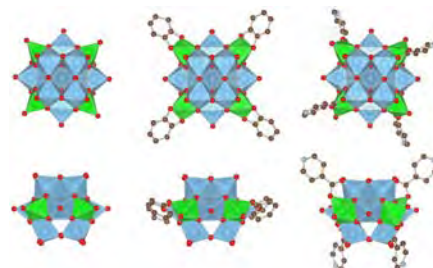


Figure 1: Semiconductor core of the pure Ti₁₇ cluster (left) and the cluster functionalized with catechol (center) and isonicotinic acid (right).

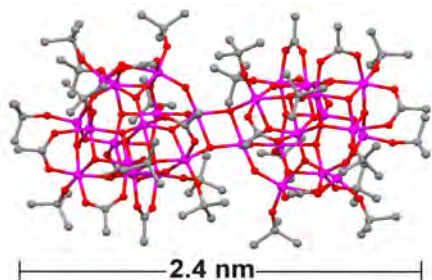


Figure 2: Structure of a new polyoxotitanate Ti₂₈O₄₀(OAc)₁₂(OBu)₂₀

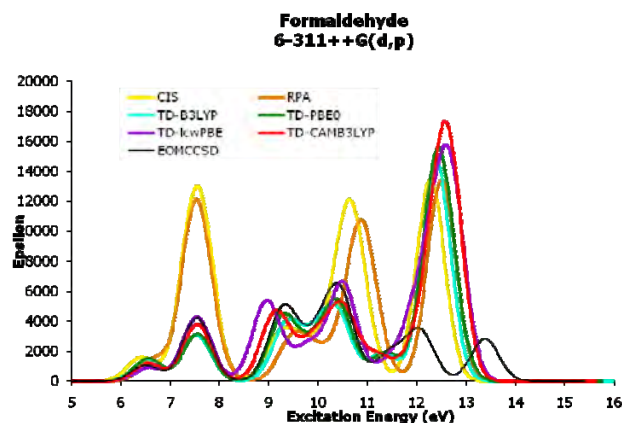
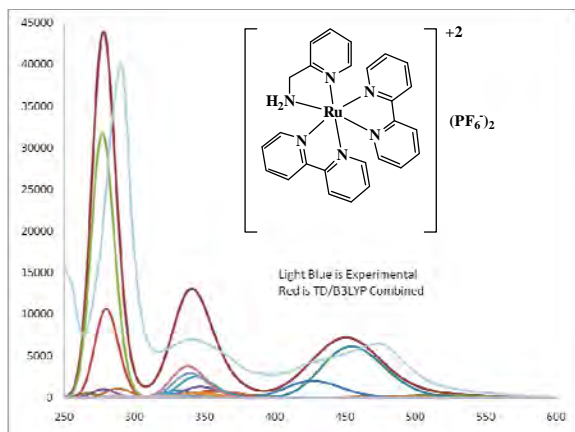
As expected deep colors are obtained when the clusters are functionalized with a range of photosensitizer dyes such as catechol, fluorone black and fluorescein, presumably due to the formation of new ligand-metal charge transfer bands. Once the precise structures are known, photo-induced electron transfer dynamics of the crystalline functionalized nanoclusters can be obtained through time-resolved X-ray diffraction² and ultra-fast femtosecond spectroscopy.

1. Benedict, J. B.; Coppens, P., *J. Am. Chem. Soc.* **2010**, 132, 2939-2944.
2. Coppens, P.; Benedict, J.; Messerschmidt, M.; Novozhilova, I.; Graber, T.; Chen, Y.-S.; Vorontsov, I.; Scheins, S.; Zheng, S.-H., *Acta Cryst A.* **2010**, A66, 179-188.

Multi-metallic Complexes for Photoinduced Reactions: Computational Efforts

Marco Allard, Brian T. Psciuk, Cláudio N. Verani,
John F. Endicott, H. Bernhard Schlegel
Department of Chemistry
Wayne State University
Detroit, Michigan 48202

Utilization of coordination complexes to harvest solar energy requires an understanding of the structure, energetics and reactivity of excited states. As part of a collaborative program aimed at the fundamental topics involved with water oxidation by multi-metallic complexes, we are surveying computational methods applicable to excited states of donor-acceptor complexes. TD-DFT methods are practical for calculating electronic excited states for a wide range of molecules, but some caution is needed for charge transfer processes. The energies and charge distributions of excited states are reflected in the position and intensity of the bands in absorption and emission spectra. Numerous studies are available that compare the accuracy of excitation energies for different density functionals, but very few studies have examined intensities. The oscillator strengths for a series of organic and inorganic systems have been calculated with TD-DFT and compared to wavefunction methods. The performance of standard, hybrid and long range corrected functionals has been examined along with basis set dependence. These studies are aimed at providing the benchmarks needed for the application of TD-DFT methods for the calculation of UV-visible spectra and for the investigation of electronic excited states of organic and inorganic and systems relevant to solar energy utilization.



Photoinduced Reactions of Multi-metallic Complexes: Spectroscopic Probes of Charge-Transfer Excited State Reactivity

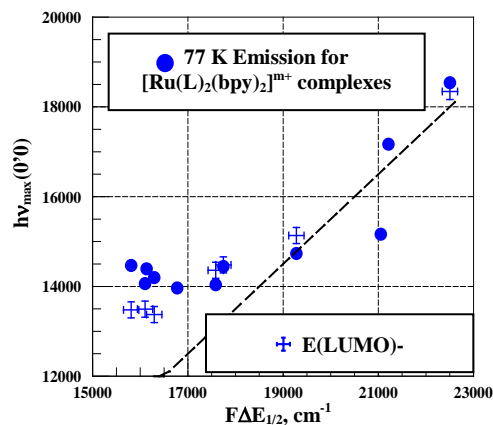
Marco M. Allard, Onduro S. Odongo, H. Bernhard Schlegel, Cláudio N. Verani
and John F. Endicott
Department of Chemistry, Wayne State University, Detroit, Michigan 48202

The utilization of transition metal complexes for efficient photoinduced electron transfer processes requires knowledge of their excited state structures and electron donor capability. We have been investigating experimental approaches to determination of the relevant properties of transition metal excited states as a part of a collaborative approach to issues related to photoinduced oxidation-reduction processes in multimetal complexes.

Direct determination of the relevant factors governing the electron-transfer reactivity excited states, such as their redox potentials and electron-transfer reorganizational energies (λ), is rarely possible. Thus, excited state redox potentials are usually inferred by combining the excited state energy with the potentials for related ground state reactions, and the relevant reorganizational energies may be inferred from vibronic side-bandshapes. We have been systematically examining both such approaches for the lowest energy excited states in simple Ru-polypyridyl complexes in order to better define the relevant parameters and guiding principles.

1. Correlations between excited state energies and ground state redox potentials.

The lowest energy absorption bands of the $[\text{Ru}(\text{L})_2(\text{bpy})_2]^{m+}$ complexes are comprised of two principal absorption envelopes which are especially well defined for complexes with $(\text{L})_2 =$ substituted acac; computational modeling indicates that the lowest energy and least intense of these envelopes is the most closely related to the HOMO-to-LUMO transitions and thereby to the differences in reduction and oxidation potentials, $\Delta E_{1/2}$. However, the correlations between $\Delta E_{1/2}$ and either the lowest energy absorption component or the calculated HOMO-to-LUMO transition energies are more shallow than expected, and the related correlations for the 77K emission energies of these complexes appear to reach a low energy limit near to $14,000 \text{ cm}^{-1}$. Similarly, the correlations between the 77K emission maxima of $\{(\text{L})_4\text{Ru}\}_n\text{dpp}\}^{n+}$ complexes and $\Delta E_{1/2}$ approach a low energy limit near $9,000\text{-}10,000 \text{ cm}^{-1}$. These observations can be attributed to the characteristically strong Ru/PP electronic mixing in these complexes.

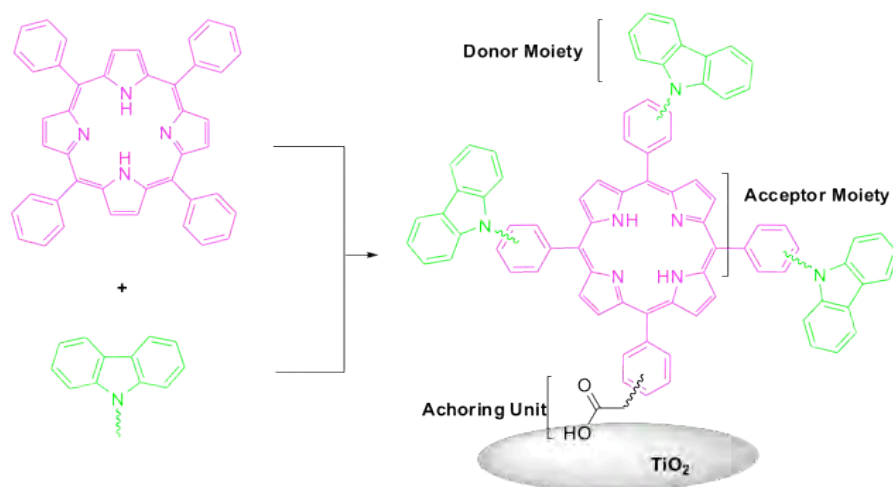


2. Excited state reorganizational energies and 77K emission bandshapes. The effective magnitudes of λ decrease with MLCT excited state energy and appear to be smaller for the $^3\text{MLCT}$ than for the related Franck-Condon excited states. The variations of vibronic bandshapes in the emission plateau region differ from those in the “normal” region and are being further investigated.

Nanoscaled Components for Improved Efficiency in a Multipanel Photocatalytic Water-Splitting System

Marye Anne Fox and James K Whitesell
Department of Chemistry and Biochemistry
University of California, San Diego
La Jolla, CA 92093-0358

The most successful charge-transfer sensitizers employed in DSSCs are polypyridylruthenium complexes, which yield solar-to-electric power conversion efficiencies of 10-11% with simulated sunlight. The main drawback of these ruthenium-based sensitizers is their long term instability and lack of absorption in the red region of the visible spectrum. The use of porphyrins as dyes on DSSCs is particularly attractive given their primary role in photosynthesis and the relative ease with which a variety of covalent or noncovalent porphyrin arrays can be constructed. Herein, a new series of porphyrin dyes are designed and synthesized (Figure 1):



As shown in Figure 1, these porphyrin dyes contain π -conjugated carbazole units as donor moieties for intramolecular charge transfer and a carboxyl group as an anchoring unit for the attachment of the dyes onto nanoparticulate TiO_2 . A variety of these dyes are being prepared in order to provide a broad range of spectral absorption profiles.

Multimetallic Complexes for Photoinduced Reactions: Synthetic and Surface-based Efforts

Rajendra Shakya, Frank D. Lesh, Rama Shanmugan, Debashis Basu, Marco M. Allard,
H. Bernhard Schlegel, John F. Endicott, Cláudio N. Verani*

Department of Chemistry
Wayne State University
Detroit, MI-48202

A comprehensive effort is under development at Wayne State University aiming at water oxidation by modular supramolecular multimetallic complexes. Such complexes can incorporate reactive sites, antennae, and acceptors capable of accumulating and shuffling multiple electrons. In order to proceed, we are employing synthetic, redox-, spectroscopic-, surface-, and computation-based techniques to understand photoinduced electron transfer, charge separation and efficient dioxygen production in bulk and on surfaces.

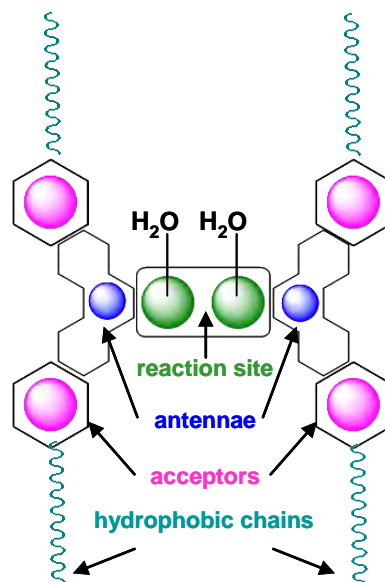
To date we have succeeded on the synthesis of modular heterometallic complexes that involve (i) tetrametallic species that merge antennae and active sites, (ii) bimetallic species that merge antennae and acceptors, and (iii) species that merge antenna and amphiphiles and allow for Langmuir-Blodgett film formation.

(i) The tetrametallic species: Multistep synthetic routes were used to isolate phenanthroline-modified Robson-type macrocyclic complexes with cores $[\text{Ru}^{\text{II}}\text{M}_A\text{M}_A\text{Ru}^{\text{II}}]$ ($\text{M}_A = \text{Cu}(\text{II}), \text{Ni}(\text{II})$) aiming at $\text{Mn}(\text{II})$. These species were characterized by spectrometric and spectroscopic methods and allow for the study of concerted excitation of two electrons from the antennae to an acceptor such as methylviologen. The generation of two “holes” enables the study of proton-coupled electron transfer from the Mn-based active sites to the antenna.

(ii) The bimetallic species: Phenanthroline-modified Jaeger-type macrocyclic complexes with cores $[\text{Co}^{\text{III}}\text{Ru}^{\text{II}}]$ were isolated and allow for the incorporation of Co-containing acceptor modules to Ru-based antennae.

(iii) Species merging antenna and amphiphiles: Ru-based modules $[\text{Ru}^{\text{II}}\text{L}^{\text{amph}}]$ incorporate amphiphiles and allow for the study of film formation at the air/water interface. Pyridine-rich amphiphiles gave the best films as judged by collapse pressures and Brewster angle microscopy. Phenolate-based amphiphiles are redox-active and showed rich electrochemical behavior indicating that the amphiphile itself can act as electron acceptor.

Future work involves the assembly of systems with $[(\text{Co}^{\text{III}})_2\text{Ru}^{\text{II}}(\text{Mn}^{\text{II}})_2\text{Ru}^{\text{II}}(\text{Co}^{\text{III}})_2]$ cores that display a topology such as {acceptors[antenna(catalyst)antenna]acceptors}.



All Inorganic Binuclear Charge Transfer Chromophores: Structure, Electron Transfer Kinetics, and Redox Properties

Tanja Cuk, Walter Weare, Marisa MacNaughtan, and Heinz Frei
Physical Biosciences Division, Lawrence Berkeley National Laboratory
Berkeley, CA 94720

Separation of photophysical and catalytic functions in a photosynthetic unit provides maximum flexibility for simultaneously optimizing the chromophoric properties (optimal coverage of the solar spectrum) and the rate of multi-electron catalysis while at the same time enabling the close matching of redox potentials of light absorber and catalyst. The latter is essential for converting the maximum fraction of solar photon energy to chemical energy of the fuel. Oxo-bridged heterobinuclear metal-to-metal charge-transfer units anchored in nanoporous silica scaffolds we have developed in the past few years are robust visible light chromophores that offer a wide choice of donor and acceptor metal centers. By selecting appropriate metals and oxidation states, the potentials of donor or acceptor centers can be closely matched with the energetic requirements for catalytic water oxidation or CO₂ reduction.

TiOMn^{II} units anchored on silica nanopores absorb across the visible spectrum and generate transient donor (Mn^{III}) and acceptor centers (Ti^{III}) of desired redox potential. We have conducted a detailed characterization of structural, electron transfer and photochemical properties of the charge transfer unit that provides the basis for use in integrated photosynthetic assemblies. Ti and Mn K-edge EXAFS and L-edge X-ray absorption spectroscopy provided insight into the coordination geometry of the metal centers. By developing completely transparent mesoporous silica membranes, the visible light Ti^{IV}OMn^{II} → Ti^{III}OMn^{III} charge-transfer absorption could be recorded in transmission mode, thus obviating diffuse reflectance measurements of strongly scattering pressed wafers of MCM-41 or SBA-15 particles that previously prevented accurate determination of reaction quantum efficiencies. Laser flash photolysis revealed an unusually long lifetime of the Ti^{III}OMn^{III} excited state of 1.8 ± 0.3 microsecond at room temperature, which is attributed to a strong polarization of the local and remote silica environment upon light-triggered electron transfer from Mn to Ti resulting in a substantial reorganization barrier for back electron transfer.¹ The long lifetime is consistent with the observed photoredox activity of this chromophore² and other oxo-bridged heterobinuclear units anchored on silica surfaces, which makes them suitable as visible light electron pumps for driving multi-electron catalysts (e.g. TiOCr^{III}—Ir oxide nanocluster units for water oxidation).³

The observed complete charge transfer from Mn to Ti upon absorption of visible light (potential of excited acceptor -0.3V) opens up opportunities for exploring spatially directed synthesis of metal cluster catalysts at the acceptor site for multi-electron reduction catalysis. Initial experiments that seek to demonstrate the feasibility of this synthetic approach will be discussed.

¹ Cuk, T.; Weare, W.; Frei, H. *J. Phys. Chem. C* **2010**, *114*, 000.

² Wu, X.; Weare, W.; Frei, H. *Dalton Trans.* **2009**, 10114.

³ Han, H.; Frei, H. *J. Phys. Chem. C* **2008**, *112*, 16156.

Photochemical Formation of Hydride Donors and Their Reactivities

Etsuko Fujita,¹ Diane Cabelli,¹ Brian Cohen,¹ Takashi Fukushima,² James T. Muckerman,¹
Dmitry E. Polyansky,¹ Koji Tanaka,² Randolph Thummel,³ and Ruifa Zong³

¹ Chemistry Department, Brookhaven National Laboratory, Upton, NY 11973-5000

² Coordination Chemistry Laboratories, Institute for Molecular Science, 5-1 Higashi-yama,
Myodaiji, Okazaki, Aichi 444-8787, Japan

³ Department of Chemistry, 136 Fleming Bldg, University of Houston, Houston, TX 77204-5003

We have shown that a polypyridylruthenium complex with an NAD⁺/NADH model ligand, [Ru(bpy)₂(pbn)]²⁺ (**[1]**²⁺, bpy = 2,2'-bipyridine, pbn = 2-(2'-pyridyl)-benzo[*b*]-1,5-naphthyridine), undergoes proton-coupled two-electron reduction cleanly to give [Ru(bpy)₂(pbnHH)]²⁺ (**[1•HH]**²⁺, pbnHH = 5,10-dihydro-2-(2'-pyridyl)-benzo[*b*]-1,5-naphthyridine) upon irradiation with visible light (300-600 nm) in a triethylamine (TEA) containing acetonitrile solution with a quantum yield of 0.21 at 355 nm via disproportionation of the π -stacking dimer of the protonated one-electron-reduced species.^{1,2}

A related complex [Ru(bpy)₂(ipbn)]²⁺ (**[2]**²⁺, ipbn = 2-(2'-pyridyl)-benzo[*b*]-1,8-naphthyridine) also cleanly gives [Ru(bpy)₂(ipbnHH)]²⁺ (**[2•HH]**²⁺) upon irradiation, however, our pulse radiolysis and nmr experiments indicate a different pathway via the C–C bonded dimer of the protonated one-electron-reduced species. The C–C bonded dimer is stable in neutral or acidic aqueous solution, but disproportionates in a basic solution or in acetonitrile.

While both complexes can transfer their hydrides to Ph₃C⁺, **[2•HH]**²⁺, in which the hydride is away from the Ru coordination sphere, transfers it 100 times faster than **[1•HH]**²⁺. Ground-state and excited-state properties of these complexes will be discussed.

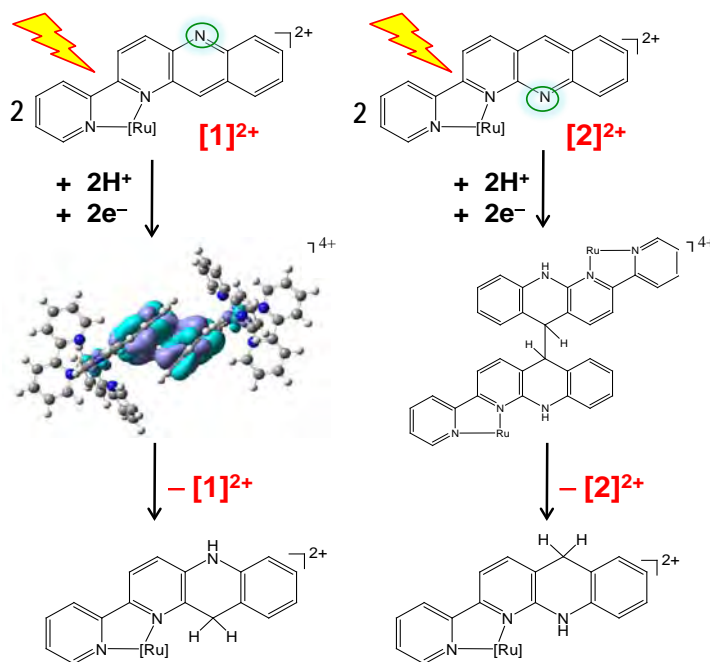


Fig.1. Mechanism of photogeneration of hydride donors, **[1•HH]**²⁺ and **[2•HH]**²⁺, in a TEA containing acetonitrile. [Ru] indicates Ru(bpy)₂.

References

- 1 Polyansky, D. E.; Cabelli, D.; Muckerman, J. T.; Fukushima, T.; Tanaka, K.; Fujita, E. *Inorg. Chem.* **2008**, *47*, 3958-3968.
- 2 Fukushima, T.; Fujita, E.; Muckerman, J. T.; Polyansky, D. E.; Wada, T.; Tanaka, K., *Inorg. Chem.*, **2009**, *48*, 11510-11512

Charge Injection Behavior of Dye:ZnO Nanocrystal Dyads as a Function of Excited State Potential of the Ruthenium-Based Dye

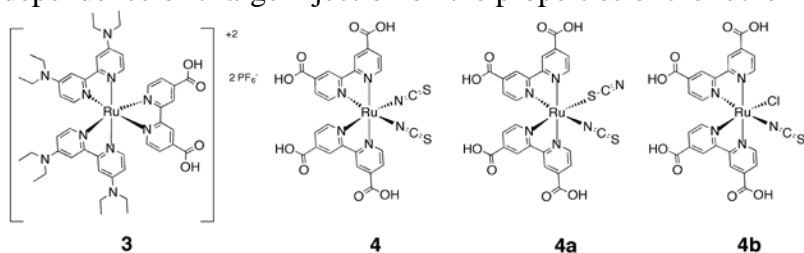
Ryan Hue, Julia Saunders, Adam Huss, Raghu Chitta, Kent Mann, David Blank and Wayne L. Gladfelter

Department of Chemistry
University of Minnesota
Minneapolis, MN 55455

Despite the fact that the excited states of the tris(bipyridine) ruthenium complexes, $[\text{Ru}(\text{bpy})_2(\text{dcb})](\text{PF}_6)_2$ (1) and $[\text{Ru}(\text{t-Bu}_2\text{bpy})_2(\text{dcb})](\text{PF}_6)_2$ (2), where dcb = 4,4'-dicarboxy-2,2'-bipyridine, t-Bu₂bpy = 4,4'-di-tert-butyl-2,2'-bipyridine, are quenched upon adsorption on heat-treated, nanocrystalline ZnO films, isolated ZnO nanocrystals (diameters = 3 - 5 nm) do not quench the excited state. Confirmation that the dye complexes were bound to the ZnO nanocrystals is based on infrared spectroscopy and fluorescence polarization anisotropy measurements as well as differences in solubility that allowed separation of the unbound complexes from the (dye)_n:ZnO dyads. The hypothesis that the lack of quenching resulted from an increase in the ZnO conduction band edge was tested by increasing the excited state oxidation potential of the dye.

Towards this end the new compound $[\text{Ru}(\text{deabpy})_2(\text{dcb})](\text{PF}_6)_2$ (3) (deabpy = 4,4'-bis(diethylamino)-2,2'-bipyridine) was synthesized. No luminescence was observed for the parent diacid species 3, whereas the doubly deprotonated species (3a) emits with a λ_{max} at 728 nm. The diethylamino substituents were predicted to increase the excited state oxidation potential. Using spectroscopic and electrochemical studies the excited state oxidation potential of 3a was calculated to be -1.23V (vs. NHE) which is 0.5 V higher in energy than that of 1. Steady state luminescence studies confirm that ZnO nanocrystals quench the excited state of 3a. Ultrafast photophysical studies to probe for the evidence of electron transfer within this dyad system are underway.

A series of ruthenium dyes having excited state potentials between 1 and 3 include $\text{Ru}(\text{dcb})_2(\text{NCS})_2$ (4), commonly known as N3, and its dianionic form, N719, which were prepared by modification to existing literature methods. Chromatographic separation of the final intermediate (the tetraester of 4), allowed the isolation of the known N,S isomer 4a, and the new chloroisothiocyanato compound, 4b. Details of these synthetic procedures will be presented. Using pump-probe methods, clear spectroscopic evidence of charge injection from N719 ($E^+/E^* = -0.98$ V) into a 3 nm ZnO crystal was observed. These experiments demonstrate the dependence of charge injection on the properties of the ruthenium dyes.



Electron Transfer Parameters from Spectroscopy

Naoki Ito, Tamal Mukherjee and Ian R. Gould
Department of Chemistry and Biochemistry
Arizona State University
Tempe, AZ 85287

We summarize some recent work that further explores the quantitative relationships between optical and thermal electron transfer processes.

Transition Dipole Moments and Electronic Coupling Matrix Elements. The central assumption in quantitative studies of optical electron transfer is the Mulliken-Hush (MH) relationship for the transition dipole moment (M), Eq. 1.

$$M = \frac{V \Delta\mu}{h\nu} \quad (1)$$

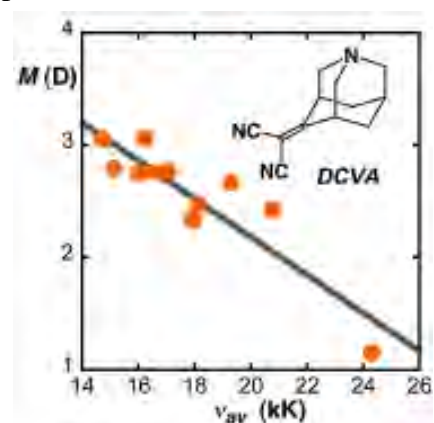
$$\int \epsilon \nu d\nu = \frac{8 N \pi^3}{3000 h^3 c \ln 10} n V^2 \Delta\mu^2 \quad (2)$$

$$k_f = \frac{64 \pi^4}{3 h^3 c^3} n \nu_{av} V^2 \Delta\mu^2 \quad (3)$$

In the weak coupling limit characteristic of electron transfer processes, the absorption and emission intensity is derived exclusively from mixing of ground (AD) and excited (A^-D^+) states, determined by the energy gap ($h\nu$) and the electronic coupling matrix element V . Important consequences of the MH relationship are that

CT absorption and emission bands should have a frequency dependent M , and the radiative rate constant k_f should exhibit a linear dependence on emission frequency instead of the usual frequency cubed dependence. Here we test the MH relationship experimentally.

M for absorption and emission processes have been evaluated for dicyanovinylazaadamantane (DCVA) using Eqs. 1 - 3, where ν_{av} is the average emission or absorption frequency and $\Delta\mu$ the dipole moment difference for AD and A^-D^+ , estimated to be 20 D for DCVA. A plot of k_f versus ν_{av} is linear and M is decreases linearly with increasing ν_{av} , as predicted by Eq. 1. The average value for V from the k_f measurements is 2300 cm^{-1} , and V from the absorption spectra is 1450 cm^{-1} .



Optical Bandwidth and Reorganization Parameters: Hydrogen-Bonding. Spectral bandshape analysis has been used to quantify the effects of hydrogen bonding on electron transfer parameters for DCVA in protic solvents. Hydrogen bonding weakens with increasing temperature, as evidenced by small red shifts in the CT emission with increasing temperature (compared to blue shifts in aprotic solvents), but hydrogen bonding is present up to the boiling points of methanol and ethanol. The reorganization energies in protic solvents and their temperature dependencies are not predictable by conventional continuum theories. Compared to the values expected based on the Pekar factor, hydrogen bonding in methanol increases both the energy gap between the AD and A^-D^+ states and the reorganization energy for charge recombination by almost 0.2 eV.

Detailed investigations of the differences in the reorganization parameters for charge separation and charge recombination reactions will also be presented.

Charged Defects in Excitonic Semiconductors: Their Number, Chemistry and Influence

Brian A. Gregg, Ziqi Liang, Michael Woodhouse, Russel A. Cormier
Chemical and Materials Science Center
National Renewable Energy Laboratory
Golden, Colorado 80401

Entropy, which favors defect formation, is more dominant when the enthalpy of crystal formation is low. Thus even “perfect” crystals of van der Waals-bonded organic semiconductors may have 6 – 12 orders of magnitude more defects than crystalline silicon. Charged defects often control the observed electrical and photoconversion properties of organic semiconductors yet little is known about them and they are often ignored. We have been studying the nature of these defects via several approaches. Characterizing pristine semiconductors with purposely added charged defects of known energy levels (dopants) resulted in a simple theoretical model of doping and transport that emphasized the role of the electrostatic perturbations caused by charges in such a low dielectric medium. One unshielded charge perturbs the energy levels of some 10,000 neighboring molecules. At concentrations typically observed in π -conjugated polymers, there are practically no energy levels that are *not* perturbed by the charges. This consideration alone can explain the previously mysterious appearance of energetic correlations and low-field Poole-Frenkel mobilities in π -conjugated polymers, without recourse to any of the “correlated disorder” models of transport.

Another approach involves probing the electroactive defects in poly(3-hexylthiophene), P3HT, by employing chemical reactions designed to react only at such defects. Reacting P3HT with electrophiles eliminated some anionic defects, while nucleophiles removed some cationic defects. These treatments resulted in doubling the exciton diffusion length, stabilizing the polymer against photodegradation and increasing the carrier mobility in the best case by a factor of 15. This highlights the influence of defects in π -conjugated polymers, and shows that targeted chemical treatments can tune the semiconducting properties in predictable ways.

A third approach to studying defects was to investigate the physical and optoelectronic properties of non-conjugated polymers based on perylene diimides and compare them to π -conjugated polymers. The optical properties, exciton diffusion length and band edge positions of these new polymers (see figure) were measured. Carrier mobility is moderately high at $5 \times 10^{-4} \text{ cm}^2/\text{Vs}$.

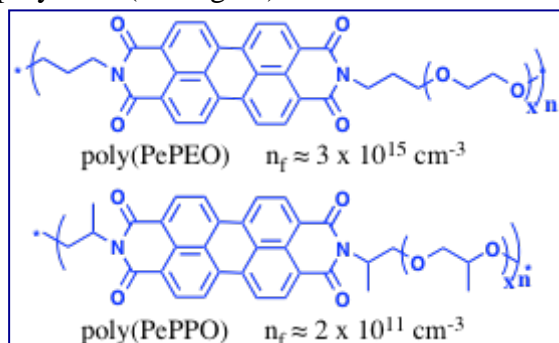


Figure. Two new families of perylene diimide polymers that have a surprisingly large difference in equilibrium charge density.

The conductivity in the three polyoxyethylene-based polymers ($\sim 10^{-7} \text{ S/cm}$) is much higher than in the two polyoxypropylene-based polymers ($\sim 10^{-11} \text{ S/cm}$). Rigorous deionizing has no effect on the conductivity. The free electron density, derived from the n-type charged defect density, is $\sim 3 \times 10^{15} \text{ cm}^{-3}$ in the polyoxyethylene-based polymers and $\sim 2 \times 10^{11} \text{ cm}^{-3}$ in the polyoxypropylene-based polymers. We have not yet found a reasonable explanation for this huge difference in free carrier density between ostensibly very similar polymer types.

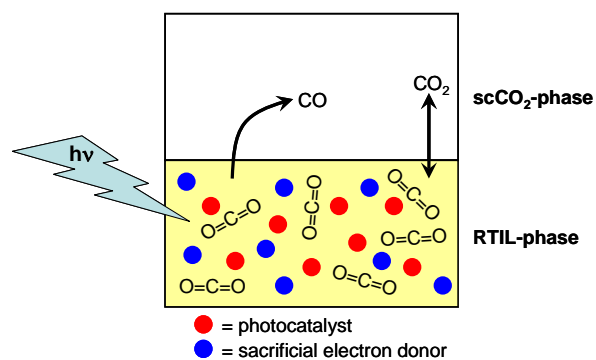
Biphasic Ionic Liquid-Supercritical CO₂ Systems for the Photocatalytic Reduction of CO₂

David C. Grills

Chemistry Department
Brookhaven National Laboratory
Upton, NY 11973-5000

We are investigating the use of alternative media to improve the efficiency of photocatalytic processes for the reduction of CO₂ to CO and other useful products, with transition metal complexes as catalysts. Our approach is to replace conventional organic solvents with either supercritical CO₂ (scCO₂), or biphasic solvent systems consisting of room temperature ionic liquids (RTILs) and scCO₂. Using scCO₂ as a solvent for these reactions has the advantage that the concentration of CO₂ is much higher (*e.g.* ~20M @ 3000 psi, 35°C), thus accelerating reaction steps that involve CO₂. Furthermore, the elimination of coordinating solvent molecules means that the active site of the catalyst is more readily available for reaction with CO₂. We have synthesized a series of new CO₂-soluble homogeneous catalysts, [Re(4,4'-(C_xF_{2x+1}CH₂CH₂CH₂)₂-2,2'-bpy)(CO)₃L]ⁿ (x = 6 and 8; L = Cl⁻ (n = 0), P(OCH₂CF₃)₃ (n = 1+, x = 6 only), and CO (n = 1+, x = 6 only); bpy = bipyridine), using the fluorinated [B(Ar_F)₄]⁻ anion for the cationic complexes. These catalysts exhibit a high solubility in scCO₂ due to the inclusion of fluorinated groups. Although their photophysical properties in scCO₂ are suitable for CO₂ reduction, photocatalysis in scCO₂ has been hindered by the fact that efficient sacrificial electron donors such as triethanolamine (TEOA) are not soluble in scCO₂, requiring the less efficient, but CO₂-soluble, donor triethylamine to be used.

Biphasic RTIL/scCO₂ solvent systems offer advantages over pure scCO₂ and conventional solvents. These include: (i) the RTIL can be chosen to be weakly- or non-coordinating, leaving the active metal center free to react with CO₂; (ii) scCO₂ is reasonably soluble in RTILs, meaning that the advantage of a high CO₂ concentration is maintained; (iii) efficient sacrificial electron donors, *e.g.* TEOA, are soluble in many RTILs; (iv) polar or charged catalysts can easily dissolve in RTILs without the need for synthetic modifications; and (v) the RTIL, catalyst and electron donor will not leech out into the scCO₂ phase, even at high pressures (see schematic diagram to the left).



In this poster we present results on the efficiency of the photocatalytic reduction of CO₂ to CO in a series of neat RTILs and in biphasic RTIL/scCO₂ systems, using ReCl(bpy)(CO)₃ as a photocatalyst. These data are compared with similar experiments performed in DMF. Turnover numbers for the catalytic production of CO are >10× higher in the biphasic systems than in neat scCO₂. RTILs that have been investigated include 1-butyl-1-

methylpyrrolidinium tetracyanoborate, 1-ethyl-3-methylimidazolium tetracyanoborate, and 1-ethyl-3-methylimidazolium trifluoromethanesulfonate. The choice of RTIL anion is shown to be critical in determining the overall catalytic efficiency.

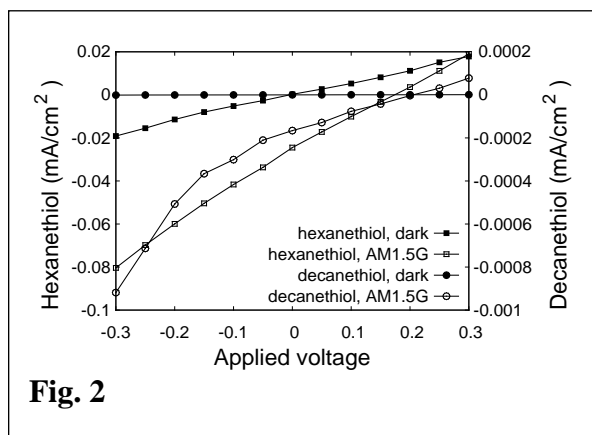
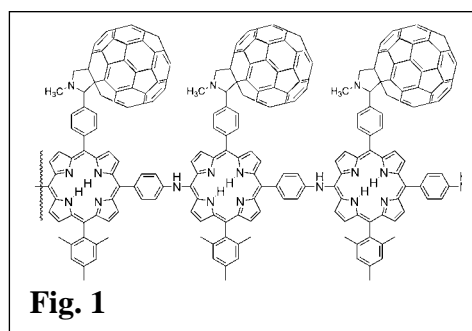
Porphyrin-Fullerene Polymers for Solar Energy Conversion

Devens Gust, Thomas A. Moore, Ana L. Moore, Paul A. Liddell, Gerdenis Kodis, Bradley Brennan and James Bridgewater

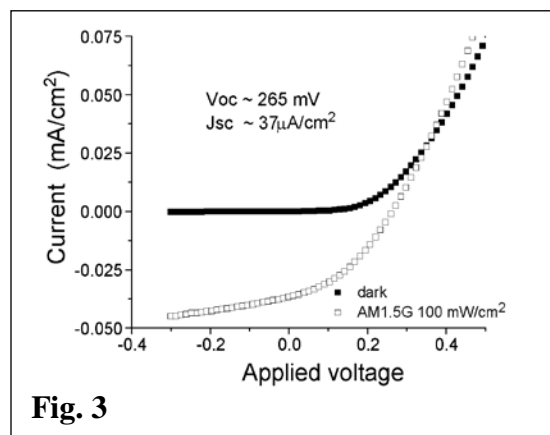
Center for Bioenergy and Photosynthesis, Department of Chemistry and Biochemistry
Arizona State University
Tempe, AZ 85287

Solar energy conversion using low cost materials holds promise for making renewable electricity generation more economically competitive with traditional, fossil fuel based production. One class of potentially low cost materials that has shown promise for solar electricity generation is blends of electron donating semiconductive organic polymers and electron accepting species. Photovoltaics utilizing this type of active layer have demonstrated power conversion efficiencies over 5% while also enabling inexpensive production methods.

We have developed electropolymers based on covalently linked porphyrin donors and fullerene acceptors (Fig. 1). Initial studies of electropolymerized films on transparent conductive oxide (TCO) substrates utilizing mercury contacts demonstrated their ability to produce photocurrent. Those experiments relied only on the difference between the contact materials to provide the asymmetry required for preferential injection of electrons and holes into opposite contacts. We have since explored the effects of contact surface modification on the selectivity of the contacts for either electron or hole extraction. Modification of the TCO substrates with silanes and modification of the mercury contacts with thiols can have substantial effects on dark currents, photocurrents and photovoltages (Fig. 2). In another approach, asymmetrization by coating the polymer film with a layer of evaporated C₆₀ followed by aluminum also yields promising results (Fig. 3).



thin film s on various substrates, opening up new



applications and analytical methods.

Anion and Cation Doping of TiO₂ for Visible Light Photoactivity

T. Ohsawa^a, M.A. Henderson^a, V. Shutthanandan^b, A.N. Mangham^a, and S.A. Chambers^a

^aChemical and Materials Science Division

^bEnvironmental Molecular Sciences Laboratory

Pacific Northwest National Laboratory

Richland, WA 99352

A limitation of TiO₂ as a photocatalyst is the fact that its optical absorptivity does not sufficiently overlap with the solar spectrum. A critical issue of research has been whether or not the bandgap of TiO₂ can be engineered through cation and anion doping. We have examined the hole-mediated photodecomposition of trimethyl acetate (TMA) as a probe for the visible-light photoactivity of nitrogen-doped rutile and anatase TiO₂ materials. Well-characterized films of N-doped TiO₂ were grown using molecular beam epitaxy (MBE), with photochemical studies undertaken in the same vacuum system. Previous work¹ has demonstrated that N doping (< 2% level) of anatase TiO₂(001) results in visible light photodecomposition of TMA at the same per-photon rate as seen with UV light, but that comparable levels of N-doping in rutile TiO₂(110) do not result in detectable levels of photochemistry. This behavior in anatase is tentatively ascribed to greater hole ‘detrapping’ rates than in rutile.

More recent work has shown that the absence of visible-light activity in N-doped rutile TiO₂ is independent of the orientation of the surface plane for the three main crystallographic terminations of this material (i.e., (100), (110) and (001)).² However, the UV-induced photochemistry of TMA shows strong orientational dependence in N-doped rutile. Fig. 1 shows rate constant data for photodecomposition

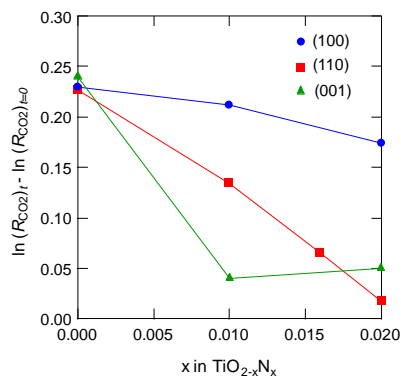


Fig. 1: UV photodecomposition rates of TMA as a function of N-doping.

of comparable coverages of TMA on three rutile surfaces as a function of N-doping level. The rates for all three surfaces were similar in the absence of N doping, but the activities in the (110) and (001) cases decreased relative to that in the (100) case as a function of N-doping. Using channeling measurements, we show that this difference in the photoactivity of N-doped rutile TiO₂(100) is due to a difference of the N-dopant location in the rutile lattice.

We have also begun preparing samples of Fe-doped and N+Fe co-doped rutile TiO₂(110) films. For Fe alone, X-ray photoemission spectroscopy (XPS) shows that Fe³⁺ species dominate at concentrations of 0.5-2 at%. However, analysis by XPS at low take-off angles indicates that the Fe is strongly segregated at the surface of the films, even after capping the doped region with ~200 Å of pure rutile. In contrast, films of Fe and N co-doped rutile TiO₂(110) showed little or no Fe segregation. Studies are ongoing with XANES, EXAFS and NRA to examine the oxidation state and local environment of the Fe species. UV-VIS analysis and photochemistry will explore the optical properties and photoactivities of these films.

1. T. Ohsawa et al., **Phys. Rev. B** 79 (2009) 085401; **J. Phys. Chem. C** 112 (2008) 20050.
2. T. Ohsawa, et al. **J. Phys. Chem. C** 104 (2010) 6595.

Highly Reducing Porphyrin/Metal-Alkylidyne Dyads

Benjamin M. Lovaasen, Daniel C. O'Hanlon, Davis Moravec, and Michael D. Hopkins

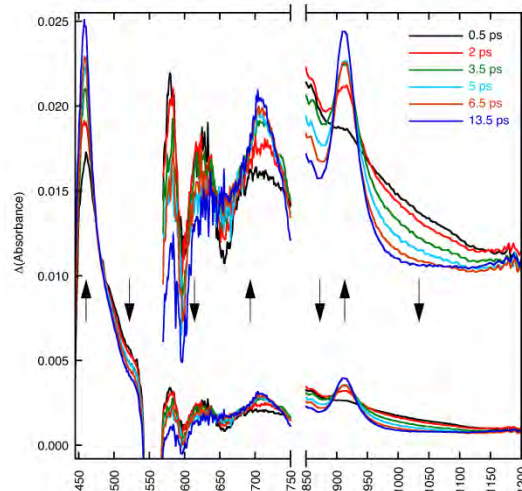
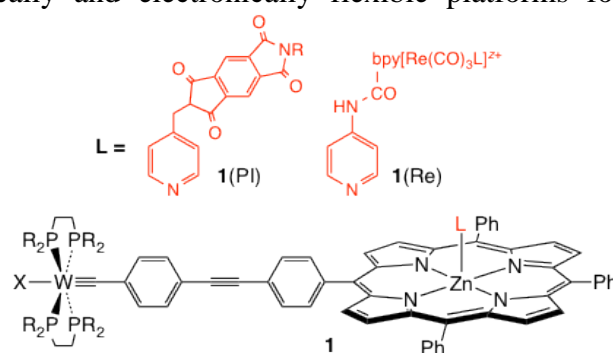
Department of Chemistry
The University of Chicago
Chicago, Illinois 60637

Metal-alkylidyne compounds possess desirable properties relevant to the artificial photosynthetic conversion of CO₂ to solar fuels: they have highly reducing excited states; can be incorporated into π -conjugated molecular wires that control electron transfer; and participate in proton-coupled electron-transfer reactions that eliminate the need for conventional sacrificial donors. We have focused our attention on porphyrin/metal-alkylidyne dyads and assemblies, typified by **1**, because they provide synthetically and electronically flexible platforms for applying these properties to photosensitized CO₂ reduction.

Our most recent work on porphyrin/alkylidyne assemblies has centered on understanding their energy-transfer and electron-transfer processes and kinetics. In nonpolar solvents, **1** and Zn-ligated derivatives **1L** with non-redox-active L ligands (e.g., L = substituted pyridines) exhibit phosphorescence from the ³(d_{xy}← π^* (WCR))

state, the lifetimes of which are 20–1300 \times longer than for free WCR due to an excited-state equilibrium between the emissive state and the nonluminescent Zn(TPP) T₁ state. Recent visible/near-IR transient-absorption spectroscopic studies of **1** and **1**(py) demonstrate that energy transfer proceeds from the initially formed Zn(TPP) S₁ state to the phosphorescent WCR state via the Zn(TPP) T₁ state, with S₁→T₁ intersystem crossing rates that are 10³ times faster than in free Zn(TPP). In more polar solvents (THF, CH₂Cl₂), in contrast, WCR phosphorescence and Zn(TPP) fluorescence of **1** are completely quenched and Zn(TPP) S₁ excitation rapidly ($\tau < 5$ ps) produces the strongly reducing [Zn(TPP)]⁻—[W]⁺ charge-separated state, which decays with a lifetime of 425 ps. This is an unusual example of a Zn(TPP) assembly in which the porphyrin functions as the primary electron acceptor. The charge-recombination lifetime for **1** greatly exceeds those found for other such assemblies (< 25 ps).

The reduced porphyrin in the [Zn(TPP)]⁻—[W]⁺ charge-separated state of **1** can be oxidized by an appended electron acceptor. Recent transient-absorption spectra of **1**(PI) in CH₂Cl₂ demonstrate that Zn(TPP) S₁ excitation rapidly produces [PI]⁻—Zn(TPP)—[W]⁺, which possesses a lifetime in the range of a few nanoseconds. The triad **1**(Re), containing the CO₂ reduction-catalyst precursor [Re(bpy)(CO)₃L]⁺, has been prepared and is expected to operate similarly; this triad is currently under study.



Ultrafast Transient Absorption Microscopy Studies of Carrier Dynamics in Epitaxial Graphene

Libai Huang¹, Gregory V. Hartland², Li-Qiang Chu³, Luxmi⁴, Randall M. Feenstra⁴, Chuanxin Lian⁵, Kristof Tahy⁵, Huili Xing⁵

¹Notre Dame Radiation Laboratory, ²Department of Chemistry and Biochemistry, ³Department of Chemical and Biomolecular Engineering, ⁵Department of Electrical Engineering, University of Notre Dame, Notre Dame, IN 46556-5670, and ⁴Department of Physics, Carnegie Mellon University, Pittsburg, PA 15213

Energy exchange between the electrons and phonons is particularly important to electron transport, and understanding this process will be vital for the realization of future graphene-based electronics. Epitaxial growth is a promising approach for practical applications, as it has the ability to prepare graphene on a large scale and supported on a substrate. However, epitaxially grown graphene is highly inhomogeneous, with variations in the sample thickness occurring over length scale of a few micrometers. It is also not clear how substrate interactions affect the carrier dynamics. Here we present transient absorption microscopy as a novel tool to characterize graphene, and to interrogate the charge carrier dynamics. This technique has the ability to directly image carrier dynamics with a diffraction-limited spatial resolution and a time resolution of ~ 200 fs. The intensity of the transient absorption signal is shown to correlate with the number of graphene layers. The carrier cooling exhibits a bi-exponential decay, consisting of an instrument-response limited fast decay time τ_1 (< 0.2 ps) and a slower decay time τ_2 . The value of τ_2 was found to increase with increasing pump fluence. The fast decay is assigned to coupling between the electrons and optical phonons in graphene, and the slower decay is attributed to the hot phonon effect. At high pump intensities the slow decay reaches a limiting value, which is assigned to the relaxation time of the optical phonons. The contribution of the slow component to the overall decay was found to vary with spatial position in the sample. This is attributed to differences in coupling between the graphene and the substrate. Transient absorption images at different delay times reveal variation in optical phonon lifetime that was not related to graphene thickness. These results point to transient absorption microscopy as a potentially important tool for characterizing the electrical conductivity of graphene through measurement of the lifetime of optical phonon modes excited by charge carrier relaxation.

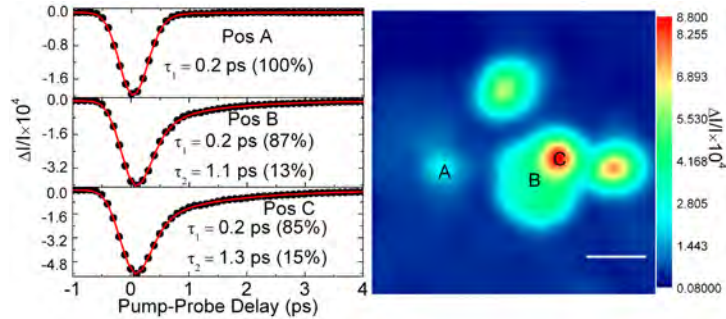


Figure 1. Transient absorption traces recorded at three different positions as marked in the right image. Transient absorption traces were fitted with a bi-exponential decay convoluted with a Gaussian response function. Experimental data are black filled circles and fits are red solid lines. Scale bar in the right image is $1 \mu\text{m}$.

Uncommon Approaches to Investigating Water Oxidation Catalysis

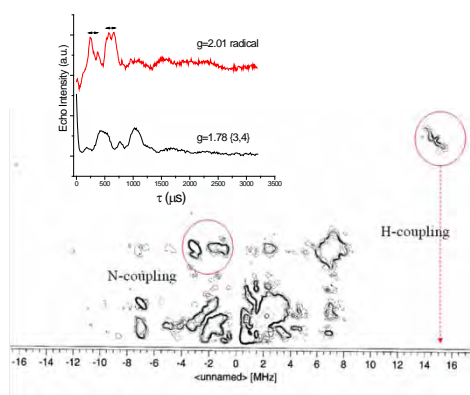
Jamie Stull,* Sergei V. Lymar,[†] Aurora Clark, James K. Hurst

Chemistry Department
Washington State University
Pullman, WA 99164-4630

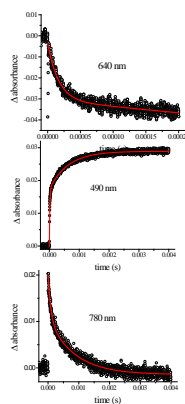
The “blue dimer”, i.e., $\text{cis,cis-}[\text{Ru}^{\text{III}}(\text{bpy})_2(\text{OH}_2)]_2\text{O}^{4+}$ (hereafter denoted **{3,3}**), undergoes $4e^-$ oxidation to generate the catalytically active form (**{5,5}**), in which the aqua ligands are fully deprotonated to ruthenyl oxo atoms. ^{18}O -isotope labeling studies define two major pathways in which O-O bond formation occurs either (1) between the coordinated oxo atom and a solvent molecule or (2) between two solvent molecules. Experimental and computational studies suggest that pathway (1) involves concerted addition of H_2O across the $(\text{Ru}^{\text{V}}=\text{O})_2\text{O}$ core in **{5,5}** via homolytic cleavage of the H-OH bond to give a $\text{Ru}^{\text{IV}}(\text{OOH})\text{-O-Ru}^{\text{IV}}(\text{OH})$ intermediate, which then decomposes to the final products. We have proposed that the highly unusual pathway (2) is initiated by a homolytic cleavage similar to pathway (1), but with the OH fragment adding to a bipyridine ligand. This radical intermediate then undergoes a set of hydrolytic and internal redox steps leading ultimately to O_2 formation from two solvent molecules. Consistent with this mechanism, we have observed anomalous signals suggestive of a ligand radical species in the cryogenic EPR spectra of **{5,5}**, and near-IR optical absorption bands suggestive of bpy-OH adducts in a photocatalytic system. Decay of both these signals occurs with the same rate constant as O_2 evolution.

Ongoing pulsed EPR studies have provided ENDOR and ESEEM evidence of electron-proton coupling within the **{5,5}** signal, which is not seen in the other paramagnetic states of the catalyst (e.g., **{3,4}**). A comparison of the 1D-ESEEM spectra for **{3,4}** and **{5,5}** is given in panel a of the accompanying figure, with a HYSCORE plot that identifies both the N- and H-couplings in **{5,5}**. Transient spectra obtained from pulse radiolysis studies indicate that, rather than undergoing simple electron transfer, OH^\bullet adds to the bipyridine ring in **{3,3}** and **{3,4}** (panel b), and DFT calculations on a hypothetical monomeric model of the catalytic site, i.e., $(\text{NH}_3)_3(\text{bpy})\text{Ru}^{\text{V}}=\text{O}^{3+}$, indicate that addition of H_2O to the ring to form $(\text{NH}_3)_3(\text{bpy-OH}^\bullet)\text{Ru}^{\text{IV}}\text{-OH}^{3+}$ is thermodynamically feasible and gives rise to a predicted EPR signal very similar to the one observed for **{5,5}** (panel c). When completed, these studies should allow rigorous evaluation of the potential role of N-heterocyclic ligands in catalysis.

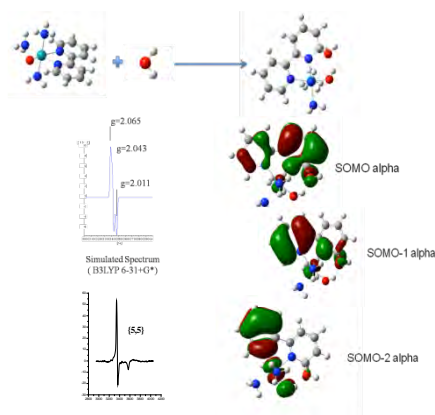
panel a:



panel b: $\{3,3\} + \text{OH}^\bullet \rightarrow \{3,4\text{-OH}\} \rightarrow \text{P}$



panel c:



Directed Charge and Energy Transfer in Semiconductor Nanocrystals and Heterostructures

E. Ryan Smith, Barbara Hughes, Matt Beard, Arthur Nozik, Justin Johnson
National Renewable Energy Laboratory
1617 Cole Blvd, Golden, CO 80401

Improved synthetic control over the shape, size, composition, and quality of semiconductor nanocrystals (NC) samples has provided a wealth of new structures with unique properties. In many cases the impetus for a particular type of structure is to direct energy or charge transfer through the production of type I or type II energy level schemes. The photophysical and photochemical implications of these new samples for light harvesting are often discussed but not well understood. We have applied two complementary techniques, polarization anisotropy (PA) and cross-polarized transient grating (CPTG), to investigate the time scales and yields of energy and charge transfer in CdSe and PbSe nanostructured systems.

Polarization anisotropy, applied in a time-resolved fashion in either emission or absorption, uncovers the transition dipole moment directions of absorption and emission as a function of time. At type II interfaces, transitions can initially exist as isolated in either compound or as a charge-transfer (CT) transition across the interface (i.e., a so-called indirect transition). The anisotropy is a probe of when CT occurs and the evolution of the CT with time, including the change in the dipole moment. CPTG has been utilized as an ultrafast probe of spin flipping in CdSe and lead chalcogenide systems,¹ and has two primary functions: (1) to uncover the exciton fine structure within the inhomogeneously broadened absorptions, and (2) to measure the degree of exciton delocalization. The CPTG signal decay is largely dictated by the exchange interaction, which is a unique probe of electron-hole overlap and thus quantization effects.

In CdSe/CdS heterostructures in solution, the PA emission signal begins at a finite value (0.1) before decreasing on a μs time scale likely due to rotational diffusion (Figure 1a). Other CdSe structures exhibit much smaller anisotropy due to the lack of asymmetry in the composition of contributing excited states. In PbS capped with oleic acid, we discover a size-dependent decay of the CPTG signal (Figure 1b), which is expected from the strong quantum confinement of the electrons and holes. We are currently investigating different shapes of including rods and “dimers,” as well as heterostructures with PbSe and CdSe. Emission largely dominated by surface traps is also observed, which has additional influence over the polarization dependent signals.

¹Johnson, J.C. et al, *Nano Letters*, **2008**, 8, 1374.

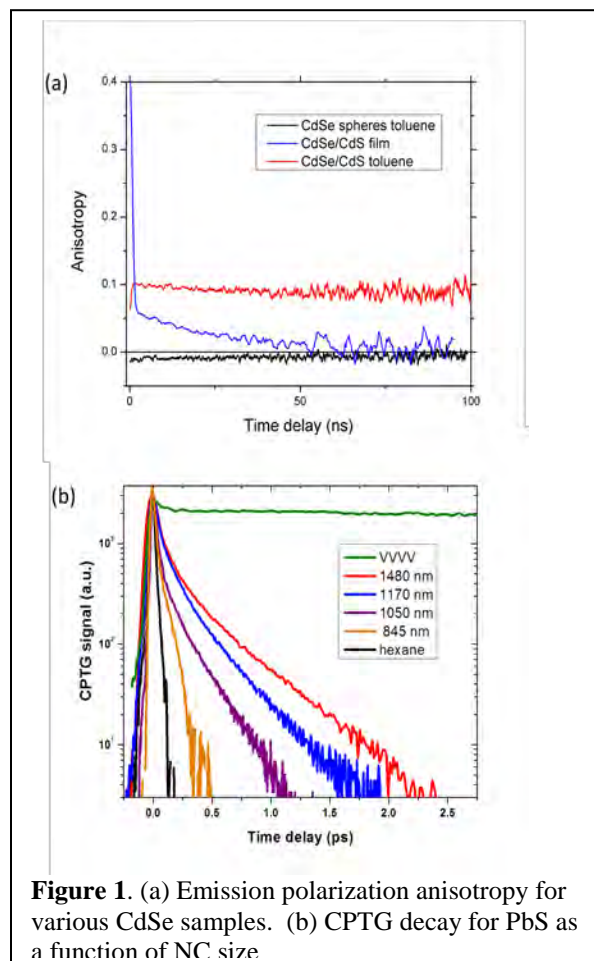


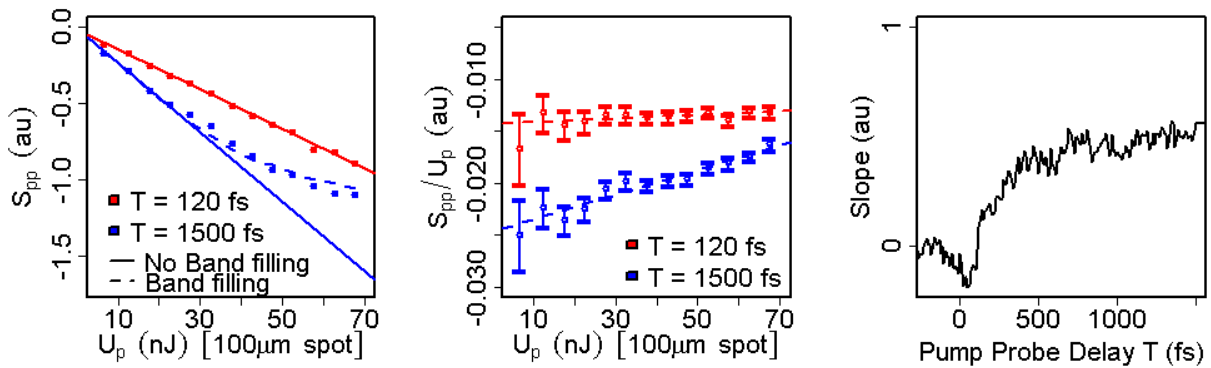
Figure 1. (a) Emission polarization anisotropy for various CdSe samples. (b) CPTG decay for PbS as a function of NC size.

Band Filling Dynamics in Lead Sulfide Quantum Dots

Byungmoon Cho, William K. Peters, Trevor L. Courtney, Robert J. Hill, and David M. Jonas
 Department of Chemistry and Biochemistry
 University of Colorado
 Boulder, Colorado 80309-0215

As a potential route to more efficient solar light harvesting, carrier multiplication has received considerable attention since kinetic signatures of Auger recombination were reported after high energy single photon excitation of semiconductor nanocrystals. At least three mechanisms have been proposed, and there are significant experimental disagreements about the Multiple Exciton Generation (MEG) yield. As there is no theoretical explanation for the observed size scaling of Auger recombination, the reverse process of MEG, something important about the mechanism of this apparent 3 body reaction (and its reverse, MEG) may be missing from the theory.

We have carried out new experiments that probe the timescale for band filling. In lead sulfide (PbS) quantum dots, the band edges (LUMO electrons and HOMO hole vacancies) are 8-fold degenerate. In experiments where a single dot can absorb 9 or more photons, the band edge reaches maximum occupancy after carrier cooling so that some carriers must remain in higher energy levels. Based on modeling of Auger measurements, Sargent and co-workers suggested these excess carriers stop contributing to the pump probe signal (S_{pp}), leading to a signal that is weaker than proportionality to the number of electron-hole pairs would suggest. S_{pp} is proportional to the pump pulse energy (U_p) when the probe immediately follows the pump at pump-probe delay $T = 120$ fs, but loses this proportionality by 1.5 ps (left panel). We assess band filling progress through the slope of (S_{pp}/U_p) vs. U_p (middle panel) up to excitation probabilities such that S_{pp} is reduced over 20% by band filling. From slope vs. T , we have first resolved the ~ 225 fs timescale of band filling in dots as an exponential rise (right panel).



This band filling timescale is very close to that on which the pump-probe signal reaches its maximum strength, which has been attributed to development of a nanocrystal Stark effect. This implies that carrier cooling is complete on the same 225 fs timescale as the Stark effect and that band filling occurs during carrier cooling or is rate-limited by carrier cooling. The mechanism of band filling is not known, but it could proceed via Auger recombination involving hot exciton configurations such as $(\text{HOMO}-1)^{-1}(\text{HOMO})^{-8}(\text{LUMO})^8(\text{LUMO}+1)^{+1}$. If so, this would indicate that Auger recombination from hot configurations is over 500 times faster than at the band edge.

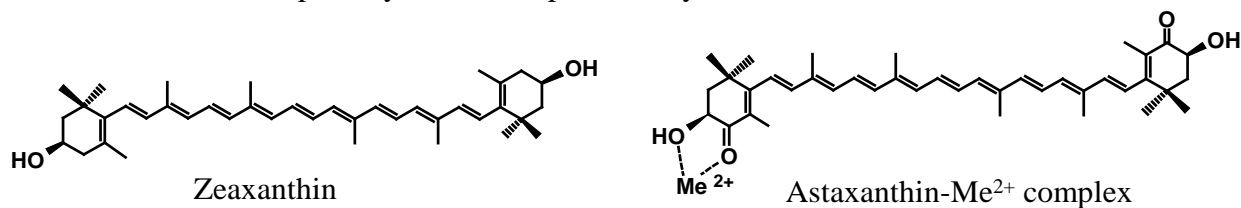
The Carotenoid Astaxanthin and its Photooxidative Role Under High Light and Salt Stress

Lowell D. Kispert, A. Ligia Focsan, Nikolay E. Polyakov, Péter Molnár,

Department of Chemistry, The University of Alabama, Tuscaloosa, AL 35487-0336 US, Inst. of Chemical Kinetics & Combustion, Institutskaya Str. 3, 630090, Novosibirsk, Russia Department of Pharmacognosy, University of Pécs, H-7624 Pécs, Rókus u. 2, Pécs, Hungary,

Carotenoids are a class of pigments wide spread in nature, which also serve as antennas, photoprotective devices and intermediate electron carriers in photosynthetic reaction centers. Recently zeaxanthin has been shown to form charge transfer complex (radical cation) in the presence of strong light and converts to violaxanthin in low light. We have also shown that proton lost from the radical cation ($\text{Car}^{\bullet+}$) forms a neutral radical ($\# \text{Car}^{\bullet}$) which can also quench the excited state of bacteriochlorophyll. We have extended our study to astaxanthin - a carotenoid similar to zeaxanthin except for the addition of a keto group to both ends of the OH substituted cyclohexene rings. We have shown that photo-oxidation of astaxanthin on silica-alumina produces also a mixture of radicals, namely radical cations and neutral radicals formed as a result of proton loss. The identities of the radicals were confirmed through the determination of Mims ENDOR spectra and comparison with density functional theory calculations. Besides losing protons from the methyl positions, astaxanthin can lose its proton at the 3(3') position giving rise to a neutral radical lower in energy. Furthermore, deprotonation of the OH group might form a radical anion allowing complexation with metals.

The accumulation of astaxanthin in some unicellular green algae is generally thought to be a survival strategy of the algae under photooxidative and salt stress. Algae has the ability to synthesize and accumulate about twice the astaxanthin content under high light, or under high light in the presence of excess of ferrous ions (Steinbrenner, J.; Linden, H. *Plant Physiol.* **2001**, *125*, 810-817). Though some photoprotective mechanisms have been suggested, the function of astaxanthin in photosynthetic center is still questioned. We have shown that the ability of carotenoids to scavenge peroxy radicals increases significantly with increase of the redox potential. The high antioxidant activity of astaxanthin may result from its higher reduction potential among the carotenoids we have studied earlier. Another feature of astaxanthin is the presence of two oxygen atoms in the cyclohexene ring. It is known that such compounds are able to form stable complexes with divalent metal ions. In the present study astaxanthin- Me^{2+} complexes (Me = Ca, Zn and Fe) were investigated in detail by different techniques (UV-Vis, NMR, EPR, IR and MS-spectroscopy). The ability of astaxanthin to form complexes with metal ions can increase the efficiency of photoinduced electron transfer from carotenoid to metal atom in artificial solar cells, photosynthetic and photocatalytic devices.



Photodriven Water Oxidation by New Carbon-Free Molecular Catalysts

Qiushi Yin, Yurii V. Geletii, Guibo Zhu, Claire Besson, Yu Hou, Zhuangqun Huang, Tianquan Lian, Djamaladdin G. Musaev and Craig L. Hill

*Department of Chemistry and Cherry L. Emerson Center for Scientific Computation,
Emory University, Atlanta, Georgia 30322*

A current key focus of our ongoing solar photochemistry work is to investigate photodriven oxidation of H₂O to O₂ catalyzed by our carbon-free, stable, molecular, water oxidation catalysts (WOCs). We first sought to assess the impact of WOC ground state potential on the rates, yields and quantum yields for O₂ production from water. Toward this end we achieved the synthesis of {[Ru₄O₄(OH)₂(H₂O)₄](γ -PW₁₀O₃₆)₂}⁸⁻ (**2**), the isostructural analogue of our thoroughly characterized initial WOC, the silicon based complex {[Ru₄O₄(OH)₂(H₂O)₄](γ -SiW₁₀O₃₆)₂}¹⁰⁻ (**1**) but with P(V) replacing Si(IV) in the polytungstate ligands.¹ This substitution reduces the charge on the catalyst by two units which makes the potentials for **2** more positive than those for **1**. The new catalyst, **2**, efficiently catalyzes visible-light-driven water oxidation using [Ru(bpy)₃]²⁺, as a photosensitizer, and persulfate, [S₂O₈]²⁻, as a sacrificial electron acceptor but the rates and overall yields of O₂ are 30% lower than **1**, consistent with the O₂ producing step being rate limiting.

We also sought to determine if light-driven water oxidation could be achieved by our recently reported tetra-cobalt polyoxometalate WOC, which is the fastest homogeneous WOC reported to date. The long-established [Ru(bpy)₃]²⁺-visible light-persulfate system does efficiently result in catalytic water oxidation (see Figure 1). The relative rates of the elementary processes and other features of the mechanism are under investigation.

Synthesis of a Mn₄O₄ unit stabilized by polytungstate ligands has been achieved and its water oxidation activity is under investigation.²

Central to sustained photodriven catalytic water oxidation is the stability of all components under irradiation and catalytic conditions. Our kinetic studies find that photodegradation of the Ru(polypyridine) sensitizers limits overall turnover (TON) in these systems, thus we are studying these photodegradation processes.

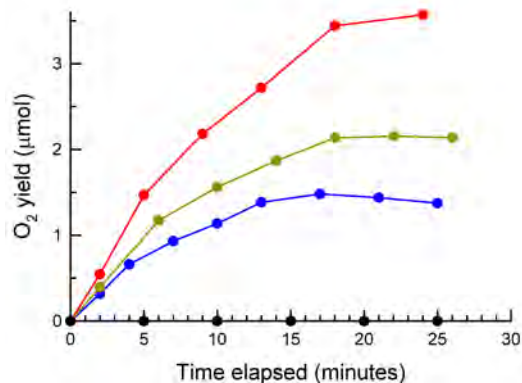


Figure. O₂ evolution using 1 mM [Ru(bpy)₃]²⁺ (photosensitizer), and 0.0032 mM (red), 0.00128 mM (yellow-green), and 0.000512 mM tetra-cobalt WOC, **2** (pH 8 Na phosphate buffer with 2.5 mM sodium persulfate).

References

- (1) Besson, C.; Huang, Z.; Geletii, Y. V.; Lense, S.; Hardcastle, K. I.; Musaev, D. G.; Lian, T.; Proust, A.; Hill, C. L. *Chem. Commun.*, **2010**, 46, 2784–2786.
- (2) Fang, X.; Speldrich, M.; Schilder, H.; Cao, R.; O'Halloran, K.; Hill, C. L.; Kögerler, P. *Chem. Commun.* **2010**, 46, 2760–2762.

Single-Walled Carbon Nanotube Photophysics

Xiaoyong Wang, Andrea J. Lee, Lisa J. Carlson, Julie A. Smyder, and Todd D. Krauss
Department of Chemistry
University of Rochester
Rochester, NY 14627-0216

Single-walled carbon nanotubes (SWNTs) are tubular graphitic molecules with high aspect ratios and exceptional electronic and optical properties, such as the ability to be either metallic or semiconducting depending on their molecular structure. Single semiconducting SWNTs display remarkably stable and size-tunable photoluminescence at near-infrared (NIR) wavelengths, making them fundamentally interesting and technologically relevant materials. However, individual SWNTs have a photoluminescence (PL) quantum yield (QY) of about 1%, much less than other NIR emitting nanomaterials such as semiconductor quantum dots. It is currently not understood whether the poor QY of SWNTs is an intrinsic property or the result of extrinsic quenching mechanisms indicative of non-optimal sample quality.

We will discuss that the addition of reducing agents to an aqueous solution of SWNTs results in an enormous enhancement of the QY for individual SWNTs to unprecedented values of ~30% (Figure 1). These unexpectedly high QY values indicate that SWNTs are intrinsically bright emitters, and that current understanding of the optical properties of SWNTs has largely been obtained from defective SWNTs having their PL partially quenched. The availability of a bright and steady source of NIR photons will greatly facilitate the development of new technology in several fields including biological imaging and optoelectronics. To that end, we will also present studies of multiple electron-hole pair generation (MEG) in isolated SWNTs using ultrafast transient absorption (TA) spectroscopy. Absorption of single photons with energies corresponding to three times the SWNT energy gap ($\hbar\omega = 3E_g$) results in an electron-hole pair generation efficiency of 130% per photon. Our results suggest that the multiple electron-hole pair generation threshold in SWNTs can be close to the limit defined by energy conservation ($\hbar\omega = 2E_g$), which is highly relevant to the potential of MEG as a viable route to enhancing the efficiency of solar cells.

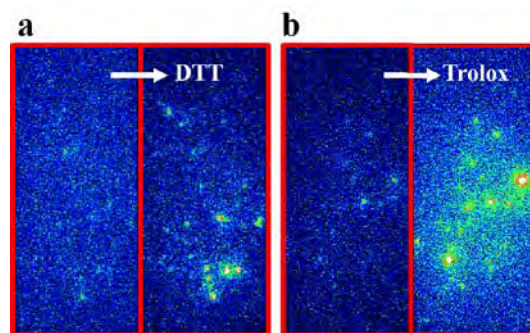


Figure 1. Fluorescence images of individual SWNTs before and after adding a) Dithiothreitol (DTT) and b) Trolox. The horizontal dimension for each fluorescence image is ~20 μm .

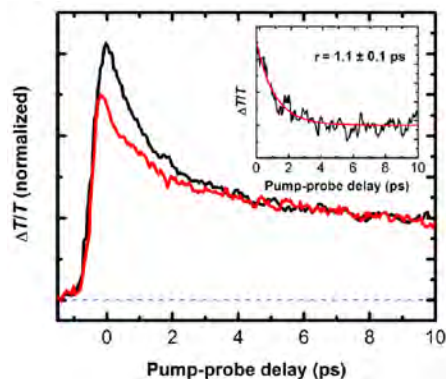


Figure 1. (a) TA spectra measured under 800 nm (red) and 335 nm (black) excitation at low pump fluence where the average number of electron-hole pairs per SWNT $N_0 \approx 0.25$. Spectra are normalized at late decay times. Inset shows the difference between the two curves indicating the presence of MEG at 335 nm.

Interfacial Charge Separation and Recombination Dynamics in Nanoparticle-Sensitizer-Water Oxidation Catalyst Triads

Zhuangqun Huang, Quishi Yin, Zhen Luo, Jie Song, Yurii V. Geletii, Karl S. Hagen, Djamaladdin G. Musaev, Craig L. Hill, Tianquan Lian

Department of Chemistry and Emerson Center of Scientific Computing
Emory University
Atlanta, GA 30322

In the previous funding period, we demonstrated a photo-driven water oxidation system based on all-inorganic molecular (soluble) catalysts for H₂O oxidation, [$\{\text{Ru}_4\text{O}_4(\text{OH})_2(\text{H}_2\text{O})_4\}(\gamma\text{-SiW}_{10}\text{O}_{36})_2\}^{10-}$ (or Ru-POM), Ru(bpy)₃ sensitizers, and sacrificial electron acceptors.¹ In this presentation, we report the performance of the catalysts in a photoelectrochemical cell that split water into H₂ and O₂ with sun light (without sacrificial electron acceptor). In the photoelectron-chemical cell, protons are reduced to form H₂ in the Pt cathode. The photoanode consists of nanoporous oxide - sensitizer- catalyst triads or colored oxide-catalyst dyads, in which photo-illumination of the dyads or triads lead to the oxidation of water to form O₂ and H⁺. The performances of various catalysts/sensitizer/oxide assemblies are characterized by measuring the photocurrent of the cell. To gain insight into the difference in their performance, we have carried out transient absorption study of interfacial charge separation and recombination dynamics in these dyads and triads.

1) TiO₂-Ru(dpbpy)(bpy)₂-Ru(POM) triads: In this triad, the excitation of the sensitizer [Ru(dpbpy)(bpy)₂] lead to ultrafast charge transfer to TiO₂. This process is monitored by transient absorption in the visible and mid-IR. The oxidized sensitizer can then oxidize the Ru(POM) catalyst. The rates of the electron injection and catalyst oxidation processes are studied as a function of the sensitizer and the catalyst as well as the solution pH. The understanding of these processes will also be guided by studies of the same systems using recently developed computational method.²

2) Fe₂O₃-RuPOM dyads: In an effort to construct all inorganic systems for photo-catalytic oxidation of water, we have started to examine the use of low band-gap oxide nanoparticles as light harvesting photoanode. We showed that with addition of the catalysts, the photocurrent is greatly enhanced. The incident-photon-current-conversion efficiency exceeds 35% at an external bias of 1.4 V. Ongoing studies are examining the dynamics of electron-hole recombination and hole capture by the catalysts in the Fe₂O₃-RuPOM dyads.

References:

[1] Geletii, Y. V.; Huang, Z. Q.; Hou, Y.; Musaev, D. G.; Lian, T. Q.; Hill, C. L. *J. Am. Chem. Soc.*, **2009**, *131*, 7522-7523. [2] Kaledin, A. L.; Huang, Z.; Lian, T.; Geletii, Y. V.; Hill, C. L.; Musaev, D. G. *J. Phys. Chem. A*, **2010**, *114*(1), pp 73-80.

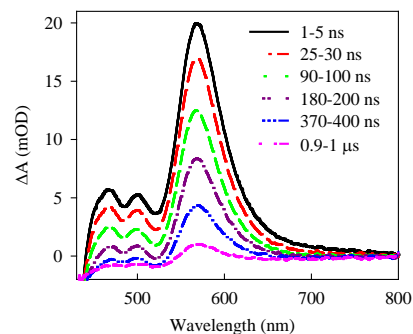
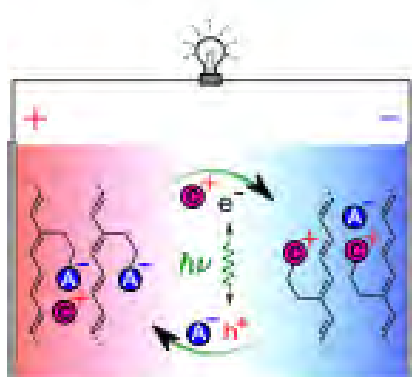


Fig. 1. Transient absorption spectra of $\alpha\text{-Fe}_2\text{O}_3$ after 400 nm excitation.

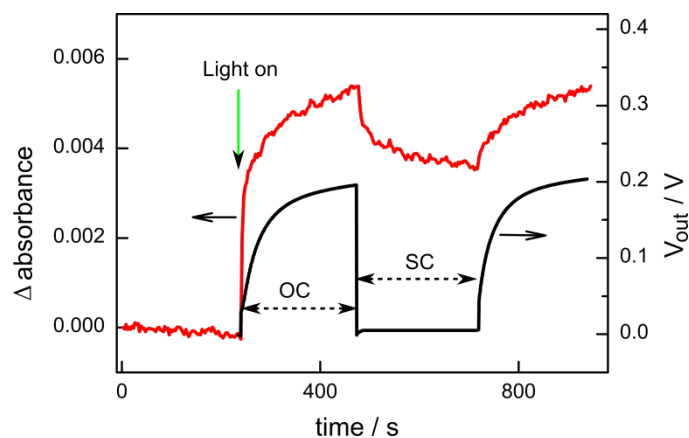
Photochemical Doping of Conjugated Ionomer Interfaces

Stephen Robinson, Fuding Lin, Ethan Walker, and Mark Lonergan
Department of Chemistry
University of Oregon
Eugene, OR 97403

We present studies on the photochemical doping and photovoltaic effect at organic semiconductor interfaces characterized by an asymmetry in ionic carriers rather than the more traditional asymmetry in electronic carriers or frontier orbitals. An example of such a system is shown in Figure 1A; it is based on ionically functionalized polyacetylenes (polyacetylene ionomers). Ion exchange driven by the asymmetry in mobile ion content is hypothesized to lead to a built-in electric field that can drive the initial separation of photogenerated charge carriers. We further hypothesize that the motion of photogenerated charge carriers is accompanied by the migration of ions leading to photochemical doping and the formation of a p-n junction: anions and holes move into the anionomer to p-dope it, and cations and electrons move into the cationomer to n-dope it (Figure 1A). Evidence for the photochemical doping process comes from transient absorption measurements at 1300nm that follow the absorbance of the mid-gap state created by doping (Figure 1B), and the time dependence of the open-circuit voltage and short-circuit current density. The doping level is theorized to change adaptively as needed to support the photovoltaic effect, and a model is presented for the maximum open-circuit potential that can be achieved based on the Fermi level difference developed by the photochemical doping process. The model predicts a stronger dependence of the V_{oc} on illumination level than for a more traditional p-n junction, and that the maximum V_{oc} obtainable depends strongly on the ion concentration. The analysis of the photoresponse to place limits on the built-in potential created by the ionic asymmetry is also discussed.



A.



B.

Figure 1. (A) Schematic of the photochemical doping of the interface between anion-conducting and cation-conducting mixed electronic/ionic conductors based on polyacetylene ionomers. (B) Change in absorbance at 1305nm (red) and potential (black) resulting from illumination at 532nm with a power of 30mW under open-circuit (oc) and short-circuit (sc) conditions.

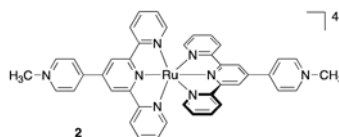
Computational and experimental insights into photoinduced oxidation of $[\text{Ru}(\text{mptpy})_2]^{4+}$ and $[\text{Ru}(\text{bpy})_3]^{2+}$ photosensitizers

Alexey Kaledin, Yurii V. Geletii, Zhuangqun Huang, Tianquan Lian, Craig L. Hill, and Djamaladdin G. Musaev

Department of Chemistry and Cherry L. Emerson Center for Scientific Computation, Emory University, Atlanta, Georgia 30322

Recently, we have shown that the carbon-free, stable, molecular, $\{[\text{Ru}_4\text{O}_4(\text{OH})_2(\text{H}_2\text{O})_4](\gamma\text{-SiW}_{10}\text{O}_{36})_2\}^{10-}$ (1) catalyst efficiently catalyzes visible-light-driven water oxidation using $[\text{Ru}(\text{bpy})_3]^{2+}$, as a photosensitizer, and persulfate, $[\text{S}_2\text{O}_8]^{2-}$, as a sacrificial electron acceptor [1]. However, the $[\text{Ru}(\text{bpy})_3]^{2+}$ sensitizer has a relatively narrow absorption window and is not oxidatively stable under the photocatalytic conditions. Therefore, one way to improve the performance of this homogeneous visible-light driven artificial photosynthetic system is to replace the $[\text{Ru}(\text{bpy})_3]^{2+}$ with a better light absorber. One candidate class of dyes is $[\text{Ru}(\text{mptpy})_2]^{4+}$, (2), where $\text{mptpy} = 4'(4\text{-methylpyridinio})\text{-}2,2':6,2''\text{-terpyridine}$.

We investigated the electron transfer mechanism between a single electron donor $[\text{Ru}(\text{mptpy})_2]^{4+}$ and one (complexation scheme 1:1) or two (complexation scheme 1:2) persulfate molecules, $[\text{S}_2\text{O}_8]^{2-}$, acting as electron acceptors, in both water and acetonitrile [2]. In these studies we used integrated computational (density functional and exciton interaction theories) and experimental (transient absorption, static and time-resolved fluorescence spectroscopy and other) techniques.



The goals of our studies were: (1) to study the excited state properties of $[\text{Ru}(\text{mptpy})_2]^{4+}$ and electron transfer dynamics in 1:1 and 1:2 complexes; (2) to compare the results for $[\text{Ru}(\text{mptpy})_2]^{4+}$ with those recently reported [3] for $[\text{Ru}(\text{bpy})_3]^{2+}$; and (3) to extend the less-demanding and more insightful transition charge density model (TCDM) approach.

It was found that the excitation energy of $[\text{Ru}(\text{mptpy})_2]^{4+}$ is about 0.4-0.5 eV smaller than that of $[\text{Ru}(\text{bpy})_3]^{2+}$, which is consistent with the measured absorption maxima of 445 nm and 507 nm, for $[\text{Ru}(\text{bpy})_3]^{2+}$ and $[\text{Ru}(\text{mptpy})_2]^{4+}$, respectively. The smaller excitation energy in $[\text{Ru}(\text{mptpy})_2]^{4+}$ correlates with much slower electron transfer rates to persulfate compared to $[\text{Ru}(\text{bpy})_3]^{2+}$. The quenching of the photoexcited $[\text{Ru}(\text{mptpy})_2]^{4+}$ by $[\text{S}_2\text{O}_8]^{2-}$ occurs via an unimolecular mechanism with formation of a weak ion-pair complex $\{[\text{Ru}(\text{mptpy})_2]^{4+} \cdots ([\text{S}_2\text{O}_8]^{2-})_n\}$, where $n = 1$ and 2 . The calculated(measured) electron transfer lifetimes in water are $1/\kappa_1 = 199.4$ (298) ns and $1/\kappa_2 = 108.4$ (149) ns, for the 1:1 and 1:2 complexes, respectively. The effect of solvent polarity on electron transfer rates is found to be significant: the less polar acetonitrile slows the rate by an order of magnitude compared to water.

References:

- [1] Geletii, Y. V.; Huang, Z. Q.; Hou, Y.; Musaev, D. G.; Lian, T. Q.; Hill, C. L. *J. Am. Chem. Soc.*, **2009**, *131*, 7522-7523
- [2] Kaledin, A. L.; Huang, Z.; Yin, Q.; Dunphy, E. L.; Constable, E. C.; Housecroft, C. E.; Geletii, Y. V.; Lian, T.; Hill, C. L.; Musaev, D. G. *J. Phys. Chem. A*, **2010**, *in press*
- [3] Kaledin, A. L.; Huang, Z.; Lian, T.; Geletii, Y. V.; Hill, C. L.; Musaev, D. G. *J. Phys. Chem. A*, **2010**, *114*(1), pp 73-80.

Heterometallic Solids for Solar Photoconversion

Paul A. Maggard

Department of Chemistry
North Carolina State University
Raleigh, NC 27695-8204

Atomic and particle-level modulations of advanced metal-oxides and -oxides/organics (e.g., $MM'OL$; M/M' = transition metals with d^0 and d^{10} electron configurations; L = coordinating ligand) have been investigated for use in driving photocatalytic reactions, such as most notably the water-splitting reactions to produce H_2 and/or O_2 . Our results show that new heterometallic solids containing a combination of d^0/d^{10} electron configurations (e.g., $Cu(I)/Nb(V)$) represent an effective approach to achieving visible-light bandgap sizes with favorable band energies stemming from metal-to-metal transitions. Significant research progress has been made in two main areas: 1) The incorporation of structure-directing ligands into heterometallic oxides, and 2) the use of flux reactions for tuning particle sizes and compositions.

Using hydrothermal synthetic methods, more than fifteen different ligands have been incorporated into numerous (>30) hybrid structures in the M/M' ($M = Cu, Ag$; $M' = V, Nb, Re$) systems and that demonstrate the impact of the $M-ReO_4$ connectivities and the M coordination environments on their bandgap sizes ($\sim 2.1 - 3.9$ eV), valence-band energies, and absorption coefficients. In the Ag/Re and Cu/Re systems, for example, hybrid structures containing from isolated clusters to extended networks have been found. In parallel, molten-salt flux reactions have also been investigated toward the synthesis of heterometallic oxides in the $MM'O$ ($M = Cu, Ag$, $M' = Nb/Ta$) systems. For example, in recent research we have demonstrated that the copper(I) tantalates, $Cu_5Ta_{11}O_{30}$ and $Cu_3Ta_7O_{19}$, can be prepared in high purity using a $CuCl$ flux. Compared to $NaTaO_3$, the Cu $3d$ orbitals yield significantly smaller bandgap sizes of ~ 2.59 eV for the former and ~ 2.47 eV for the latter, and which stem from a metal-to-metal charge transfer between primarily the Cu $3d$ and Ta $5d$ orbitals, as shown in Figure 1. Current research also includes the first flux syntheses and investigations of $CuNbO_3$, $CuNb_3O_8$, and $CuNb_{13}O_{33}$, with even smaller bandgap sizes of ~ 1.47 eV, ~ 2.02 eV, and ~ 2.25 eV, respectively. The new solid solutions $(Cu_{2-x}Na_x)Ta_4O_{11}$ and $(Cu_{1-x}Na_x)Nb_{13}O_{33}$ have also been investigated in these systems, wherein the bandgap sizes can be tuned widely from $\sim 4.40 - 2.65$ eV and $\sim 3.05 - 2.25$ eV, respectively, by adjusting the %Cu. These results have yielded a new understanding of some of the key factors leading to visible-light bandgap sizes, strong optical absorption, and suitable band-level energies for use in driving the water-splitting reactions.

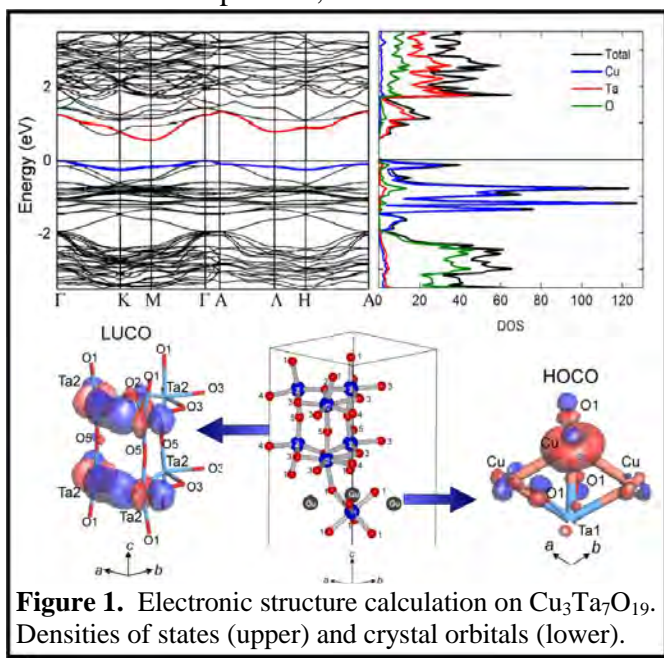


Figure 1. Electronic structure calculation on $Cu_3Ta_7O_{19}$. Densities of states (upper) and crystal orbitals (lower).

Nanostructured Photocatalytic Water Splitting Systems

Seung-Hyun Anna Lee, Landy K. Bladell, John Swierk, Nina I. Kovtyukhova, W. Justin Youngblood, Kazuhiko Maeda, Megan A. Kolarz, Lucas Jellison, and Thomas E. Mallouk

Department of Chemistry, The Pennsylvania State University, University Park, PA 16802

Thomas A. Moore, Ana L. Moore, and Devens Gust

Department of Chemistry and Biochemistry, Arizona State University, Tempe, AZ 85287

This project is exploring strategies for assembling photocatalytic and photoelectrochemical water splitting systems based on molecular sensitizers, oxide semiconductors, and catalyst nanoparticles. As in natural photosynthesis, the relative rates of forward and back electron transfer reactions are sensitive to structure on the molecular length scale. The goals of improving the efficiency and stability of molecular water splitting systems thus drive us to explore new ways to configure their components and to study light-driven electron transfer rates.

We recently reported (Youngblood et al., *J. Am. Chem. Soc.* **2009**, 131, 926) water splitting in a photoelectrochemical cell containing Ru-tris(bipyridyl) sensitizers that bridge between $\text{IrO}_2 \cdot n\text{H}_2\text{O}$ nanoparticles and the surface of a porous TiO_2 electrode. Under 450 nm illumination, the cell produces O_2 at the anode and H_2 at a Pt counter electrode with an applied bias of ≥ 350 mV. The quantum efficiency of the system is low (0.9%) due to rapid back electron transfer from TiO_2 to the oxidized sensitizer. In efforts to decrease the rate of back electron transfer we have investigated TiO_2 films with a thin layer of insulating oxide. Transient spectroscopy of Ru-dye- $\text{IrO}_2 \cdot n\text{H}_2\text{O}$ diads adsorbed onto a $\text{TiO}_2/\text{ZrO}_2$ film electrode shows slower back electron transfer (~ 0.53 ms) than that observed with a sensitized TiO_2 film (~ 0.37 ms). The slower recombination rate at the core-shell electrode is consistent with steady-state photoelectrochemical measurements, which show about a factor of two improvement in quantum efficiency for water oxidation. The timescale of photocurrent transients suggests that the diffusion of protons generated in the photoanode reaction may limit the current for water oxidation. We are now exploring strategies for buffering the nanopore network of the photoanode.

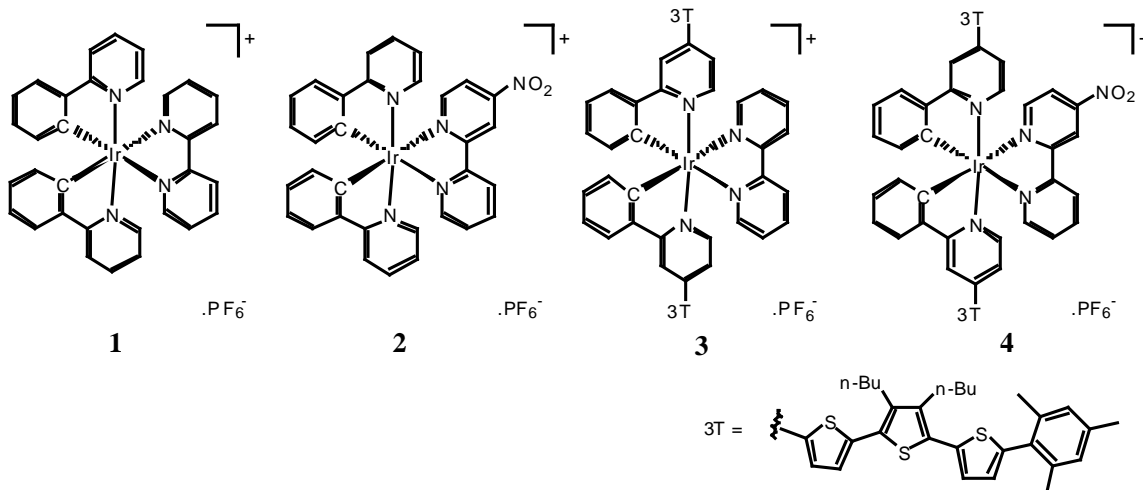
An alternative design for photoelectrochemical water splitting involves a hydrogen-evolving photocathode and a dark anode for oxygen evolution. This design avoids the stability problem of anode photosensitizers at the potential of water oxidation. Our recent experiments with platinized niobate nanosheets and nanoscrolls show high quantum yields for water reduction using Ru-tris(bipyridyl)-phosphonate sensitizers and EDTA as a sacrificial electron donor. We are now exploring layer-by-layer assembly of layered metal oxide semiconductors, sensitized by Ru-tris(bipyridyl) complexes and porphyrins, as a way to couple similar structures to high surface area transparent conductor electrodes. Our previous experiments with these multilayer donor-acceptor structures have shown that it is possible to achieve millisecond charge separation lifetimes, which should be adequate for hydrogen evolution from Pt nanoparticles on the surface of the nanosheets. In order to prepare high surface area photocathodes, we have grown transparent conducting nanowires and nanotubes of tin-doped indium oxide (ITO) by electrochemically-assisted deposition in anodic alumina membranes, followed by annealing at 600°C . A mechanistic study shows that Sn-O-In linkages are formed from Sn(IV) and In(III) ions in nitrate-containing supporting electrolytes, but their formation is inhibited in chloride-containing solutions. Exploiting the surface chemistry of the alumina pore walls allows one to switch the growth mode between nanotube and nanowire ITO arrays.

New Cyclometallated Iridium Dyes with Nitro Bipyridine Acceptors and Oligothiophene Secondary Electron Donors

Kyle R. Schwartz, Raghu Chitta, Jon N. Bohnsack, Darren J. Cecknowicz, David A. Blank, Wayne L. Gladfelter and Kent R. Mann

Department of Chemistry
University of Minnesota
Minneapolis, MN 55455

The primary goal of this research is to investigate and understand the relationship between structure, energetics and dynamics in a set of well-defined electron/energy donor-acceptor dyads and triads. We are studying novel dyes for this research that contain cyclometallated cationic Ir(III) complexes $[\text{Ir}(\text{C}^{\wedge}\text{N})_2(\text{N}^{\wedge}\text{N})]^+$ ($\text{C}^{\wedge}\text{N}$ = cyclometalating ligand, $\text{N}^{\wedge}\text{N}$ = diimine ligand) with ligands substituted with terthiophenes (3Ts) as potential donors and nitro substituents as potent acceptors to direct the charge transfer in a vectorial manner. Functionalization of these Ir(III) complexes with secondary electron donors (SED) such as 3Ts not only increases the panchromatic nature of the dyes but also stabilizes the charge separated state generated upon photoexcitation by allowing the hole to reside on the SED and the electron on nitro substituted bipyridine (4-NO₂-bpy) resulting in a long-lived charge separated state. Information about the primary photophysical events occurring within these Ir(III) complexes will provide a better understanding of the electron transfer dynamics of ZnO nanocrystals decorated with similar complexes with modified anchoring groups. Studies of the UV-vis, cyclic voltametry, spectroelectrochemistry, time resolved photoluminescence and femtosecond transient absorption experiments to confirm the formation of radical ion pairs are underway.

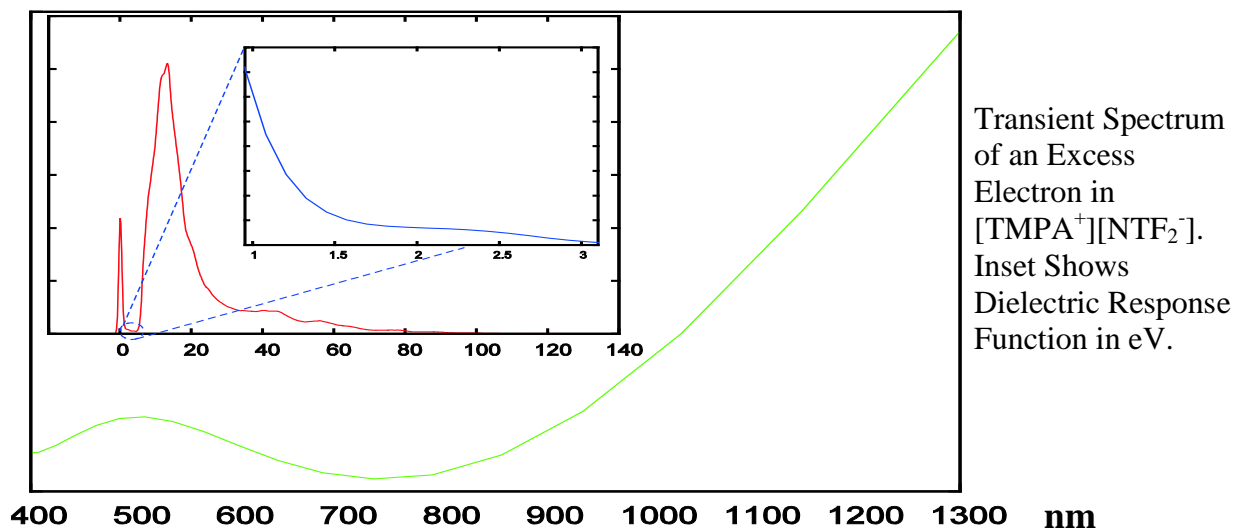


Control complexes: $[\text{Ir}(\text{ppy})_2(\text{bpy})]\text{PF}_6$ (**1**), $[\text{Ir}(\text{ppy})_2(4\text{-NO}_2\text{-bpy})]\text{PF}_6$ (**2**); those bearing SEDs: $[\text{Ir}(3\text{T-ppy})_2(\text{bpy})]\text{PF}_6$ (**3**) $[\text{Ir}(3\text{T-ppy})_2(4\text{-NO}_2\text{-bpy})]\text{PF}_6$ (**4**) (ppy = 2-phenylpyridine, 3T-ppy = 3',4'-dibutyl-5-mesityl-5''-(4-2-phenylpyridine)-2,2':5',2''-terthiophene, bpy = 2,2'-bipyridine, 4-NO₂-bpy = 4-nitro-2,2'-bipyridine).

Excess Electron Spectrum and Heterogeneity in Room Temperature Ionic Liquids

Mario del Popolo[†], Jorge Kohanoff[†], David Coker[‡], H.V.R. Annapureddy^{*}, Claudio J. Margulis^{*}. QUB, Belfast UK[†]; UCD, Dublin, Ireland[‡]; Department of Chemistry, University of Iowa, Iowa City, Iowa, 52242^{*}

Part a ([†],[‡],^{*}): Room-temperature ionic-liquids (RTILs) are new media being studied for their potential in a variety of different academic and industrial areas including electron transport and radioactive material processing. The interactions between excess electrons, very strong reducing agents, and room-temperature ionic-liquids are by no means fully understood. Pulse radiolysis studies as well as electron photodetachment studies have opened a window of opportunity to address these problems¹⁻². In this poster we present preliminary results on our study of excess electron and hole localization in different solid, liquid and gas phase aromatic and aliphatic RTIL systems. This work attempts to rationalize the different features in the transient optical spectrum of the excess electron and correlates these features with issues of mobility and possible reactivity.



Part b (^{*}): We have recently found that fluorescence spectroscopy as well as excited state intramolecular electron transfer reactions can be absorption wavelength dependent in RTILs³⁻⁴. In this context, part of our current research effort is to identify the structural and dynamical connections between “local environment” heterogeneous reactivity and the particular nature and arrangements of the ions involved. To this effect, in this poster we present preliminary results that attempt to address the so called “pre-peak” observed in x-ray and neutron scattering studies of certain RTILs which is often ascribed to long range ordering and a possible indication of structural heterogeneity⁵.

(1) Wishart, J. F. *Ionic Liquids as Green Solvents: Progress and Prospects* **2003**, 856, 381. (2) Funston, A. M.; Wishart, J. F. *Acs Sym Ser* **2005**, 901, 102. (3) Hu, Z. H.; Margulis, C. J. *P Natl Acad Sci USA* **2006**, 103, 831. (4) Annapureddy, H. V. R.; Margulis, C. J. *J Phys Chem B* **2009**, 113, 12005. (5) Triolo, A.; Russina, O.; Bleif, H. J.; Di Cola, E. *J Phys Chem B* **2007**, 111, 4641.

Dynamical Arrest and Non-Gaussian Energy Gap Fluctuations in Natural and Artificial Photosynthesis

Dmitry V. Matyushov

Department of Chemistry/Physics, Arizona State University
Tempe, AZ 85281

All designs of natural and artificial photosynthetic schemes involve same basic components: energy input, electron hopping, and the output used for electricity generation or catalytic storage in chemical bonds. Since charge recombination is a strongly downhill process, avoiding this wasteful reaction necessitates fast, nearly activationless forward transitions. The standard theories of electron transport between molecules (Marcus) suggest that the energy of the nuclear medium reorganization is lost to heat in each activationless hop. With the typically anticipated reorganization energy of 1 eV almost entire input energy of 1--2 eV should be lost in just a couple of hops. Despite this generic inefficiency, suggested by standard models, natural energy chains achieve quite remarkable efficiency, which is hard to reconcile with $\lambda \approx 0.7$ eV commonly attributed to proteins. Likewise, primary charge separation in bacterial photosynthesis has an energetic efficiency much higher than the standard scheme of activationless transitions would suggest [1,2].

We found two mechanisms of overcoming the efficiency bottlenecks in our studies of primary charge separation in bacterial reaction centers [1,2]. We showed that the equilibrium reorganization energy for this reaction, ca. 1.5 eV, far exceeds the values required to fit the measured reaction rate. The inclusion of

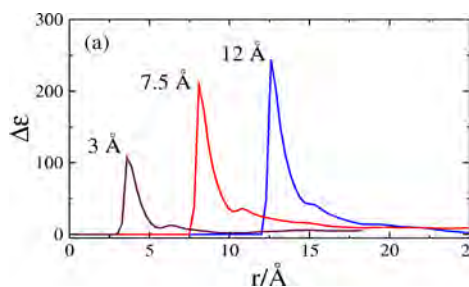


Fig. 1: Excess dielectric constant of hydration shell around nanoparticles with the radius shown in the plot.

a nonergodic cutoff of the nuclear fluctuations [3] reduced this reorganization energy to about 0.35 eV. This mechanism, however, cannot be applied to slower reactions on the nano-second time-scale. For these reactions, there is yet another mechanism achieving the same goal of the free energy efficiency. We found that interfacial water around proteins is polarized in a ferroelectric cluster with a non-zero net dipole moment. The thermal motions of this polarized cluster create non-Gaussian fluctuations of the electrostatic potential. The result is about an order of magnitude lower loss of free energy per hop than in the standard mechanism.

We want to extend our observations in natural photosynthetic systems to reactants used in artificial photosynthesis schemes. We have initiated studies of charge-transfer kinetics in colloidal particles with sizes comparable to proteins [4]. Numerical simulations of model non-polar particles, resembling in their hydrophobicity Ag nanoparticles, have shown a steady increase in the interfacial polarity as the size of the nanoparticle approaches that of a typical globular protein (Fig. 1).

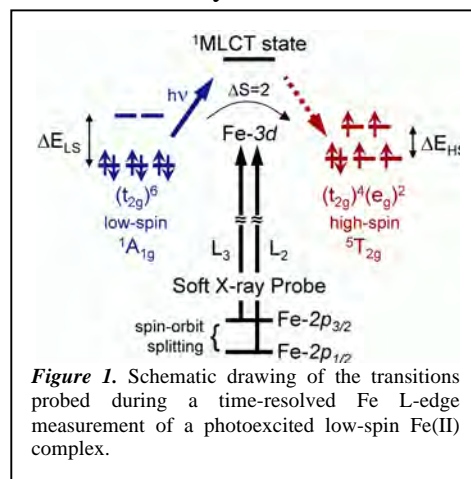
1. D. N. LeBard, V. Kapko, D. V. Matyushov, Energetics and Kinetics of Primary Charge Separation in Bacterial Photosynthesis, *J. Phys. Chem. B* **112** (2008) 10322.
2. D. N. LeBard and D. V. Matyushov, Energetics of bacterial photosynthesis, *J. Phys. Chem. B*, **113** (2009) 12424.
3. D. V. Matyushov, Nonergodic activated kinetics in polar media, *J. Chem. Phys.* **130** (2009) 164522.
4. A. Friesen and D. V. Matyushov, Cavity-water interface in polar, *PRL* (submitted, arXiv:1001.4476v1).

First-row Transition Metal Complexes as Chromophores for Solar Energy Conversion

Allison Brown, Lindsey Jamula, and James K. McCusker*
Department of Chemistry
Michigan State University
East Lansing, MI 48824

All energy conversion strategies can be described in terms of three principle steps: capture, convert, and store. In the case of solar, capture implies the absorption of radiant energy that can lead to charge separation for the creation of electric and/or chemical potential. The most successful approaches to date have employed transition metal complexes of Ru(II); although functionally competent, conversion strategies that rely on second- and third-row elements such as ruthenium will ultimately face a scalability problem stemming from the coupled issues of scarce natural abundance and limited resource capitalization. With these considerations in mind, our research efforts are focusing on the development of chromophores based on earth-abundant elements (specifically iron and copper). During the past year, we have made two significant advances in our efforts: one in the area of methodology, the other in the form of a new Fe(II) compound that exhibits properties that we believe hold promise for applications in solar cells.

Time-resolved Iron L-edge X-ray Absorption Spectroscopy. Our ongoing collaboration with Robert Schoenlein's group at Lawrence Berkeley National Laboratory has resulted in the first successful application of time-resolved soft x-ray absorption spectroscopy to a molecule in solution. Specifically, we examined a low-spin Fe(II) complex in the Fe L-edge x-ray region of the spectrum subsequent to $^1A_1 \rightarrow ^1MLCT$ excitation in the visible. At these energies one probes the $2p \rightarrow 3d$ absorption of the metal, thereby providing a direct measure of changes in bonding (e.g., energies, population, etc.) associated with the d-orbitals associated with excited-state dynamics (Figure 1). The data from these experiments provided an unprecedented level of detail concerning changes in metal-ligand interactions as a result of the low-spin to high-spin conversion that occurs following MLCT excitation of the compound. The time resolution of the experiment is presently limited to ca. 70 ps, however, modifications now in progress will improve this to ca. 100 fs: this should allow us to directly examine electronic structure dynamics associated with deactivation of charge transfer states, an important goal of our research program.



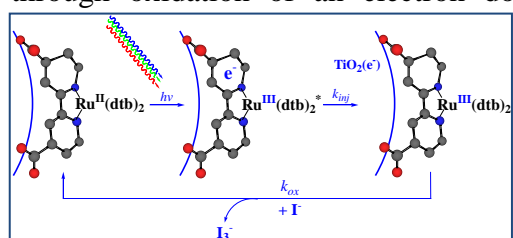
[Fe(tripy)₂](PF₆)₂: The First Emissive Fe(II) Complex. We have recently had a significant breakthrough in our efforts to create Fe(II) complexes that are viable as sensitizers for semiconductor-based solar cells. The compound consists of a modified terpyridyl-based ligand that forms a bis-adduct with Fe(II), yielding a strongly colored, low-spin complex. Surprisingly, this compound exhibits a weak emission near 800 nm when excited in a low-temperature optical glass. The change in electronic structure that gives rise to this novel property will be discussed, as will our plans to capitalize on this observation for possible applications in DSSCs.

Electron Transfer Dynamics in Efficient Molecular Solar Cells

Shane Ardo, John Rowley, and Gerald J. Meyer

Departments of Chemistry and Materials Science & Engineering,
Johns Hopkins University, Baltimore, MD 21218

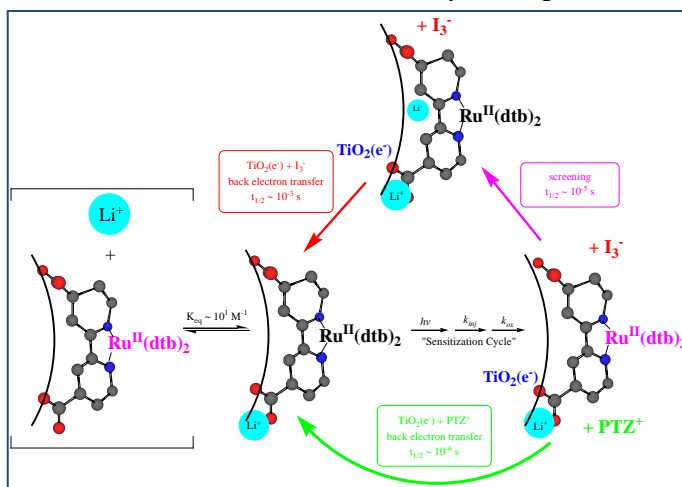
The sensitized nanocrystalline semiconductor thin films developed by Grätzel and coworkers for application in regenerative dye-sensitized solar cells are comprised of interconnected anatase TiO₂ nanocrystallites functionalized with ruthenium–polypyridyl compounds. The Ru(II) coordination compounds can rapidly and quantitatively undergo three consecutive charge-transfer reactions shown schematically: 1) light absorption through metal-to-ligand charge transfer (MLCT) excitation; 2) excited-state electron injection into TiO₂; and 3) reduction through oxidation of an electron donor present in the solution electrolyte. In principle,



immediately after completion of this cycle the sensitizer is “regenerated” and could repeat the “sensitization cycle” again. Under 1 sun illumination each sensitizer repeats this cycle on average about twice per second. At the condition of maximum power generation, approximately 10 injected electrons are estimated to reside in each TiO₂ nanocrystallite. This poster

addresses the influence injected electrons have on the individual steps of the sensitization cycle.

We have shown that injected electrons have a profound influence on the absorption spectrum of Ru(II) sensitizers that did not undergo excited state injection. Pulsed-laser excitation of a sensitized nanocrystalline thin film immersed in 0.5 M LiI acetonitrile electrolyte at open circuit, resulted in the expected rapid excited-state injection and donor oxidation to yield TiO₂(e⁻)s and oxidized iodide. However, the MLCT absorption spectra of the Ru(II) coordination compounds differed from that which was initially excited. The spectral data were consistent with an underlying Stark effect of magnitude ~ 270 MV/m, corresponding to a ~ 40 mV potential drop. The amplitude of the Stark effect decreased over time periods where TiO₂(e⁻) + I₃⁻ → charge recombination was absent, behavior attributed to “screening” of the electric field by interfacial ionic reorganization.



In the absence of iodide, or with phenothiazine donors, the magnitude of the Stark effect decreased concomitantly with interfacial charge recombination. Unambiguous identification of a Stark effect on the excited-state sensitizers was also accomplished. The unique relative orientation of the electric field and sensitizer afforded by the nanocrystal geometry resulted in unidirectional shifts in the absorption and photoluminescence spectra of the Ru(II) coordination compounds giving rise to first-derivative like spectra.

Metal-to-Ligand Charge Transfer Excited States on Surfaces and in Rigid Media: Application to Energy Conversion

Thomas J. Meyer, John M. Papanikolas
Department of Chemistry
University of North Carolina
Chapel Hill, N.C. 27599-3290

Encapsulating $\text{Ru}(\text{NN})_3^{2+}$ complexes (where NN = 1,10-phenanthroline (phen), 2,2'-bipyridine (bpy), 4,4'-dimethyl-2,2'-bipyridine (dmb), and 4-methyl-4'-vinyl-2,2'-bipyridine (vbpy)) in freeze-pump-thaw degassed PEG-DMA film (PEG-DMA = Polyethylene (glycol dimethacrylate)) in 1 cm path length air free cuvettes allowed for accurate determination of the photophysical properties of the Ru(II) complexes in the rigid medium. This in situ preparation technique in the 1 cm cells yielded reliable relative emission quantum yields by: 1) collecting the spectra in completely air free conditions, 2) using identical path length cells as the $[\text{Ru}(\text{bpy})_3](\text{PF}_6)_2$ standard, and 3) by reproducible sample placement inside the fluorimeter. A significantly longer MLCT lifetime for $\text{Ru}(\text{phen})_3^{2+}$ in PEG-DMA film ($\tau_{\text{obs}} = 2000$ ns) versus fluid ($\tau_{\text{obs}} = 930$ ns) was observed, while only a slight increase was seen for $\text{Ru}(\text{bpy})_3^{2+}$ and $\text{Ru}(\text{dmb})_3^{2+}$ in the film. Comparison of the emission spectral fitting results for $\text{Ru}(\text{dmb})_3^{2+}$ and $\text{Ru}(\text{vbpy})_3^{2+}$ show that the vinyl group of vbpy copolymerizes with PEG-DMA and incorporates $\text{Ru}(\text{vbpy})_3^{2+}$ into the polymer network. Once the $\text{Ru}(\text{vbpy})_3^{2+}$ chromophores are copolymerized within the PEG-DMA network, the vinyl substituents are chemically modified to alkyl groups and the excited state characteristics of $\text{Ru}(\text{vbpy})_3^{2+}$ fall in line with $\text{Ru}(\text{dmb})_3^{2+}$. The ground- and excited-state $\text{Ru}(\text{NN})_3^{2+}/\text{PEG-DMA}$ interactions manifested in the observed photophysics will be discussed.

In the mixed polymer $[\text{PS-CH}_2\text{CH}_2\text{NHC(O)-Ru}^{\text{II}}(\text{am})_{17}(\text{Os}^{\text{II}})_3](\text{PF}_6)_{40}$, rapid intra-strand $\text{Ru}^{\text{II}} \rightarrow \text{Os}^{\text{II}}$ energy transfer previously observed in fluid solution was investigated in PEG-DMA film to suppress macromolecular motion. The comparison of transient emission-time profiles in solid PEG-DMA and CH_3CN solution shows that intra-strand energy transfer rates are comparable in both environments, and that attachment of the chromophores to the polystyrene backbone is the dominant contributor to the excited-state energy transfer barrier.

- (1) "Photophysical Properties of MLCT Excited States in Films from Polymerizable Fluids." Troy E. Knight, Anna M. Goldstein, M. Kyle Brennaman, Thomas Cardolaccia, Joseph M. DeSimone, and Thomas J. Meyer. *J. Phys. Chem. B* **2010** submitted.
- (2) "Efficient, Long-Range Energy Migration in Ru^{II} Polypyridyl Derivatized Polystyrenes in Rigid Media. Antennae for Artificial Photosynthesis." Cavan N. Fleming, M. Kyle Brennaman, John M. Papanikolas, and Thomas J. Meyer. *Dalton Trans.* **2009**, 3903-3910.

Photocatalytic Water Oxidation at the GaN (1010) – Water Interface

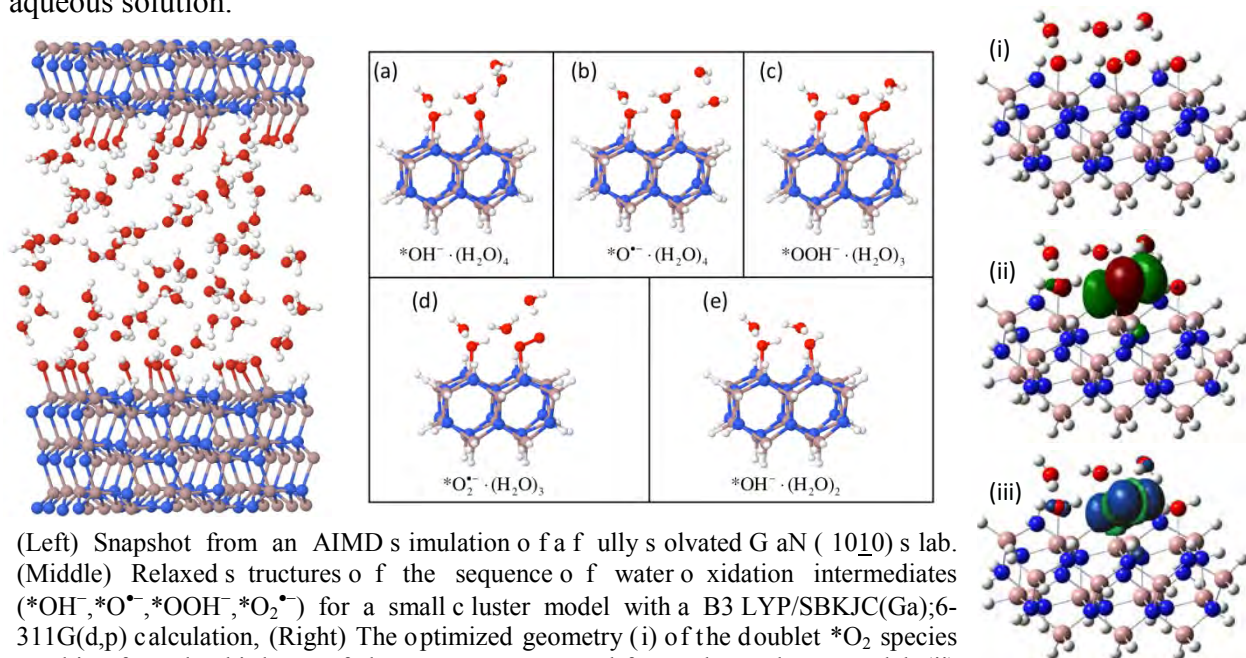
J. T. Muckerman,^{1,2} Y. A. Small,² X. Shen,³ M. S. Hybertsen,²
J. Wang,³ P. B. Allen,³ M. V. Fernandez-Serra,³ E. Fujita¹

¹Chemistry Department, Brookhaven National Laboratory, Upton, NY 11973-5000

²Center for Functional Nanomaterials, Brookhaven National Laboratory, Upton, NY 11973-5000

³Department of Physics, Stony Brook University, Stony Brook, NY 11794-3800

Domènec and co-workers have observed that the GaN/ZnO semiconductor alloy serves, in the presence of a sacrificial electron scavenger, as a photocatalyst for solar water oxidation, producing H^+ and O_2 at the aqueous/semiconductor interface. With a suitable co-catalyst, the same solar photoexcitation process also generates H_2 from H^+ with much lower overall efficiency. The active sites, mechanisms, and reaction intermediates are not known. The active GaN/ZnO alloy facet and the details of the alloy composition and structure at the catalytically active interface with water are also unknown. Since pure GaN also functions as a water-splitting UV photocatalyst, we focus on this simpler example to propose a detailed water oxidation mechanism. We start by using *ab initio* molecular dynamics (AIMD) calculations to explore the details of solvation at the GaN (1010) – water interface. We then propose a detailed water oxidation mechanism consisting of a series of four proton-coupled electron-transfer (PCET) steps. We use Density Functional Theory (DFT) calculations, applied to cluster models chosen with reference to our simulations of the extended interface, to probe the structure of the solvated interface and reactive intermediates. Nearby solvent is explicitly simulated with the farther solvent being treated by an implicit solvation model. Based on the calculations, we obtain the standard free energies for sequential proton-coupled one-electron oxidation. The results are discussed in terms of their implications for water oxidation at semiconductor surfaces and their relationship to the analogous known one-electron water oxidation reactions in homogeneous aqueous solution.



(Left) Snapshot from an AIMD simulation of a fully solvated GaN (1010) slab. (Middle) Relaxed structures of the sequence of water oxidation intermediates ($*OH^-$, $*O^-$, $*OOH^-$, $*O_2^-$) for a small cluster model with a B3LYP/SBKJC(Ga);6-311G(d,p) calculation, (Right) The optimized geometry (i) of the doublet $*O_2$ species resulting from the third step of electron-proton removal from a large cluster model; (ii) its β -LUMO; and (iii) its spin density. The surface species is clearly identified as $*O_2^-$.

Tuning the Photophysical Properties of Group IV Nanocrystals

Nathan R. Neale and Daniel A. Ruddy
Chemical and Materials Science Center
National Renewable Energy Laboratory
Golden, CO 80401

Group IV nanocrystals (NCs) are under intense scrutiny as a nontoxic class of nanomaterials for solar photoconversion. Recently, Beard et al. demonstrated that 9.5 nm Si NCs with an effective band gap (E_g) of 1.20 eV produced via gas-phase synthesis exhibit multiple exciton generation (MEG). Controlling the size & shape (and, therefore, the photophysical properties) of Group IV NCs via solution-phase routes has been problematic, but a 2009 report by Klimov and coworkers detailed the preparation of 3.2–6.4 nm Ge NCs (effective $E_g = 0.95$ –1.20 eV; cf. bulk Ge $E_g = 0.67$ eV) via a high temperature solution-phase reduction method. However, fine control over Group IV nanoparticle size & shape analogous to that achieved for binary compound semiconductor NCs (e.g., III-V, II-VI, IV-VI) still remains elusive.

We have been interested in developing synthetic strategies to Group IV NCs, particularly Si. In the literature report on Ge NCs, a Ge(II) precursor (GeI_2) is mixed with hexadecylamine and reduced by *n*-butyllithium in the presence of octadecene, which caps the growing nanoparticles to form octadecyl-terminated Ge NCs (Ge-C_{18}). As no Si(II) precursor exists, we have attempted similar reductions using SiI_4 , but initial experiments have yielded no Si NCs. We believe that the reason for the reactivity difference between GeI_2 and SiI_4 lies in the reaction mechanism.

Coupled with our Si NC studies, we have prepared emissive Ge NCs via an adaptation of the literature procedure. Using pure GeI_2 , our Ge-C_{18} NCs have a size of 4.4 ± 1.3 nm (TEM) resulting in a broad photoluminescence (PL) response (FWHM = 160 nm; $\lambda_{\text{max}} \sim 750$ nm). Although the PL broadness is consistent with the literature values, the PL λ_{max} is blue-shifted by ca. 400 nm relative to that reported for this particle size regime (the cause of this discrepancy is still under investigation). To manipulate the particle size, we have been exploring a selective seeded growth method. Reactions using both GeI_2 and GeI_4 have resulted in larger particles (5.9 ± 1.4 nm) and a red-shifted absorption onset relative to those made from pure GeI_2 , while using only GeI_4 resulted in smaller particles and a blue-shifted absorption onset (Fig. 1). We propose that the larger particles result from initial GeI_2 conversion to Ge NC seeds, which then grow via Ge addition from slower reduction of the GeI_4 precursor. Currently we are exploring related reactions to tune the NC size further as well as to provide insight into the details of the reaction mechanism.

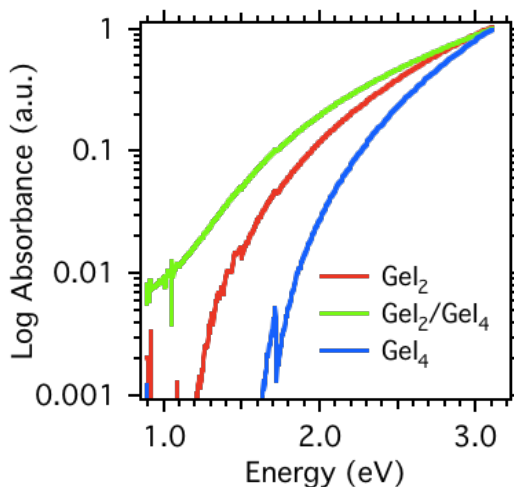


Figure 1. Absorbance spectra (hexanes solution) of Ge-C_{18} NCs prepared from different precursors.



First Principles Studies of Optical Absorption and Charge Separation At Donor-Acceptor Interfaces in Organic Nanostructures

P. Doak, P. Darancet, S. Sharifzadeh, E. Isaacs, and J. B. Neaton
Molecular Foundry, Lawrence Berkeley National Lab, Berkeley, CA 94720, USA

Organic, molecular, and other nanostructure-based solar cells are currently being explored as components for efficient and inexpensive artificial photosynthetic platforms. Fundamentally different from more costly silicon solar cells, organic solar cells rely on a high density of nanoscale interfaces to separate and transport electrons and holes. Despite their considerable promise, the role of these interfaces on key processes involved in solar energy conversion—absorption, exciton formation, charge separation, and charge transport—remains poorly understood. In this work, we use first principles calculations to predict optical absorption and examine charge separation in covalently-linked donor-acceptor molecules, a model organic solar cell system, for which all interfaces—donor-acceptor, donor-electrode, and acceptor-electrode—are assembled and tailored bond-by-bond with chemical control. Using density functional theory (DFT) and many body perturbation theory (MBPT) calculations of both electron addition and removal energies using the GW approximation, and neutral excitations using a Bethe-Salpeter equation (BSE) approach, we explore a series of small asymmetric molecules containing covalently-linked aromatic moieties based on thiophene, durene and tetrafluoro-, dinitrile-, and methoxy-benzene. By explicit calculation of exciton binding energies and molecular energy level alignment, the relationship between type II heterojunction electronic structure, charge separation, and optical absorption is critically examined, and the influence of the metal contacts and binding groups on junction electronic level alignment is computed. In addition, the efficacy of DFT and MBPT for quantitative studies is discussed in the context of recent experiments on organic molecules; organic semiconductor crystals, such as pentacene, C60, and PTCDA; and the metal-organic interface through comparison with experiment. This work was funded by the Helios Solar Energy Research Center, which is supported by the Director, Office of Science, Office of Basic Energy Sciences of the U.S. Department of Energy under Contract No. DE-AC02-05CH11231. Portions of this work were performed at the Molecular Foundry, Lawrence Berkeley National Laboratory, and were supported by the U.S. Department of Energy, Office of Science, Office of Basic Energy Sciences, under Contract DE-AC02-05CH11231.

Rapid Synthesis/Screening and Nano-Structuring of Oxide Semiconductor Photocatalysts

Allen J. Bard and C. Buddie Mullins
Departments of Chemistry and Chemical Engineering
University of Texas at Austin
Austin, TX 78712

We employ a variation of scanning electrochemical microscopy (SECM) for rapid screening of photocatalysts in which the ultramicroelectrode tip is replaced by an optical fiber that illuminates a photocatalyst array allowing the activity of each photocatalyst “spot” to be quickly determined. Multi-component doped metal oxide semiconductor arrays are fabricated using a computer controlled piezo-dispenser head with a stepping motor-operated XYZ stage which produces a pattern of ~ 200 μm sized electrocatalyst spots on a substrate (e.g., FTO). The first component (metal-salt solution) is loaded and dispensed followed sequentially by the other components and then heated in a furnace to the desired reaction temperature. Different potentials can be applied to the working electrode (arrays), while the optical fiber tip scans the arrays about

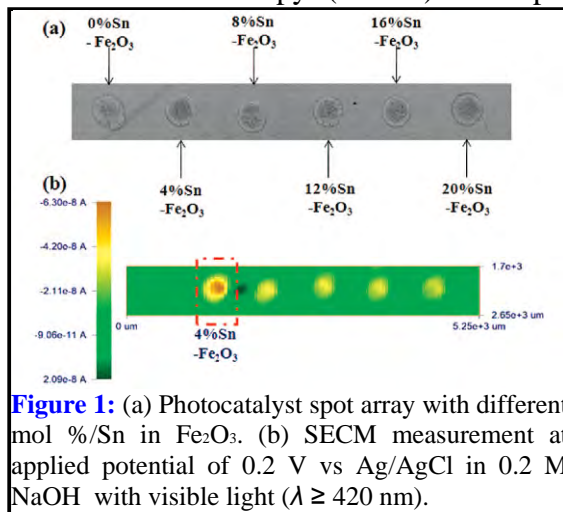


Figure 1: (a) Photocatalyst spot array with different mol %/Sn in Fe_2O_3 . (b) SECM measurement at applied potential of 0.2 V vs Ag/AgCl in 0.2 M NaOH with visible light ($\lambda \geq 420$ nm).

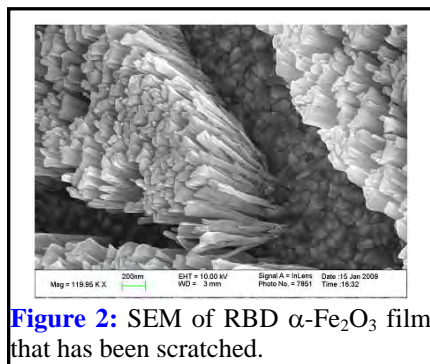


Figure 2: SEM of RBD $\alpha\text{-Fe}_2\text{O}_3$ film that has been scratched.

50 μm above the array surface. The photocurrent produced at a given potential during the scan is measured and recorded as a false-color image. Figure 1 displays an example SECM scan for $\alpha\text{-Fe}_2\text{O}_3$ films doped with different levels of Sn (see *J. Phys. Chem. C* **113**, 6719 (2009)) suggesting that Sn-doping at the level of 4% is optimal.

Promising doped semiconductor materials with complex stoichiometries, identified through screening tests, are then fabricated into nano-structured thin films using reactive ballistic deposition (RBD), altering the structure and composition to tune photocatalytic and optical properties. RBD involves the metallic component(s) of the film being evaporated at a glancing angle onto the substrate through an ambient of reactive gas (e.g., oxygen) to create high surface area films composed of arrays of nano-columnar structures (e.g., Figure 2; N. Hahn, *et al.*, *ACS Nano* ASAP (2010)) with high internal porosity. $\alpha\text{-Fe}_2\text{O}_3$ RBD films doped with titanium have been characterized and tested electrochemically (see Figure 3) and are generally consistent with the rapid screening SECM results showing that 2% Ti-doping of the iron oxide is optimal for water oxidation by photoelectrocatalysis.

50 μm above the array surface. The photocurrent produced at a given potential during the scan is measured and recorded as a false-color image. Figure 1 displays an example SECM scan for $\alpha\text{-Fe}_2\text{O}_3$ films doped with different levels of Sn (see *J. Phys. Chem. C* **113**, 6719 (2009)) suggesting that Sn-doping at the level of 4% is optimal.

Promising doped semiconductor materials with complex stoichiometries, identified through screening tests, are then fabricated into nano-structured thin films using reactive ballistic deposition (RBD), altering the structure and

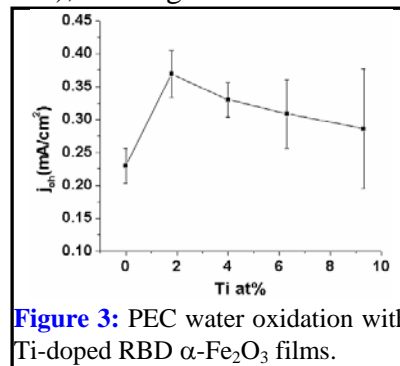


Figure 3: PEC water oxidation with Ti-doped RBD $\alpha\text{-Fe}_2\text{O}_3$ films.

D/A Couplings in Binuclear Metal Complexes and the Role of Competing Ligands

Marshall D. Newton
Chemistry Department, Brookhaven National Laboratory
Upton, New York 11973-5000

Bridge-mediated D/A coupling between redox sites in binuclear transition metal complexes is sensitive to the electronic manifolds of the ligands, especially the central bridging and exterior axial ligands. We assess this situation in an effective 2-state (2-st) framework, or in an enlarged (n -state, $n > 2$) reduced space, selected to accommodate low-lying ligand states. Each chosen space (defined by n adiabatic states (eigenstates) of the system, $\Psi_i^{a(4)}$, $i = 1, n$) yields a corresponding set of diabatic states ($\Psi_i^{d(4)}$), in terms of which important quantities such as coupling elements ($H_{DA}^{d(n)}$), D/A separation ($r_{DA}^{d(n)}$), effective D,A size ($r_D^{d(n)}, r_A^{d(n)}$), and reorganization energy ($\lambda_{DA}^{d(n)}$) are expressed. We focus on electron transfer (ET) processes, obtaining $\Psi_i^{d(4)}$ as defined by the maximum-charge-separation criterion underlying the Generalized Mulliken Hush (GMH) model. Results are illustrated for three different mixed-valence binuclear Ru complexes (each with a pyrazine bridge (Ru-pz-Ru)), using a frozen-orbital model with n ranging from 2 to 6, based on DFT calculations for the fully-reduced systems (Ru²⁺/Ru²⁺). The GMH approach imposes local adiabaticity for multiple states on a given site (here, pz). The calculations show conformity with the distance scale separation required by GMH, namely, $r_{DA}^{d(n)} \gg r_D^{d(n)}, r_A^{d(n)}$.

Analysis of the calculated coupling and associated D and A states shows that the 2-st coupling, which we find to be the most appropriate estimate of the effective D/A coupling, involves crucial mixing with intervening bridge states (D and A ‘tails’), while increasingly larger state spaces for the same system yield increasingly more localized D and A states (and weaker coupling), with H_{DA} tending to approach the limit of ‘bare’ or ‘through space’ coupling. In terms of perturbation theory (PT), a superexchange (se) model is found to be quantitatively valid for the complex with outer pyridine ((py)₂) ligands, and still useful semi-quantitatively for the (CO)₂ and Creutz-Taube complexes. Nevertheless, for all three complexes, the overall 2-st coupling ($H_{DA}^{d(2)}$) is too strong to satisfy the separate PT requirements for use of the Golden Rule (GR) in modelling the kinetics. Even in cases where the 2-st model is adequate for modeling ET coupling, a multistate analysis is still valuable in facilitating the decomposition of D/A coupling in terms of the se model.

The present results help to reconcile seemingly contradictory assertions in the recent literature regarding the proper role of multi-state frameworks in the formulation of coupling for both intra- and intermolecular ET systems. The new results presented here are compared in detail with other reported results, many of which are in conformity with the trends observed here, but with others showing different behavior. This latter behavior may reflect special interference effects arising from the qualitative features of the adiabatic states constituting the n -space and their relative ordering, a topic warranting further calculations and analysis.

Multiple Exciton Collection in a Sensitized Photovoltaic System Results in Quantum Yields Greater than One

Justin B. Sambur^{#*}, Thomas Novet⁺ and B. A. Parkinson^{*}

^{*}Department of Chemistry and School of Energy Resources
University of Wyoming
Laramie, WY 80271

[#]Department of Chemistry
Colorado State University
Fort Collins, CO 80523

⁺ Voxtel Inc
Beaverton, OR 97006

Multiple exciton generation, the creation of two electron hole pairs from one high energy photon, is well established in bulk semiconductors but the efficiency and magnitude of this effect remains controversial in quantum confined systems like semiconductor nanocrystals. We use a photoelectrochemical system composed of PbS nanocrystals chemically bound to TiO₂ single crystals to demonstrate the collection of photocurrents with quantum yields greater than one. The electronic coupling and favorable energy level alignment of PbS nanocrystals to bulk TiO₂ energy levels make this a suitable system to quickly extract multiple excitons before they recombine. Our results have implications for increasing the efficiency of photovoltaic devices by avoiding losses due to the thermalization of photogenerated carriers.

Surface femtochemistry of alkali atom photodesorption from noble metal surfaces

Hrvoje Petek

Department Physics and Astronomy

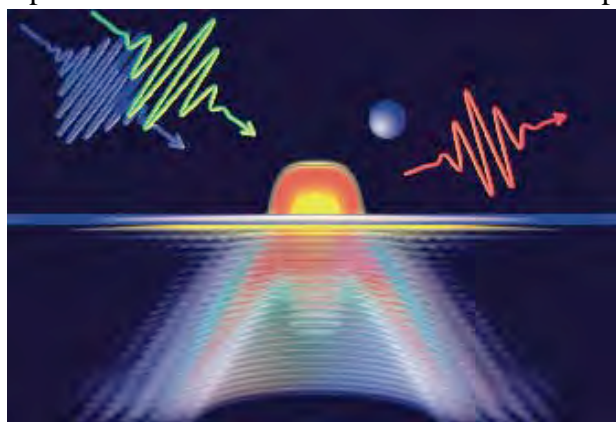
University of Pittsburgh

Pittsburgh, PA 15260

We have investigated the femtosecond time scale electron and nuclear dynamics in photodesorption of alkali atoms from noble metal surfaces by time-resolved two-photon photoemission (TR-2PP) spectroscopy.¹⁻³ In the zero coverage limit, alkali atoms chemisorb on metal surfaces in ionic form. Photoinduced charge transfer excitation with ~ 3 eV photons prepares alkali atoms in their neutral state at the position of the ionic ground state. The strong Coulomb repulsion between neutral alkali atoms and their image charges initiates dissociative wave packet motion. Photoexcitation of the excited state with a delayed 3 eV probe pulse can induce photoemission from the evolving excited state.

We have investigated by TR-2PP the surface photodesorption of the Cs/Ag(111) system. Pump-probe two-pulse correlation measurements (2PC) indicate unusually long lifetime for the 6s resonance of Cs, which make it possible to follow the photodesorption dynamics for several hundred femtoseconds. Below the time zero energy of 6s resonance, 2PC measurements follow nonexponential kinetics that can be modeled with an exponential rise and decay. If we attribute the rise to the nuclear wave packet motion and the decay to the resonant charge transfer from 6s state to the conduction band continuum of the metal substrate, we would conclude that the nuclear wave packet motion as the excited electronic state decays on ~ 200 fs time scale and the bond length increases by 0.7 \AA . The situation is not so simple, however.

2PC measurements as a function of photoemission angle show that the observed kinetics measurements are strongly emission angle dependent. For low-density alkali atoms, one would expect to measure the same excited state population independent of the emission angle.



Therefore, the angular dependence must have a different origin, most likely the electron rather than nuclear dynamics. The angle dependence of 2PC measurements arises either from the evolution of the electronic wave function in the intermediate state (Fig. 1), or the electron tunneling effects in near threshold photoemission. We are investigating these possibilities by ultrafast photoemission momentum microscopy, at the MPI for Microstructure Physics and by theory.

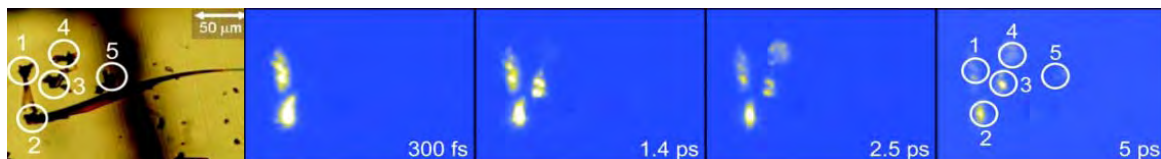
Figure 1. The calculated Cs 6s state electronic wave packet seen above (top) and below (bottom) metal surface.

- (1) Petek, H.; Weida, M. J.; Nagano, H.; Ogawa, S. *Science* **2000**, 288, 1402-1404.
- (2) Petek, H.; Ogawa, S. *Annu. Rev. Phys. Chem.* **2002**, 53, 507-531.
- (3) Zhao, J. et al.. *Phys. Rev. B* **2008**, 78, 085419-7.

Femtosecond Emission Microscopy of Exciton Dynamics in Semiconductor Nanoparticles

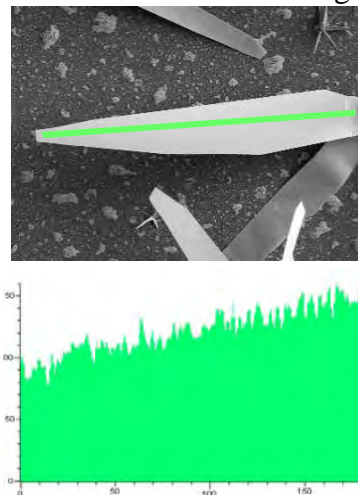
Jianhua Bao, Lars Gundlach and Piotr Piotrowiak
Department of Chemistry
Rutgers University
Newark, New Jersey 07102

Recent efforts of our group concentrated on the development of new ultrafast fluorescence microscopy techniques and applying them to investigate electron and energy transfer processes in nanostructured systems. The temporal resolution of commercial microscopes is inadequate for the study of these events which occur on femtosecond and short picosecond time scales. To overcome this limitation we constructed a Kerr-gated microscope capable of collecting wide-field emission ‘movies’ with an unprecedented resolution of 100 fs (see below). Ultrafast fluorescence microscopy combines the temporal and spectral resolution of femtosecond pump-probe spectroscopy with the ability to image and monitor individual objects, down to the single particle level. The technique is general and can be applied both to ‘hard’ and ‘soft’, molecular materials.



Selected 100 fs frames of a luminescence “movie” showing the inhomogeneous temporal response of a group of CdS_xSe_{1-x} nanobelts. The complete movie is available on the JPC site. The dark-field view of the cluster is shown on the left.

Using our instrument we were able to analyze the photoluminescence dynamics in individual CdSSe nanobelts and resolve the competing linear and non-linear charge recombination channels. CdSSe and other ternary semiconductor nanoparticles are excellent candidates for solar energy conversion applications. Thanks to the small lattice mismatch a wide range of bandgaps from 1.7 to 2.4 eV (508 to 718 nm) can be obtained. This unusually broad tunability can be further augmented in nanosized CdSSe by quantum size effects. As a result, optimal matching of the solar spectrum for light harvesting can be achieved. We initiated a project aimed at controlled growth CdSSe nanobelts and nanowires with large bandgap gradients. The initial results are promising. The SEM-EDS scan on the right shows the sulfur content along the main axis of a less than 20 nm thick, 100x15 μm nanobelt. We are currently refining the growth procedures. The ultrafast fluorescence microscope will be used to probe the exciton relaxation along the bandgap gradient, with the long-term goal of achieving controlled, directional flow of the generated carriers. In earlier experiments on the CdSS nanobelts without intentionally introduced composition gradients we observed sub-picosecond localization of the emission at the tip of the particle. It is important to understand whether such localization occurs due to shape-induced confinement effects or results from composition inhomogeneity.



Imaging Proton-Coupled Electron Transfer Pathways in Natural Photosynthesis

Oleg G. Poluektov, Lisa M. Utschig, David M. Tiede

Chemical Sciences and Engineering Division

Argonne National Laboratory

Argonne, IL 60439

K. V. Lakshmi

Department of Chemistry and Chemical Biology

Rensselaer Polytechnic Institute

Troy, NY 12180

The goal of our research is to understand the function of the protein in optimizing solar energy conversion. Specifically we investigate: the protein's role in controlling optimal pathways for proton-coupled ET (PCET) reactions; the response of the protein to rapid charge transfer and separation; and local cofactor site structure related to conformationally gated ET. The experimental approach includes the application of a suite of advanced, multi-frequency, time-resolved magnetic resonance techniques together with capabilities to prepare specialized RC samples. Here we report on the application of time-resolved (TR) electron-nuclear double resonance (ENDOR) spectroscopy at high magnetic field. ENDOR is a unique technique which allows direct measurement of the distribution of the spin densities of unpaired electrons wave function and reconstruction of the geometry of the protein environment via magnetic nuclei coupling with electron spin.

Q_A relaxation following photoinduced ET. Owing to transient features of the TR-ENDOR technique, the spin density distribution can be followed in time and provides important information about the protein environment's response to photoinduced ET. Spectral analysis of the ²H-ENDOR of deuterated Q_A substituted into protonated purple bacterial RCs demonstrates that positions of the ENDOR lines, recorded shortly after ET, do not coincide with the positions of the same peaks in the thermalized spectrum. These shifts provide direct spectroscopic evidence of protein environmental reorganization that accommodates the donor-acceptor CS state. TR-ENDOR provides evidence that ET induces a small-scale reorganization at the level of the global H-bonding network.

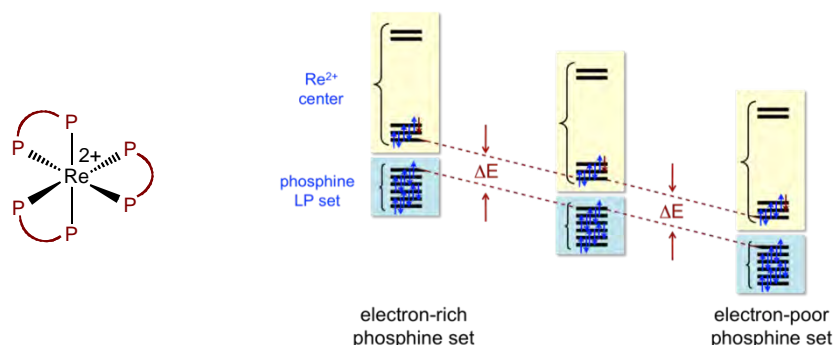
PCET at the TyrD Residue of Photosystem II. TyrD in PSII can be oxidized at cryogenic temperatures, T < 10 K, where both proton and protein motions are limited. Annealing this state at a slightly higher temperature allows proton movement and relaxation of the protein environment. ²H ENDOR spectroscopy was used to investigate the sequence of events that lead to PCET at the TyrD site of PSII. These studies provide 'snapshots' of functional PCET intermediates and make it possible to directly observe the mechanism of PCET in biological energy transduction. Our results show that electron transfer, proton movement and associated conformational changes of the TyrD-binding pocket are individual steps of the PCET reaction.

Localization of the protons involved in PCET in bacterial RCs. Orientational dependence of the matrix proton TR-ENDOR spectra of deuterated purple bacteria RCs in deuterated buffer allows us to identify a number of exchangeable protons involved in the ET process. These protons are located close to the primary acceptor pheophytin and belong to Trp100L and Glu104L amino acid residues. This finding supports our previous hypothesis that matrix relaxation responsible for the ET regulation in the bacterial RCs occurs around the pheophytin cofactor.

Advances in Re(II) Photo-oxidant Complex Chemistry

Dean M. Roddick, Jeramie J. Adams, and Navamoney Arulsamy
Department of Chemistry, Dept. 3838
University of Wyoming
Laramie, WY 82071

We have previously reported new Re(II) polyphosphine systems based on the novel highly-oxidizing excited state (HOES) complex $(dmpe)_3Re^{2+}$ ($dmpe = Me_2PCH_2CH_2PMe_2$), which was the subject of chloride and arene emission quenching studies by Sullivan *et al* in 2006. Primary findings were (1) Increased emission lifetime for more electron-rich $(depe)_3Re^{2+}$ ($depe = Et_2PCH_2CH_2PEt_2$) relative to $(dmpe)_3Re^{2+}$, (2) A quenching of emission for $(R_2PCH_2PR_2)_3Re^{2+}$ systems with single methylene diphosphine chelate bridges, and (3) An insensitivity of absorption and emission energies for $(R_2P(CH_2)_nPR_2)_3Re^{2+}$ ($n = 1$ or 2 ; $R = Me, Et, Ph$) despite a 500 mV ground state variation in $E_0(Re^{2+}/Re^+)$ between $+0.16$ and $+0.6V$. This invariance is ascribed to a compensating shift in metal orbital energies with the energy of the phosphine donor set which determine the LMCT energy gap:



Current research focuses on the development and study of a wider variety of Re(II) polyphosphines. Efforts to prepare the arylphosphine chelate $(dppe)_3Re^{2+}$ ($dppe = Ph_2PCH_2CH_2PR_2$) afforded only the *trans* bis-chelate *trans*- $(dppe)_2ReI_2$. A new phenylene-bridged tris chelate, $[(1,2-C_6H_4(PMe_2)_2)_3Re^{2+}]$, however, has been prepared and characterized. *trans*- $(dppe)_2ReI_2$ provides a starting point for the synthesis of a more flexible class of tetragonally-distorted Re(II) compounds *trans*- $(dppe)_2Re(L)_2^{2+}$. The nitrile complex *trans*- $(dppe)_2Re(MeCN)_2^{2+}$ has been prepared by iodide abstraction with Ag^+ in acetonitrile. However, abstraction in the presence of $L = PR_3$ or py leads to Re(III) products. Abstraction under an atmosphere of CO does give the blue dicarbonyl complex *trans*- $(dppe)_2Re(CO)_2^{2+}$. The photophysical properties of new Re(II) systems will be presented.

Concurrent with synthetic studies, photoredox quenching studies (in collaboration with Russell Schmehl, Tulane University) have focused on the $(dmpe)_3Re^{2+}$ and $(depe)_3Re^{2+}$ systems. Quenching is observed for a wide range of aromatics; however, charge-separated aryl radical cations are only observed for readily oxidized alkoxy- and amino-aromatics. This variation in charge recombination and separation is believed to stem from inner- and outer-sphere reorganization energies.

Microwave Absorption Studies of Charge Transfer at Planar Bulk Heterojunction Interfaces

Garry Rumbles, Andrew Ferguson, David Coffey, Smita Dayal, and Nikos Kopidakis.

Chemical and Materials Center
National Renewable Energy Laboratory
Golden, Colorado 80401-3393

We report on studies of photo-induced electron transfer between conjugated polymers blended with fullerenes, as well as some new studies of donor-acceptor bi-layer systems of vapor-deposited molecular thin films, and solution-deposited conjugated polymers on colloidal quantum dot arrays. Using flash photolysis, transient microwave conductivity (fp-TRMC) we have studied exciton transfer and dissociation at the interfaces formed between in these systems. The technique is proving to be an invaluable tool, providing us with the ability to probe the yield and kinetics of the formation of mobile carriers created in nanoscale donor-acceptor networks.

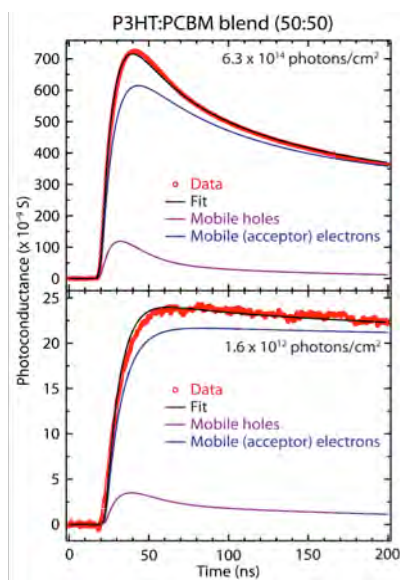


Figure 1 – TRMC transients at low and high laser fluences on a 50:50 blend of PCBM in P3HT. The modeling shows that the absorption signal is dominated by electrons in PCBM clusters.

Our recent work on the investigation of blends of fullerenes in conjugated polymers, demonstrates that we are able to detect the formation of fullerene clusters through the presence of a microwave absorption signal that is a signature for mobile electrons and that is distinct from the mobile holes in the donor polymer. A result from one of our modeling efforts is shown in Figure 1 for a 50:50 blend of a fullerene (PCBM) in poly(3-hexylthiophene). This study has enabled us to understand the kinetics of the excitons and charge carriers in bulk heterojunctions, which is the foundation of the prototypical solar cell created from these blends. We can now demonstrate that the ability to detect fullerene clusters of this type provides us with an invaluable method for probing nanoscale morphologies in these complex blends. This effect will be reported through the studies of a range of new conjugated polymers and substituted fullerenes.

The complex morphologies exhibited by the blends, although of technological value, make the fundamental investigation of the photophysics that occurs at the interface a difficult one to study. To overcome this issue we are constructing planar heterojunctions using vapor-deposited molecules, such as phthalocyanines and perylenes, onto C_{60} , and not its soluble derivative, PCBM, often used in blends. Such systems, studied by fp-TRMC, enable us to understand the role of both exciton dissociation, and the transfer of the exciton energy to the fullerene, followed by back transfer the hole. By attaching electrodes to the multi-layer constructs, we are able to extract the photo-generated carriers, and compare the yields with those measured by microwave absorption. We will also report some studies of planar interfaces formed between an assembled array of colloidal quantum dots with a layer of conjugated polymer deposited on top. By changing the nature of the bi-functional ligands that couple the QDs, we are able to probe the influence of electronic coupling and the role of nanoscale networks on the primary photo-induced electron transfer processes.

Characterizing Coupled Charge Transport with Multiscale Simulations

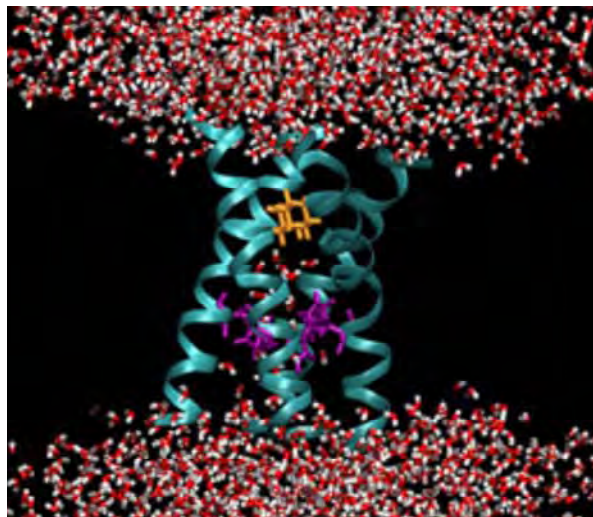
Jessica M.J. Swanson

Chemical Sciences and Engineering, Argonne National Laboratory
9700 S. Cass Ave. Bldg. 200, Argonne, IL 60439

This research aims to establish computational methods to characterize reactions involving electron transfer coupled to proton dynamics/transport, herein termed *coupled charge transport*. This phenomenon enables efficient (i.e., little wasted energy) multi-electron chemistry (oxidation/reduction reactions) from single photon excitations by stabilizing intermediate species. Incorporating similar coupled charge transport processes into artificial catalysts may be essential to obtain the requisite efficiency for breakthrough alternative energy technologies.

The goals of this work are three-fold: 1) to gain mechanistic insights into coupled charge transport processes that will aid in the development new energy-relevant catalysts and materials, 2) to fill the gap in current theoretical investigations of coupled charge transport by treating systems in aqueous environments that involve proton *transport* to or through multiple molecules (as opposed to *transfer* from donor to acceptor), and 3) to build a theoretical program to complement the experimental work in Argonne's Solar Conversion Group. One of the group's central aims is to understand multi-electron reactions involving coupled charge transport at the molecular, atomic and electronic levels. Attaining this level of physical insight is expected to demand complementary experimental and theoretical breakthroughs.

Herein, the early stages of a computational method called Coupled Charge Transport Molecular Dynamics (CCT-MD) will be described and its use on a model system demonstrated. CCT-MD combines *ab initio* calculations with the necessary statistical sampling (via simulation) to describe quantum processes, which occur on the *femto-* to *pico-*second timescale, coupled to transport over the *nano-* to *milli-* second time scales for complex systems involving hundreds to thousands of atoms. The basic strategy in CCT-MD will be to describe proton solvation and transport in a multi-configuration representation, which wraps the electronic delocalization of the excess proton into classical Newtonian dynamics of the nuclei, while simultaneously accounting for transitions between electronic states. The model system studied herein is a transmembrane tetra-helix bundle containing two protonatable Histidine residues and the surrounding membrane and aqueous environment (see figure). Results for an electronic transition and the coupled proton dynamics will be discussed.



Tetrahelix Model System containing two histidine residues and an explicitly solvated excess proton (membrane not shown for clarity).

Single-Chain, Helical Wrapping of Individualized, Single-Walled Carbon Nanotubes by Ionic Poly(Aryleneethynylene)s: New Compositions for Photovoltaic Systems

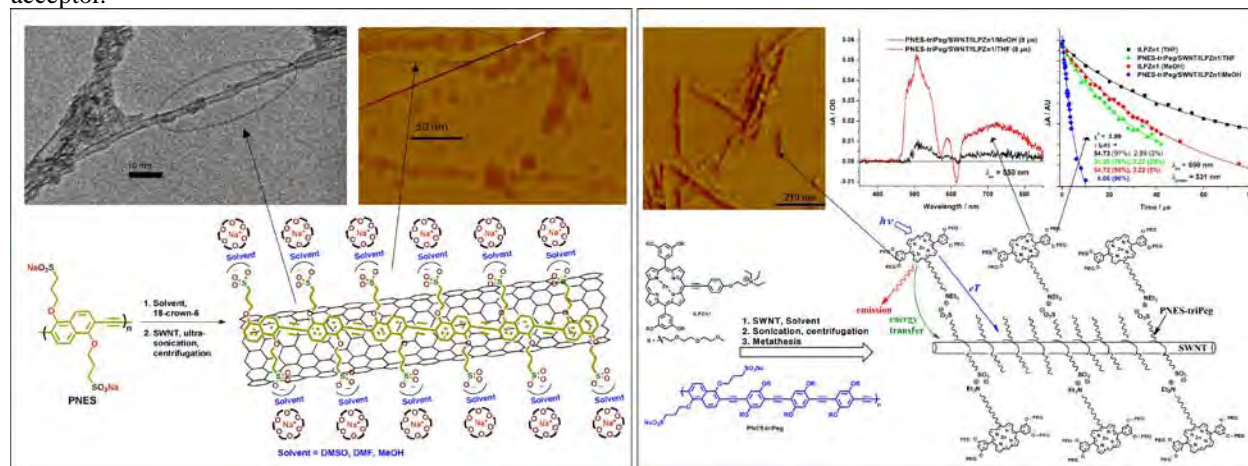
Pravas Deria,^a Youn K. Kang,^b One-Sun Lee,^b Sang Hoon Kim,^c Tae-Hong Park,^b Ian Stanton,^a Dawn A. Bonnell,^c Jeffery G. Saven,^b and Michael J. Therien^a

^aDepartment of Chemistry, French Family Science Center, 124 Science Drive, Duke University, Durham, NC 27708

^bDepartment of Chemistry, University of Pennsylvania, 231 South 34th Street, Philadelphia, PA 19104

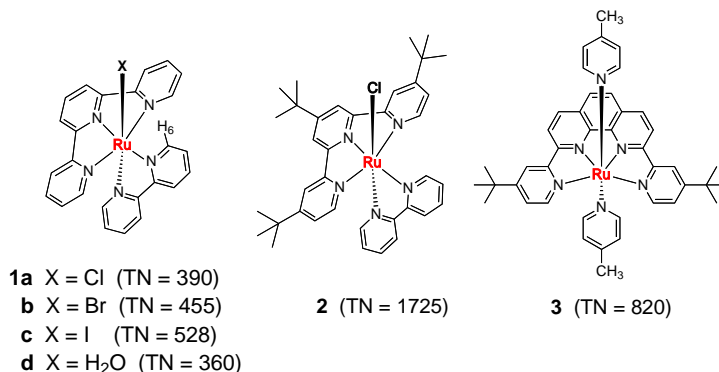
^cDepartment of Materials Science and Engineering, University of Pennsylvania, 3231 Walnut Street, Philadelphia, PA 19104;

Amphiphilic, linear conjugated poly[*p*-{2,5-bis(3-propoxysulfonicacidsodiumsalt)}phenylene]ethynylene (**PPES**) and poly[2,6-{1,5-bis(3-propoxysulfonicacidsodiumsalt)}naphthylene]ethynylene (**PNES**) efficiently disperse single-walled carbon nanotubes (SWNTs) under ultra-sonication conditions into the aqueous phase. Vis-NIR absorption spectroscopy, atomic force microscopy (AFM), and tunneling electron microscopy (TEM) demonstrate that these solubilized SWNTs are individualized. AFM and TEM data reveal that the interaction of **PPES** and **PNES** with SWNTs gives rise to self-assembled superstructures in which a polymer monolayer helically wraps the nanotube surface; the observed **PPES** and **PNES** pitch lengths confirm structural predictions made via MD simulations. Following appropriate metathesis reactions, these self-assembled polymer-nanotube systems can be dissolved in organic solvents; AFM and TEM data confirm that the **PNES** helical wrapping structure observed for individualized SWNTs in aqueous solution persists in nonaqueous media. Steady-state and time-resolved spectroscopic studies reveal that these structures maintain established SWNT semi-conducting and conducting properties, regardless of solvent. These superstructures can be subjected to metathesis reactions that non-covalently deliver auxiliary redox centers to the SWNT backbone, suitable for photo-activated electron transfer to a polymer-wrapped nanotube acceptor.

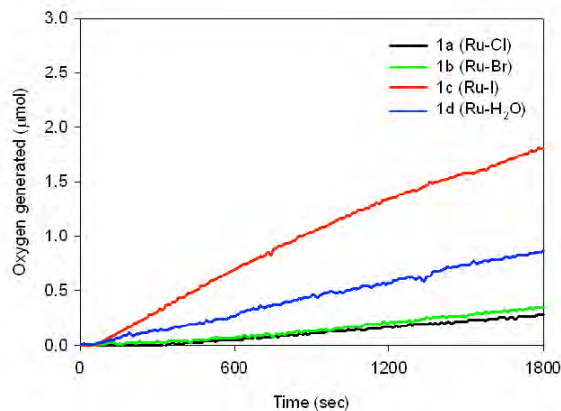


Further Observations on Water Oxidation Catalyzed by Mononuclear Ru(II) Complexes

Ruifa Zong, Nattawut Kaveevivitchai, Maya El Ojaimi, and Randolph P. Thummel
Department of Chemistry, 136 Fleming Building, University of Houston,
Houston, TX 77204-5003



There has been considerable recent discussion concerning the oxidation of water using mononuclear Ru-based catalysts.¹ In our study, a synthetic approach has been followed to help better understand factors that contribute to the design of an effective catalyst. Complexes of the general type [Ru(bpy)(tpy)X]⁺ (bpy = 2,2'-bipyridine, tpy = 2,2'; 6',2"-terpyridine, X = halogen or other monodentate), along with others, have been studied. The catalysts are evaluated by using Ce(IV) as a sacrificial oxidant. Besides variation of the bi- and tridentate ligands, we have also examined different monodentates such as the halogens: chloride, bromide, and iodide. The H₆ proton on the bpy ligand is a very sensitive indicator as to the nature of X. The counter-ion, reaction medium, and cerium source are also found to have some effect. We find that the hydrolysis of **1a** and **1b** is considerably faster than **1c**, yet the rate of oxygen generation and the turnover number using the iodo-complex (**1c**) as catalyst is greater than the other halo-complexes and also greater than the aqua-complex (**1d**). The mechanistic implications of these studies will be presented.



Reference

1. Tseng, H.-W.; Zong, R.; Muckerman, J. T.; Thummel, R. *Inorg. Chem.* **2008**, *47*, 11763-11773.

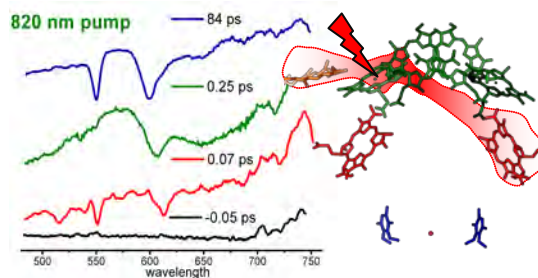
Mapping Structure with Function in Natural and Biomimetic Photosynthetic Architectures

David M. Tiede¹, Karen L. Mulfort¹, Nina Ponomarenko¹, Lin X. Chen¹, Lisa M. Utschig¹, Oleg G. Poluektov¹, and Libai Huang² and Gary Wiederrecht³

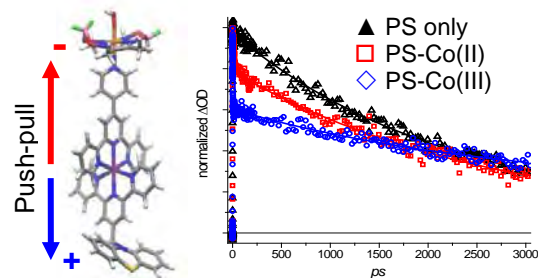
¹Chemical Sciences and Engineering Division and ³Center for Nanoscale Materials, Argonne National Laboratory, Argonne, IL 60439, ²Radiation Laboratory, University of Notre Dame Notre Dame, IN 46556

Natural photosynthetic architectures are characterized by hierarchical, modular designs and module-specific protein host-cofactor guest chemistries. This partitioning of photochemical function allows the individual light-harvesting, charge separation, water-splitting and reductive fuels tasks of solar energy conversion to be optimized within individual functional modules, which can then be integrated for overall solar energy conversion function. In this program we are investigating correlations between structure and photosynthetic function in natural photosynthetic and supramolecular biomimetic architectures.

Ultrafast mapping of photosynthetic solar energy flow. We have used polarization selective ultrafast spectroscopy of cryogenically cooled (100 K) single reaction center crystals from *Rhodobacter sphaeroides* to reveal remarkable new features of the earliest events in photosynthetic solar energy capture. The earliest excited state produced by selective cofactor excitation was found to be highly delocalized across multiple reaction center cofactors and decays within 0.25 ps to form a localized excited state on the bacteriochlorophyll dimer. The delocalization pattern differs markedly depending upon the cofactor chosen for excitation. The results are suggestive of different networks of electronic coupling, and allow excited state photochemistry to be mapped onto the atomic coordinate structure of the bacterial reaction center.



Supramolecular cobaloxime-based H₂ photocatalysts. We are investigating structure-function correlations for hydrogen-evolving supramolecular motifs that are designed to probe the photosensitizer-catalyst distance, geometry, coupling motif, and potential for through-bond as well as through-space photo-induced electron transfer pathways. For photosensitizer-cobalt H₂ catalyst (PS-Co(III) or II) assemblies connected by axially-coordinated pyridyl linkers, a large variation is found in the rate and extent of multiphasic photo-induced electron transfer (PET) that is independent of reaction driving force. The results suggest that PET is limited by electronic coupling and configurational dispersion and suggest design strategies for next-generation photocatalyst architectures.



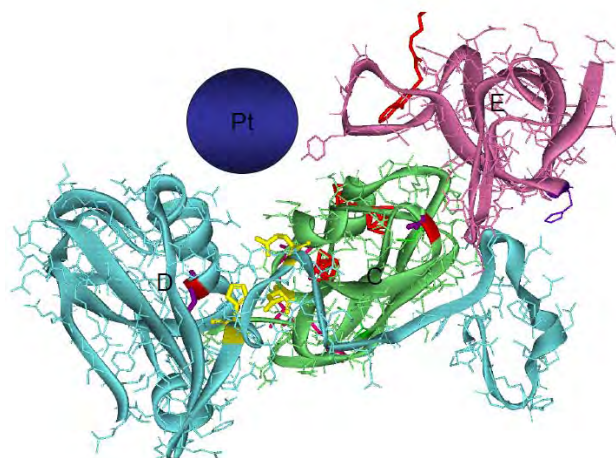
Photosynthetic Interprotein and Biohybrid Electron Transfer

Lisa M. Utschig, Oleg G. Poluektov, Lin X. Chen, Jenny V. Lockard, Sergey D. Chemerisov,
Karen Mulfort, David M. Tiede
Chemical Science and Engineering Division
Argonne National Laboratory
Argonne, IL 60439

Photosynthetic reaction center (RC) proteins are finely tuned molecular systems optimized for solar energy conversion. The primary reaction in RCs involves rapid, sequential electron transfer that results in stable charge separation. Following efficient charge separation, the energy captured is utilized in a series of reactions that ultimately drive the chemical conversion of CO₂ into carbohydrates. Our group has initiated efforts to mimic Nature and make use of the initial light-initiated RC reactions to drive non-native chemical reactions for solar fuels production. To this end, recent work is focused on understanding structure-function relationships in natural photosynthetic systems with the intent of applying this knowledge to the design and optimization of novel biohybrid systems. Specifically, we are initiating research efforts to understand native protein docking events and interprotein electron transfer from Photosystem I (PSI) to its native acceptor proteins, ferredoxin (Fd) or flavodoxin (Fld). Our experimental approach utilizes both specialized “spin-edited” samples and multifrequency pulsed electron paramagnetic resonance (EPR) techniques as well as X-ray absorption fine structure (XAFS) spectroscopy.

Studies of PSI electron transfer to the Fd and Fld acceptor proteins suggest that electron transfer in PSI-acceptor protein complexes are more efficient than in PSI alone. Using fully deuterated Fld, we can distinguish the EPR signals of reduced Fld and oxidized primary donor P⁺ at X- and D-band. We have examined the light-induced EPR spectra of PSI-Fld and surprisingly observe low temperature ET, with a 1:1 yield of P⁺:Fld⁻ formation. Furthermore, we detect Fld-induced changes in the time-resolved EPR spectra PSI-Fld complex. These Fld-induced changes may relate to Fd-induced effects observed with X-band EPR that show facile reduction of Cu²⁺ sites in the presence of Fd. XAFS studies of PSI Cu²⁺ sites provide the first direct experimental evidence of light-induced structural changes in PSI. Our working premise is that acceptor protein binding induces conformational changes in PSI that facilitate highly efficient electron transfer through the terminal Fe-S clusters.

Capitalizing on these fundamental RC results, we have initiated efforts to link catalysts on the stromal end of PSI. We have developed methods to prepare Pt-nanoparticle complexes with PSI and hypothesize that Pt-nanoparticles are mimicking native acceptor protein binding to a stromal ridge provided by PSI (Figure). Initial measurements of our PSI-Pt nanoparticle complexes show photocatalytic H₂ production rates comparable to rates for Pt nanoparticles directly linked via a molecular wire to the terminal F_B cluster of PSI. This work with Pt nanoparticles proves that the stromal binding pocket is a reasonable target location for attaching molecular catalysts and provides a key experimental system for photofunctional hybrid system development.



Imaging of Energy and Charge Transport in Nanoscale Systems

Jao van de Lagemaat[†] and Manuel Romero[‡]

[†]Chemical Sciences and Materials Sciences Center

[‡]National Center for Photovoltaics

National Renewable Energy Laboratory

Golden, Colorado, 80401

Recent developments in the scientific study of nanoscale matter by spectroscopic and microscopic techniques have made possible increased scientific insight into the fundamental interaction of matter and energy at small scales. Often, applications of these phenomena depend on the extraordinary and sometimes unexpected properties of electrons and excitons when confined to small spaces. The techniques that address these phenomena either have a good energy resolution, a good spatial resolution, or a good temporal resolution, but not all at the same time. The current project aims to investigate nanoscale energy and charge flow in photochemical conversion systems by expanding a technique based on scanning tunneling luminescence to also include energetic resolution and temporal resolution

In previous work, we have shown that the single particle tunneling luminescence from CdSe:ZnS core-shell quantum dots bound to gold substrates was due to the creation of localized surface plasmons that transfer their energy to the quantum dots.¹ In current work,² we have demonstrated that exciton transport in organic semiconductors such as P3HT can be effectively studied using tip-enhanced tunneling luminescence (Fig. 1). Energy transfer from the surface plasmon between the tip and the substrate excites the polymer. When there is an acceptor (i.e. PCBM) interface nearby, electron transfer should occur and no luminescence should be observed. When no acceptor is nearby, luminescence should be relatively efficient. Indeed, it was found that upon annealing of the mixes, strong spatial inhomogeneities arose in the local, tunneling induced luminescence that correlate to the phase segregation observed in such heterojunction blends. This indicates that our technique can be used to determine exciton diffusion length and to study exciton transport in such systems.

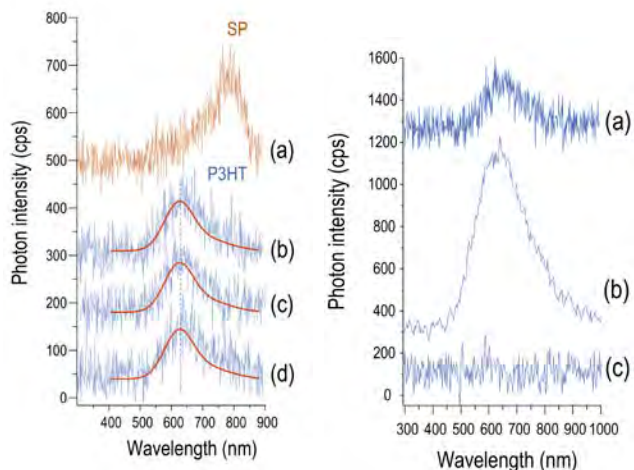


Fig 1. (left) Tunneling luminescence of P3HT layers on a gold substrate. The presence of the P3HT extinguishes the gold surface plasmon. (right) tunneling induced luminescence of P3HT on (a) gold, (b) silver, and (c) ITO.

¹ M. J. Romero and J. van de Lagemaat. *Phys. Rev. B* **80**, 2009, 115432

² M. J. Romero, A. J. Morfa, T. H. Reilly III, J. van de lagemaat, M. Al-Jassim, *Nano Lett* **9**, 2009, 3904

Transport and Bimolecular Electron Transfer in Ionic Liquids

James F. Wishart and Masao Gohdo
Chemistry Department
Brookhaven National Laboratory
Upton, NY 11973

Ionic liquids are complex fluids that display domain-like structure on the nanometer scale, often exhibiting multiple disordered phases as well as dynamic heterogeneity on the femtosecond to nanosecond time scales.[1] As highlighted in several DOE BES Basic Research Needs reports and recent literature, ionic liquids are emerging as important components in systems that employ charge transfer and the transport of molecules and charge to produce, store and efficiently utilize energy.[2,3] Fundamental studies of these phenomena in ionic liquids are needed to provide the knowledge base for successful use of these interesting materials. As part of a 5-group collaboration on the fundamentals of electron transfer and dynamics in ionic liquids, the studies at BNL focus on pulse radiolysis and flash photolysis studies of diffusion and electron transfer phenomena in ionic liquids, including the use of pressure dependence to elucidate anomalous diffusion mechanisms and the details of solvation dynamics. We will present our early results on comparisons of electron transfer reactions involving neutral versus charged reactants, which have been shown to have significantly different mobilities in ionic liquids.

1. *Spotlight on Ionic Liquids*, E. W. Castner and J. F. Wishart, *J. Chem. Phys.* **132**, 120901 (2010).
2. *Guest Commentary: Importance of ionic liquid solvation dynamics to their applications in advanced devices and systems* J. F. Wishart, *J. Phys. Chem. Lett.* **1**, (2010) in press. DOI: 10.1021/jz100532k.
3. *Energy applications of ionic liquids* J. F. Wishart, *Energy Environ. Sci.*, **2**, 956 - 961 (2009).

Basic Studies and Novel Approaches for Photoelectrosynthesis

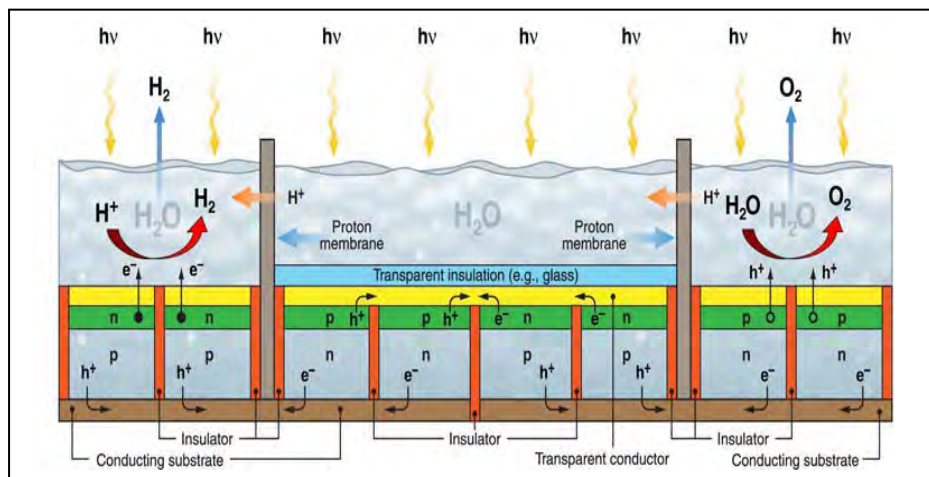
J.A. Turner, N.R. Neale, H. Branz, A.J. Frank, M. Beard, S.H. Wei, A.J. Nozik (P.I.)

Postdocs: D.A. Ruddy, J.Ma, J. Oh, F. Toor, P.T. Erslef

Chemical and Materials Science Center
and National Center for Photovoltaics
National Renewable Energy Laboratory
Golden, CO, 80401-3393

Abstract

Novel approaches to efficient solar water splitting based on abundant and low cost silicon micron and nanoscale structures are being investigated. These will be based on (1) Si micron-sized and nanoscale-sized patterned segregated cubes to avoid photocorrosive/photooxidative catastrophic failure, (2) macroscale p-n junctions between n-and p-doped nanocrystalline films formed from Si nanocrystals (NCs), and (3) Si nanowires that form p-n junctions connected in series electrically but illuminated in parallel.



(1) A photoelectrolysis cell based on Si microcubes arranged in 4 panels is shown in the Figure. By using isolated, micron-sized photoelectrolysis cells operating independently in parallel, the spreading of local photocorrosion is

prevented, and the failure of one set of cells does not affect the others.

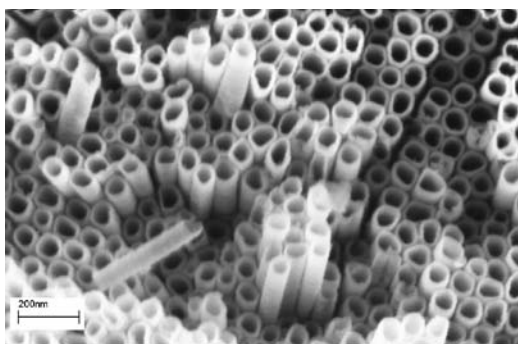
(2) Because of quantum confinement, Si NCs will have bandgaps (HOMO-LUMO) that are determined by their size and can exceed their bulk bandgaps (1.12 eV for Si). Thus, the NC bandgaps can range from 1.2-2.0 eV for Si NCs with sizes from 10 to 3.5 nm, respectively. Two nanocrystalline p-n junctions with two different bandgaps can be formed into tandem type photochemical diode structures to generate sufficient photovoltage to split H_2O .

(3) In a combination of 1 and 2, co-axial p-n Si quantum wires (also called nanowires (NWs)) arranged in 2 or 4 panels similar to the figure, except that the NWs form carpet-like arrays rather than QD arrays of microspheres or microcubes. Two panels can be used if the wires are thin enough ($< 5-7$ nm) to be in the quantized regime such that the sum of the two photovoltages in the 2 series-connected p-n NWs is about 1.8 to 2 volts, sufficient to drive the water splitting reaction.

Ultra-stable Molecule-Surface Architectures at Metal Oxides

Michelle Cooperrider, Ryan Franking, Kacie Louis, Michael McCoy, and Robert J. Hamers
Department of Chemistry
University of Wisconsin-Madison
Madison, WI 53706

Oxide materials are widely known for their catalytic properties. Our work is focusing on the development and application of surface chemistries that will enable oxide materials to be linked with organic molecules to enhance light absorption and catalytic properties, and as means for preparing self-assembled nanoscale heterostructures. To address this need, we are exploring new fundamental chemistry for making highly stable molecular interfaces to oxide materials, with a goal of developing a toolkit of reactions that can be used to achieve self-assembled photocatalytic systems. In the early stages of this work, we have been investigating the use of photochemical reactions to link organic alkenes to oxide materials and exploring multi-step syntheses on nanostructured oxides. Studies of photochemical grafting are motivated by the fact



TiO₂ nanotubes fabricated by electrochemical etching of Ti

that our studies have shown that molecular layers formed by this route can have unprecedented chemical stability in contact with aqueous media. More recently we have been investigating the factors that control the mechanism of this reaction, including formation of monolayers vs. multilayers and the influence of different substitutional groups of the reactant molecules on the subsequent photochemistry. We have also been using time-resolved microwave reflectivity measurements to characterize carrier lifetimes with the intent of studying how surface functional groups impact lifetimes of electrons and

holes. Ongoing studies are using TiO₂ in multiple forms including single crystals, nanocrystalline thin films, and as high surface-area nanotubes like those shown at left.

A major goal of our work is to enable development of versatile surface chemistries that will enable multi-step synthesis for linking complex structures such as molecular catalysts to surfaces. Our efforts this far have focused on using ligand-exchange reactions to link propionic and/or 3,4-dihydroxybenzaldehyde (DHBA) to metal oxide surfaces, particularly TiO₂ and Fe₂O₃. DHBA contains a free aldehyde group that can be used as a handle for subsequent surface chemistry via Schiff base formation. Using this approach we have succeeded in performing multi-step syntheses on TiO₂ nanoparticles to control properties such as aqueous stability over a wide range of pH. Because simple carboxylic-modified surfaces are unstable at low pH, the above ideas are also being applied to multidentate ligands. A specific target of ongoing work is to enable “click” chemistry for forming catalytically active oxide-oxide heterojunctions via simple wet-chemical routes. Thus far we have succeeded in making and characterizing alkyne-modified nanoparticles, with complementary efforts to form azide-modified nanoparticles ongoing. These studies will enable chemical methods to be used for the self-assembly of novel oxide-based photocatalysts..

Metal-Linked Artificial Oligopeptides as Scaffolds toward Photoinitiated Molecular Wires

Carl P. Myers, Joy A. Gallagher, Seth Ostheimer and Mary Elizabeth Williams*

Department of Chemistry
The Pennsylvania State University
University Park, PA 16802

Controlled assembly of multimetallic artificial oligopeptides using modular, interchangeable units provides a library of architectures for photoinitiated charge separation. Artificial oligopeptides are cross-linked by metal bonds, and act as scaffolds to make heterofunctional and heterometallic structures. We synthesize modular amino acid units linked by amide bonds to construct multimetallic oligopeptides with unique sequences. Directed self-assembly of the peptides using metal chelation will ultimately be employed to construct useful supramolecular structures for photochemical conversion of energy.

Multifunctional aminoethylglycine (aeg) derivatized $[\text{Ru}(\text{bpy})_3]^{2+}$ complexes with pendant bipyridine (bpy) ligands coordinate Cu^{2+} to form coordinative chain crosslinks in a “hairpin loop” motif.¹ We recently reported the synthesis and characterization of a series of Ru aeg “hairpins” in which the relative aeg chain length and number of pendant bpy ligands is varied.² Coordination of Cu^{2+} causes quenching of the excited state Ru species; the degree of quenching efficiency depends on the location and number of coordinated Cu ions. These data reveal only a shallow decrease in k_{nr} with increasing distance between the Ru and Cu complexes, suggestive of excited state electron transfer as the quenching mechanism.

Figure 1. General structural motifs of the Ru aeg hairpin, where Ru is $\text{Ru}(\text{bpy})_2$, M is a second transition metal, L is bpy, and n is the number of repeat units on the chain.

More recent studies have focused on transient absorption spectroscopy to determine the excited state quenching mechanism in the di- heterometallic Ru hairpins.³ Analogs containing Ni, Pd, Pt, Co and Cd have been prepared for comparison of the photodynamics as a function of relative redox and spectroscopic properties.⁴ The structures have been further elaborated by preparing Ru complexes containing two and three “hairpin”-modified bpy ligands, which are reacted with metal ions to make tri- and tetra- metallic assemblies.⁵ In proof of concept experiments, di- and trimetallic Ru-Pd structures have been used for photoinduced catalytic dimerization of styrene,⁶ demonstrating the potential for using these structures to study artificial photosynthesis.

¹ Myers, C. P.; Gilmartin, B. P.; Williams, M. E. “Aminoethylglycine-Functionalized $\text{Ru}(\text{bpy})_3^{2+}$ with Pendant Bipyridines Self-Assemble Multimetallic Complexes by Cu and Zn Coordination” *Inorg. Chem.* **2008**, *47*, 6738.

² Myers, C. P.; Miller, J. R.; Williams, M. E. “Impacts of the Location and Number of $[\text{Cu}(\text{bpy})_2]^{2+}$ Crosslinks on the Emission Photodynamics of $[\text{Ru}(\text{bpy})_3]^{2+}$ with Pendant Oligo(aminoethylglycine) Chains” *J. Am. Chem. Soc.* **2009**, *42*, 15291.

³ Myers, C. P.; Rack, J. J.; Williams, M. E. “Transient Absorption Spectroscopy of Ru-M Complexes Linked by Aminoethylglycine Show Quenching Mechanisms that Vary with Bound Metal.” *In preparation*

⁴ Ostheimer, S.; Myers, C.P.; Williams, M. E. “Aminoethylglycine-Functionalized $\text{Ru}(\text{bpy})_3^{2+}$ with Pendant Bipyridines Form Heterometallic Complexes with Cd, Ni, Co, Pt, and Pd with Variable Photophysical and Redox Behaviors”, in preparation

⁵ Myers, C. P.; Ostheimer, S.; Miller, J. R.; Williams, M. E. “Aminoethylglycine-Functionalized $\text{Ru}(\text{bpy})_3^{2+}$ Di- and Tri-Hairpin Complexes Form Controlled Tri-Heterometallic Structures with Pd^{2+} and Cu^{2+} .”

⁶ Myers, C. P.; Williams, M. E.* “Aminoethylglycine-Functionalized $\text{Ru}(\text{bpy})_3^{2+}$ Complexes with Pendant $\text{Pd}(\text{bpy})(\text{CH}_3)(\text{X})$ Photocatalytically Dimerize Styrene.” *In preparation.*

List of Participants

Participants List – 32nd DOE Solar Photochemistry Research Meeting

Joel Ager
Lawrence Berkeley National Laboratory
1 Cyclotron Rd.
Berkeley, CA 94720
Phone: 510-486-6715
E-Mail: JWAger@lbl.gov

Neal Armstrong
University of Arizona
Department of Chemistry
Tucson, AZ 85721
Phone: 520-621-8242
E-Mail: nra@email.arizona.edu

Paul Barbara
University of Texas Austin
CNM
Austin, TX 78712
Phone: 512-694-8903
E-Mail: p.barbara@mail.utexas.edu

Allen Bard
University of Texas at Austin
1 University Station A5300
Austin, TX 78712-0165
Phone: 512-471-3761
E-Mail: ajbard@mail.utexas.edu

Tunna Baruah
University of Texas at El Paso
500 W. University Avenue
El Paso, TX 79968
Phone: 915-747-7529
E-Mail: tbaruah@utep.edu

Victor Batista
Yale University
225 Prospect St
New Haven, CT 06520
Phone: 203-432-6672
E-Mail: victor.batista@yale.edu

Matt Beard
National Renewable Energy Laboratory
1617 Cole Blvd
Golden, CO 80007
Phone: 303-384-6781
E-Mail: matt.beard@nrel.gov

Jeffrey Blackburn
National Renewable Energy Laboratory
16523 Denver West Parkway
Golden, CO 80401
Phone: 303-384-6649
E-Mail: jeffrey.blackburn@nrel.gov

David Blank
University of Minnesota
207 Pleasant St SE
Minneapolis, MN 55455
Phone: 612-624-0571
E-Mail: blank@umn.edu

Andrew Bocarsly
Princeton University
Frick Laboratory
Princeton, NJ 8544
Phone: 609-258-3888
E-Mail: bocarsly@princeton.edu

David Bocian
University of California, Riverside
Department of Chemistry
Riverside, CA 92521
Phone: 951-827-3660
E-Mail: David.Bocian@ucr.edu

Kara Bren
University of Rochester, Department of Chemistry
120 Trustee Rd.
Rochester, NY 14627-0216
Phone: 585-275-4335
E-Mail: bren@chem.rochester.edu

Participants List – 32nd DOE Solar Photochemistry Research Meeting

Karen J Brewer
Virginia Tech
Department of Chemistry
Blacksburg, VA 24061-0212
Phone: 540-231-6579
E-Mail: kbrewer@vt.edu

Gary Brudvig
Yale University
Department of Chemistry
New Haven, CT 06520-8107
Phone: 203-432-5202
E-Mail: gary.brudvig@yale.edu

Louis E. Brus
Chemistry Department, Columbia University
3000 Broadway
New York, NY 10706
Phone: 212-854-4041
E-Mail: leb26@columbia.edu

Emilio Bunel
Argonne National Laboratory
9700 S. Cass Ave., Bldg. 205
Argonne, IL 60439
Phone: 630-252-4309
E-Mail: ebunel@anl.gov

Ian Carmichael
Notre Dame Radiation Laboratory
University of Notre Dame
Notre Dame, IN 46556
Phone: 574-631-4502
E-Mail: carmichael.1@nd.edu

Edward Castner, Jr.
Rutgers, The State University of New Jersey
610 Taylor Road
Piscataway, NJ 08854-8066
Phone: 732-445-2564
E-Mail: ed.castner@rutgers.edu

Elaine Chandler
Helios SERC, LBL
1 Cyclotron Rd
Berkeley, CA 94708
Phone: 510-486-6854
E-Mail: eachandler@lbl.gov

Lin Chen
Argonne National Lab/Northwestern University
9700 S. Cass Ave.
Argonne, IL 60439
Phone: 630-252-3533
E-Mail: lchen@anl.gov

Kyoung-Shin Choi
Purdue University
Department of Chemistry
West Lafayette, IN 47907
Phone: 765-494-0049
E-Mail: kchoi1@purdue.edu

Philip Coppens
University at Buffalo, SUNY
732 NSc Complex, Amherst Camps
Buffalo, NY 14260-3000
Phone: 716-645-4273
E-Mail: coppens@buffalo.edu

Robert Crabtree
Yale University
225 Prospect St,
New Haven, CT 06520-8107
Phone: 203-432-3925
E-Mail: robert.crabtree@yale.edu

Carol Creutz
BNL Chemistry
Bldg. 555A
Upton, NY 11973
Phone: 631-344-4359
E-Mail: ccreutz@bnl.gov

Participants List – 32nd DOE Solar Photochemistry Research Meeting

Niels Damrauer
University of Colorado at Boulder
Campus Box 21
Boulder, CO 80309
Phone: 303-735-1280
E-Mail: niels.damrauer@colorado.edu

Richard Eisenberg
University of Rochester
Department of Chemistry
Rochester, NY 14620
Phone: 585-275-5573
E-Mail: eisenberg@chem.rochester.edu

C. Michael Elliott
Colorado State University
Department of Chemistry
Fort Collins, CO 80523
Phone: 970-491-5204
E-Mail: elliott@lamar.colostate.edu

John Endicott
Wayne State University
Detroit, MI 48202
Phone: 313-577-2607
E-Mail: jfe@chem.wayne.edu

Gregory Fiechtner
DOE/Basic Energy Sciences
19901 Germantown Road SC22-11
Germantown, MD 20874-1920
Phone: 301-903-8509
E-Mail: gregory.fiechtner@science.doe.gov

Graham Fleming
Lawrence Berkeley National Lab
221 Hildebrand Hall
Berkeley, CA 94720
Phone: 510-643-2735
E-Mail: grfleming@lbl.gov

Marye Anne Fox
UCSD
5926 Sagebrush Rd.
La Jolla, CA 92037
Phone: 858-534-5335
E-Mail: mafox@ucsd.edu

Arthur Frank
NREL
1617 Cole Blvd.
Golden, CO 80401
Phone: 303-384 6262
E-Mail: afrank@nrel.gov

Heinz Frei
Lawrence Berkeley National Laboratory
1 Cyclotron Road
Berkeley, CA 94720
Phone: 510-486-4325
E-Mail: HMFrei@lbl.gov

Richard A Friesner
Columbia University
3000 Broadway, MC 3110
New York, NY 10027
Phone: 212-854-7606
E-Mail: ec31@columbia.edu

Etsuko Fujita
Brookhaven National Laboratory
Chemistry Department
Upton, NY 11973-5000
Phone: 631-344-4356
E-Mail: fujita@bnl.gov

Elena Galoppini
Rutgers University
73 Warren Street
Newark, NJ 07102
Phone: 973-353-5317
E-Mail: galoppin@rutgers.edu

Participants List – 32nd DOE Solar Photochemistry Research Meeting

Bruce Garrett
Pacific Northwest National Laboratory
PO Box 999 (K9-90)
Richland, WA 99352
Phone: 509-372-6344
E-Mail: bruce.garrett@pnl.gov

Wayne Gladfelter
University of Minnesota
Department of Chemistry
Minneapolis, MN 55455
Phone: 612-624-4391
E-Mail: wlg@umn.edu

Ian Gould
Arizona State University
Dept of Chem and Biochem
Tempe, AZ 85287
Phone: 480-965-7278
E-Mail: igould@asu.edu

Richard Greene
U.S. Department of Energy
19901 Germantown Road SC22-11
Germantown, MD 20874-1920
Phone: 301-903-6190
E-Mail: richard.greene@science.doe.gov

Brian Gregg
National Renewable Energy Laboratory
1617 Cole Blvd
Golden, CO 80401
Phone: 303-384-6635
E-Mail: brian.gregg@nrel.gov

David Grills
Brookhaven National Laboratory
Chemistry Department, Bldg 555
Upton, NY 11973-5000
Phone: 631-344-4332
E-Mail: dcgrills@bnl.gov

Devens Gust
Arizona State University
Dept. of Chemistry and Biochemistry
Tempe, AZ 85287
Phone: 480-965-4547
E-Mail: gust@asu.edu

Robert Hamers
University of Wisconsin
1101 University Avenue
Madison, WI 53706
Phone: 608-262-6371
E-Mail: rjhamers@wisc.edu

Alexander Harris
Brookhaven National Laboratory
Chemistry Department, Bldg 555
Upton, NY 11973
Phone: 631-344-4301
E-Mail: alexh@bnl.gov

Michael Henderson
Pacific Northwest National Laboratory
PO Box 999, MS K8-87
Richland, WA 99338
Phone: 509-371-6527
E-Mail: ma.henderson@pnl.gov

Craig Hill
Emory University
1515 Dickey Dr NE
Atlanta, GA 30322
Phone: 404-727-6611
E-Mail: chill@emory.edu

Dewey Holten
Washington University in St. Louis
Chemistry, One Brookings Drive
St. Louis, MO 63130
Phone: 314-935-6502
E-Mail: holten@wustl.edu

Participants List – 32nd DOE Solar Photochemistry Research Meeting

Michael Hopkins
The University of Chicago
Department of Chemistry
Chicago, IL 60637
Phone: 773-702-6490
E-Mail: mhopkins@uchicago.edu

Libai Huang
University of Notre Dame
223 A Radiation Lab
Notre Dame, IN 46556
Phone: 573-631-2657
E-Mail: lhuang2@nd.edu

Joseph Hupp
Northwestern University
2145 Sheridan Road
Evanston, IL 60208
Phone: 847-491-3504
E-Mail: j-hupp@northwestern.edu

James Hurst
Washington State University
Department of Chemistry
Pullman, WA 99164
Phone: 509-432-3194
E-Mail: hurst@wsu.edu

Justin Johnson
National Renewable Energy Laboratory
1617 Cole Blvd
Golden, CO 80401
Phone: 303-384-6190
E-Mail: justin.johnson@nrel.gov

David Jonas
University of Colorado
215 UCB
Boulder, CO 80309-0215
Phone: 303-492-3818
E-Mail: david.jonas@colorado.edu

Prashant Kamat
University of Notre Dame
235 Radiation Laboratory
Notre Dame, IN 46556
Phone: 574-261-5411
E-Mail: pkamat@nd.edu

David Kelley
University of California, Merced
5200 N. Lake Rd.
Merced, CA 95344
Phone: 209-228-4354
E-Mail: dfkelley@ucmerced.edu

Lowell Kispert
The University of Alabama, Department of Chemistry
Shelby Hall Room 1007 D
Box 870336, 250 Hackberry Lane
Tuscaloosa, AL 35487-0336
Phone: 205-348-7134
E-Mail: lkispert@bama.ua.edu

Valeria Kleiman
University of Florida
PO BOX 117200
Gainesville, FL 32611
Phone: 352-392-4656
E-Mail: kleiman@ufl.edu

Todd Krauss
University of Rochester
120 Trustee Road
Rochester, NY 14627-0216
Phone: 585-275-5093
E-Mail: krauss@chem.rochester.edu

Frederick Lewis
Northwestern University
Department of Chemistry
Evanston, IL 60208
Phone: 847-491-3441
E-Mail: fdl@northwestern.edu

Participants List – 32nd DOE Solar Photochemistry Research Meeting

Nathan Lewis
Caltech
1200 E. California Blvd.
Pasadena, CA 91125
Phone: 626-395-6335
E-Mail: nslewis@caltech.edu

Tianquan Lian
Emory University
1515 Dickey Drive
Atlanta, GA 30322
Phone: 404-727-6649
E-Mail: tlian@emory.edu

Jonathan Lindsey
NC State University
Department of Chemistry
Raleigh, NC 27695-8204
Phone: 919-515-6406
E-Mail: jlindsey@ncsu.edu

Mark Lonergan
University of Oregon
1253 Department of Chemistry
Eugene, OR 97403-1253
Phone: 541-346-4748
E-Mail: lonergan@uoregon.edu

Sergei Lyamar
Brookhaven National Laboratory
Chemistry Department, BNL
Upton, NY 11973
Phone: 631-344-4333
E-Mail: lyamar@bnl.gov

Paul Maggard
North Carolina State University
2620 Yarbrough Drive
Raleigh, NC 27695-8204
Phone: 919-515-3616
E-Mail: Paul_Maggard@ncsu.edu

Thomas Mallouk
Penn State University
Department of Chemistry
University Park, PA 16802
Phone: 814-863-9637
E-Mail: tem5@psu.edu

Kent Mann
University of Minnesota
Chemistry Department
Minneapolis, MN 55455
Phone: 612-625-3563
E-Mail: krmann@umn.edu

Diane Marceau
Department of Energy
19901 Germantown Road
Germantown, MD 20874
Phone: 301-903-0235
E-Mail: diane.marceau@science.doe.gov

Claudio Margulis
University of Iowa
118 IATL
Iowa City, IA 52242
Phone: 319-335-0615
E-Mail: claudio-margulis@uiowa.edu

Mark Maroncelli
Penn State
104 Chemistry Building
University Park, PA 16802
Phone: 814-865-0898
E-Mail: maroncelli@psu.edu

Dmitry Matyushov
Arizona State University
PO Box 871605
Tempe, AZ 85287-1504
Phone: 480-965-0057
E-Mail: dmitrym@asu.edu

Participants List – 32nd DOE Solar Photochemistry Research Meeting

James McCusker
Michigan State University
Department of Chemistry
East Lansing, MI 48824
Phone: 517-355-9715
E-Mail: jkm@chemistry.msu.edu

Thomas Meyer
UNC-Chapel Hill
Dept of Chemistry
Chapel Hill, NC 27599-3290
Phone: 919-843-8312
E-Mail: tjmeyer@unc.edu

Gerald Meyer
Johns Hopkins
3400 N Charles St.
Baltimore, MD 21218
Phone: 410-516-7319
E-Mail: meyer@jhu.edu

John Miller
Brookhaven National Lab
Chemistry 555
Upton, NY 11973
Phone: 631-344-4354
E-Mail: jrmiller@bnl.gov

Ana Moore
Arizona State University
Chemistry & Biochemistry
Tempe, AZ 85287-1604
Phone: 480-965-2953
E-Mail: amoore@asu.edu

Thomas Moore
Arizona State University
Chemistry & Biochemistry
Tempe, AZ 85287-1604
Phone: 480-965-3308
E-Mail: tmoore@asu.edu

James Muckerman
Brookhaven National Laboratory
Chemistry Department
Upton, NY 11973-5000
Phone: 631-344-4368
E-Mail: muckerma@bnl.gov

Charles Mullins
University of Texas at Austin
Dept. of Chem. Engr. and Chem
Austin, TX 78712-0231
Phone: 512-471-5817
E-Mail: mullins@che.utexas.edu

Djamaladdin Musaev
Emory University, Chemistry Dept.
1515 Dickey Dr.
Atlanta, GA 30322
Phone: 404-727-2382
E-Mail: dmusaev@emory.edu

Nathan Neale
National Renewable Energy Laboratory
1617 Cole Blvd
Golden, CO 80401
Phone: 303-384-6165
E-Mail: nathan.neale@nrel.gov

Jeffrey Neaton
Lawrence Berkeley National Lab
1 Cyclotron Rd
Berkeley, CA 94720
Phone: 510-486-4527
E-Mail: jbneaton@lbl.gov

Marshall Newton
Brookhaven National Laboratory
Chemistry Department
Upton, NY 11973
Phone: 631-344-4366
E-Mail: newton@bnl.gov

Participants List – 32nd DOE Solar Photochemistry Research Meeting

Arthur Nozik
NREL/Univ Colorado
1617 Cole Blvd
Golden, CO 80401
Phone: 303-384-6603
E-Mail: anozik@nrel.gov

John Papanikolas
University of North Carolina at Chapel Hill
Department of Chemistry
Chapel Hill, NC 27599
Phone: 919-962-1619
E-Mail: john_papanikolas@unc.edu

Bruce Parkinson
University of Wyoming
Department of Chemistry
Laramie, WY 82071
Phone: 307-766-9891
E-Mail: bparkin1@uwoyo.edu

Hrvoje Petek
University of Pittsburgh
Department of Physics and Astr
Pittsburgh, PA 15260
Phone: 412-624-3599
E-Mail: petek@pitt.edu

Laurence Peter
Department of Chemistry, University of Bath
Claverton Down
Bath, - BA2 7AY UK
Phone: +44 1225 386502
E-Mail: l.m.peter@bath.ac.uk

Piotr Piotrowiak
Rutgers University
73 Warren Street
Newark, NJ 07304
Phone: 973-353-5318
E-Mail: piotr@andromeda.rutgers.edu

Oleg Poluektov
Argonne National Laboratory
9400 S. Cass Ave
Argonne, IL 60439
Phone: 630-252-3546
E-Mail: Oleg@anl.gov

Dmitry Polyansky
Brookhaven National Laboratory
Chemistry, Bldg. 555
Upton, NY 11973
Phone: 631-344-4315
E-Mail: dep@bnl.gov

Oleg Prezhdo
University of Washington
Department of Chemistry
Seattle, WA 98195
Phone: 206-221-3931
E-Mail: prezhdo@u.washington.edu

Yulia Pushkar
Purdue University
525 Northwestern Ave.
West Lafayette, IN 47907
Phone: 765-496-3279
E-Mail: YPushkar@purdue.edu

Jeff Pyun
University of Arizona
1306 E University Blvd.
Tucson, AZ 85721
Phone: 520-626-1834
E-Mail: jpyun@email.arizona.edu

John Reynolds
University of Florida
PO Box 117200
Gainesville, FL 32611
Phone: 352-392-9151
E-Mail: cgoogins@chem.ufl.edu

Participants List – 32nd DOE Solar Photochemistry Research Meeting

Dean Roddick
University of Wyoming
Chemistry, Dept. 3838, 1000 E.
Laramie, WY 82071
Phone: 307-766-2535
E-Mail: dmr@uwo.edu

Charles Schmuttenmaer
Yale University, Department of Chemistry
225 Prospect St, PO Box 208107
New Haven, CT 06520-8107
Phone: 203-432-5049
E-Mail: charles.schmuttenmaer@yale.edu

Garry Rumbles
National Renewable Energy Lab
1617 Cole Boulevard
Golden, CO 80401-3393
Phone: 303-885-3581
E-Mail: garry.rumbles@nrel.gov

Mark Spitler
Department of Energy
1000 Independence Ave, SW
Washington, DC 20585
Phone: 301-903-4568
E-Mail: mark.spitler@science.doe.gov

S. Scott Saavedra
Univ. of Arizona, Dept. of Chemistry & Bioch.
1306 E University
Tucson, AZ 85721
Phone: 520-621-9761
E-Mail: saavedra@email.arizona.edu

Robert Stack
DOE Office of Science
Germantown, MD 20874
Phone: 301-903-5652
E-Mail: robert.stack@science.doe.gov

Kirk Schanze
Chemistry Department, University of Florida
PO Box 117200
Gainesville, FL 32611-7200
Phone: 352-392-9133
E-Mail: kschanze@chem.ufl.edu

Jessica Swanson
ANL
9700 S. Cass Ave, Bldg. 200
Argonne, IL 60439
Phone: 630-252-3579
E-Mail: jswanson@anl.gov

H. Bernhard Schlegel
Dept. of Chemistry, Wayne State University
5101 Cass Ave.
Detroit, MI 48202
Phone: 313-577-2562
E-Mail: hbs@chem.wayne.edu

Michael Therien
Duke University
Box 90347
Durham, NC 27708
Phone: 919-684-0785
E-Mail: ian.foley@duke.edu

Russell Schmehl
Tulane University
Department of Chemistry
New Orleans, LA 70118
Phone: 504-862-3566
E-Mail: russ@tulane.edu

Mark Thompson
University of Southern California
Department of Chemistry
Los Angeles, CA 90089
Phone: 213-740-6402
E-Mail: met@usc.edu

Participants List – 32nd DOE Solar Photochemistry Research Meeting

Randolph Thummel
University of Houston
136 Fleming
Houston, TX 77204-5003
Phone: 713-743-2734
E-Mail: thummel@uh.edu

David Tiede
Argonne National Laboratory
9700 South Cass Ave.
Argonne, IL 60439
Phone: 630-252-3539
E-Mail: tiede@anl.gov

William Tumas
NREL
1617 Cole Blvd.
Golden, CO 80401
Phone: 303-384-7955
E-Mail: bill.tumas@nrel.gov

John Turner
National Renewable Energy Laboratory
1617 Cole Blvd.
Golden, CO 80401
Phone: 303-275-4270
E-Mail: jturner@nrel.gov

Lisa Utschig
Argonne National Laboratory
9700 S. Cass Ave.
Argonne, IL 60439
Phone: 630-252-3544
E-Mail: utschig@anl.gov

Jao van de Lagemaat
NREL
1617 Cole Blvd.
Golden, CO 80403
Phone: 303-384-6143
E-Mail: jao.vandelagemaat@nrel.gov

Claudio Verani
Wayne State University
5101 Cass Ave.
Detroit, MI 48310
Phone: 313-577-1076
E-Mail: cnverani@chem.wayne.edu

Michael Wasielewski
Northwestern University
2145 Sheridan Rd.
Evanston, IL 60208
Phone: 847-467-1423
E-Mail: m-wasielewski@northwestern.edu

Emily Weiss
Department of Chemistry, Northwestern University
2145 Sheridan Rd
Evanston, IL 60208-3113
Phone: 847-491-3095
E-Mail: e-weiss@northwestern.edu

James Whitesell
UCSD
5926 Sagebrush Rd
La Jolla, CA 92037
Phone: 858-349-3182
E-Mail: jkwhitesell@mac.com

David Whitten
Center for Biomedical Engineering
University of New Mexico
Albuquerque, NM 87131-0001
Phone: 505-277-5736
E-Mail: whitten@langmuir.acs.org

James Wishart
Brookhaven National Laboratory
Chemistry Department
Upton, NY 11973
Phone: 631-344-4327
E-Mail: wishart@bnl.gov

Author Index

Adachi, Takuji.....	60	Ceckanowicz, Darren J.....	155
Adams, Jeramie J.....	170	Chambers, S. A.....	141
Allard, Marco.....	130, 131, 133	Chemerisov, Sergey D.....	176
Allen, Laura J.....	122, 126	Chen, Lin X.....	127, 175, 176
Allen, P. B.....	161	Chitta, Raghu.....	136, 155
Amick, Tyson J.....	21	Cho, Byungmoon.....	146
Annappureddy, H. V. R.....	156	Choi, Kyoung-Shin.....	11
Arachchige, Shamindri.....	84	Chu, Li-Qiang.....	143
Ardo, Shane.....	159	Clark, Aurora.....	144
Armstrong, Neal R.....	117	Coffey, David.....	171
Arulsamy, Navamoney.....	170	Cohen, Brian.....	135
Arzhantsev, Sergei.....	94	Coker, David.....	156
Asaoka, Sadayuki.....	57	Colvin, Michael T.....	44
Ashbrook, Lance.....	21	Cook, Andrew.....	57
Attenkofer, Klaus.....	127	Cooperrider, Michelle.....	180
Bang, Jin Ho.....	103	Coppens, Philip.....	129
Bao, Jianhua.....	168	Cormier, Russel A.....	138
Baranowski, Alex J.....	125	Courtney, Trevor L.....	146
Barbara, Paul F.....	60	Crabtree, Robert H.....	122, 124, 126, 128
Bard, Allen J.....	164	Creutz, Carol.....	81
Baruah, Tunna.....	119	Cuk, Tanja.....	134
Basu, Debashis.....	133	Damrauer, Niels H.....	69
Batista, Victor S.....	122, 124, 126, 128	Darancet, P.....	163
Beard, Matt.....	120, 145, 179	Dayal, Smita.....	171
Benedict, Jason B.....	129	del Popolo, Mario.....	156
Besson, Claire.....	148	Deria, Pravas.....	173
Blackburn, Jeff.....	120	Doak, P.....	163
Blakemore, James D.....	124	Draggich, Jeff.....	91
Blank, David A.....	136, 155	Eisenberg, Richard.....	123
Blasdel, Landy K.....	154	El Ojaimi, Maya.....	174
Bocarsly, A. B.....	121	Elliott, C. Michael.....	21
Bocian, David F.....	50	Endicott, John F.....	130, 131, 133
Bohnsack, Jon N.....	155	Erslef, P. T.....	179
Bolinger, Joshua C.....	60	Erwin, Patrick.....	118
Bonnell, Dawn A.....	173	Feenstra, Randall M.....	143
Branz, H.....	179	Ferguson, Andrew.....	120, 171
Bren, Kara L.....	123	Fernandez-Serra, M. V.....	161
Brennan, Bradley.....	140	Fleming, Graham R.....	71
Brewer, Karen J.....	84	Focsan, A. Ligia.....	147
Bricaud, Quentin.....	63	Fox, Marye Anne.....	132
Bridgewater, James.....	140	Frank, Arthur J.....	98, 179
Brown, Allison.....	158	Franking, Ryan.....	180
Brudvig, Gary W.....	122, 124, 126, 128	Frei, Heinz.....	134
Brumback, Karin.....	122	Friesner, Richard A.....	36
Brus, Louis.....	111	Fude, Feng.....	63
Cabelli, Diane.....	135	Fujita, Etsuko.....	135, 161
Carlson, Lisa J.....	149	Fukushima, Takashi.....	135
Carmieli, Raanan.....	44	Gallagher, Joy A.....	181
Castner, Edward W., Jr.....	125	Galoppini, Elena.....	24

Geletii, Yurii V.....	148, 150, 152	Kispert, Lowell D.....	147
Gladfelter, Wayne L.....	136, 155	Kleiman, Valeria D.....	63
Gohdo, Masao.....	178	Kodis, Gerdenis.....	140
Gould, Ian R.....	137	Kohanoff, Jorge.....	156
Gregg, Brian A.....	138	Kolarz, Megan A.....	154
Grills, David C.....	139	Kömürlü, Sevnur.....	63
Grumstrup, Erik M.....	69	Kopidakis, Nikos.....	120, 171
Gu, Jing.....	91	Kovtyukhova, Nina I.....	154
Gundlach, Lars.....	168	Krauss, Todd D.....	123, 149
Gust, Devens.....	140	Lakshmi, K. V.....	169
Hagen, Karl S.....	150	Lazorski, Megan.....	21
Hamers, Robert J.....	180	Lebkowsky, Kristi.....	91
Hartland, Gregory V.....	143	Lee, Andrea J.....	149
Henderson, M. A.....	141	Lee, One-Sun.....	173
Hill, Craig L.....	148, 150, 152	Lee, Seoung Ho.....	63
Hill, Robert J.....	146	Lee, Seung-Hyun Anna.....	154
Holland, Patrick L.....	123	Lesh, Frank D.....	133
Holt, Josh.....	120	Lewis, Frederick D.....	41
Holten, Dewey.....	50	Lewis, Nathan S.....	7
Hopkins, Michael D.....	142	Li, Gonghu.....	126
Hou, Yu.....	148	Li, Xiang.....	94
Huang, Libai.....	143, 175	Lian, Chuanxin.....	143
Huang, Zhuangqun.....	148, 150, 152	Lian, Tianquan.....	148, 150, 152
Hue, Ryan.....	136	Liang, Min.....	94
Hughes, Barbara.....	145	Liang, Ziqi.....	138
Hupp, Joseph T.....	14	Liddell, Paul A.....	140
Hurst, James K.....	144	Lightcap, Ian.....	103
Huss, Adam.....	136	Lin, Fuding.....	151
Hybertsen, M. S.....	161	Lindsey, Jonathan S.....	50
Imahori, H.....	57	Liu, Haitao.....	111
Isaacs, E.....	163	Lockard, Jenny V.....	127, 176
Ito, Naoki.....	137	Lonergan, Mark.....	151
Jamula, Lindsey.....	158	Louis, Kacie.....	180
Jellison, Lucas.....	154	Lovaasen, Benjamin M.....	142
Jennings, Guy.....	127	Luo, Zhen.....	150
Jiang, Zhong-Jie.....	108	Luxmi.....	143
Jin, Hui.....	94	Lymar, Sergei V.....	79, 144
Johnson, Justin C.....	98, 145	Ma, J.....	179
Jonas, David M.....	146	MacNaughtan, Marisa.....	134
Jung, Naeyoung.....	111	Maeda, Kazuhiko.....	154
Kaledin, Alexey.....	152	Maggard, Paul A.....	153
Kamat, Prashant V.....	103	Mallouk, Thomas E.....	154
Kang, Soon Hyung.....	98	Mangham, A. N.....	141
Kang, Youn K.....	173	Mann, Kent R.....	136, 155
Kaveevivitchai, Nattawut.....	174	Manpadi, Madhuri.....	125
Keets, K.....	121	Mara, Michael W.....	127
Keller, Julia M.....	57	Margulis, Claudio J.....	156
Kelley, David F.....	108	Maroncelli, Mark.....	94
Kim, Sang Hoon.....	173	Matyushov, Dmitry V.....	157

McCoy, Michael.....	180	Polyansky, Dmitry E.	135
McCusker, James K.....	158	Ponomarenko, Nina.....	175
McIlroy, Sean.....	57	Prezhdo, Oleg.....	31
McNamara, William R.	122, 126, 128	Psciuk, Brian T.....	130
Meekins, Benjamin.....	103	Pyun, Jeffry.....	117
Meyer, Gerald J.....	159	Reynolds, John R.....	63
Meyer, Thomas J.....	160	Richter, Christiaan.....	126
Miller, John R.....	57	Ricks, Annie Butler.....	44
Milot, Rebecca L.....	122, 124, 126, 128	Robinson, Stephen.....	151
Mirafzal, Hoda.....	108	Roddick, Dean M.	170
Mistry, Kevin.....	120	Romero, Manuel.....	177
Miura, Tomoaki.....	44	Rowley, John.....	159
Molnár, Péter.....	147	Roy, Durba.....	94
Moore, Ana L.....	140	Ruddy, Daniel A.....	162, 179
Moore, Gary F.....	124	Rumbles, Garry.....	120, 171
Moore, Thomas A.....	140	Ryu, Sunmin.....	111
Moravec, Davis.....	142	Saavedra, S. Scott.....	117
Morris, A. J.....	121	Sambur, Justin B.....	166
Muckerman, James T.	135, 161	Santos, Cherry S.....	125
Mukherjee, Tamal.....	137	Saunders, Julia.....	136
Mulfort, Karen L.....	175, 176	Saven, Jeffery G.....	173
Mullins, C. Buddie.....	164	Schanze, Kirk S.....	57, 63
Musaev, Djamaladdin G.....	148, 150, 152	Schlegel, H. Bernhard.....	130, 131, 133
Myers, Carl P.....	181	Schlenker, Cody.....	118
Neale, Nathan R.....	98, 162, 179	Schmehl, Russell.....	91
Neaton, J. B.....	163	Schmuttermaer, Charles....	122,124,126,128
Nelson, Jeremy J.....	21	Schwartz, Kyle R.....	155
Neuberger, Amelia.....	91	Scott, Amy M.....	44
Newton, Marshall D.....	165	Sedai, Baburam.....	84
Novet, Thomas.....	166	Shakya, Rajendra.....	133
Nozik, Arthur J.....	98, 145, 179	Shanmugan, Rama.....	133
Odongo, Onduro S.....	131	Sharifzadeh, S.....	163
Oh, J.....	179	Shaw, Ryan.....	84
O'Hanlon, Daniel C.....	142	Shen, X.....	161
Ohsawa, T.....	141	Shibano, Yuki.....	57
Olguin, Marco.....	119	Shutthanandan, V.....	141
Ostheimer, Seth.....	181	Small, Y. A.....	161
Palma, Julio L.....	122	Smith, E. Ryan.....	145
Papanikolas, John M.....	160	Smolentsev, Grigory.....	127
Park, Tae-Hong.....	173	Smyder, Julie A.....	149
Parkinson, B. A.....	166	Snoeberger, Robert C., III.....	126, 128
Patel, Dan.....	63	Soldatov, Alexander.....	127
Perez, Dolores.....	118	Song, Hee-eun.....	124, 128
Petek, Hrvoje.....	167	Song, Jie.....	150
Peter, Laurence.....	3	Sreearunothai, Paiboon.....	57
Peters, William K.....	146	Stanton, Ian.....	173
Piotrowiak, Piotr.....	168	Stickrath, Andrew B.....	127
Poluektov, Oleg G.....	169, 175, 176	Stull, Jamie.....	144
Polyakov, Nikolay E.....	147	Swanson, Jessica M. J.....	172

Swierk, John	154
Tahy, Kristof	143
Takeda, Norihiko.....	57
Tanaka, Koji	135
Therien, Michael J.....	173
Thompson, Mark	118
Thummel, Randolph P.....	135, 174
Tiede, David M.....	169, 175, 176
Toor, F.	179
Traub, Matt C.	60
Turner, J.A.....	179
Tvrdy, Kevin	103
Utschig, Lisa M.	169, 175, 176
Vallett, Paul	69
van de Lagemaat, Jao	177
Vella, Jarrett	63
Verani, Cláudio N.....	130, 131, 133
Walker, Ethan.....	151
Wang, J.....	161
Wang, Xiaoyong.....	149
Wasielewski, Michael R.....	44
Wasinger, Erik C.	127
Weare, Walter.....	134
Wei, S. H.	179
White, Travis.....	84
Whitesell, James K.	132
Wiederrecht, Gary	175
Williams, Lawrence J.	125
Williams, Mary Elizabeth.....	181
Wishart, James F.	178
Woodhouse, Michael.....	138
Xing, Huili.....	143
Yin, Qushi	148, 150
Youngblood, W. Justin.....	154
Zeitler, E. L.	121
Zhang, Xiaoyi.....	127
Zhu, Guibo.....	148
Zong, Ruifa.....	135, 174
Zope, R. R.	119